USGS
science for a changing world

DOE/ID-22258

Prepared in cooperation with the U.S. Department of Energy

Determining Three-Dimensional Hydrologic Processes in the Eastern Snake River Plain Aquifer Using Geochemical Mass-Balance Modeling, Idaho National Laboratory, Eastern Idaho

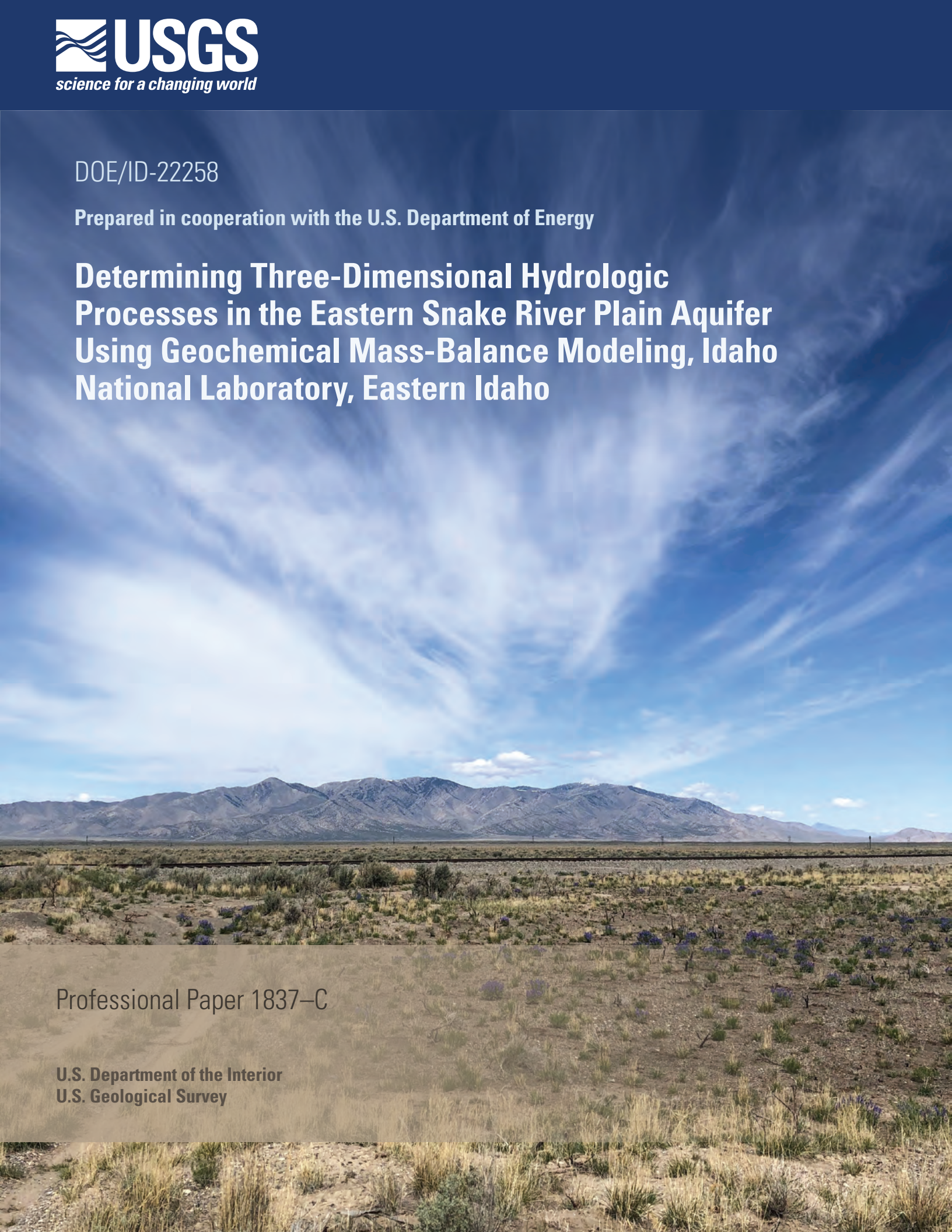

Professional Paper 1837–C

U.S. Department of the Interior
U.S. Geological Survey

Cover. Eastern Snake River Plain looking west towards the Lost River Range, Idaho. Photograph by Kerri C. Treinen, U.S. Geological Survey, May 2021.

Determining Three-Dimensional Hydrologic Processes in the Eastern Snake River Plain Aquifer Using Geochemical Mass-Balance Modeling, Idaho National Laboratory, Eastern Idaho

By Gordon W. Rattray

DOE/ID-22258

Prepared in cooperation with the U.S. Department of Energy

Professional Paper 1837–C

U.S. Department of the Interior
U.S. Geological Survey

U.S. Geological Survey, Reston, Virginia: 2023

For more information on the USGS—the Federal source for science about the Earth, its natural and living resources, natural hazards, and the environment—visit https://www.usgs.gov or call 1–888–ASK–USGS.

For an overview of USGS information products, including maps, imagery, and publications, visit https://store.usgs.gov/.

Suggested citation:
Rattray, G.W., 2023, Determining three-dimensional hydrologic processes in the eastern Snake River Plain aquifer using geochemical mass-balance modeling, Idaho National Laboratory, eastern Idaho, with contributions by Treinen, K.C.: U.S. Geological Survey Professional Paper 1837–C (DOE/ID 22258), 133 p., https://doi.org/10.3133/pp1837C.

Associated data for this publication:
Jurgens, B.C., 2018, Data for tritium deposition in precipitation in the United States, 1953–2012: U.S. Geological Survey data release, https://doi.org/10.5066/P92CEFXN.

Related reports:
Rattray, G.W., 2018, Geochemistry of groundwater in the eastern Snake River Plain aquifer, Idaho National Laboratory and vicinity, eastern Idaho: U.S. Geological Survey Professional Paper 1837–A (DOE/ID-22246), 198 p., https://doi.org/10.3133/pp1837A.

Rattray, G.W., 2019, Evaluation of chemical and hydrologic processes in the eastern Snake River Plain aquifer based on results from geochemical modeling, Idaho National Laboratory, eastern Idaho: U.S. Geological Survey Professional Paper 1837–B (DOE/ID-22248), 85 p., https://doi.org/10.3133/pp1837B.

Rattray, G.W., and Paces, J.B., 2023, Evaluation of hydrologic processes in the eastern Snake River Plain aquifer using uranium and strontium isotopes, Idaho National Laboratory, eastern Idaho, with contributions by Treinen, K.C.: U.S. Geological Survey Professional Paper 1837–D (DOE/ID-22259), 65 p., https://doi.org/10.3133/pp1837D.

ISSN 2330-7102 (online)

Contents

Figures

Tables

Conversion Factors

U.S. customary units to International System of Units

Multiply	By	To obtain
	Length	
inch (in.)	2.54	centimeter (cm)
foot (ft)	0.3048	meter (m)
mile (mi)	1.609	kilometer (km)
	Area	
acre	0.4047	hectare (ha)
square mile (mi^2)	2.590	square kilometer (km^2)
	Flow rate	
cubic foot per second (ft^3/s)	0.02832	cubic meter per second (m^3/s)
	Radioactivity	
picocurie per liter (pCi/L)	0.037	becquerel per liter (Bq/L)
	Hydraulic conductivity	
foot per day (ft/d)	0.3048	meter per day (m/d)
	Hydraulic gradient	
foot per mile (ft/mi)	0.1894	meter per kilometer (m/km)

International System of Units to U.S. customary units

Multiply	By	To obtain
	Length	
millimeter (mm)	0.03937	inch (in.)
meter (m)	3.281	foot (ft)
kilometer (km)	0.6214	mile (mi)

Temperature in degrees Fahrenheit (°F) may be converted to degrees Celsius (°C) as follows:

$°C = (°F - 32) / 1.8.$

Temperature in degrees Celsius (°C) may be converted to degrees Fahrenheit (°F) as follows:

$°F = (1.8 \times °C) + 32.$

Datums

Vertical coordinate information is referenced to the National Geodetic Vertical Datum of 1929 (NGVD 29).

Horizontal coordinate information is referenced to the North American Datum of 1927 (NAD 27).

Altitude, as used in this report, refers to distance above the vertical datum.

Supplemental Information

Specific conductance is given in microsiemens per centimeter at 25 degrees Celsius (µS/cm at 25 °C).

Concentrations of chemical constituents in water are given in either milligrams per liter (mg/L) or micrograms per liter (µg/L).

Phase mole transfer amounts are given in micromoles per kilogram of water (µmol/kg water).

Activities for radioactive constituents in water are given in picocuries per liter (pCi/L).

Abbreviations

ABSB	Arco-Big Southern Butte
ATRC	Advanced Test Reactor Complex
AVH	axial volcanic highland
BC	Birch Creek
BLR	Big Lost River
BLT	Big Lost Trough
bwt	below water table
CFA	Central Facilities Area
DOE	U.S. Department of Energy
ESRP	eastern Snake River Plain
INL	Idaho National Laboratory
INTEC	Idaho Nuclear Technology and Engineering Center
LLR	Little Lost River
MLMS	multilevel monitoring system
MLW	multilevel wells
NAD	normalized absolute difference
RPD	relative percent difference
RSD	relative standard deviation
RWMC	Radioactive Waste Management Complex
SI	saturation index
USGS	U.S. Geological Survey

Determining Three-Dimensional Hydrologic Processes in the Eastern Snake River Plain Aquifer Using Geochemical Mass-Balance Modeling, Idaho National Laboratory, Eastern Idaho

By Gordon W. Rattray

Abstract

Waste constituents discharged to the eastern Snake River Plain aquifer at the U.S. Department of Energy (DOE) Idaho National Laboratory (INL) pose risks to the water quality of the aquifer. To understand these risks, the U.S. Geological Survey, in cooperation with the DOE, used geochemical mass-balance modeling to identify three-dimensional hydrologic processes in that portion of the aquifer underlying the southwestern part of the INL that affect the movement of groundwater and waste constituents. Modeling was performed using water chemistry of 74 water samples collected from 30 wells. Fifty-four of the water samples were collected from 11 wells equipped with multilevel monitoring systems with vertically discrete sampling zones that encompass the upper 750 feet of the aquifer. Water samples from these multilevel wells were collected during 2007–13, a period when conditions in the aquifer were approximately steady-state because there was little or no recharge from the Big Lost River.

The primary source of water in groundwater at the multilevel wells during 2007–13 was the Big Lost River. Other sources of water include groundwater from the Little Lost River valley, precipitation, and wastewater. Horizontal groundwater-flow directions appear to be similar in both the shallow and deep parts of the aquifer, and surface-water sources of water in most deep groundwater shows that groundwater moves downward. Surface-water sources of water in deep groundwater noticeably decrease within and below the Matuyama flow and associated sedimentary interbeds, which indicates that these units are semi-impermeable and retard the downward movement of groundwater.

Introduction

The eastern Snake River Plain (ESRP) aquifer is an important resource for the State of Idaho because it is the sole source of drinking water for about 200,000 people and supplies water for industry and for about 900,000 acres of irrigated farmland (Idaho Department of Environmental Quality, 2015). The U.S. Department of Energy (DOE) established the Idaho National Laboratory (INL) on the ESRP in eastern Idaho in 1949. Nuclear research activities at the INL produced liquid and solid chemical and radiochemical wastes that were disposed to the subsurface at various INL facilities (fig. 1). The disposal of these wastes resulted in detectable concentrations of some waste constituents in the ESRP aquifer (Davis and others, 2013).

The presence of chemical and radiochemical wastes in the ESRP aquifer may pose risks to the water quality of the aquifer, which is a concern of the State of Idaho, DOE, and the public. To understand these risks to groundwater quality, the U.S. Geological Survey (USGS), in cooperation with the DOE, has maintained an extensive water-quality monitoring network at the INL since 1949 (Bartholomay, Maimer, and others, 2017). From 2005 to 2012, 11 multilevel wells (MLW) were added to the monitoring network (fig. 1); these wells, equipped with multilevel monitoring systems (MLMS), provide water-quality data from multiple aquifer depths in the southwestern part of the INL (Bartholomay and Twining, 2010; Bartholomay and others, 2015). In addition to providing information about risks to groundwater quality from waste constituents, water-quality data are used in geochemistry studies to understand chemical and hydrologic processes in the ESRP aquifer and to determine how these processes affect the concentrations and movement of waste constituents in the aquifer. Results from geochemistry studies also provide information that may be used to improve, constrain, and (or) calibrate groundwater-flow models of the ESRP aquifer at the INL (Fisher and others, 2012).

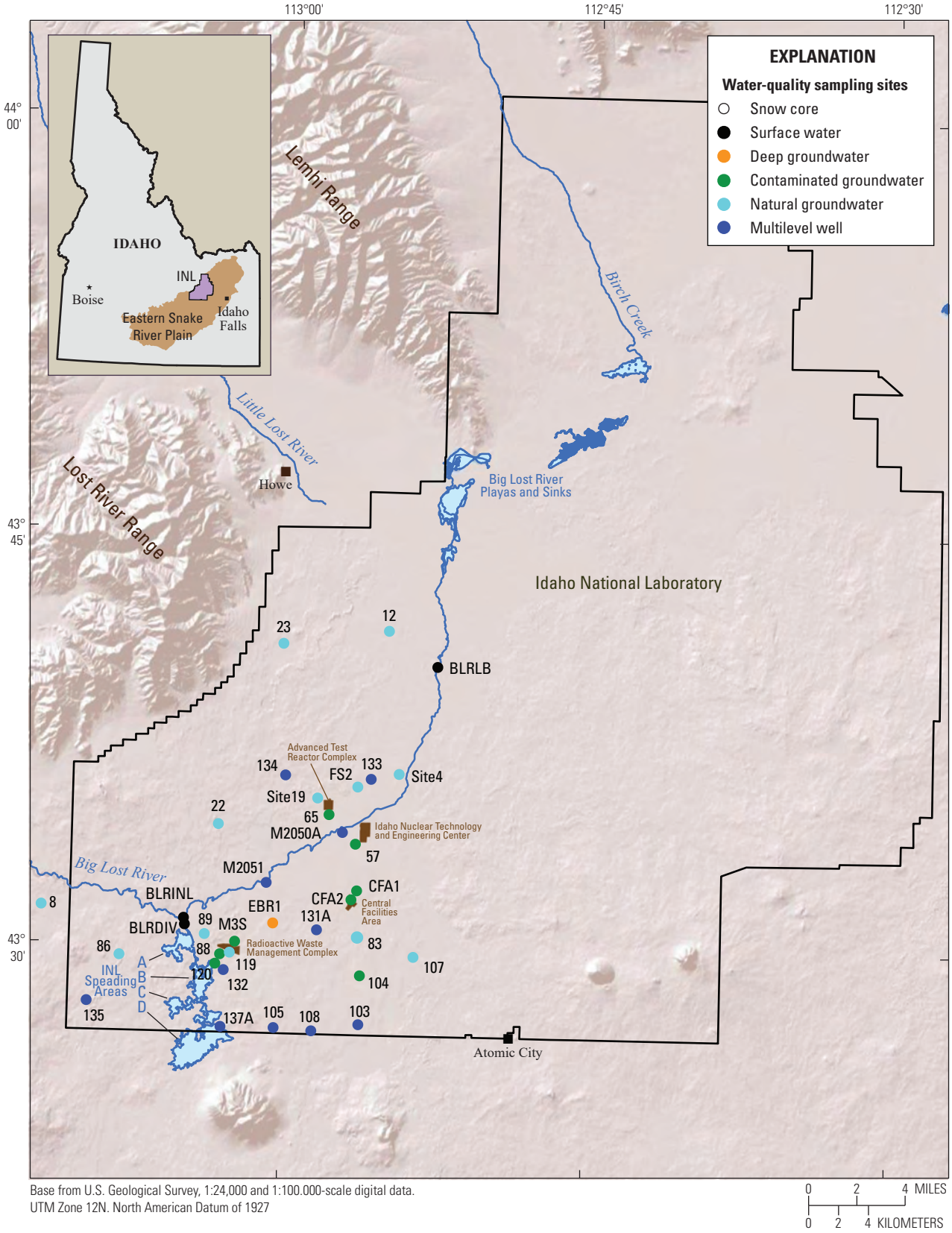

Figure 1. Geographic features and water-quality sampling sites at and near the Idaho National Laboratory (INL) and vicinity, eastern Idaho. See table 1 for site details.

Chapters A and B of Professional Paper 1837 (Rattray, 2018, 2019) identified chemical and hydrologic processes in the shallow ESRP aquifer at the INL through evaluation of surface-water and groundwater chemistry and geochemical mass-balance modeling. This report (Chapter C) describes geochemical mass-balance modeling done to investigate these same chemical and hydrologic processes in both shallow and deep groundwater of the ESRP aquifer in the southwestern part of the INL. Consequently, this report describes chemical reactions and the three-dimensional movement of groundwater in both the shallow and deep aquifer, whereas the previous chapters (Rattray, 2018, 2019) only described chemical reactions and the two-dimensional movement of groundwater in the shallow aquifer. Most waste constituents at the INL were discharged to and reside in that portion of the aquifer underlying the southwestern part of the INL (Bartholomay, Maimer, and others, 2017), so this report identifies the chemical and hydrologic processes that affect the three-dimensional movement of most waste constituents in the ESRP aquifer in the southwestern part of the INL.

Purpose and Scope

The objectives of this report were (1) to use geochemical mass-balance modeling to identify chemical reactions and hydrologic processes (sources of recharge, mixing of water, and groundwater-flow directions) in the upper 750 feet (ft) of the ESRP aquifer in the southwestern part of the INL; and (2) to understand how these processes affect the movement of groundwater and, hence, waste constituents in the aquifer. Water-quality data are available at multiple, discrete aquifer depths from 11 MLW (MIDDLE 2050A, MIDDLE 2051, USGS 103, USGS 105, USGS 108, USGS 131A, USGS 132, USGS 133, USGS 134, USGS 135, and USGS 137A) (table 1). Wells USGS 133 and USGS 134 are located north and upgradient of the other nine MLW (fig. 1). Consequently, chemistry data representing the deep aquifer were not available for producing geochemical models of the deeper zones at these two MLW. However, chemistry data from wells USGS 133 and USGS 134 were used in geochemical models for the other nine MLW.

Modeling was performed using the inverse modeling capability of the computer code PHREEQC (Parkhurst and Appelo, 2013) and the water chemistry from 74 water samples collected from 30 sites (fig. 1). Fifty-four of the water samples were collected from vertically discrete water sampling zones from the 11 MLW from 2007 to 2013, and the other 20 water samples were collected from open boreholes from 1978 to 1996. A complete list of the chemical and isotopic data used in geochemical modeling effort is available in section, "Geochemistry Data." The data presented in this report are available from the USGS National Water Information System at https://dx.doi.org/10.5066/F7P55KJN using the site numbers listed in table 1 (U.S. Geological Survey, 2021).

Description of Study Area

The study area includes groundwater from MLW in the southwestern part of the INL where waste constituents from the Advanced Test Reactor Complex (ATRC), Idaho Nuclear Technology and Engineering Center (INTEC), and Radioactive Waste Management Complex (RWMC) reside. This area is defined on the south, west, north, and east by the southern and western boundaries of the INL, the Big Lost River (BLR), and an imaginary line between the INTEC and MLW USGS 103 (fig. 1). The study area encompasses approximately 130 square miles (mi^2) of eastern Idaho, the ESRP, and the southwestern part of the INL. The ESRP is a relatively flat topographic depression with elevations at the INL ranging from about 4,800 to 5,300 ft. The climate at the INL is semi-arid with mean annual temperature of 42.3 degrees Fahrenheit (°F) and a mean annual precipitation of 8.4 inches (in.) (period of record 1950 to 2014, National Oceanic and Atmospheric Administration, 2015).

Geology

The ESRP is a structural depression that formed in the wake of the Yellowstone Hot Spot. The Yellowstone Hot Spot moved progressively northeastward across Idaho as the North American Plate began to move southwestward over a fixed upper mantle melting anomaly about 17 million years ago (Kuntz and others, 1992). As the ESRP subsided, it filled with silicic material from caldera eruptions, tube-fed pahoehoe basalt flows, and sediment from alluvial, fluvial, lacustrine, and eolian processes (Hodges and Champion, 2016). Consequently, the ESRP at and near the INL consists of a thick accumulation of Tertiary tuffs and rhyolites overlain by a thick sequence of numerous subhorizontal Tertiary and Quaternary basalt flows (Ackerman and others, 2006) with interfingering Tertiary and Quaternary surficial and interbed sediments (fig. 2; Doherty and others, 1979; Anderson and Liszewski, 1997).

Structural features on the ESRP associated with volcanism and subsidence include:

- The axial volcanic highland (AVH), a broad linear topographic highland trending southwest-to-northeast and formed from the accumulation of lava flows from basaltic volcanoes centered along the AVH and uplift associated with emplacement of rhyolite domes (fig. 2; Kuntz and others, 1992).
- Volcanic rift zones, which are linear to curvilinear belts of numerous geologically young volcanic structures and landforms that generally trend northwestward and are perpendicular to the AVH and the direction of regional groundwater flow (fig. 2; Kuntz and others, 1992).

Table 1. Site names, U.S. Geological Survey (USGS) site numbers, and abbreviated names for water-quality sample sites, Idaho National Laboratory, eastern Idaho (U.S. Geological Survey, 2021).

[**Site name:** Location of sites shown in figure 1. **Abbreviations:** na, not applicable; No., number]

Site name	USGS site No.	Abbreviated name
SNOW CORE		
USGS 83	na	83
SURFACE WATER		
Big Lost River below INL Diversion	13132520	BLRINL
INL Diversion at head, near Arco	13132513	BLRDIV
Big Lost River below lower Lincoln Blvd. Bridge	13132553	BLRLB
TRIBUTARY VALLEY GROUNDWATER		
Ruby Farms[1]	434751112571801	RF
DEEP GROUNDWATER		
EBR 1	433051113002601	EBR1
CONTAMINATED GROUNDWATER		
Advanced Test Reactor Complex		
USGS 65	433447112574501	65
Central Facilities Area		
CFA 1	433204112562001	CFA1
CFA 2	433144112563501	CFA2
USGS 104	432856112560801	104
Idaho Nuclear Technology and Engineering Center		
USGS 57	433344112562601	57
Radioactive Waste Management Complex		
RWMC M3S	433008113021801	M3S
USGS 88	432940113030201	88
USGS 120	432919113031501	120
NATURAL GROUNDWATER		
Fire Station 2	433548112562301	FS2
Site 4	433617112542001	Site4
Site 19	433522112582101	Site19
USGS 8	433121113115801	8
USGS 12	434126112550701	12
USGS 22	433422113031701	22
USGS 23	434055112595901	23
USGS 83	433023112561501	83
USGS 86	432935113080001	86
USGS 89	433005113032801	89
USGS 107	432942112532801	107
USGS 117	432955113025901	117
USGS 119	432945113023401	119
GROUNDWATER FROM MULTILEVEL WELLS		
MIDDLE 2050A	433409112570500	M2050A
Zone 15	433409112570515	M2050AZ15
Zone 12	433409112570512	M2050AZ12
Zone 9	433409112570509	M2050AZ9

Table 1. Site names, U.S. Geological Survey (USGS) site numbers, and abbreviated names for water-quality sample sites, Idaho National Laboratory, eastern Idaho (U.S. Geological Survey, 2021).—Continued

[**Site name:** Location of sites shown in figure 1. **Abbreviations:** na, not applicable; No., number]

Site name	USGS site No.	Abbreviated name
GROUNDWATER FROM MULTILEVEL WELLS—Continued		
Zone 6	433409112570506	M2050AZ6
Zone 3	433409112570503	M2050AZ3
MIDDLE 2051	433217113004900	M2051
Zone 12	433217113004912	M2051Z12
Zone 9	433217113004909	M2051Z9
Zone 6	433217113004906	M2051Z6
Zone 3	433217113004903	M2051Z3
Zone 1	433217113004901	M2051Z1
USGS 103	432714112569701	103
Zone 17	432714112560723	103Z17
Zone 15	432714112560720	103Z15
Zone 12	432714112560716	103Z12
Zone 9	432714112560712	103Z9
Zone 6	432714112560708	103Z6
Zone 3	432714112560704	103Z3
Zone 1	432714112560702	103Z1
USGS 105	432703113001801	105
Zone 13	432703113001818	105Z13
Zone 11	432703113001815	105Z11
Zone 8	432703113001811	105Z8
Zone 5	432703113001807	105Z5
Zone 2	432703113001803	105Z2
USGS 108	432659112582601	108
Zone 11	432659112582616	108Z11
Zone 9	432659112582613	108Z9
Zone 7	432659112582610	108Z7
Zone 4	432659112582606	108Z4
Zone 1	432659112582602	108Z1
USGS 131A	433036112581800	131A
Zone 12	433036112581815	131AZ12
Zone 8	433036112581810	131AZ8
Zone 5	433036112581806	131AZ5
Zone 3	433036112581803	131AZ3
USGS 132	432906113025000	132
Zone 17	432906113025022	132Z17
Zone 14	432906113025018	132Z14
Zone 11	432906113025014	132Z11
Zone 8	432906113025010	132Z8
Zone 5	432906113025006	132Z5
Zone 1	432906113025001	132Z1

Table 1. Site names, U.S. Geological Survey (USGS) site numbers, and abbreviated names for water-quality sample sites, Idaho National Laboratory, eastern Idaho (U.S. Geological Survey, 2021).—Continued

[**Site name:** Location of sites shown in figure 1. **Abbreviations:** na, not applicable; No., number]

Site name	USGS site No.	Abbreviated name
GROUNDWATER FROM MULTILEVEL WELLS—Continued		
USGS 133	433605112554300	133
Zone 10	433605112554312	133Z10
Zone 7	433605112554308	133Z7
Zone 4	433605112554305	133Z1
Zone 1	433605112554301	133Z10
USGS 134	433611112595800	134
Zone 15	433611112595819	134Z15
Zone 12	433611112595815	134Z12
Zone 9	433611112595811	134Z9
Zone 6	433611112595807	134Z6
Zone 3	433611112595804	134Z3
USGS 135	432753113093600	135
Zone 10	432753113093613	135Z10
Zone 7	432753113093609	135Z7
Zone 4	432753113093605	135Z4
Zone 1	432753113093601	135Z1
USGS 137A	432701113025800	137A
Zone 5	432701113025807	137AZ5
Zone 4	432701113025805	137AZ4
Zone 3	432701113025803	137AZ3
Zone 1	432701113025801	137AZ1

[1]Location of sites shown in Rattray (2019), fig. 7.

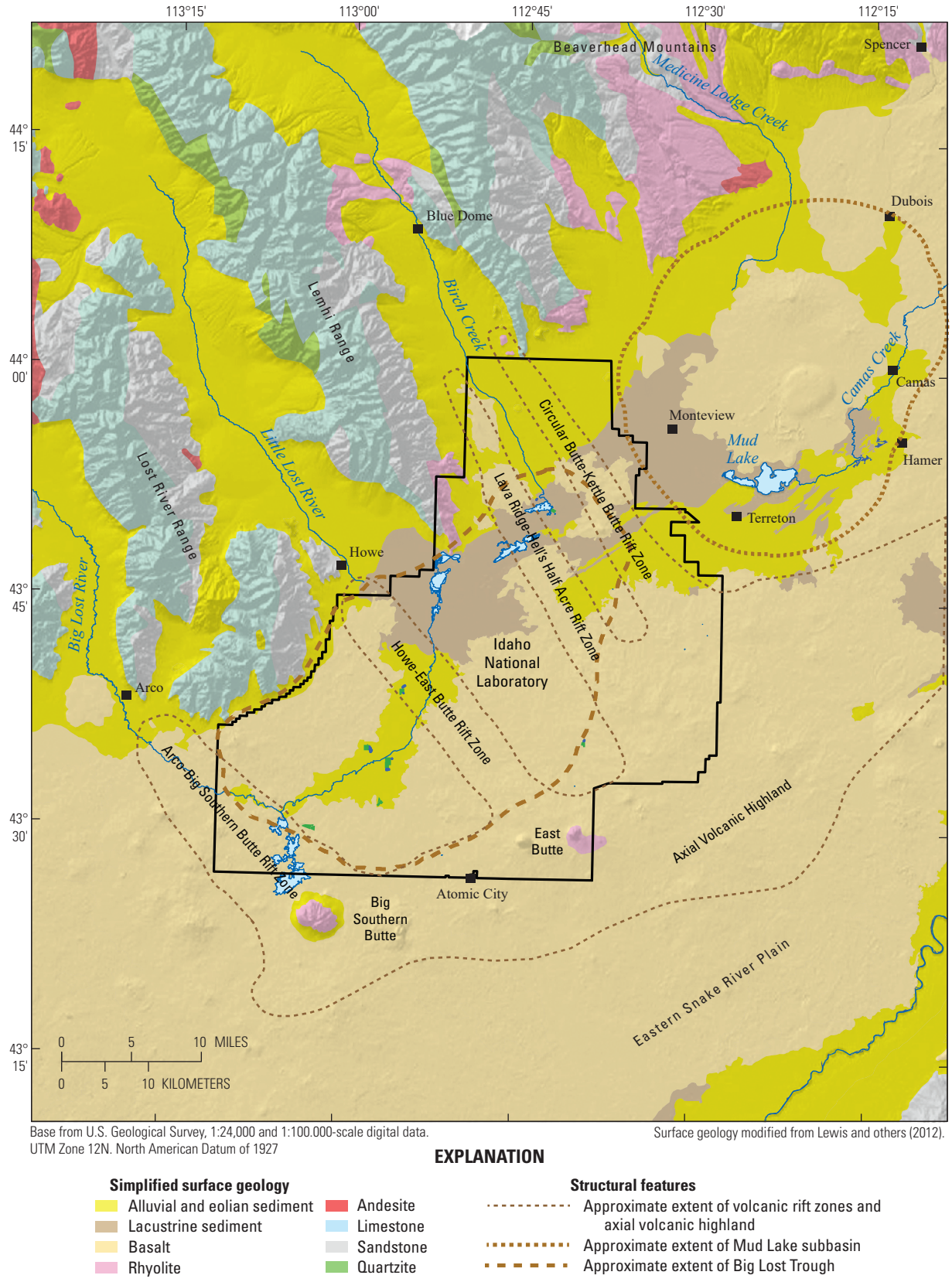

Figure 2. Surface geology and structural features, Idaho National Laboratory and vicinity, eastern Idaho. Surface geology modified from Lewis and others (2012).

- Volcanic vent corridors, which are narrow zones in and near (and parallel to) volcanic rift zones that contain known or inferred volcanic vents, fissures, and dikes (Anderson and others, 1999).
- Caldera boundaries and (potentially) buried faults (Ginsbach, 2013).
- The Big Lost Trough (BLT) and Mud Lake subbasin, long-lived sedimentary basins that were part of Pleistocene Lake Terreton (fig. 2; Gianniny and others, 2002).

Stratigraphic sequences extending from land surface to 1,700 ft below land surface (bls) were mapped in the southwestern part of the INL (fig. 3) using paleomagnetic data, petrography, geophysical logs, and the age of basalt flows (Hodges and Champion, 2016). The stratigraphic sequences were composed of numerous basalt flows,[1] with basalt comprising about 82–97 percent of the stratigraphic sequence and sediment and rhyolite (or felsic rocks) comprising the remainder (North Wind, Inc., 2006; Twining and others, 2008; Hodges and others, 2012). Cross sections indicate that many stratigraphic units have an eastward dip between MLW USGS 135 and USGS 103 (fig. 3*A* and 3*B*) and a southern dip between MLW USGS 132 and USGS 137A (fig. 3*C*) and MLW USGS 131A and USGS 105 (fig. 3*D*). Thus, the actual dip of many stratigraphic units in the southwestern part of the INL may be to the southeast.

Mineralogy

The minerals in the aquifer matrix are the minerals in the basalt and sediment that compose the aquifer and any secondary minerals such as calcite, silica (crystalline, cryptocrystalline, or amorphous), clay, and opaques that are present in the aquifer (Knobel and others, 1997). Basalt at the INL is composed of phenocrysts, a fine-grained matrix, and volcanic glass. Common minerals in basalt, in typical order of abundance, are plagioclase (An_{50-70}), pyroxene (augite to ferroaugite), olivine (Fo_{80-90}), and iron oxides (Kuntz and others, 1992; Knobel and others, 1997).

The most abundant minerals in sediment were quartz, clays, and plagioclase. Calcite and pyroxene were present in lesser amounts and dolomite, olivine, and hematite were present in small amounts (Rightmire and Lewis, 1987; Bartholomay and others, 1989; Bartholomay, 1990; Reed and Bartholomay, 1994). The most abundant clay minerals measured from sedimentary interbeds at the INL were smectites,[2] illite, and kaolinite (Rightmire and Lewis, 1987; Reed and Bartholomay, 1994), with illite generally considered to be of detrital origin (Rightmire, 1984). Gypsum (or anhydrite) was identified in evaporite deposits associated with lacustrine sediment (Blair, 2002; Geslin and others, 2002) and may be present throughout the INL in eolian sediment (Wood and Low, 1988).

Hydrology

Hydrologic features in the southwestern part of the INL are the Big Lost River (BLR), INL spreading areas (fig. 1), and the ESRP aquifer. The BLR is an ephemeral stream on the ESRP, with annual discharge varying significantly (fig. 4) depending on the amount of annual precipitation in the surrounding mountains (Ackerman and others, 2006; Bartholomay, Maimer, and others, 2017). During the past 50 years, mean annual discharge of the BLR onto the INL has fluctuated between zero and greater than 100 cubic feet per second (ft^3/s) in response to short-term (3–8 year) wet-dry climate cycles (fig. 4), with localized, episodic infiltration from the BLR occurring during wet climate cycles (Bennett, 1990). Beginning in 1965, water from the BLR has been periodically diverted to the INL spreading areas for flood control (figs. 1 and 4; streamgage 13132513, INL diversion at head, near Arco, Idaho). Water infiltrates readily from the spreading areas (Nimmo and others, 2002) and some channel locations (Bennett, 1990) and may be rapidly transported vertically and (or) horizontally (owing to low permeability basalt or sediment layers) over long distances through the unsaturated zone.[3]

The ESRP aquifer at the INL is a heterogeneous, unconfined, fractured-basalt aquifer (Ackerman and others, 2006). The aquifer is composed of hundreds of interfingered layers of discontinuous basalt flows and sediment, and the thickness of individual basalt flows is estimated to range from 2 to 100 ft (Anderson and Liszewski, 1997). Depth from land surface to the base of the aquifer in the southwestern part of the INL is estimated to be 2,000–3,000 ft (Ackerman and others, 2006, fig. 14).

The thickness of the unsaturated zone (depth to water from land surface to water table) in the southwestern part of the INL ranges from about 400 ft at Site 4 to about 770 ft at USGS 8 (fig. 1). Perched groundwater zones have formed within the unsaturated zone beneath the ATRC, INTEC, and RWMC owing to localized infiltration of water from the BLR, wastewater infiltration ponds, and facility operational losses such as leaky pipes (U.S. Department of Energy, 2011) in conjunction with localized low permeability geologic materials that impede the downward movement of water (Cecil and others, 1991; Bartholomay and Tucker, 2000; Davis and others, 2013).

[1]The naming of basalt flows herein uses the convention of Hodges and Champion (2016, p. 8), which uses the term "basalt flow" and its definition from the North American Stratigraphic Code to mean the smallest formal lithostratigraphic unit of volcanic rock flows.

[2]The smectite group of clay minerals includes the clay mineral montmorillonite (Deer and others, 1983).

[3]Water infiltrating from the INL spreading areas traveled a horizontal distance of about 4,300 ft in 4 months, a transport rate of about 36 feet per day (Nimmo and others, 2002).

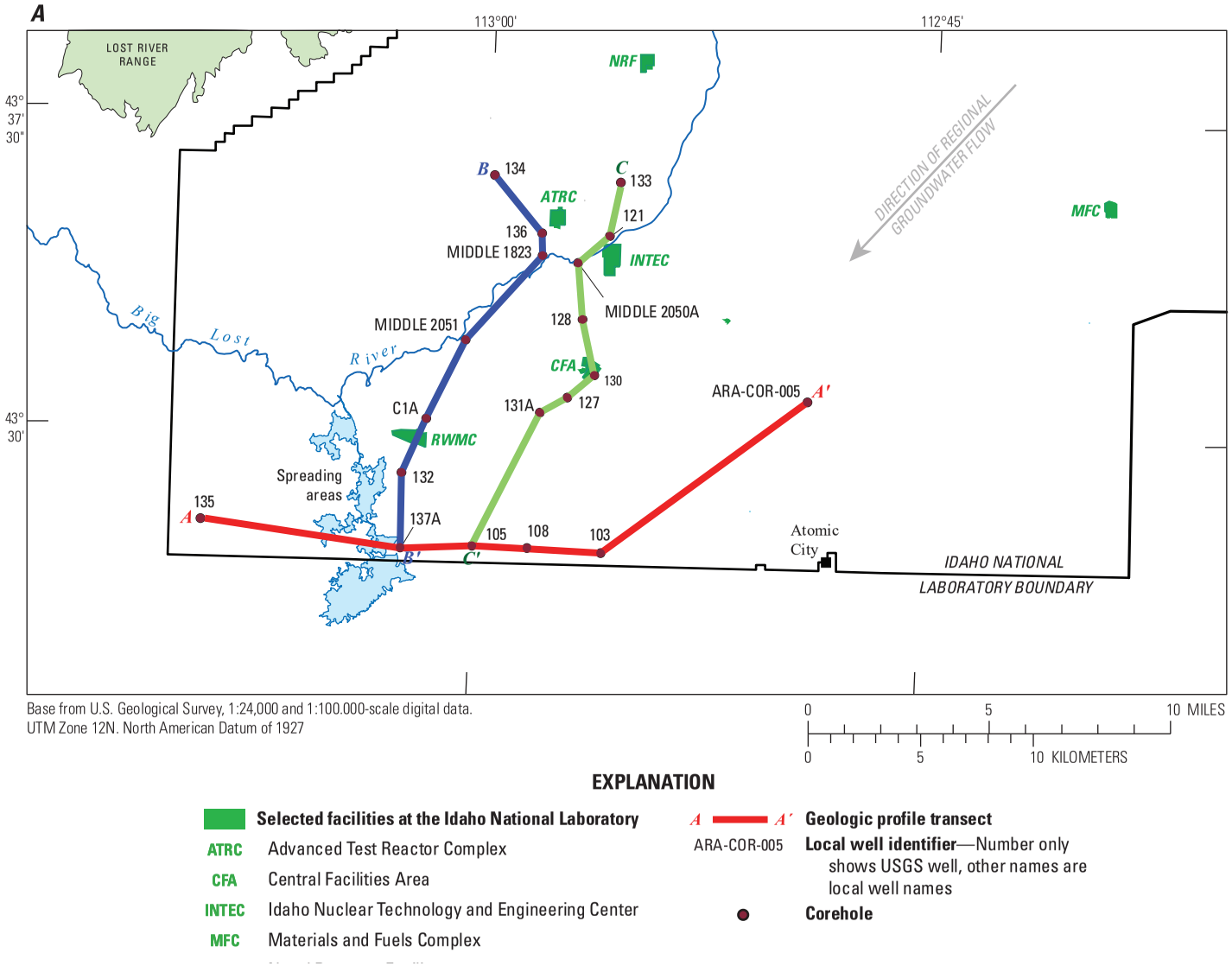

Figure 3. Stratigraphic units, coreholes, multilevel well water sampling zones, and tritium activities in groundwater in the southwestern part of the Idaho National Laboratory, eastern Idaho. *A*. Map showing geologic profile transects and location of coreholes. *B*. Geologic profile transect *A*–*A*′. *C*. Geologic profile transect *B*–*B*′. *D*. Geologic profile transect *C*–*C*′. Figure and unit labels modified from Hodges and Champion (2016).

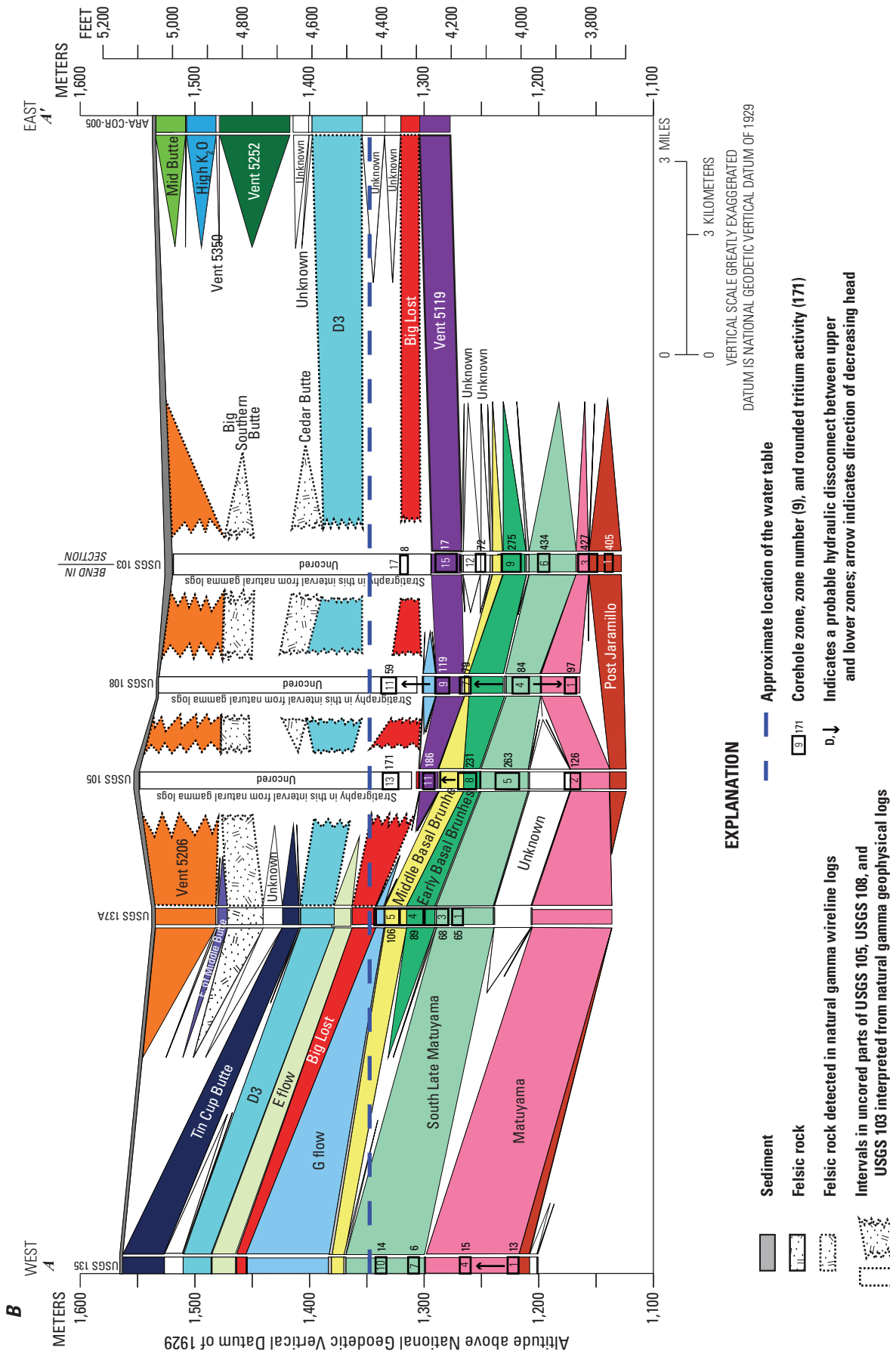

Figure 3.—Continued

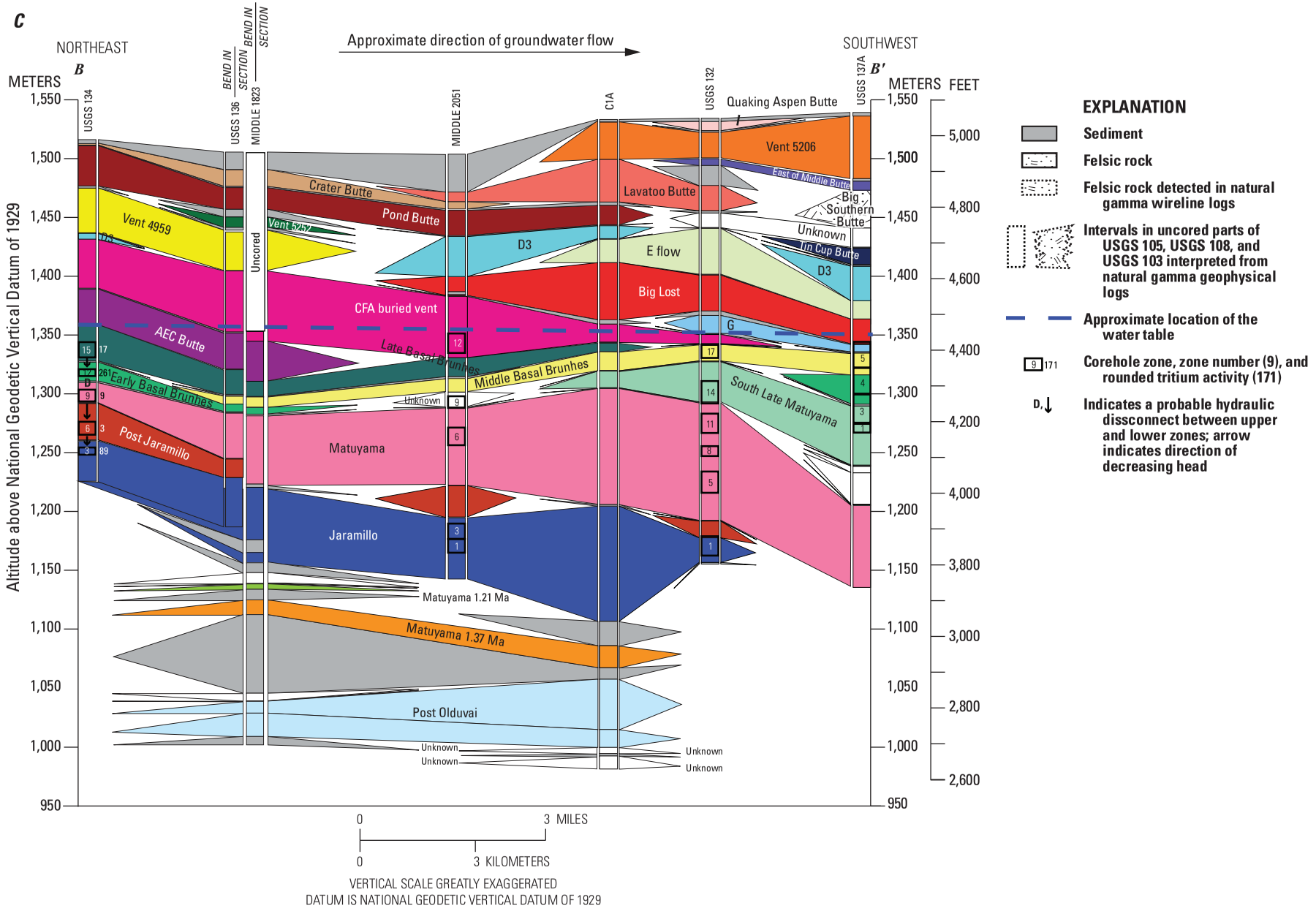

Figure 3.—Continued

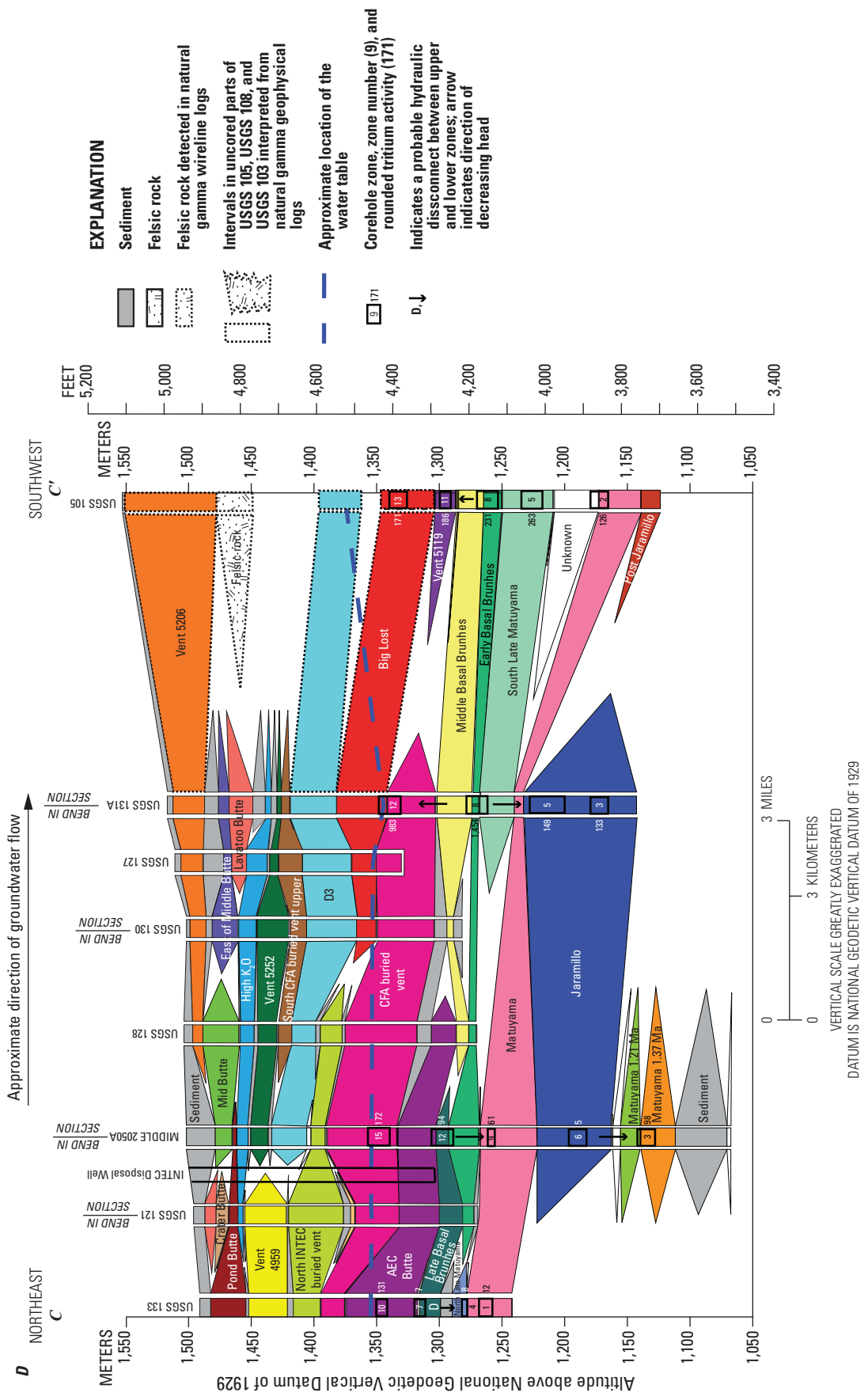

Figure 3.—Continued

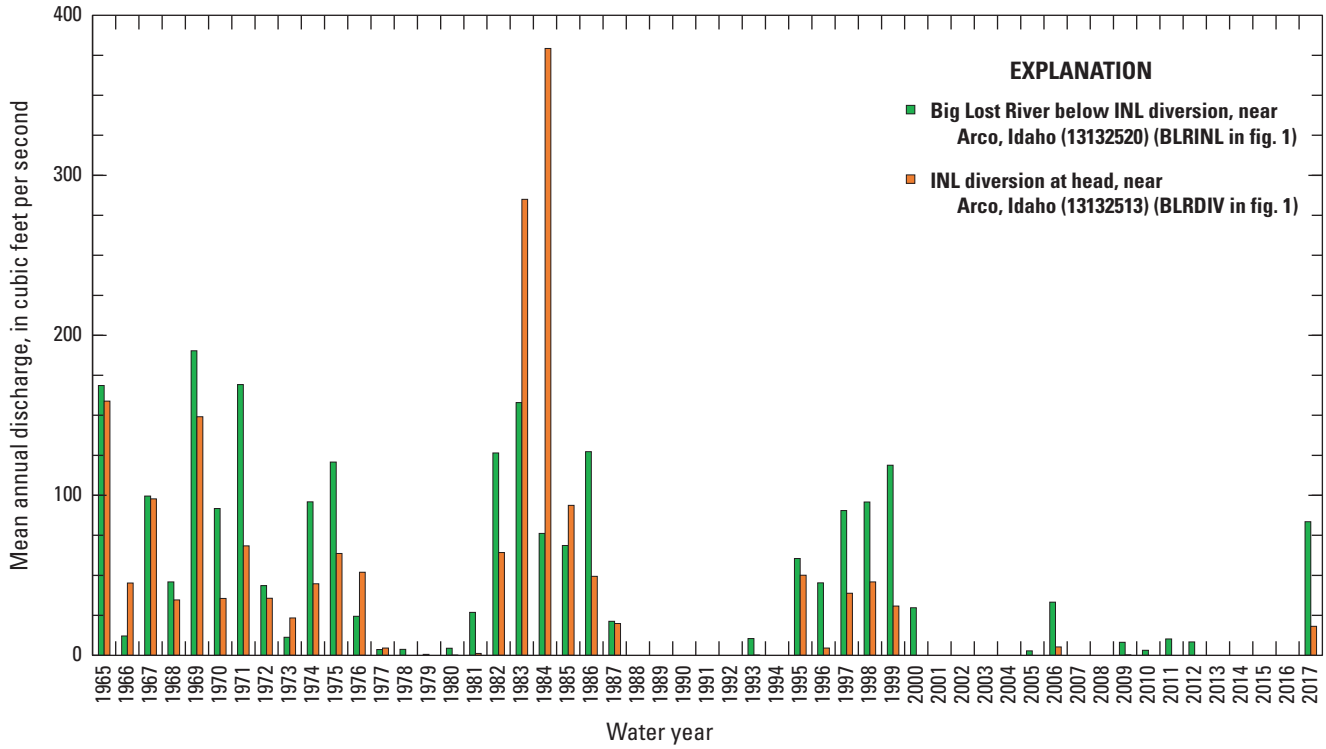

Figure 4. Mean annual discharge at streamgages Big Lost River below Idaho National Laboratory (INL) diversion, near Arco, Idaho, and INL diversion at head, near Arco, Idaho, INL, eastern Idaho. A water year is the 12-month period from October 1, for any given year, through September 30 of the following year. A water year is designated by the calendar year in which it ends. Data are available from the National Water Information System (NWIS) at https://doi.org/10.5066/F7P55KJN (U.S. Geological Survey, 2021).

Potential sources of recharge to the ESRP aquifer in the southwestern part of the INL include:

- Streamflow infiltration from the BLR channel and the INL spreading areas (fig. 1; Bennett, 1990; Busenberg and others, 2001; Nimmo and others, 2002);
- Inflow of **tributary valley groundwater**[4] from the BLR and Little Lost River valleys west and north of the INL (fig. 2; Rattray, 2019);
- Inflow of mountain front groundwater from the Lost River Range (fig. 1) northwest of the INL (Rattray, 2019);
- Inflow of **regional groundwater** from the northeast (fig. 3*A*; Rattray, 2018, 2019);
- Infiltration of precipitation across the surface of the ESRP (Ackerman and others, 2006; Rattray, 2019); and
- Injection or infiltration of wastewater at INL facilities (fig. 1; Davis and others, 2015).

Because of the subhorizontal structure of the fractured basalt aquifer and its large horizontal conductivity (Ackerman and others, 2006), groundwater moves rapidly in the horizontal direction through the rubble- and sediment-filled interflow zones between basalt flows (Whitehead, 1992). In addition, structural features in the aquifer may impede and (or) enhance horizontal and (or) vertical flow. For example, structural features in the southwestern part of the INL include the Arco-Big Southern Butte rift zone (fig. 2) and several volcanic vent corridors (Anderson and others, 1999, fig. 7). Consequently, this part of the INL contains numerous volcanic vents, fissures, and dikes. Volcanic vents and noneruptive fissures are highly porous and may cut across highly permeable zones in and between basalt layers (Anderson and others, 1999), so they may provide conduits for the rapid vertical movement of groundwater. In contrast, dikes have lower permeability, and they may impede the horizontal movement of groundwater if they have a large lateral and vertical extent (Anderson and others, 1999).

Although upward and downward vertical groundwater movement occurs in the aquifer (Mann, 1986; Ackerman and others, 2006; Rattray, 2015), significant vertical movement may be constrained to areas where:

- Vertical fractures are abundant (Whitehead, 1992);

[4]Definitions of water types highlighted in **bold** are presented in the glossary (and may reference data presented in chapters A and B of Professional Paper 1837 [Rattray, 2018, 2019]).

- Vertically oriented fissures and dikes associated with volcanic rift zones or vent corridors are present (Anderson and others, 1999);
- The aquifer thins or thickens (Ackerman and others, 2006, fig. 24); and
- A vertical head gradient forms, where head decreases with depth, in response to either significant amounts of infiltrating water from the BLR or INL spreading areas percolating downward and ponding above the water table; and
- Local confined conditions caused by relatively impermeable basalt and (or) fine-grained sediment layers.

Porosity of the fractured basalt ranges from 0.05 to 0.27, although these values are dependent upon scale and the methods used to determine them (Ackerman and others, 2006). However, porosity and permeability are low in the massive interiors of basalt flows and higher in the interflow zones (Welhan, Clemo, and others, 2002; Welhan, Johannesen, and others, 2002; Ackerman and others, 2006). Hydraulic conductivities (*K*) estimated from single-well aquifer tests indicate that the aquifer in the southwestern part of the INL has extreme heterogeneity in *K*, with *K* ranging more than five orders of magnitude (log *K* of -2.00 to >3.36 feet per day [ft/d]; Rattray, 2018, table 11, Southwest INL Area).

Water-table contours for April 1989 for the ESRP aquifer were interpolated from 481 water-level measurements (water-level data presented in Rattray, 2018, table 1-1) using the natural neighbor technique (Sibson, 1981). Water-table contours (fig. 5) indicate that groundwater in the southwestern part of the INL generally flows south or southwest with a hydraulic gradient of about 3–4 feet per mile (ft/mi). Average linear flow velocities, estimated from model ages of environmental tracers (Busenberg and others, 1993, 2001) and assumed first-arrival times of waste constituents in groundwater (Barraclough and others, 1981; Pittman and others, 1988; Mann and Beasley, 1994; Cecil and others, 2000), range from 3 to 20 ft/d (Ackerman and others, 2006).

Horizontal groundwater-flow directions at different depths in the aquifer were determined from contours of 2012 hydraulic head data from three discrete ranges of aquifer depth (0–106, 247–335, and 520–655 feet below water table) (fig. 6). The contours were prepared from hydraulic head data from all 11 (7 for the 520–655 feet below water table range of aquifer depth)[5] MLW (Twining and Fisher, 2015) using the same technique as for the 1989 water table (fig. 5). The altitude range of hydraulic head data for the three successively deeper discrete ranges of aquifer depth were 4,416.5–4,463.5, 4,416.5–4,457.3, and 4,420.1–4,446.6 feet above the National Geodetic Vertical Datum of 1929.

Hydraulic head decreased from an altitude of 4,450 ft near the ATRC and INTEC to an altitude of 4,420 ft near USGS 132 and the southern boundary of the INL (fig. 6). Although individual contours may not be precise owing to the limited number of hydraulic head data for each discrete range of aquifer depth, the general similarity of the contours between shallow and deep groundwater (figs. 5 and 6) indicates that southern and southwestern groundwater-flow directions probably prevail throughout the upper 700 ft of the aquifer. More specifically, the horizontal flow directions appear to be south to southwest in the eastern part of the study area, south in the western part, and possibly southeast in the western part of the study area at the 247–335 range of aquifer depth. The hydraulic gradient at all three depths was about 4.2 ft/mi between the INTEC and USGS 131A and about 2.3 ft/mi between USGS 131A and USGS 105.

Vertical hydraulic head and water temperature profiles collected from MLW (fig. 7; note variable ranges of hydraulic head and water temperature on *x*-axes) provide information about the three-dimensional hydrogeology of the ESRP aquifer in the southwestern part of the INL. For example, hydraulic head profiles appear to be influenced by lithology, with boreholes located in the Arco-Big Southern Butte rift zone (fig. 2; boreholes USGS 103, USGS 105, USGS 108, USGS 132, USGS 135, and USGS 137A) typically having a smaller range of head (fig. 7) than boreholes located in the BLT (fig. 2; boreholes MIDDLE 2050A, MIDDLE 2051, USGS 131A, USGS 133, USGS 134). The smaller range of head for boreholes in the rift zone was attributed to a high level of vertical connectivity between fractured basalts due to the high concentration of volcanic vents and fissures in the rift zone, whereas the larger range of head for boreholes in the BLT was attributed to the greater quantities of subhorizontally layered sediment that produced confining beds and slow vertical water movement (Fisher and Twining, 2011). Water temperature profiles for boreholes in the BLT increase with depth (fig. 7), indicative of conductive heat flow associated with the geothermal gradient. This temperature profile suggests horizontal groundwater flow is the dominant flow pattern. In contrast, temperature profiles for boreholes in the Arco-Big Southern Butte rift zone are either stable or decrease with depth, indicative of convective heat flow and the downward movement of water (Fisher and Twining, 2011).

Previous Investigations

The USGS, in collaboration with an INL contractor, began installing MLW in 2005. Annual water-quality sampling of MLW commenced at multiple, discrete-depth, sampling zones for selected water-quality constituents that included waste constituents discharged to the aquifer from INL facilities. The annual water-quality sampling program has increased in scope to include MLW installed since 2005. Results from annual sampling of MLW are presented in periodic updates of "Hydrologic Conditions" reports (Davis, 2010; Davis and others, 2013; Bartholomay, Maimer, and others, 2017), reports by U.S. Department of Energy (2007, 2008), Bartholomay and Twining (2010), and Bartholomay and others (2015).

[5]Hydraulic head data were not available for the 520–655 range of aquifer depth from MLW USGS 133, USGS 134, USGS 135, and USGS 137A.

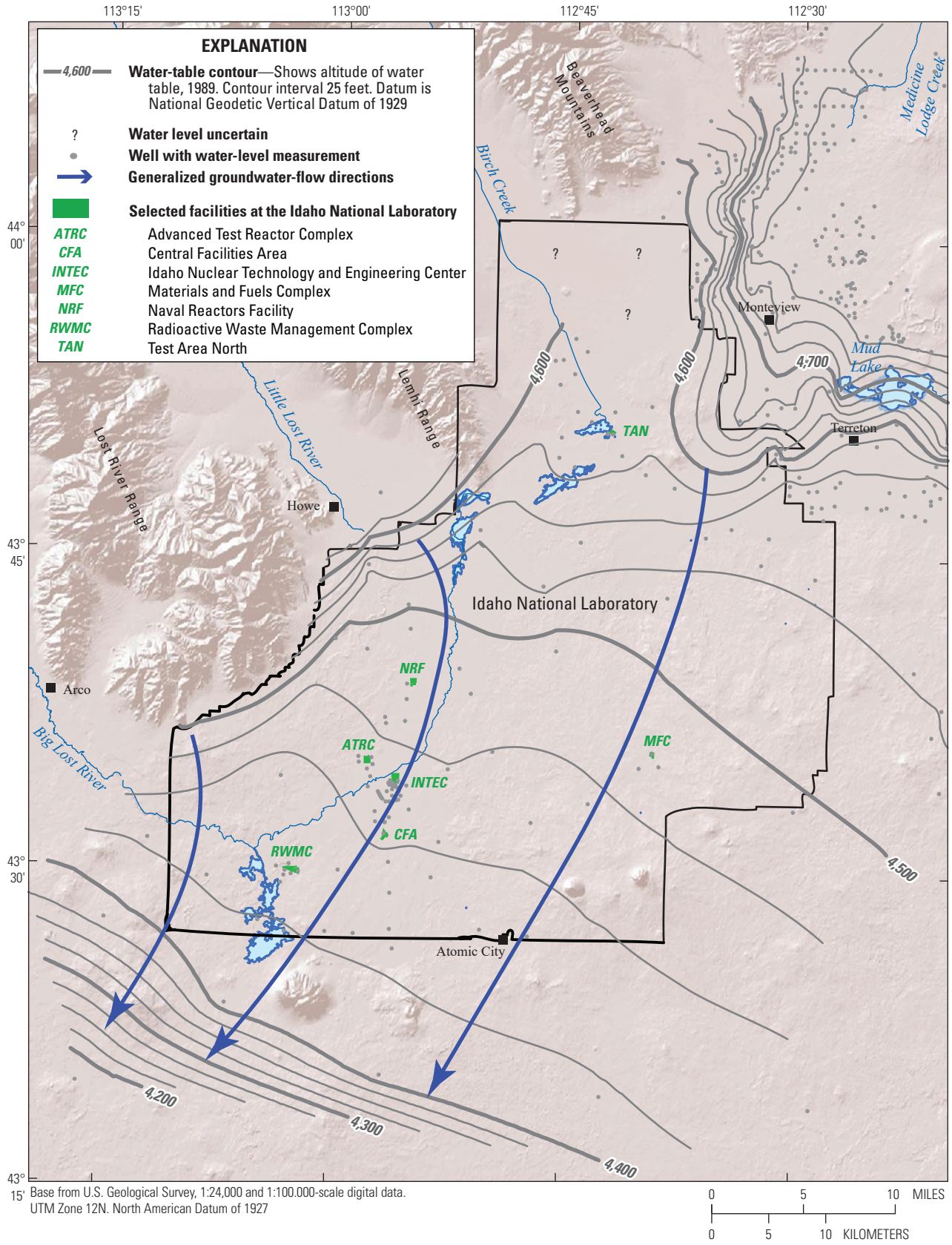

Figure 5. Areal distribution of wells with water-level measurements and 1989 water-table contours, Idaho National Laboratory, eastern Idaho. Figure modified from Rattray (2018, fig. 6).

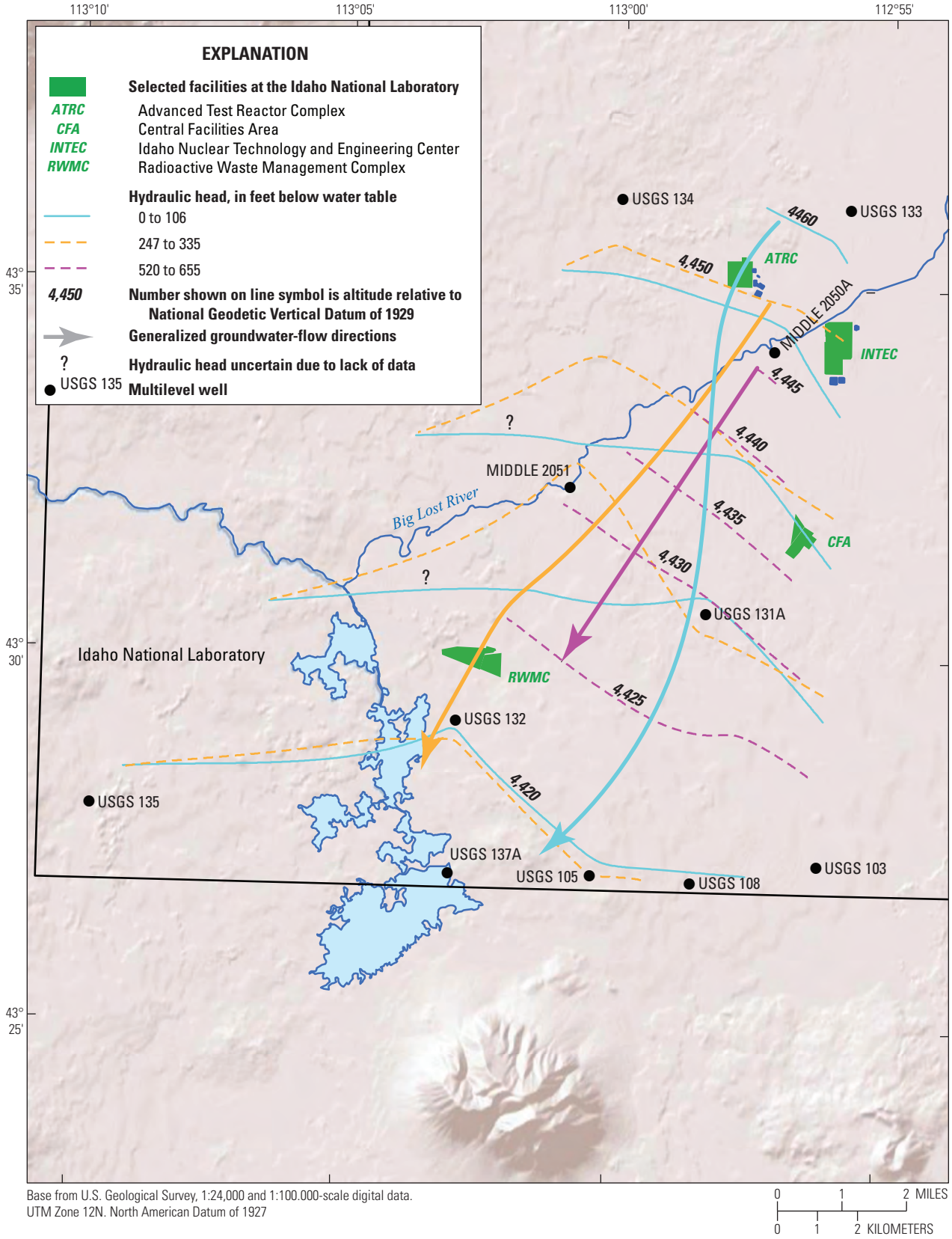

Figure 6. Hydraulic head at three discrete ranges of aquifer depth, Idaho National Laboratory, eastern Idaho, 2012. Location of sites is shown in figure 1. More information is available from the National Water Information System (NWIS) at https://doi.org/10.5066/F7P55KJN (U.S. Geological Survey, 2021).

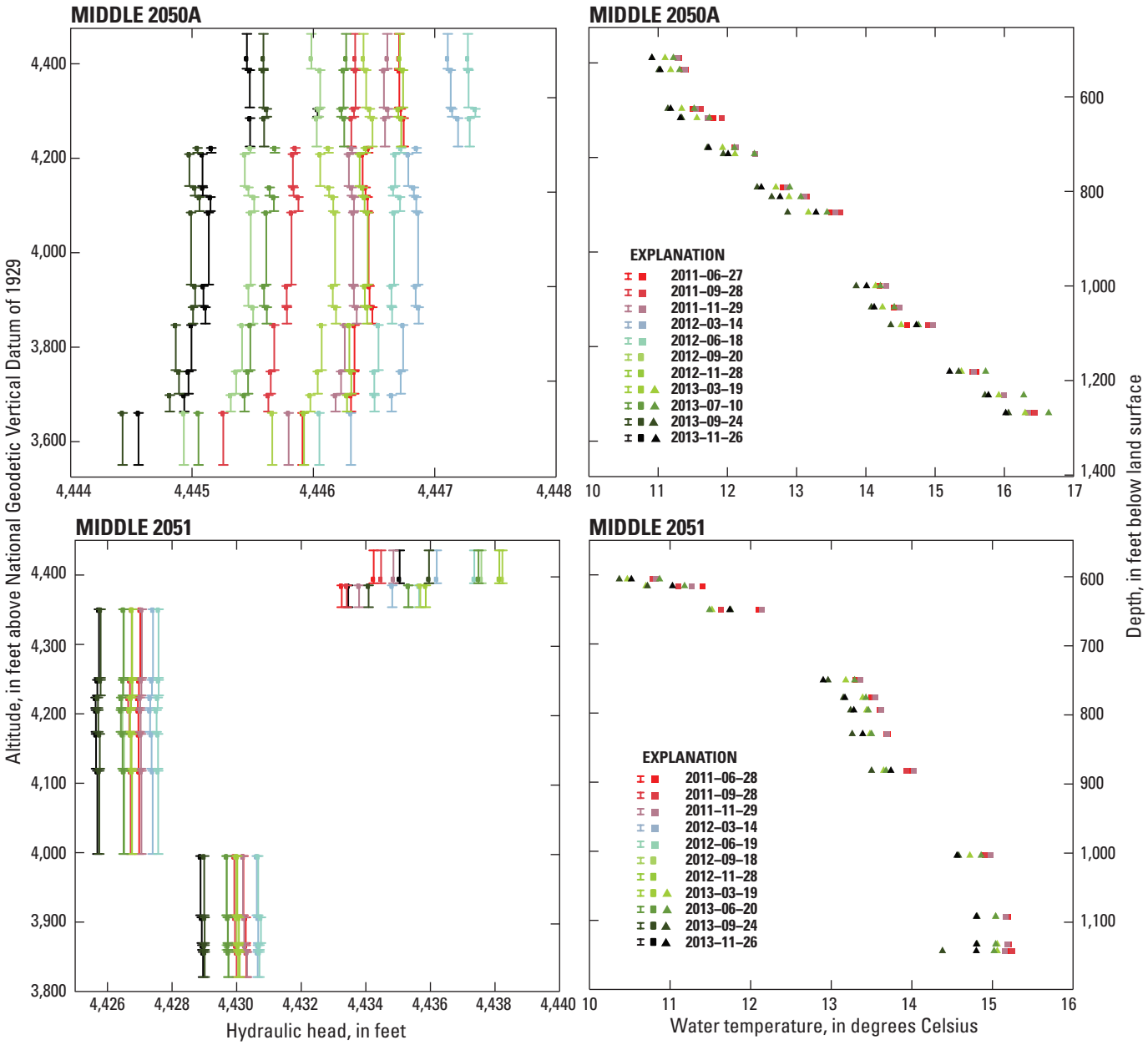

Figure 7. Hydraulic head and water temperature at boreholes MIDDLE 2050A, MIDDLE 2051, USGS 103, USGS 105, USGS 108, USGS 131A, USGS 132, USGS 135, and USGS 137A, Idaho National Laboratory, eastern Idaho. USGS. U.S. Geological Survey. More information is available from the National Water Information System (NWIS) at https://doi.org/10.5066/F7P55KJN (U.S. Geological Survey, 2021).

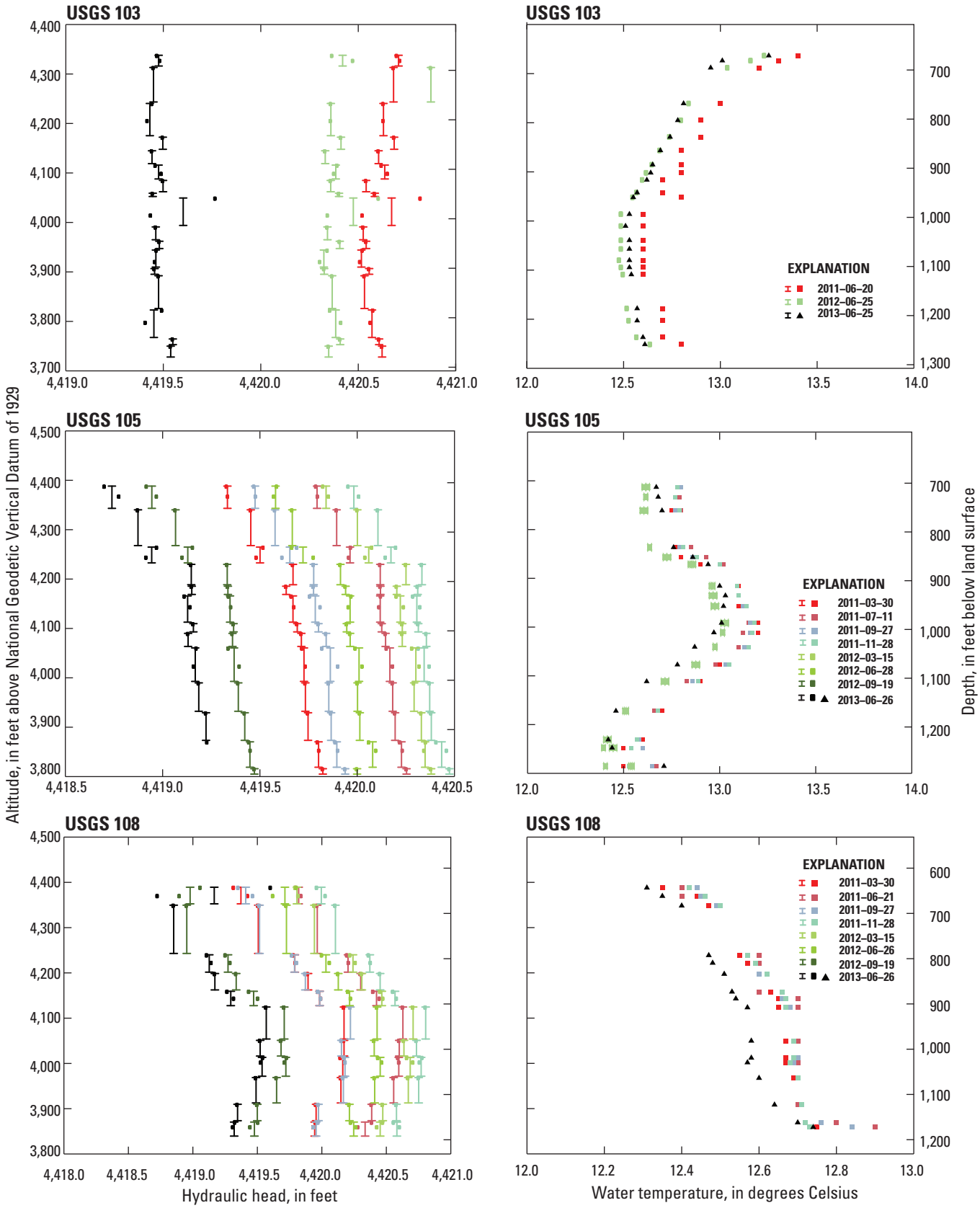

Figure 7.—Continued

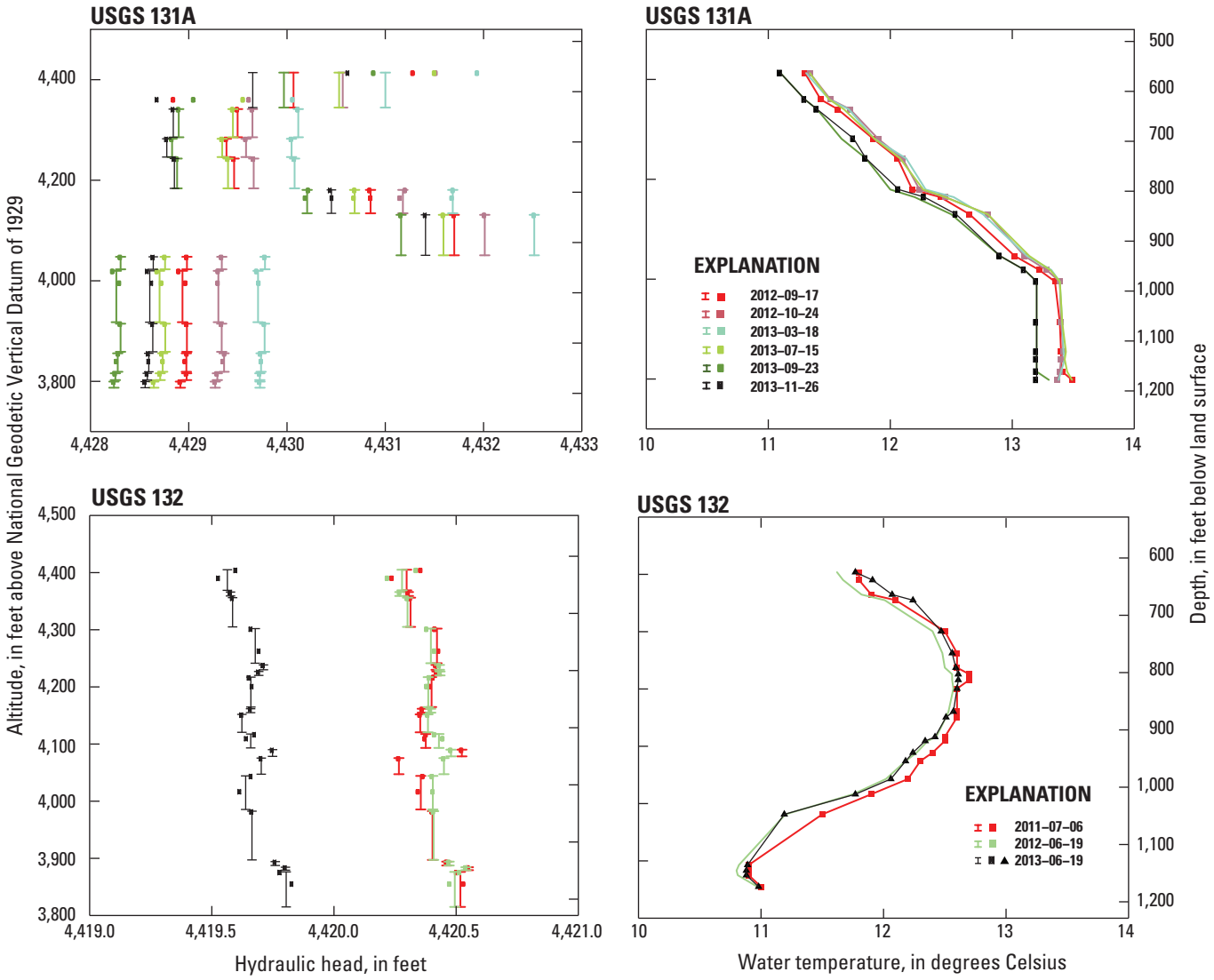

Figure 7.—Continued

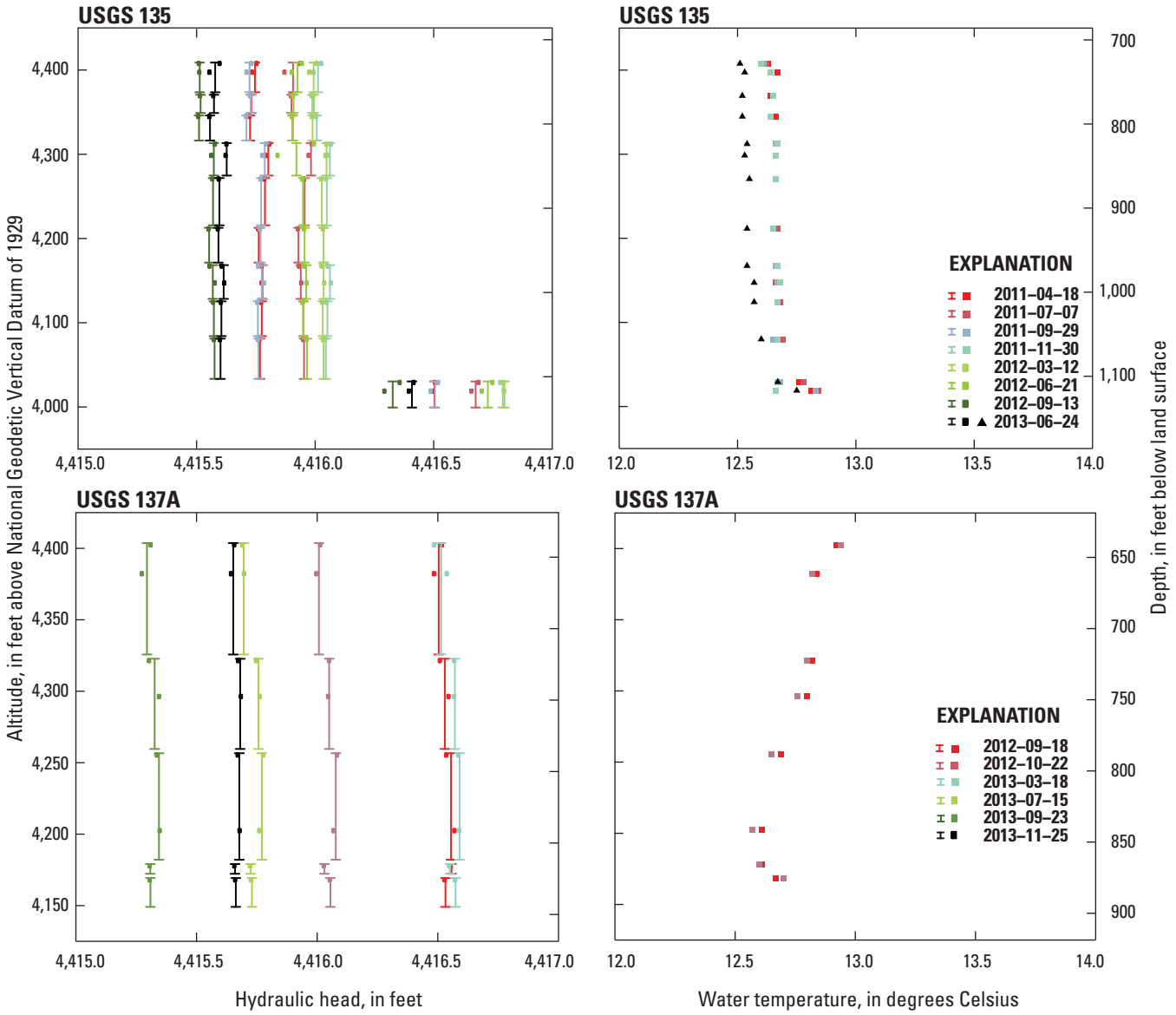

Figure 7.—Continued

Prior to installation of MLW, collection of water-quality samples from discrete aquifer depths were limited in space and time and were analyzed for a limited number of chemical constituents. These water-quality samples and analyses are presented in Peckham (1959), Jones (1961), Olmsted (1962), Robertson and others (1974), Mann (1986), Mann and Cecil (1990), Fromm and others (1994), and U.S. Department of Energy (2004, 2007). Results from these water-quality analyses are briefly summarized in Bartholomay and others (2015).

Water-quality analyses from MLW were used to interpret the sources of water to MLW (Bartholomay and Twining, 2010; Bartholomay and others, 2015). For example, Bartholomay and others (2015) noted the presence of waste constituents in deep water from MLW along the southern boundary of the INL and suggested that this result supports the interpretation of Ackerman and others (2006) that groundwater moves downward in the southwestern part of the INL.

Bartholomay, Hodges, and others (2017) investigated the correlation between basalt stratigraphy and the presence or absence of waste constituents in MLW to better understand the three-dimensional movement of wastewater discharged at site facilities. Wastewater was discharged from the ATRC and INTEC to the land surface or through a disposal well penetrating the upper 150 ft of the aquifer beginning in 1952. Routine use of the disposal well for subsurface discharge of low- and intermediate-level radioactive wastewater at INTEC ended in 1984. Use of the old percolation ponds at ATRC for land surface wastewater disposal ceased in 1993 with the installation of lined evaporation ponds (U.S. Department of Energy, 2011; Bartholomay, Maimer, and others, 2017). As

a result of this discharge of wastewater, waste constituents such as tritium, entered the aquifer beneath these site facilities in the CFA buried vent and (or) the AEC Butte basalt flows (fig. 3*A*, 3*C*, 3*D*). Subsequently, high tritium activities, assumed to be from wastewater (that is, the activities are above the proposed natural background of 75 pCi/L; Orr and others, 1991), were measured in groundwater from MLW downgradient of site facilities. These high tritium activities have been found at significant depths below the water table at MLW, and frequently reside in basalt flows that are stratigraphically beneath the CFA buried vent and (or) the AEC Butte basalt flow (fig. 3*A*, 3*C*, 3*D*). This downward movement of tritium (and wastewater) suggests that there is a significant downward movement of groundwater in the southwestern part of the INL.

Geochemistry Data

Water samples were collected from (1) snowpack, (2) surface water as either a grab sample (Big Lost River below lower Lincoln Blvd Bridge [BLRLB]; fig. 1) or an equal width increments sample (Big Lost River below INL Diversion [BLRINL]), (3) open wells with either dedicated or portable pumps, and (4) multilevel wells (MLW) with bailers. The sampling zone depths at MLW range from the water table to about 748 feet below the water table (ft bwt) (table 2).

Comprehensive sets of water-quality data were collected from MLW on an annual basis for several years following well completion. However, only one set of data from each MLW included a low-level tritium analysis, and these are the datasets included in this report. A comprehensive suite of MLW water-quality data is available from NWIS (U.S. Geological Survey, 2021). The water-quality data collected from MLW were collected during an extended dry climate cycle that began in 2001 (fig. 4), which means that the study area approximated a steady-state system when water samples were collected from MLW. Consequently, any variability between the currently available annual water-quality datasets from specific MLW should be small.

Sample collection followed procedures and guidelines documented in the National Field Manual for the Collection of Water-Quality Data (U.S. Geological Survey, variously dated) and U.S. Geological Survey (USGS) Idaho National Laboratory (INL) Project Office Quality Assurance Plans that were in place at the time of sample collection (Mann, 1996; Knobel and others, 2008; Bartholomay and others, 2014). Additional sample collection information, as well as analytical method information, are presented in reports (and references therein) from which the chemistry data in this report were compiled. These reports are:

- Rightmire and Lewis (1987)—Chemistry data for the snow sample (USGS 83; fig. 1) collected in 1978.
- Knobel and others (1992, 1999)—Chemistry data for a few samples of **contaminated groundwater** (USGS 57, USGS 65, and USGS 88) and **natural groundwater** (USGS 119)[6] collected in 1989 or 1991.
- Busenberg and others (2000)—Chemistry data for surface water, **deep groundwater**, and all other contaminated or natural groundwater samples collected from 1995 to 1997.
- Bartholomay and Twining (2010) and Bartholomay and others (2015)—Chemistry data for samples of **groundwater from MLW** collected from 2008 to 2013.

The chemical and radiochemical constituents included in this report are (1) those needed for geochemical modeling, (2) select waste constituents discharged from site facilities, and (3) select other constituents that provide additional information regarding the source of water at different sites. These constituents include:

- Field parameters (water temperature, pH, specific conductance, and alkalinity) and dissolved gases (dissolved oxygen [O_2] and carbon dioxide [CO_2]) (table 3).
- Major ions (calcium [Ca], magnesium [Mg], sodium [Na], potassium [K], bicarbonate [HCO_3^-], chloride [Cl], sulfate [SO_4^{2-}], fluoride [F], nitrite plus nitrate [NO_3^-; nitrite is unstable in the oxidizing environment of the eastern Snake River Plain (ESRP) aquifer]) and silica (SiO_2) (table 4).
- Dissolved metals (aluminum [Al], barium [Ba], chromium [Cr], iron [Fe], lithium [Li], manganese [Mn], strontium [Sr], and uranium [U]) (table 5).
- Stable isotopes (hydrogen-2/hydrogen-1 [δ^2H],[7] oxygen-18/oxygen-16 [$\delta^{18}O$], and carbon-13/carbon-12 [$\delta^{13}C$]) (table 6).
- The radionuclide tritium [^3H] (table 6).

If only one measurement of either alkalinity or bicarbonate was reported for a water sample, then the value of the other parameter was determined using the conversion factor in Hem (1992, p. 57). The partial pressures of CO_2 were determined from speciation calculations with PHREEQC (Parkhurst and Appelo, 2013).

[6]The tritium analysis for USGS 119 was from a water sample collected in 2017 (table 6).

[7]The delta (δ) notation for isotope ratios is explained in Rattray (2019, appendix 1, eq. 1-1).

Table 2. Site information, including site name, U.S. Geological Survey site number, location, altitude, well depths, open intervals, approximate depths to water, depths of open intervals below water table, water use, aquifer material, hydraulic conductivity, and model layer, Idaho National Laboratory, eastern Idaho.

[Well construction information from Busenberg and others (1998); Idaho Department of Water Resources (2014); Bartholomay, Hodges, and others (2017); and Bartholomay, Maimer, and others (2017). Snow core sample location was a snow grab-sample collected at USGS 83 (Rightmire and Lewis, 1987). **Site name:** Alternate names used in other reports shown in table 1. **Approximate depth of open intervals below water table:** Range of depth may include multiple open intervals. **Estimated hydraulic conductivity:** Data from Anderson and others (1999). **Groundwater from multilevel wells:** Wells USGS 103, USGS 105, and USGS 108 were drilled as open boreholes in 1980 (Fisher and Twining, 2011; Twining and Fisher, 2012) and data from these open boreholes were used in Rattray (2018, 2019). In 2006 and 2008, these wells were deepened and fitted with packer systems at discrete depths (Fisher and Twining, 2011; Twining and Fisher, 2012). Data from these later multilevel wells are used in this report (U.S. Geological Survey, 2021). **Datums:** horizontal, North American Datum of 1927 (NAD 27); vertical, National Geodetic Vertical Datum of 1929 (NGVD 29). **Abbreviations:** CFA, Central Facilities Area; INL, Idaho National Laboratory; na, not applicable; nd, not determined; No., number; RWMC, Radioactive Waste Management Complex; USGS, U.S. Geological Survey. **Units:** ft, foot; ft bls, foot below land surface; ft bwt, foot below water table; ft/d, foot per day]

Site name (fig. 1)	USGS site No.	Latitude (decimal degrees)	Longitude (decimal degrees)	Altitude of land-surface (ft)	Depth of well (ft bls)	Approximate extent of open intervals (ft bls)	Approximate depth to water table (ft bls)	Approximate depth of open intervals below water table (ft bwt)	Water use	Aquifer lithology	Estimated hydraulic conduc-tivity (ft/d as log K)	Model layer
SNOW CORE												
USGS 83	433023112561501	43.506305	–112.938407	4,941	na	na	na	na	na	na	na	na
SURFACE WATER												
Big Lost River below INL Diversion (BLRINL)	13132520	43.515833	–113.081944	5,000	na	na	na	na	na	na	na	na
Big Lost River below lower Lincoln Blvd Bridge (BLRLB)	13132553	43.670740	–112.875829	4,820	na	na	na	na	na	na	na	na
DEEP GROUNDWATER												
EBR1	433051113002601	43.513698	–113.008156	5,024	1,075	600-1,075	586	14–489	Production	Basalt	0.43	1–4
CONTAMINATED GROUNDWATER												
Advanced Test Reactor Complex												
USGS 65	433447112574501	43.579587	–112.963923	4,925	498	456–498	468	0–30	Monitoring	Basalt	2.45	1
Central Facilities Area												
CFA1	433204112562001	43.534304	–112.939588	4,928	639	440–685	479	0–206	Production	Basalt	1.08	1–3
CFA2	433144112563501	43.528779	–112.943916	4,932	681	521–681	471	50–210	Production	Basalt	1.04	1–3
USGS 104	432856112560801	43.482149	–112.936423	4,988	700	550–700	558	0–142	Monitoring	Basalt	–1.03	1, 2
Idaho Nuclear Technology and Engineering Center												
USGS 57	433344112562601	43.562140	–112.941386	4,922	582	477–582	469	8–113	Monitoring	Basalt	2.18	1, 2

Table 2. Site information, including site name, U.S. Geological Survey site number, location, altitude, well depths, open intervals, approximate depths to water, depths of open intervals below water table, water use, aquifer material, hydraulic conductivity, and model layer, Idaho National Laboratory, eastern Idaho.—Continued

[Well construction information from Busenberg and others (1998); Idaho Department of Water Resources (2014); Bartholomay, Hodges, and others (2017); and Bartholomay, Maimer, and others (2017). Snow core sample location was a snow grab-sample collected at USGS 83 (Rightmire and Lewis, 1987). **Site name:** Alternate names used in other reports shown in table 1. **Approximate depth of open intervals below water table:** Range of depth may include multiple open intervals. **Estimated hydraulic conductivity:** Data from Anderson and others (1999). **Groundwater from multilevel wells:** Wells USGS 103, USGS 105, and USGS 108 were drilled as open boreholes in 1980 (Fisher and Twining, 2011; Twining and Fisher, 2012) and data from these open boreholes were used in Rattray (2018, 2019). In 2006 and 2008, these wells were deepened and fitted with packer systems at discrete depths (Fisher and Twining, 2011; Twining and Fisher, 2012). Data from these later multilevel wells are used in this report (U.S. Geological Survey, 2021). **Datums:** horizontal, North American Datum of 1927 (NAD 27); vertical, National Geodetic Vertical Datum of 1929 (NGVD 29). **Abbreviations:** CFA, Central Facilities Area; INL, Idaho National Laboratory; na, not applicable; nd, not determined; No., number; RWMC, Radioactive Waste Management Complex; USGS, U.S. Geological Survey. **Units:** ft, foot; ft bls, foot below land surface; ft bwt, foot below water table; ft/d, foot per day]

Site name (fig. 1)	USGS site No.	Latitude (decimal degrees)	Longitude (decimal degrees)	Altitude of land-surface (ft)	Depth of well (ft bls)	Approximate extent of open intervals (ft bls)	Approximate depth to water table (ft bls)	Approximate depth of open intervals below water table (ft bwt)	Water use	Aquifer lithology	Estimated hydraulic conduc-tivity (ft/d as log K)	Model layer
CONTAMINATED GROUNDWATER —Continued												
Radioactive Waste Management Area												
RWMC M3S	433008113021801	43.502209	–113.039251	5,016	633	603–633	590	13–43	Monitoring	Basalt	nd	1
USGS 88	432940113030201	43.494407	–113.051377	5,021	663	587–635	590	0–45	Monitoring	Basalt	–0.77	1
USGS 120	432919113031501	43.488570	–113.054274	5,040	705	638–705	617	21–88	Monitoring	Basalt	3.36	1
NATURAL GROUNDWATER												
Fire Station 2 (FS2)	433548112562301	43.596573	–112.940553	4,902	510	427–511	420	7–91	Production	Basalt	nd	1
Site 4	433617112542001	43.604907	–112.906385	4,795	495	422–497	401	21–96	Monitoring	Basalt	nd	1
Site 19	433522112582101	43.589440	–112.973468	4,926	860	472–842	471	1–371	Monitoring	Basalt	2.23	1–4
USGS 8	433121113115801	43.522269	–113.200122	5,195	812	782–812	770	12–42	Monitoring	Basalt	2.84	1
USGS 83	433023112561501	43.506305	–112.938407	4,941	752	516–752	501	15–251	Monitoring	Basalt	0.58	1–3
USGS 86	432935113080001	43.492903	–113.134568	5,077	691	48–691	652	0–39	Monitoring	Basalt	0.81	1
USGS 107	432942112532801	43.494913	–112.891808	4,918	690	270–690	482	0–208	Monitoring	Basalt	2.52	1–3
USGS 119	432945113023401	43.495632	–113.043524	5,032	705	639–705	685	0–20	Monitoring	Basalt	–2.00	1
GROUNDWATER FROM MULTILEVEL WELLS												
MIDDLE 2050A												
Zone 15	433409112570515	43.569207	–112.952325	4,928	1,378	465–539	479	0–60	Monitoring	Basalt	nd	1
Zone 12	433409112570512	–	–	–	–	643–703	–	164–224	–	Basalt	nd	2, 3
Zone 9	433409112570509	–	–	–	–	790–807	–	311–328	–	Basalt	nd	4
Zone 6	433409112570506	–	–	–	–	999–1,041	–	520–562	–	Basalt	nd	5
Zone 3	433409112570503	–	–	–	–	1,180–1,227	–	701–748	–	Basalt	nd	5

Table 2. Site information, including site name, U.S. Geological Survey site number, location, altitude, well depths, open intervals, approximate depths to water, depths of open intervals below water table, water use, aquifer material, hydraulic conductivity, and model layer, Idaho National Laboratory, eastern Idaho.—Continued

[Well construction information from Busenberg and others (1998); Idaho Department of Water Resources (2014); Bartholomay, Hodges, and others (2017); and Bartholomay, Maimer, and others (2017). Snow core sample location was a snow grab-sample collected at USGS 83 (Rightmire and Lewis, 1987). **Site name:** Alternate names used in other reports shown in table 1. **Approximate depth of open intervals below water table:** Range of depth may include multiple open intervals. **Estimated hydraulic conductivity:** Data from Anderson and others (1999). **Groundwater from multilevel wells:** Wells USGS 103, USGS 105, and USGS 108 were drilled as open boreholes in 1980 (Fisher and Twining, 2011; Twining and Fisher, 2012) and data from these open boreholes were used in Rattray (2018, 2019). In 2006 and 2008, these wells were deepened and fitted with packer systems at discrete depths (Fisher and Twining, 2011; Twining and Fisher, 2012). Data from these later multilevel wells are used in this report (U.S. Geological Survey, 2021). **Datums:** horizontal, North American Datum of 1927 (NAD 27); vertical, National Geodetic Vertical Datum of 1929 (NGVD 29). **Abbreviations:** CFA, Central Facilities Area; INL, Idaho National Laboratory; na, not applicable; nd, not determined; No., number; RWMC, Radioactive Waste Management Complex; USGS, U.S. Geological Survey. **Units:** ft, foot; ft bls, foot below land surface; ft bwt, foot below water table; ft/d, foot per day]

Site name (fig. 1)	USGS site No.	Latitude (decimal degrees)	Longitude (decimal degrees)	Altitude of land-surface (ft)	Depth of well (ft bls)	Approximate extent of open intervals (ft bls)	Approximate depth to water table (ft bls)	Approximate depth of open intervals below water table (ft bwt)	Water use	Aquifer lithology	Estimated hydraulic conduc-tivity (ft/d as log K)	Model layer
GROUNDWATER FROM MULTILEVEL WELLS—Continued												
MIDDLE 2051												
Zone 12	433217113004912	43.537943	–113.014548	4,997	1,179	562–609	564	0–45	Monitoring	Basalt	nd	1
Zone 9	433217113004909	–	–	–	–	748–771	–	184–207	–	Basalt	nd	2, 3
Zone 6	433217113004906	–	–	–	–	826–876	–	262–312	–	Basalt	nd	3,4
Zone 3	433217113004903	–	–	–	–	1,090–1,128	–	526–564	–	Basalt	nd	5
Zone 1	433217113004901	–	–	–	–	1,140–1,176	–	576–612	–	Basalt	nd	5
USGS 103												
Zone 17	432714112560723	43.453678	–112.93598	5,007	1,279	670–691	585	85–106	Monitoring	Basalt	2.94	1, 2
Zone 15	432714112560720	–	–	–	–	767–832	–	182–247	–	Basalt	nd	2, 3
Zone 12	432714112560716	–	–	–	–	892–920	–	307–335	–	Basalt	nd	4
Zone 9	432714112560712	–	–	–	–	958–1,014	–	373–429	–	Basalt	nd	4
Zone 6	432714112560708	–	–	–	–	1,063–1,098	–	478–513	–	Basalt	nd	4, 5
Zone 3	432714112560704	–	–	–	–	1,184–1,240	–	599–655	–	Basalt	nd	5
Zone 1	432714112560702	–	–	–	–	1,257–1,279	–	672–694	–	Basalt	nd	5
USGS 105												
Zone 13	432703113001818	43.450852	–113.005770	5,095	1,290	707–752	673	34–79	Monitoring	Basalt	2.80	1
Zone 11	432703113001815	–	–	–	–	830–862	–	157–189	–	Basalt	nd	2
Zone 8	432703113001811	–	–	–	–	929–982	–	256–309	–	Basalt	nd	3, 4
Zone 5	432703113001807	–	–	–	–	1,035–1,102	–	362–429	–	Basalt	nd	4
Zone 2	432703113001803	–	–	–	–	1,225–1,276	–	552–603	–	Basalt	nd	5

Table 2. Site information, including site name, U.S. Geological Survey site number, location, altitude, well depths, open intervals, approximate depths to water, depths of open intervals below water table, water use, aquifer material, hydraulic conductivity, and model layer, Idaho National Laboratory, eastern Idaho.—Continued

[Well construction information from Busenberg and others (1998); Idaho Department of Water Resources (2014); Bartholomay, Hodges, and others (2017); and Bartholomay, Maimer, and others (2017). Snow core sample location was a snow grab-sample collected at USGS 83 (Rightmire and Lewis, 1987). **Site name:** Alternate names used in other reports shown in table 1. **Approximate depth of open intervals below water table:** Range of depth may include multiple open intervals. **Estimated hydraulic conductivity:** Data from Anderson and others (1999). **Groundwater from multilevel wells:** Wells USGS 103, USGS 105, and USGS 108 were drilled as open boreholes in 1980 (Fisher and Twining, 2011; Twining and Fisher, 2012) and data from these open boreholes were used in Rattray (2018, 2019). In 2006 and 2008, these wells were deepened and fitted with packer systems at discrete depths (Fisher and Twining, 2011; Twining and Fisher, 2012). Data from these later multilevel wells are used in this report (U.S. Geological Survey, 2021). **Datums:** horizontal, North American Datum of 1927 (NAD 27); vertical, National Geodetic Vertical Datum of 1929 (NGVD 29). **Abbreviations:** CFA, Central Facilities Area; INL, Idaho National Laboratory; na, not applicable; nd, not determined; No., number; RWMC, Radioactive Waste Management Complex; USGS, U.S. Geological Survey. **Units:** ft, foot; ft bls, foot below land surface; ft bwt, foot below water table; ft/d, foot per day]

Site name (fig. 1)	USGS site No.	Latitude (decimal degrees)	Longitude (decimal degrees)	Altitude of land-surface (ft)	Depth of well (ft bls)	Approximate extent of open intervals (ft bls)	Approximate depth to water table (ft bls)	Approximate depth of open intervals below water table (ft bwt)	Water use	Aquifer lithology	Estimated hydraulic conduc-tivity (ft/d as log K)	Model layer
GROUNDWATER FROM MULTILEVEL WELLS—Continued												
USGS 108												
Zone 11	432659112582616	43.449572	–112.974813	5,031	1,194	642–679	612	30–67	Monitoring	Basalt	2.98	1
Zone 9	432659112582613	–	–	–	–	791–830	–	179–218	–	Basalt	nd	2, 3
Zone 7	432659112582610	–	–	–	–	872–904	–	260–292	–	Basalt	nd	3
Zone 4	432659112582606	–	–	–	–	1,018–1,060	–	406–448	–	Basalt	nd	5
Zone 1	432659112582602	–	–	–	–	1,161–1,194	–	549–582	–	Basalt	nd	5
USGS 131A												
Zone 12	433036112581815	43.510194	–112.971861	4,989	1,189	562–632	546	16–86	Monitoring	Basalt	nd	1
Zone 8	433036112581810	–	–	–	–	795–842	–	249–296	–	Basalt	nd	3
Zone 5	433036112581806	–	–	–	–	956–1,058	–	410–512	–	Basalt	nd	4
Zone 3	433036112581803	–	–	–	–	1,120–1,157	–	574–611	–	Basalt	nd	5
USGS 132												
Zone 17	432906113025022	43.485096	–113.048313	5,029	1,214	624–660	607	17–53	Monitoring	Basalt	nd	1
Zone 14	432906113025018	–	–	–	–	727–787	–	120–180	–	Basalt	nd	2
Zone 11	432906113025014	–	–	–	–	812–864	–	205–257	–	Basalt	nd	3
Zone 8	432906113025010	–	–	–	–	911–935	–	304–328	–	Basalt	nd	4
Zone 5	432906113025006	–	–	–	–	984–1,043	–	377–436	–	Basalt	nd	4
Zone 1	432906113025001	–	–	–	–	1,152–1,214	–	545–607	–	Basalt	nd	5
USGS 133												
Zone 10	433605112554312	43.601435	–112.929664	4,890	766	448–480	431	17–49	Monitoring	Basalt	nd	1
Zone 7	433605112554308	–	–	–	–	556–591	–	125–160	–	Basalt	nd	2

Table 2. Site information, including site name, U.S. Geological Survey site number, location, altitude, well depths, open intervals, approximate depths to water, depths of open intervals below water table, water use, aquifer material, hydraulic conductivity, and model layer, Idaho National Laboratory, eastern Idaho.—Continued

[Well construction information from Busenberg and others (1998); Idaho Department of Water Resources (2014); Bartholomay, Hodges, and others (2017); and Bartholomay, Maimer, and others (2017). Snow core sample location was a snow grab-sample collected at USGS 83 (Rightmire and Lewis, 1987). **Site name:** Alternate names used in other reports shown in table 1. **Approximate depth of open intervals below water table:** Range of depth may include multiple open intervals. **Estimated hydraulic conductivity:** Data from Anderson and others (1999). **Groundwater from multilevel wells:** Wells USGS 103, USGS 105, and USGS 108 were drilled as open boreholes in 1980 (Fisher and Twining, 2011; Twining and Fisher, 2012) and data from these open boreholes were used in Rattray (2018, 2019). In 2006 and 2008, these wells were deepened and fitted with packer systems at discrete depths (Fisher and Twining, 2011; Twining and Fisher, 2012). Data from these later multilevel wells are used in this report (U.S. Geological Survey, 2021). **Datums:** horizontal, North American Datum of 1927 (NAD 27); vertical, National Geodetic Vertical Datum of 1929 (NGVD 29). **Abbreviations:** CFA, Central Facilities Area; INL, Idaho National Laboratory; na, not applicable; nd, not determined; No., number; RWMC, Radioactive Waste Management Complex; USGS, U.S. Geological Survey. **Units:** ft, foot; ft bls, foot below land surface; ft bwt, foot below water table; ft/d, foot per day]

Site name (fig. 1)	USGS site No.	Latitude (decimal degrees)	Longitude (decimal degrees)	Altitude of land-surface (ft)	Depth of well (ft bls)	Approximate extent of open intervals (ft bls)	Approximate depth to water table (ft bls)	Approximate depth of open intervals below water table (ft bwt)	Water use	Aquifer lithology	Estimated hydraulic conductivity (ft/d as log K)	Model layer
GROUNDWATER FROM MULTILEVEL WELLS—Continued												
Zone 4	433605112554305	–	–	–	–	686–696	–	255–265	–	Basalt	nd	3
Zone 1	433605112554301	–	–	–	–	725–766	–	294–335	–	Basalt	nd	4
USGS 134												
Zone 15	433611112595819	43.603003	–113.000352	4,969	887	554–590	513	41–77	Monitoring	Basalt	nd	1
Zone 12	433611112595815	–	–	–	–	639–652	–	126–139	–	Basalt	nd	2
Zone 9	433611112595811	–	–	–	–	691–720	–	178–207	–	Basalt	nd	2, 3
Zone 6	433611112595807	–	–	–	–	782–818	–	269–305	–	Basalt	nd	3, 4
Zone 3	433611112595804	–	–	–	–	846–868	–	333–355	–	Basalt	nd	4
USGS 135												
Zone 10	432753113093613	43.464759	–113.160730	5,136	1,137	727–762	717	10–45	Monitoring	Basalt	nd	1
Zone 7	432753113093609	–	–	–	–	823–861	–	106–144	–	Basalt	nd	2
Zone 4	432753113093605	–	–	–	–	968–1,008	–	251–291	–	Basalt	nd	3
Zone 1	432753113093601	–	–	–	–	1,106–1,137	–	389–420	–	Basalt	nd	4
USGS 137A												
Zone 5	432701113025807	43.450760	–113.049615	5,054	895	640–718	628	12–90	Monitoring	Basalt	2.78	1
Zone 4	432701113025805	–	–	–	–	721–784	–	93–156	–	Basalt	nd	2
Zone 3	432701113025803	–	–	–	–	787–862	–	159–234	–	Basalt	nd	2, 3
Zone 1	432701113025801	–	–	–	–	875–895	–	247–267	–	Basalt	nd	3

Table 3. Measurements of field parameters and calculated partial pressure of carbon dioxide for water-quality analyses from precipitation (snow core), surface water, and groundwater, Idaho National Laboratory, eastern Idaho.

[Data from Bartholomay and Twining (2010), Bartholomay and others (2015), Bartholomay, Maimer, and others (2017), and Rattray (2018). Snow core sample location was a snow grab-sample collected at USGS 83 (Rightmire and Lewis, 1987). **Site name:** Alternate names used in other reports shown in table 6. **Approximate depth of open intervals below water table:** Range of depth may include multiple open intervals. **Dissolved oxygen:** Dissolved oxygen (O_2) values followed by an E indicate that no measurement of O_2 was made on the date shown and that the O_2 value in the table was estimated as the mean value of all O_2 measurements for that site in U.S. Geological Survey National Water Information System (NWIS) through December 2015 (U.S. Geological Survey, 2021). **Carbon dioxide:** Calculated with PHREEQC (Parkhurst and Appelo, 2013). **Abbreviations:** CFA, Central Facilities Area; Idaho National Laboratory; na, not applicable; nd, not determined; RWMC, Radioactive Waste Management Complex; USGS, U.S. Geological Survey. **Units:** ft bwt, foot below water table; mm-dd-yyyy, month, day, year; pH, negative base-10 logarithm of the hydrogen ion activity; µS/cm, microsiemen per centimeter at 25 degrees °C; mg/L, milligram per liter; $CaCO_3$, calcium carbonate; $LogPCO_2$, base-10 logarithm of carbon dioxide partial pressure. **Symbols:** °C, temperature, in degrees Celsius; %, percent]

Site name (fig. 1)	Approximate depth of open intervals below water table (ft bwt)	Date sampled (mm-dd-yyyy)	Water temperature (°C)	pH (units)	Specific conductance (µS/cm at 25 °C)	Alkalinity (mg/L as $CaCO_3$)	Dissolved oxygen (mg/L)	Carbon dioxide ($LogPCO_2$)
SNOW CORE								
USGS 83	na	02-02-1978	Frozen	5.0	16	nd	nd	–3.0
SURFACE WATER								
Big Lost River below INL Diversion (BLRINL)	na	06-02-1995	15.0	8.4	262	108	7.2	–3.4
Big Lost River below lower Lincoln Blvd Bridge (BLRLB)	na	06-19-1995	12.5	7.7	[1]337	101	7.3E	–2.7
DEEP GROUNDWATER								
EBR 1	14–489	10-16-1996	18.8	8.2	279	116	6.7	–3.1
CONTAMINATED GROUNDWATER								
Advanced Test Reactor Complex								
USGS 65	0–30	05-16-1991	14.0	8.0	600	123	8.6	–2.9
Central Facilities Area								
CFA 1	0–206	07-16-1996	12.3	7.9	567	131	9.5	–2.8
CFA 2	50–210	07-16-1996	12.1	7.9	745	122	8.4	–2.8
USGS 104	0–142	07-15-1996	12.3	8.1	327	128	9.0	–3.0
Idaho Nuclear Technology and Engineering Center								
USGS 57	8–113	05-13-1991	14.5	7.8	674	121	8.3	–2.7
Radioactive Waste Management Area								
RWMC M3S	13–43	07-22-1996	13.7	8.1	368	144	7.4E	–2.9
USGS 88	0–45	04-04-1989	14.0	8.2	600	93	8.5	–3.2
USGS 120	21–88	07-17-1996	12.0	8.2	444	153	10.2	–3.0

Table 3. Measurements of field parameters and calculated partial pressure of carbon dioxide for water-quality analyses from precipitation (snow core), surface water, and groundwater, Idaho National Laboratory, eastern Idaho.—Continued

[Data from Bartholomay and Twining (2010), Bartholomay and others (2015), Bartholomay, Maimer, and others (2017), and Rattray (2018). Snow core sample location was a snow grab-sample collected at USGS 83 (Rightmire and Lewis, 1987). **Site name:** Alternate names used in other reports shown in table 6. **Approximate depth of open intervals below water table:** Range of depth may include multiple open intervals. **Dissolved oxygen:** Dissolved oxygen (O_2) values followed by an E indicate that no measurement of O_2 was made on the date shown and that the O_2 value in the table was estimated as the mean value of all O_2 measurements for that site in U.S. Geological Survey National Water Information System (NWIS) through December 2015 (U.S. Geological Survey, 2021). **Carbon dioxide:** Calculated with PHREEQC (Parkhurst and Appelo, 2013). **Abbreviations:** CFA, Central Facilities Area; INL, Idaho National Laboratory; na, not applicable; nd, not determined; RWMC, Radioactive Waste Management Complex; USGS, U.S. Geological Survey. **Units:** ft bwt, foot below water table; mm-dd-yyyy, month, day, year; pH, negative base-10 logarithm of the hydrogen ion activity; µS/cm, microsiemen per centimeter at 25 degrees °C; mg/L, milligram per liter; $CaCO_3$, calcium carbonate; $LogPCO_2$, base-10 logarithm of carbon dioxide partial pressure. **Symbols:** °C, temperature, in degrees Celsius; %, percent]

Site name (fig. 1)	Approximate depth of open intervals below water table (ft bwt)	Date sampled (mm-dd-yyyy)	Water temperature (°C)	pH (units)	Specific conductance (µS/cm at 25 °C)	Alkalinity (mg/L as $CaCO_3$)	Dissolved oxygen (mg/L)	Carbon dioxide ($LogPCO_2$)
NATURAL GROUNDWATER								
Fire Station 2	7-91	10-16-1996	11.3	8.0	447	167	9.1	–2.8
Site 4	21–96	10-16-1996	11.3	8.1	369	157	7.5E	–2.9
Site 19	1–371	07-16-1996	15.2	8.0	387	164	8.1	–2.8
USGS 8	12–42	10-08-1996	11.4	8.0	376	165	8.0	–2.8
USGS 83	15–251	04-11-1995	11.8	8.2	282	101	6.1	–3.2
USGS 86	0–39	10-11-1996	10.0	8.3	332	109	11.4	–3.3
USGS 107	0–208	10-09-1996	14.9	8.1	399	144	9.1	–2.9
USGS 119	0–20	04-03-1989	15.0	8.3	298	94	8.4	–3.3
GROUNDWATER FROM MULTILEVEL WELLS								
MIDDLE 2050A								
Zone 15	0–60	08-27-2008	11.8	7.7	421	164	7.6	–2.5
Zone 12	164–224	08-27-2008	12.9	7.7	351	149	9.8	–2.5
Zone 9	311–328	08-26-2008	13.1	7.7	398	170	7.8	–2.5
Zone 6	520–562	08-26-2008	13.9	7.6	384	164	9.8	–2.4
Zone 3	701–748	08-26-2008	14.8	7.7	379	172	6.7	–2.5
MIDDLE 2051								
Zone 12	0–45	08-25-2008	11.6	7.5	346	154	7.6	–2.3
Zone 9	184–207	08-25-2008	13.7	7.6	383	154	9.8	–2.4
Zone 6	262–312	08-21-2008	13.8	7.7	390	158	10.3	–2.5
Zone 3	526–564	08-21-2008	15.2	7.6	366	146	9.3	–2.4
Zone 1	576–612	08-21-2008	15.1	7.6	366	144	10.7	–2.4

Table 3. Measurements of field parameters and calculated partial pressure of carbon dioxide for water-quality analyses from precipitation (snow core), surface water, and groundwater, Idaho National Laboratory, eastern Idaho.—Continued

[Data from Bartholomay and Twining (2010), Bartholomay and others (2015), Bartholomay, Maimer, and others (2017), and Rattray (2018). Snow core sample location was a snow grab-sample collected at USGS 83 (Rightmire and Lewis, 1987). **Site name:** Alternate names used in other reports shown in table 6. **Approximate depth of open intervals below water table:** Range of depth may include multiple open intervals. **Dissolved oxygen:** Dissolved oxygen (O_2) values followed by an E indicate that no measurement of O_2 was made on the date shown and that the O_2 value in the table was estimated as the mean value of all O_2 measurements for that site in U.S. Geological Survey National Water Information System (NWIS) through December 2015 (U.S. Geological Survey, 2021). **Carbon dioxide:** Calculated with PHREEQC (Parkhurst and Appelo, 2013). **Abbreviations:** CFA, Central Facilities Area; INL, Idaho National Laboratory; na, not applicable; nd, not determined; RWMC, Radioactive Waste Management Complex; USGS, U.S. Geological Survey. **Units:** ft bwt, foot below water table; mm-dd-yyyy, month, day, year; pH, negative base-10 logarithm of the hydrogen ion activity; µS/cm, microsiemen per centimeter at 25 degrees °C; mg/L, milligram per liter; $CaCO_3$, calcium carbonate; $LogPCO_2$, base-10 logarithm of carbon dioxide partial pressure. **Symbols:** °C, temperature, in degrees Celsius; %, percent]

Site name (fig. 1)	Approximate depth of open intervals below water table (ft bwt)	Date sampled (mm-dd-yyyy)	Water temperature (°C)	pH (units)	Specific conductance (µS/cm at 25 °C)	Alkalinity (mg/L as $CaCO_3$)	Dissolved oxygen (mg/L)	Carbon dioxide ($LogPCO_2$)
GROUNDWATER FROM MULTILEVEL WELLS—Continued								
USGS 103								
Zone 17	85–106	08-20-2008	13.6	8.3	304	100	5.5	–3.3
Zone 15	182–247	08-19-2008	14.1	7.7	342	125	12.4	–2.6
Zone 12	307–335	08-19-2008	13.3	7.7	315	125	10.8	–2.6
Zone 9	373–429	08-18-2008	13.3	7.7	343	140	8.9	–2.6
Zone 6	478–513	08-18-2008	13.2	7.7	360	140	9.2	–2.6
Zone 3	599–655	08-18-2008	12.9	7.7	357	140	10.2	–2.6
Zone 1	672–694	08-19-2008	13.1	7.7	364	138	10.0	–2.6
USGS 105								
Zone 13	34–79	09-16-2010	12.8	7.9	357	136	6.7	–2.8
Zone 11	157–189	09-16-2010	12.8	7.9	362	144	8.8	–2.7
Zone 8	256–309	09-15-2010	13.1	8.0	363	141	10.1	–2.9
Zone 5	362–429	09-15-2010	13.0	7.9	359	140	9.6	–2.8
Zone 2	552–603	09-15-2010	12.6	7.9	357	144	11.4	–2.7
USGS 108								
Zone 11	30–67	06-23-2011	12.4	7.9	356	140	5.9	–2.8
Zone 9	179–218	06-23-2011	12.6	7.9	379	144	7.2	–2.7
Zone 7	260–292	06-23-2011	12.7	7.8	392	156	8.6	–2.6
Zone 4	406–448	06-22-2011	12.7	7.8	402	154	7.4	–2.6
Zone 1	549–582	06-22-2011	12.9	7.5	408	163	9.4	–2.3

Table 3. Measurements of field parameters and calculated partial pressure of carbon dioxide for water-quality analyses from precipitation (snow core), surface water, and groundwater, Idaho National Laboratory, eastern Idaho.—Continued

[Data from Bartholomay and Twining (2010), Bartholomay and others (2015), Bartholomay, Maimer, and others (2017), and Rattray (2018). Snow core sample location was a snow grab-sample collected at USGS 83 (Rightmire and Lewis, 1987). **Site name:** Alternate names used in other reports shown in table 6. **Approximate depth of open intervals below water table:** Range of depth may include multiple open intervals. **Dissolved oxygen:** Dissolved oxygen (O_2) values followed by an E indicate that no measurement of O_2 was made on the date shown and that the O_2 value in the table was estimated as the mean value of all O_2 measurements for that site in U.S. Geological Survey National Water Information System (NWIS) through December 2015 (U.S. Geological Survey, 2021). **Carbon dioxide:** Calculated with PHREEQC (Parkhurst and Appelo, 2013). **Abbreviations:** CFA, Central Facilities Area; INL, Idaho National Laboratory; na, not applicable; nd, not determined; RWMC, Radioactive Waste Management Complex; USGS, U.S. Geological Survey. **Units:** ft bwt, foot below water table; mm-dd-yyyy, month, day, year; pH, negative base-10 logarithm of the hydrogen ion activity; µS/cm, microsiemen per centimeter at 25 degrees °C; mg/L, milligram per liter; $CaCO_3$, calcium carbonate; $LogPCO_2$, base-10 logarithm of carbon dioxide partial pressure. **Symbols:** °C, temperature, in degrees Celsius; %, percent]

Site name (fig. 1)	Approximate depth of open intervals below water table (ft bwt)	Date sampled (mm-dd-yyyy)	Water temperature (°C)	pH (units)	Specific conductance (µS/cm at 25 °C)	Alkalinity (mg/L as $CaCO_3$)	Dissolved oxygen (mg/L)	Carbon dioxide ($LogPCO_2$)
GROUNDWATER FROM MULTILEVEL WELLS—Continued								
USGS 131A								
Zone 12	16–86	07-17-2013	11.5	8.0	365	139	7.9	–2.9
Zone 8	249–296	07-16-2013	12.4	7.9	435	148	8.7	–2.7
Zone 5	410–512	07-16-2013	13.4	8.0	401	161	8.4	–2.8
Zone 3	574–611	07-16-2013	13.4	8.0	399	167	8.7	–2.8
USGS 132								
Zone 17	17–53	08-14-2008	11.9	7.9	478	140	6.9	–2.8
Zone 14	120–180	08-13-2008	13.3	7.9	364	144	8.4	–2.7
Zone 11	205–257	08-13-2008	12.7	7.8	358	140	9.3	–2.7
Zone 8	304–328	08-13-2008	12.4	7.7	356	136	10.2	–2.6
Zone 5	377–436	08-12-2008	12.7	7.9	353	136	8.9	–2.8
Zone 1	545–607	08-12-2008	11.4	7.9	366	146	9.5	–2.7
USGS 133								
Zone 10[2]	17–49	09-24-2007	11.3	7.6	339	132	5.9	–2.5
Zone 7	125–160	09-02-2008	11.9	7.6	349	138	11.1	–2.5
Zone 4	255–265	09-02-2008	11.9	7.6	367	145	11.4	–2.5
Zone 1	294–335	09-02-2008	11.4	7.6	442	186	13.8	–2.4
GROUNDWATER FROM MULTILEVEL WELLS—Continued								

Table 3. Measurements of field parameters and calculated partial pressure of carbon dioxide for water-quality analyses from precipitation (snow core), surface water, and groundwater, Idaho National Laboratory, eastern Idaho.—Continued

[Data from Bartholomay and Twining (2010), Bartholomay and others (2015), Bartholomay, Maimer, and others (2017), and Rattray (2018). Snow core sample location was a snow grab-sample collected at USGS 83 (Rightmire and Lewis, 1987). **Site name:** Alternate names used in other reports shown in table 6. **Approximate depth of open intervals below water table:** Range of depth may include multiple open intervals. **Dissolved oxygen:** Dissolved oxygen (O_2) values followed by an E indicate that no measurement of O_2 was made on the date shown and that the O_2 value in the table was estimated as the mean value of all O_2 measurements for that site in U.S. Geological Survey National Water Information System (NWIS) through December 2015 (U.S. Geological Survey, 2021). **Carbon dioxide:** Calculated with PHREEQC (Parkhurst and Appelo, 2013). **Abbreviations:** CFA, Central Facilities Area; INL, Idaho National Laboratory; na, not applicable; nd, not determined; RWMC, Radioactive Waste Management Complex; USGS, U.S. Geological Survey. **Units:** ft bwt, foot below water table; mm-dd-yyyy, month, day, year; pH, negative base-10 logarithm of the hydrogen ion activity; µS/cm, microsiemen per centimeter at 25 degrees °C; mg/L, milligram per liter; $CaCO_3$, calcium carbonate; $LogPCO_2$, base-10 logarithm of carbon dioxide partial pressure. **Symbols:** °C, temperature, in degrees Celsius; %, percent]

Site name (fig. 1)	Approximate depth of open intervals below water table (ft bwt)	Date sampled (mm-dd-yyyy)	Water temperature (°C)	pH (units)	Specific conductance (µS/cm at 25 °C)	Alkalinity (mg/L as $CaCO_3$)	Dissolved oxygen (mg/L)	Carbon dioxide ($LogPCO_2$)
USGS 134								
Zone 15	41–77	09-04-2008	13.0	7.9	313	128	10.0	–2.8
Zone 12	126–139	09-04-2008	13.2	7.6	392	168	8.9	–2.4
Zone 9	178–207	09-03-2008	13.8	8.0	300	129	10.5	–2.9
Zone 6	269–305	09-03-2008	14.6	7.8	327	136	10.4	–2.7
Zone 3	333–355	09-03-2008	14.5	7.2	371	128	10.3	–2.1
USGS 135								
Zone 10	10–45	09-14-2010	11.6	7.9	330	136	6.6	–2.8
Zone 7	106–144	09-14-2010	11.6	7.7	291	116	10.3	–2.7
Zone 4	251–291	09-13-2010	11.6	7.8	325	140	11.3	–2.7
Zone 1	389–420	09-13-2010	11.9	7.7	319	136	10.3	–2.6
USGS 137A								
Zone 5	12–90	07-15-2013	12.8	8.1	367	142	7.6	–3.0
Zone 4	93–156	07-15-2013	12.8	8.1	362	142	8.6	–3.0
Zone 3	159–234	07-15-2013	12.7	8.1	360	145	8.9	–2.9
Zone 1	247–267	07-15-2013	12.9	8.1	358	144	8.6	–2.9

[1]Specific conductance measurement from 1996.

[2]Chemistry data for zone 10 from USGS 133 are from September 2007 because the cation concentrations from September 2008 are lower than expected.

Table 4. Concentrations of major ions, silica, and charge balance for water-quality analyses from precipitation (snow core), surface water, and groundwater, Idaho National Laboratory, eastern Idaho.

[Data from Bartholomay and Twining (2010), Bartholomay and others (2015), Rattray (2018), and U.S. Geological Survey (2021). Snow core sample location was a snow grab-sample collected at USGS 83 (Rightmire and Lewis, 1987). Water samples in italics exceeded the acceptable charge balance. All ions except nitrate are measured in milligrams per liter; nitrate (actually nitrite plus nitrate) is measured in milligrams per liter as nitrogen. **Site name:** Alternate names used in other reports shown in table 1. **Approximate depth of open intervals below water table:** Range of depth may include multiple open intervals. **Abbreviations:** na, not applicable ; nd, not determined. **Units:** ft bwt, foot below water table; mm-dd-yy, month, day, year. **Symbol:** <, less than]

Site name (fig, 1)	Approximate depth of open intervals below water table (ft bwt)	Date sampled (mm-dd-yyyy)	Calcium	Magnesium	Sodium	Potassium	Bicarbonate	Chloride	Sulfate	Fluoride	Nitrate	Silica	Charge balance
SNOW CORE													
USGS 83	na	02-02-1978	0.1	0.2	0.2	2.2	5	0.8	3.1	0.1	nd	1.5	–33.7
SURFACE WATER													
Big Lost River below INL Diversion (BLRINL)	na	06-02-1995	35	8	5.4	1.4	126	3	18	0.2	<0.05	12	1.7
Big Lost River below lower Lincoln Blvd Bridge (BLRLB)	na	06-19-1995	31.2	7.4	4.8	1.7	123	3.1	17.5	0.21	0.2	10.7	–1.7
DEEP GROUNDWATER													
EBR 1	14–489	10-16-1996	22.6	15.3	8.0	3.1	144	7	15.7	0.2	0.4	33.8	–2.5
CONTAMINATED GROUNDWATER													
Advanced Test Reactor Complex													
USGS 65	0–30	05-16-1991	85.0	19	14	3.0	150	21	150	<0.1	1.6	21	1.4
Central Facilities Area													
CFA 1	0–206	07-16-1996	61.6	18.6	14.4	3.2	160	74	27.7	0.25	3.5	20.9	–2.3
CFA 2	50–210	07-16-1996	71.9	26.4	21.4	4.3	149	115	45.0	0.39	3.7	23.6	–0.9
USGS 104	0–142	07-15-1996	34.9	13.7	7.6	2.4	156	12.6	19.3	0.20	0.7	24.7	–2.1
Idaho Nuclear Technology and Engineering Center													
USGS 57	8–113	05-13-1991	67	18	41	3.6	148	110	35	0.3	3.7	23	1.1
Radioactive Waste Management Area													
RWMC M3S	13–43	07-22-1996	43.4	15	8.2	2.6	176	13.4	24.3	0.3	0.7	23.6	–0.6
USGS 88	0–45	04-04-1989	33.0	23	47	7.0	113	82	64	0.3	1.8	30	0.8
USGS 120	21–88	07-17-1996	34.0	18.4	25.4	4.0	186	21.7	38.0	0.26	0.8	22.4	–1.6

Table 4. Concentrations of major ions, silica, and charge balance for water-quality analyses from precipitation (snow core), surface water, and groundwater, Idaho National Laboratory, eastern Idaho.—Continued

[Data from Bartholomay and Twining (2010), Bartholomay and others (2015), Rattray (2018), and U.S. Geological Survey (2021). Snow core sample location was a snow grab-sample collected at USGS 83 (Rightmire and Lewis, 1987). Water samples in italics exceeded the acceptable charge balance. All ions except nitrate are measured in milligrams per liter; nitrate (actually nitrite plus nitrate) is measured in milligrams per liter as nitrogen. **Site name:** Alternate names used in other reports shown in table 1. **Approximate depth of open intervals below water table:** Range of depth may include multiple open intervals. **Abbreviations:** na, not applicable ; nd, not determined. **Units:** ft bwt, foot below water table; mm-dd-yy, month, day, year. **Symbol:** <, less than]

Site name (fig. 1)	Approximate depth of open intervals below water table (ft bwt)	Date sampled (mm-dd-yyyy)	Calcium	Magnesium	Sodium	Potassium	Bicarbonate	Chloride	Sulfate	Fluoride	Nitrate	Silica	Charge balance
NATURAL GROUNDWATER													
Fire Station 2	7–91	10-16-1996	54.8	17.8	8.1	2.4	204	17.6	23.5	0.19	1.2	22.7	1.8
Site 4	21–96	10-16-1996	45.3	14.1	7.8	1.8	192	10.1	19.4	0.20	0.6	22.5	–1.5
Site 19	1–371	07-16-1996	42.4	17.5	8.0	1.9	200	11.6	20.7	0.19	0.9	18.8	–2.3
USGS 8	12–42	10-08-1996	46.8	15.0	6.9	1.8	201	8.4	21.0	0.20	0.9	18.9	–1.9
USGS 83	15–251	04-11-1995	27.3	10.6	9.7	2.5	123	10.8	20.1	0.24	0.7	25.5	–1.9
USGS 86	0–39	10-11-1996	37.0	10.2	11.0	2.9	132	19.6	22.7	0.16	1.4	25.5	–1.4
USGS 107	0–208	10-09-1996	37.6	16.6	15.4	3.5	176	21.3	25.3	0.34	1.0	29.7	–1.7
USGS 119	0–20	04-03-1989	30.0	10.0	11.0	2.6	116	12.0	35.0	0.50	1.3	31	–4.3
GROUNDWATER FROM MULTILEVEL WELLS													
MIDDLE 2050A													
Zone 15	0–60	08-27-2008	53.3	16.5	9.4	2.4	200	15.5	25.7	0.2	1.0	21.5	1.6
Zone 12	164–224	08-27-2008	42.8	14.2	7.2	2.3	182	11.1	21.4	0.2	0.3	19.6	–1.5
Zone 9	311–328	08-26-2008	45.2	17.2	8.6	1.9	207	10.9	22.1	0.2	0.9	20.3	–1.9
Zone 6	520–562	08-26-2008	41.4	16.4	7.8	1.7	200	10.3	21.6	0.2	0.9	19.0	–3.8
Zone 3	701–748	08-26-2008	40.0	17.4	12.4	2.5	210	14.6	9.6	0.3	<0.04	18.7	–0.7
MIDDLE 2051													
Zone 12	0–45	08-25-2008	46.3	11.1	5.7	2.4	188	5.7	22.0	0.2	0.4	24.3	–3.0
Zone 9	184–207	08-25-2008	43.7	15.6	8.3	2.3	188	10.7	26.1	0.2	0.8	22.4	–1.6
Zone 6	262–312	08-21-2008	43.1	15.3	8.4	2.2	193	11.1	27.1	0.2	0.9	21.6	–3.8
Zone 3	526–564	08-21-2008	35.7	17.1	7.5	2.4	178	12.1	23.3	0.2	0.9	24.2	–3.4
Zone 1	576–612	8-21-2008	36.8	17.8	7.8	2.5	176	12.1	23.5	0.2	0.8	25.0	–1.2

Table 4. Concentrations of major ions, silica, and charge balance for water-quality analyses from precipitation (snow core), surface water, and groundwater, Idaho National Laboratory, eastern Idaho.—Continued

[Data from Bartholomay and Twining (2010), Bartholomay and others (2015), Rattray (2018), and U.S. Geological Survey (2021). Snow core sample location was a snow grab-sample collected at USGS 83 (Rightmire and Lewis, 1987). Water samples in italics exceeded the acceptable charge balance. All ions except nitrate are measured in milligrams per liter; nitrate (actually nitrite plus nitrate) is measured in milligrams per liter as nitrogen. **Site name:** Alternate names used in other reports shown in table 1. **Approximate depth of open intervals below water table:** Range of depth may include multiple open intervals. **Abbreviations:** na, not applicable ; nd, not determined. **Units:** ft bwt, foot below water table; mm-dd-yy, month, day, year. **Symbol:** <, less than]

Site name (fig, 1)	Approximate depth of open intervals below water table (ft bwt)	Date sampled (mm-dd-yyyy)	Calcium	Magnesium	Sodium	Potassium	Bicarbonate	Chloride	Sulfate	Fluoride	Nitrate	Silica	Charge balance
GROUNDWATER FROM MULTILEVEL WELLS—Continued													
USGS 103													
Zone 17	85–106	08-20-2008	21.6	14.6	14.7	3.1	122	18.4	23.1	0.4	0.1	6.9	–1.1
Zone 15	182–247	08-19-2008	32.9	14.5	12.9	2.9	152	14.3	22.9	0.3	0.7	30.6	0.3
Zone 12	307–335	08-19-2008	30.7	13.7	9.3	2.8	152	10.2	19.6	0.2	0.5	29.5	–1.7
Zone 9	373–429	08-18-2008	35.6	15.4	8.7	2.6	171	12.6	21.4	0.2	0.7	27.3	–2.6
Zone 6	478–513	08-18-2008	37.1	14.9	8.5	2.5	171	14.3	22.3	0.2	0.8	25.2	–3.3
Zone 3	599–655	08-18-2008	38.8	15.5	8.9	2.6	171	14.1	22.4	0.2	0.8	26.3	–1.1
Zone 1	672–694	08-19-2008	38.3	15.4	8.8	2.5	168	14.3	22.5	0.2	0.8	26.4	–1.0
USGS 105													
Zone 13	34–79	09-16-2010	39.2	14.4	11.5	2.8	166	12.4	23.6	0.2	0.7	23.8	0.9
Zone 11	157–189	09-16-2010	39.1	14.2	11.6	2.7	176	12.3	23.8	0.2	0.7	24.4	–1.5
Zone 8	256–309	09-15-2010	40.2	15.2	11.1	2.8	172	13.1	23.2	0.2	0.8	25.4	0.7
Zone 5	362429	09-15-2010	39.5	14.5	10.9	2.9	171	12.9	23.2	0.2	0.8	25.8	–0.3
Zone 2	552–603	09-15-2010	40.7	14.4	11.7	2.7	176	11.4	23.6	0.3	0.6	24.0	0.3
USGS 108													
Zone 11	30–67	06-23-2011	35.5	15.9	11.4	2.7	171	16.4	23.6	0.3	0.7	28.2	–2.6
Zone 9	179–218	06-23-2011	40.2	17.8	8.7	2.4	176	16.6	24.3	0.2	0.9	27.5	–0.5
Zone 7	260–292	06-23-2011	42.8	18.0	8.3	2.3	190	16.8	24.2	0.2	0.9	26.4	–1.7
Zone 4	406–448	06-23-2011	46.4	18.8	8.2	2.2	188	18.0	25.2	0.2	1.0	26.5	0.8
Zone 1	549–582	06-22-2011	46.2	19.3	8.3	2.4	199	17.7	25.0	0.2	0.9	24.7	–0.6

Table 4. Concentrations of major ions, silica, and charge balance for water-quality analyses from precipitation (snow core), surface water, and groundwater, Idaho National Laboratory, eastern Idaho.—Continued

[Data from Bartholomay and Twining (2010), Bartholomay and others (2015), Rattray (2018), and U.S. Geological Survey (2021). Snow core sample location was a snow grab-sample collected at USGS 83 (Rightmire and Lewis, 1987). Water samples in italics exceeded the acceptable charge balance. All ions except nitrate are measured in milligrams per liter; nitrate (actually nitrite plus nitrate) is measured in milligrams per liter as nitrogen. **Site name:** Alternate names used in other reports shown in table 1. **Approximate depth of open intervals below water table:** Range of depth may include multiple open intervals. **Abbreviations:** na, not applicable ; nd, not determined. **Units:** ft bwt, foot below water table; mm-dd-yy, month, day, year. **Symbol:** <, less than]

Site name (fig. 1)	Approximate depth of open intervals below water table (ft bwt)	Date sampled (mm-dd-yyyy)	Calcium	Magnesium	Sodium	Potassium	Bicarbonate	Chloride	Sulfate	Fluoride	Nitrate	Silica	Charge balance
GROUNDWATER FROM MULTILEVEL WELLS—Continued													
USGS 131A													
Zone 12	16–86	07-17-2013	42.7	15.2	7.9	2.4	169	16.2	23.1	0.2	0.9	24.3	–0.3
Zone 8	249–296	07-16-2013	51.8	16.8	9.6	2.7	180	26.2	27.4	0.2	1.3	25.6	0.9
Zone 5	410–512	07-16-2013	48.5	18.4	8.5	2.2	196	12.9	22.9	0.2	1.0	24.2	2.3
Zone 3	574–611	07-16-2013	48.3	18.6	8.0	2.0	204	13.2	22.9	0.2	1.1	22.4	0.4
USGS 132													
Zone 17	17–53	08-14-2008	35.8	18.1	26.1	3.8	171	35.0	40.8	0.3	1.3	24.8	–2.8
Zone 14	120–180	08-13-2008	38.4	15.4	10.7	2.8	176	11.2	25.9	0.3	0.7	25.7	–1.4
Zone 11	205–257	08-13-2008	39.6	14.5	8.9	2.6	171	10.3	24.8	0.2	0.7	25.8	–0.9
Zone 8	304–328	08-13-2008	39.3	14.4	8.9	2.6	166	10.2	24.7	0.2	0.7	25.8	0.0
Zone 5	377–436	08-12-2008	39.9	14.6	9.2	2.6	166	10.3	24.8	0.2	0.7	25.8	0.7
Zone 1	545–607	08-12-2008	38.8	14.7	11.7	2.8	178	10.7	25.4	0.2	0.7	24.9	–1.4
USGS 133													
Zone 10	17–49	09-24-2007	43.3	13.8	8.5	3.0	161	12.5	20.7	0.2	0.4	14.4	3.8
Zone 7	125–160	09-02-2008	39.8	13.2	7.6	2.7	168	12.9	21.0	0.2	0.9	24.9	–2.4
Zone 4	255–265	09-02-2008	40.2	13.6	7.1	2.1	177	12.5	20.5	0.2	0.9	23.6	–3.8
Zone 1	294–335	09-02-2008	50.4	17.8	9.0	1.8	227	13.9	22.1	0.1	1.2	19.1	–2.9
USGS 134													
Zone 15	41–77	09-04-2008	24.8	16.0	7.2	2.2	156	9.6	20.7	0.2	0.6	27.0	–6.5
Zone 12	126–139	09-04-2008	36.3	20.1	8.7	2.3	205	10.4	19.7	0.1	0.6	28.2	–2.8
Zone 9	178–207	09-03-2008	25.5	15.5	7.7	2.2	157	7.7	18.9	0.2	0.5	28.6	–5.0
Zone 6	269–305	09-03-2008	31.9	16.6	8.2	2.4	166	9.8	20.8	0.2	0.7	25.9	–1.8
Zone 3	333–355	09-03-2008	25.2	15.6	7.8	2.6	156	7.5	19.1	0.1	0.4	39.1	–4.2

Table 4. Concentrations of major ions, silica, and charge balance for water-quality analyses from precipitation (snow core), surface water, and groundwater, Idaho National Laboratory, eastern Idaho.—Continued

[Data from Bartholomay and Twining (2010), Bartholomay and others (2015), Rattray (2018), and U.S. Geological Survey (2021). Snow core sample location was a snow grab-sample collected at USGS 83 (Rightmire and Lewis, 1987). Water samples in italics exceeded the acceptable charge balance. All ions except nitrate are measured in milligrams per liter; nitrate (actually nitrite plus nitrate) is measured in milligrams per liter as nitrogen. **Site name:** Alternate names used in other reports shown in table 1. **Approximate depth of open intervals below water table:** Range of depth may include multiple open intervals. **Abbreviations:** na, not applicable ; nd, not determined. **Units:** ft bwt, foot below water table; mm-dd-yy, month, day, year. **Symbol:** <, less than]

Site name (fig, 1)	Approximate depth of open intervals below water table (ft bwt)	Date sampled (mm-dd-yyyy)	Calcium	Magnesium	Sodium	Potassium	Bicarbonate	Chloride	Sulfate	Fluoride	Nitrate	Silica	Charge balance
GROUNDWATER FROM MULTILEVEL WELLS—Continued													
USGS 135													
Zone 10	10–45	09-14-2010	42.8	11.9	7.0	1.7	166	7.6	20.3	0.2	0.8	19.1	0.2
Zone 7	106–144	09-14-2010	36.6	11.5	6.4	1.9	141	7.1	19.5	0.2	0.6	21.9	2.0
Zone 4	251–291	09-13-2010	42.9	12.2	6.8	1.8	171	7.6	20.3	0.2	0.8	19.5	–0.5
Zone 1	389–420	09-13-2010	39.2	12.7	6.6	1.9	166	7.4	20.0	0.2	0.7	18.6	–1.3
USGS 137A													
Zone 5	12–90	07-15-2013	41.2	16.3	12.7	3.0	173	13.7	26.2	0.2	0.7	27.3	2.1
Zone 4	93–156	07-15-2013	38.7	15.4	11.1	2.8	173	12.0	25.1	0.2	0.7	26.1	–0.5
Zone 3	159–234	07-15-2013	40.8	15.5	10.9	2.6	177	11.0	24.7	0.2	0.6	25.9	0.6
Zone 1	247–267	07-15-2013	39.7	15.3	11.4	2.7	176	11.0	24.7	0.2	0.7	26.2	0.0

Table 5. Concentrations of selected dissolved metals for water-quality analyses from precipitation (snow core), surface water, and groundwater, Idaho National Laboratory, eastern Idaho.

[Data from Bartholomay and Twining (2010), Bartholomay and others (2015), Rattray (2018), and U.S. Geological Survey (2021). Snow core sample location was a snow grab-sample collected at USGS 83 (Rightmire and Lewis, 1987). **Site name:** Alternate names used in other reports shown in table 1. **Approximate depth of open intervals below water table:** Range of depth may include multiple open intervals. **Abbreviations:** E, estimated value; na, not applicable; nd, not determined. **Units:** ft bwt, foot below water table; mm-dd-yy, month, day, year; µg/L, microgram per liter; mg/L, milligram per liter. **Symbol:** <, less than]

Site name (fig. 1)	Approximate depth of open intervals below water table (ft bwt)	Date sampled (mm-dd-yyyy)	Aluminum	Barium	Chromium	Iron	Lithium	Manganese	Strontium	Uranium
SNOW CORE										
USGS 83	na	02-02-1978	nd	nd	nd	nd	nd	nd	nd	nd
SURFACE WATER										
Big Lost River below INL Diversion (BLRINL)	na	06-02-1995	10	69	<5	11	<4	2	210	2.2
Big Lost River below lower Lincoln Blvd Bridge (BLRLB)	na	06-19-1995	116	60	<1	100	2	1.6	164	1.9
DEEP GROUNDWATER										
EBR 1	14–489	10-16-1996	10	21	7	34	2.7	0.4	195	2.03
CONTAMINATED GROUNDWATER										
Advanced Test Reactor Complex										
USGS 65	0–30	05-16-1991	<10	56	190	210	5	3	390	nd
Central Facilities Area										
CFA 1	0–206	07-16-1996	4	91	10	68	2.5	0.2	370	2.30
CFA 2	50–210	07-16-1996	4	96	10	158	3.6	2.8	483	2.30
USGS 104	0–142	07-15-1996	3	32	7	62	2.2	0.3	184	1.50
Idaho Nuclear Technology and Engineering Center										
USGS 57	8–113	05-13-1991	10	170	<5	4	<4	<1	360	nd
Radioactive Waste Management Area										
RWMC M3S	13–43	07-22-1996	7	45	15	51	2.4	0.1	244	2.10
USGS 88	0–45	04-04-1989	<10	22	30	7	9	6	190	nd
USGS 120	21–88	07-17-1996	5	48	9	70	3.6	1	197	2.80
NATURAL GROUNDWATER										
Fire Station 2	7–91	10-16-1996	7	20	7	56	2	0.5	303	2.00
Site 4	21–96	10-16-1996	7	nd	8	30	1.7	<0.1	231	1.90
Site 19	1–371	07-16-1996	5	49	3	55	2.5	<0.1	211	1.70
USGS 8	12–42	10-08-1996	6	70	2	45	1.3	1.1	254	2.10

Table 5. Concentrations of selected dissolved metals for water-quality analyses from precipitation (snow core), surface water, and groundwater, Idaho National Laboratory, eastern Idaho.—Continued

[Data from Bartholomay and Twining (2010), Bartholomay and others (2015), Rattray (2018), and U.S. Geological Survey (2021). Snow core sample location was a snow grab-sample collected at USGS 83 (Rightmire and Lewis, 1987). **Site name:** Alternate names used in other reports shown in table 1. **Approximate depth of open intervals below water table:** Range of depth may include multiple open intervals. **Abbreviations:** E, estimated value; na, not applicable; nd, not determined. **Units:** ft bwt, foot below water table; mm-dd-yy, month, day, year; µg/L, microgram per liter; mg/L, milligram per liter. **Symbol:** <, less than]

Site name (fig. 1)	Approximate depth of open intervals below water table (ft bwt)	Date sampled (mm-dd-yyyy)	Aluminum	Barium	Chromium	Iron	Lithium	Manganese	Strontium	Uranium
NATURAL GROUNDWATER—Continued										
USGS 83	15–251	04-11-1995	5	95	14	26	3	0.3	157	1.37
USGS 86	0–39	10-11-1996	2	19	12	37	2.3	0.8	171	1.03
USGS 107	0–208	10-09-1996	4	49	5	34	10.5	<0.1	120	2.20
USGS 119	0–20	04-03-1989	<10	28	30	6	5	4	130	nd
GROUNDWATER FROM MULTILEVEL WELLS										
MIDDLE 2050A										
Zone 15	0–60	08-27-2008	4	73	8	<8	1.4	0.1E	272	1.79
Zone 12	164–224	08-27-2008	4	35	3	<8	1.5	0.4	230	1.75
Zone 9	311–328	08-26-2008	4	46	4	<8	2.0	0.4	211	1.39
Zone 6	520–562	08-26-2008	3	42	3	<8	2.2	0.6	202	1.32
Zone 3	701–748	08-26-2008	2	61	<0.1	17	3.3	365	273	0.63
MIDDLE 2051										
Zone 12	0–45	08-25-2008	2	45	1	<8	1.6	0.2E	255	1.69
Zone 9	184–207	08-25-2008	5	54	7	<8	1.9	1.8	235	1.59
Zone 6	262–312	08-21-2008	4	58	8	<8	1.9	0.2	229	1.56
Zone 3	526–564	08-21-2008	5	34	6	<8	2.1	0.3	206	1.40
Zone 1	576–612	08-21-2008	8	34	6	7E	2.2	1.7	214	1.44
USGS 103										
Zone 17	85–106	08-20-2008	2	50	1	15	6.3	57	148	0.35
Zone 15	182–247	08-19-2008	4	28	5	<8	4.3	1.3	186	1.84
Zone 12	307–335	08-19-2008	5	28	6	<8	3.9	1.7	172	1.55
Zone 9	373–429	08-18-2008	4	39	6	<8	2.3	0.2E	193	1.44
Zone 6	478–513	08-18-2008	5	41	6	<8	2.0	0.3	191	1.39
Zone 3	599–655	08-18-2008	4	41	6	<8	2.0	0.4	200	1.47
Zone 1	672–694	08-19-2008	12	41	6	6E	2.1	0.5	203	1.50

Table 5. Concentrations of selected dissolved metals for water-quality analyses from precipitation (snow core), surface water, and groundwater, Idaho National Laboratory, eastern Idaho.—Continued

[Data from Bartholomay and Twining (2010), Bartholomay and others (2015), Rattray (2018), and U.S. Geological Survey (2021). Snow core sample location was a snow grab-sample collected at USGS 83 (Rightmire and Lewis, 1987). **Site name:** Alternate names used in other reports shown in table 1. **Approximate depth of open intervals below water table:** Range of depth may include multiple open intervals. **Abbreviations:** E, estimated value; na, not applicable; nd, not determined. **Units:** ft bwt, foot below water table; mm-dd-yy, month, day, year; µg/L, microgram per liter; mg/L, milligram per liter. **Symbol:** <, less than]

Site name (fig. 1)	Approximate depth of open intervals below water table (ft bwt)	Date sampled (mm-dd-yyyy)	Aluminum	Barium	Chromium	Iron	Lithium	Manganese	Strontium	Uranium
GROUNDWATER FROM MULTILEVEL WELLS—Continued										
USGS 105										
Zone 13	34–79	09-16-2010	5	32	6	7	2.1	5.5	227	1.74
Zone 11	157–189	09-16-2010	6	33	7	<6	2.1	0.3	236	1.83
Zone 8	256–309	09-15-2010	6	31	7	<6	2.4	0.2E	235	1.83
Zone 5	362–429	09-15-2010	6	31	8	7	2.5	0.2E	232	1.81
Zone 2	552–603	09-15-2010	7	33	8	4E	2.3	0.4	227	1.89
USGS 108										
Zone 11	30–67	06-23-2011	3	34	2	66	3.7	6.9	195	1.59
Zone 9	179–218	06-23-2011	5	37	6	<3	2.3	0.2	209	1.43
Zone 7	260–292	06-23-2011	4	39	6	<3	2.2	0.3	210	1.37
Zone 4	406–448	06-22-2011	5	42	6	<3	2.3	0.2	219	1.44
Zone 1	549–582	06-22-2011	2	41	5	<3	2.6	27	223	1.36
USGS 131A										
Zone 12	16–86	07-17-2013	3	22	11	<4	3.1	0.5	239	1.93
Zone 8	249–296	07-16-2013	4	47	11	9	2.0	0.4	291	1.84
Zone 5	410–512	07-16-2013	7	44	5	7	2.0	0.4	229	1.52
Zone 3	574–611	07-16-2013	7	41	5	<4	2.3	0.4	236	1.55
USGS 132										
Zone 17	17–53	08-14-2008	5	53	17	<8	2.9	0.1E	240	2.89
Zone 14	120–180	08-13-2008	5	39	8	<8	2.2	<0.2	223	2.07
Zone 11	205–257	08-13-2008	6	37	8	<8	1.8	0.2	222	1.75
Zone 8	304–328	08-13-2008	5	36	8	<8	1.9	0.3	214	1.78
Zone 5	377–436	08-12-2008	5	39	8	<8	1.7	0.6	218	1.80
Zone 1	545–607	08-12-2008	4	35	8	<8	1.8	0.6	230	2.31

Table 5. Concentrations of selected dissolved metals for water-quality analyses from precipitation (snow core), surface water, and groundwater, Idaho National Laboratory, eastern Idaho.—Continued

[Data from Bartholomay and Twining (2010), Bartholomay and others (2015), Rattray (2018), and U.S. Geological Survey (2021). Snow core sample location was a snow grab-sample collected at USGS 83 (Rightmire and Lewis, 1987). **Site name:** Alternate names used in other reports shown in table 1. **Approximate depth of open intervals below water table:** Range of depth may include multiple open intervals. **Abbreviations:** E, estimated value; na, not applicable; nd, not determined. **Units:** ft bwt, foot below water table; mm-dd-yy, month, day, year; µg/L, microgram per liter; mg/L, milligram per liter. **Symbol:** <, less than]

Site name (fig. 1)	Approximate depth of open intervals below water table (ft bwt)	Date sampled (mm-dd-yyyy)	Aluminum	Barium	Chromium	Iron	Lithium	Manganese	Strontium	Uranium
GROUNDWATER FROM MULTILEVEL WELLS—Continued										
USGS 133										
Zone 10	17–49	09-24-2007	1.6E	46	0.1E	<6	1.8	<0.2	220	1.32
Zone 7	125–160	09-02-2008	<2	61	5	<8	0.8E	<0.2	266	2.30
Zone 4	255–265	09-09-2008	3	49	5	7E	1.7	0.4	184	1.74
Zone 1	294–335	09-02-2008	2	59	4	16	1.4	0.6	216	1.49
USGS 134										
Zone 15	41–77	09-04-2008	3	11	6	<8	2.0	0.6	145	1.07
Zone 12	126–139	09-04-2008	2	13	4	<8	2.9	0.6	174	0.35
Zone 9	178–207	09-03-2008	3	16	6	<8	2.3	1.6	153	1.17
Zone 6	269–305	09-03-2008	2	17	6	<8	1.9	0.3	182	1.29
Zone 3	333–355	09-03-2008	1E	8	3	10	2.7	31	131	0.03
USGS 135										
Zone 10	10–45	09-14-2010	8	56	2	6	1.9	0.4	245	1.64
Zone 7	106–144	09-14-2010	5	43	2	4E	1.5	0.5	218	1.39
Zone 4	251–291	09-13-2010	6	58	2	4E	1.5	1.2	248	1.58
Zone 1	389–420	09-13-2010	6	49	2	<6	1.8	2.9	246	1.51
USGS 137A										
Zone 5	12–90	07-15-2013	6	31	7	<4	2.4	0.4	237	1.98
Zone 4	93–156	07-15-2013	7	29	6	<4	2.1	0.5	233	1.93
Zone 3	159–234	07-15-2013	7	31	6	6	2.0	0.4	231	1.95
Zone 1	247–267	07-15-2013	8	31	6	7	2.3	0.8	238	1.96

Table 6. Measurements of the stable isotope ratios of hydrogen, oxygen, and carbon and activity of tritium for water-quality analyses from precipitation (snow core), surface water, and groundwater, Idaho National Laboratory, eastern Idaho.

[Data from Bartholomay and Twining (2010), Bartholomay and others (2015), Rattray (2018), and U.S. Geological Survey (2021). Snow core sample location was a snow grab-sample collected at USGS 83 (Rightmire and Lewis, 1987). **Site name:** Alternate names used in other reports shown in table 1. **Approximate depth of open intervals below water table:** Range of depth may include multiple open intervals. **Date sampled:** Represents collection date of tritium sample if different than collection date of stable isotope ratios. **Abbreviations:** E, estimated value; na, not applicable; nd, not determined. **Units:** ft bwt, foot below water table; mm-dd-yyyy, month, day, year; ‰, per mil; pCi/L, picocuries per liter. **Symbols:** δ^2H, $\delta^{18}O$, and $\delta^{13}C$, delta notation for the stable isotope ratios of hydrogen, oxygen, and carbon; ±, plus or minus the indicated standard deviation (standard deviations are 1 sigma)]

Site name (fig. 1)	Approximate depth of open intervals below water table (ft bwt)	Date sampled (mm-dd-yyyy)	δ^2H ±1.0‰	$\delta^{18}O$ ±0.10‰	$\delta^{13}C$ ±0.1‰	Tritium (pCi/L)
SNOW CORE						
USGS 83[1]	na	02-02-1978	–141.3E	–18.70E	nd	nd
SURFACE WATER						
Big Lost River below INL Diversion (BLRINL)	na	06-02-1995	–132	–17.34	–10.15	52±1.6
Big Lost River below lower Lincoln Blvd Bridge (BLRLB)	na	05-21-1997	–132	–17.17	–10.9	nd
DEEP GROUNDWATER						
EBR 1	14–489	10-16-1996	–139.4	–18.13	–8.0	–3.2±13
CONTAMINATED GROUNDWATER						
Advanced Test Reactor Complex						
USGS 65	0–30	05-16-1991	–133.0	–16.90	–10.4	39,600±380
Central Facilities Area						
CFA 1	0–206	07-16-1996	–137.4	–17.71	–9.43	18,800±1,600
CFA 2	50–210	07-16-1996	–136.6	–17.23	–11.99±0.05	14,100±1,400
USGS 104	0–142	07-15-1996	–139.1	–18.09	–9.30±0.03	1,670±240
Idaho Nuclear Technology and Engineering Center						
USGS 57	8–113	05-13-1991	–135	–17.7	–11.3	25,600±1,400
Radioactive Waste Management Complex						
RWMC M3S	13–43	07-22-1996	–137.5	–17.98	–8.87	2,000±600
USGS 88	0–45	04-04-1989	nd	nd	nd	90±160
USGS 120	21–88	07-17-1996	–136.8	–17.61	–9.38	174.1±5.4
NATURAL GROUNDWATER						
Fire Station 2	7–91	10-16-1996	–138.7	–17.94	–9.32	36.5±1.6
Site 4	21–96	10-16-1996	–137.9	–17.74	–10.19	51.5±1.9
Site 19	1–371	07-16-1996	–139.0	–18.04	–8.35	13.4±1.0
USGS 8	12–42	10-08-1996	–136	–17.78	–9.41±0.00	47.4±0.5
USGS 83	15–251	04-11-1995	–138.9	–18.14	nd	–190±70
USGS 86	0–39	10-11-1996	–139.4	–18.13	–8.90±0.01	2.9±1.0
USGS 107	0–208	10-09-1996	–134.3	–17.55	–9.21±0.05	10.2±1.0
USGS 119	0–20	04-18-2017	nd	nd	nd	–2.3±1.6

Table 6. Measurements of the stable isotope ratios of hydrogen, oxygen, and carbon and activity of tritium for water-quality analyses from precipitation (snow core), surface water, and groundwater, Idaho National Laboratory, eastern Idaho.—Continued

[Data from Bartholomay and Twining (2010), Bartholomay and others (2015), Rattray (2018), and U.S. Geological Survey (2021). Snow core sample location was a snow grab-sample collected at USGS 83 (Rightmire and Lewis, 1987). **Site name:** Alternate names used in other reports shown in table 1. **Approximate depth of open intervals below water table:** Range of depth may include multiple open intervals. **Date sampled:** Represents collection date of tritium sample if different than collection date of stable isotope ratios. **Abbreviations:** E, estimated value; na, not applicable; nd, not determined. **Units:** ft bwt, foot below water table; mm-dd-yyyy, month, day, year; ‰, per mil; pCi/L, picocuries per liter. **Symbols:** δ^2H, $\delta^{18}O$, and $\delta^{13}C$, delta notation for the stable isotope ratios of hydrogen, oxygen, and carbon; ±, plus or minus the indicated standard deviation (standard deviations are 1 sigma)]

Site name (fig. 1)	Approximate depth of open intervals below water table (ft bwt)	Date sampled (mm-dd-yyyy)	δ^2H ±1.0‰	$\delta^{18}O$ ±0.10‰	$\delta^{13}C$ ±0.1‰	Tritium (pCi/L)
GROUNDWATER FROM MULTILEVEL WELLS						
MIDDLE 2050A						
Zone 15	0–60	08-27-2008	–134.3	–17.7	–10.34	172±5.4
Zone 12	164–224	08-27-2008	–137.9	–18.0	–11.05	93.8±3.5
Zone 9	311–328	08-26-2008	–135.0	–18.1	–8.80	60.9±2.9
Zone 6	520–562	08-26-2008	–135.7	–18.1	–8.13	5.4±1.9
Zone 3	701–748	08-26-2008	–134.7	–17.8	–13.21	97.6±3.5
MIDDLE 2051						
Zone 12	0–45	08-25-2008	–134.1	–17.3	–10.69	51.7±2.9
Zone 9	184–207	08-25-2008	–135.9	–17.9	–7.45	475±13
Zone 6	262–312	08-21-2008	–136.0	–18.0	–8.13	635±19
Zone 3	526–564	08-21-2008	–137.0	–18.0	–8.26	292±8.6
Zone 1	576–612	08-21-2008	–135.7	–18.0	–7.76	300±8.9
USGS 103						
Zone 17	85–106	08-20-2008	–135.1	–17.7	–8.79	8±1.9
Zone 15	182–247	08-19-2008	–136.2	–17.8	–9.06	16.9±1.9
Zone 12	307–335	08-19-2008	–137.7	–18.0	–9.25	72.4±2.9
Zone 9	373–429	08-18-2008	–137.8	–18.0	–8.90	275±8
Zone 6	478–513	08-18-2008	–138.1	–18.0	–8.92	434±13
Zone 3	599–655	08-18-2008	–139.2	–17.9	–8.86	427±12
Zone 1	672–694	08-19-2008	–135.0	–18.0	–8.93	405±13
USGS 105						
Zone 13	34–79	09-16-2010	–136	–17.90	–9.17	171.3±5.4
Zone 11	157–189	09-16-2010	–138	–17.84	–9.24	186.3±5.7
Zone 8	256–309	09-15-2010	–138	–17.95	–9.01	231.3±6.7
Zone 5	362–429	09-15-2010	–137	–17.95	–9.01	262.9±7.7
Zone 2	552–603	09-15-2010	–137	–17.80	–9.41	126.3±4.1
USGS 108						
Zone 11	30–67	06-23-2011	–136	–17.79	–9.15	58.8±3
Zone 9	179–218	06-23-2011	–137	–17.87	–9.00	119±3
Zone 7	260–292	06-23-2011	–136.0	–17.88	–9.02	79.3±2.4
Zone 4	406–448	06-22-2011	–137	–17.94	–9.15	83.6±3.1
Zone 1	549–582	06-22-2011	–137	–17.96	–9.17	97.4±3.3

Table 6. Measurements of the stable isotope ratios of hydrogen, oxygen, and carbon and activity of tritium for water-quality analyses from precipitation (snow core), surface water, and groundwater, Idaho National Laboratory, eastern Idaho.—Continued

[Data from Bartholomay and Twining (2010), Bartholomay and others (2015), Rattray (2018), and U.S. Geological Survey (2021). Snow core sample location was a snow grab-sample collected at USGS 83 (Rightmire and Lewis, 1987). **Site name:** Alternate names used in other reports shown in table 1. **Approximate depth of open intervals below water table:** Range of depth may include multiple open intervals. **Date sampled:** Represents collection date of tritium sample if different than collection date of stable isotope ratios. **Abbreviations:** E, estimated value; na, not applicable; nd, not determined. **Units:** ft bwt, foot below water table; mm-dd-yyyy, month, day, year; ‰, per mil; pCi/L, picocuries per liter. **Symbols:** δ^2H, $\delta^{18}O$, and $\delta^{13}C$, delta notation for the stable isotope ratios of hydrogen, oxygen, and carbon; ±, plus or minus the indicated standard deviation (standard deviations are 1 sigma)]

Site name (fig. 1)	Approximate depth of open intervals below water table (ft bwt)	Date sampled (mm-dd-yyyy)	δ^2H ±1.0‰	$\delta^{18}O$ ±0.10‰	$\delta^{13}C$ ±0.1‰	Tritium (pCi/L)
GROUNDWATER FROM MULTILEVEL WELLS—Continued						
USGS 131A						
Zone 12	16–86	07-17-2013	–138	–17.99	nd	983±26.3
Zone 8	249–296	07-16-2013	–137	–17.81	nd	1,454±38.5
Zone 5	410–512	07-16-2013	–138	–18.03	nd	149±4.86
Zone 3	574–611	07-16-2013	–137	–18.07	nd	133±4.51
USGS 132						
Zone 17	17–53	08-14-2008	–137.5	–17.7	–9.81	122±4.1
Zone 14	120–180	08-13-2008	–134.4	–17.9	–8.73	252±7.7
Zone 11	205–257	08-13-2008	–135.7	–17.8	–9.20	256±8
Zone 8	304–328	08-13-2008	–136.1	–17.8	–9.14	269±8.6
Zone 5	377–436	08-12-2008	–137.0	–17.9	–9.17	301±8.9
Zone 1	545–607	08-12-2008	–135.9	–17.8	–9.53	286±8.6
USGS 133						
Zone 10	17–49	09-02-2008	–137.6	–18.1	–8.58	131±4.1
Zone 7	125–160	09-02-2008	–136.5	–18.1	–8.95	6.9±1.8
Zone 4	255–265	09-02-2008	–137.8	–18.2	–8.83	7.9±1.7
Zone 1	294–335	09-02-2008	–135.8	–18.0	–8.87	12.4±2.2
USGS 134						
Zone 15	41–77	09-04-2008	–137.0	–18.1	–8.48	17±1.9
Zone 12	126–139	09-04-2008	–137.0	–18.1	–8.58	261±7.3
Zone 9	178–207	09-03-2008	–136.6	–18.2	–8.03	9.1±1.7
Zone 6	269–305	09-03-2008	–136.7	–18.1	–7.15	3±1.8
Zone 3	333–355	09-03-2008	–136.2	–18.2	–8.52	88.7±3.2
USGS 135						
Zone 10	10–45	09-14-2010	–137	–17.92	–9.06	14±1.9
Zone 7	106–144	09-14-2010	–138	–18.02	–9.36	6.1±1.9
Zone 4	251–291	09-13-2010	–137	–17.90	–8.87	15±2.2
Zone 1	389–420	09-13-2010	–137	–17.92	–9.29	12.8±1.9
USGS 137A						
Zone 5	12–90	07-15-2013	–137	–17.83	nd	106±3.83
Zone 4	93–156	07-15-2013	–137	–17.81	nd	89.2±3.47
Zone 3	159–234	07-15-2013	–137	–17.89	nd	67.6±2.97
Zone 1	247–267	07-15-2013	–137	–17.89	nd	64.8±2.87

[1]Stable isotope data from snow core collected at site Big Lost River below INL Diversion (Benjamin and others, 2004).

Variability and bias of water samples (Rattray, 2012, 2014) collected from MLW were evaluated with 23 replicate and 9 blank quality-assurance samples (Bartholomay and Twining, 2010; Bartholomay and others, 2015). Variability was evaluated as reproducibility with normalized absolute difference (NAD, referred to as Z-value in some of the above reports) for radiochemical and isotopic constituents and relative percent difference (RPD) or relative standard deviation (RSD) for chemical constituents. Acceptable reproducibility for each constituent was defined as an NAD, RPD, or RSD of less than 1.96, 20 percent, and 14 percent (Rattray, 2012, 2014), respectively, in at least 90 percent of the replicate samples in which the constituent was analyzed.

Reproducibility of all constituents met the acceptance criteria except for fluoride, aluminum, chromium, iron, and manganese. Acceptance criteria may not have been met for fluoride, aluminum, chromium, iron, and manganese because their concentrations were near their respective reporting levels (Rattray, 2012, 2014, 2018). However, results for fluoride, aluminum, chromium, iron, and manganese are suitable for the purposes of this report because the larger variability for concentrations of fluoride, aluminum, chromium, iron, and manganese near their reporting levels has no impact on phase mass transfers calculated with the geochemical model.

Concentrations of ions, metals, and nutrients in blank samples were nearly equal to or less than their respective reporting levels or estimated background concentrations. These results indicate that there was no bias in the environmental samples from field or laboratory procedures and methods.

Charge balance (CB) errors of 5 percent or less (absolute value) generally indicate that major ion analyses of water samples are acceptable (Freeze and Cherry, 1979). Charge balance errors for 72 of the 74 water samples in this study were equal to or less than 5 percent (table 4). Charge balance errors for the other two samples—a water sample from Zone 15 at USGS 134 and the snow core sample from USGS 83—were -6.5 and -33.7 percent, respectively. The error for the water sample from USGS 134 slightly exceeds the generally accepted criteria for CB, but this CB error is small enough that the accuracy of the chemical analyses for this sample are suitable for the purposes of this report. The CB error for the snow core sample was quite large and was caused by the calculated speciation of carbon species for this dilute and acidic (pH of 5.0; table 3) sample. Due to the dilute concentration of this sample (SpC of 16 µS/cm; table 3), however, large errors in major ion concentrations of this sample will have minimal effect on phase mass transfers during geochemical modeling.

Sources of Solutes

Identifying the potential sources of solutes in groundwater in the study area is an important step in developing an accurate geochemical model of the aquifer system. Solutes in the aquifer are derived from natural recharge, anthropogenic inputs, and water-rock interaction. Natural recharge provides the baseline concentrations of solutes in the aquifer; anthropogenic inputs provide large, localized inputs of solutes to the aquifer; and solute concentrations are modified by water-rock interaction as groundwater moves through the aquifer. Solute concentrations in the aquifer also may be modified by dispersion, diffusion, and mixing of water (including mixing of water from different aquifer depths during pumping of long, open well intervals while collecting water samples; Rattray, 2018, table 11).

Natural Recharge

Natural recharge to the study area includes infiltration of precipitation, infiltration of the Big Lost River (BLR) through the stream channel and the Idaho National Laboratory (INL) spreading areas, and groundwater inflow from adjacent areas of the eastern Snake River Plain (ESRP) aquifer (Rattray, 2018). Precipitation is only a small source of recharge at the INL (Rattray, 2019). However, because precipitation is dilute (specific conductance of 16 µS/cm at 25 °C for snow core; table 3), where recharge of precipitation does occur, it should decrease concentrations of solutes in groundwater. However, if precipitation infiltrates through the unsaturated zone near the Advanced Test Reactor Complex (ATRC), Idaho Nuclear Technology and Engineering Center (INTEC), or Radioactive Waste Management Complex (RWMC), it may transport waste constituents from the unsaturated zone to the aquifer and increase concentrations of waste constituents in the aquifer. The BLR recharge is typically more dilute than groundwater at the INL (Rattray, 2018, table 12), and because infiltration recharge from the BLR is spatially concentrated in the stream channel and the INL spreading areas recharge from the BLR may locally decrease concentrations of solutes in groundwater. The Big Lost River originates in strata chiefly composed of limestone in the mountains northwest of the INL (fig. 2), where the geology limits the groundwater concentrations of sodium, potassium, fluoride, and silica (table 4). Consequently, concentrations of these chemical species may significantly decrease in groundwater affected by recharge from the BLR. Infiltration recharge may transport dissolved oxygen and carbon dioxide to the aquifer from the atmosphere and unsaturated zone, respectively, and may produce increased concentrations of these dissolved gases in groundwater.

Groundwater inflow to the study area largely originates from tributary valleys north and northwest of the INL, although regional groundwater east of the INL may be a source of water to USGS 103 in the southeastern part of the study area (fig. 1; Rattray, 2018, 2019). Tributary valley groundwater originates in carbonate strata, whereas regional groundwater has had a significant residence time in the silicate rocks of the ESRP aquifer. Both strata typically consist of a Ca-HCO_3 type water (fig. 8; see section, "Classification of Water Types" in Rattray, 2018) for a discussion on natural groundwater, groundwater that has been modified by anthropogenic inputs, and geothermal water sources (Rattray, 2018, fig. 10). However, distinguishing between tributary valley and regional groundwater is straightforward because concentrations of calcium, magnesium, and sulfate were higher and sodium, potassium, fluoride, silica, and lithium were lower in tributary valley groundwater than in regional groundwater (Rattray, 2018).

Anthropogenic Inputs

Anthropogenic inputs potentially affecting groundwater in the study area (fig. 1) include wastewater discharge at the ATRC and INTEC (Bartholomay, Maimer, and others, 2017), application of a magnesium-chloride (Mg-Cl) brine to roads at the RWMC (Roddy, 2007; U.S. Department of Energy, 2011), and irrigation near Arco (Rattray, 2019, fig. 2). Wastewater discharge affects the chemistry of groundwater at and downgradient of these site facilities. For example, discharge of wastewater containing large amounts of sodium, chloride, sulfate, and tritium produce high concentrations or activities of these constituents in contaminated groundwater at and downgradient of the INTEC and ATRC (Rattray, 2018). Infiltration of the Mg-Cl brine may elevate concentrations of these constituents in groundwater near the RWMC (U.S. Department of Energy, 2011). Discharge of sewage to the subsurface at these facilities and at the CFA increases concentrations of nitrite plus nitrate in groundwater containing wastewater.

The amounts, locations, and methods of wastewater discharge have varied over time. For example, in 1984 discharge of low-level radioactive, chemical, and sanitary wastewater at the INTEC was changed from a 600-ft deep disposal well to infiltration ponds at the land surface (Bartholomay, Maimer, and others, 2017). Tritium activities measured in groundwater from wells USGS 57, CFA 1, and CFA 2 (table 6) reflect both the amount of tritium in discharge of wastewater from the INTEC over time and the different methods of wastewater disposal.

Irrigation near Arco (fig. 2) may affect ion concentrations in groundwater in the southwestern corner of the INL (Rattray, 2019). Irrigation water dissolves fertilizer and other soil amendments applied to the land surface and transports the dissolved ions to the aquifer (Rattray, 2015). For example, inorganic fertilizer is primarily composed of nitrogen, potassium, and phosphorus, and chemical compounds in fertilizer containing these elements also may include calcium, sodium, and sulfate. Nitrogen in fertilizer may be present in various forms, but nitrogen leached from fertilizer that infiltrates through the unsaturated zone to the aquifer will be in an oxidized form as NO_3^- (table 7). Potassium in commercial fertilizer is often present as KCl (represented with sylvite in table 7), and other soil amendments, such as gypsum or agricultural lime (typically $CaCO_3$, represented with calcite in table 7), may contribute Ca^{2+}, HCO_3^-, and SO_4^{2-} to groundwater.

Water-Rock Interaction

Water-rock interaction occurs throughout the ESRP aquifer and unsaturated zone and solutes may be dissolved from, or sorbed or precipitated onto, the aquifer matrix. In the southwestern part of the INL, potential water-rock interaction includes carbonate reactions, dissolution of evaporite minerals, weathering of silicate minerals, and precipitation of goethite (Rattray, 2018, 2019).

Water-rock interactions are driven by the thermodynamic state of water as well as that of the other relevant phases contacting the water, such as the minerals that compose the aquifer matrix. Thus, the thermodynamic state of water places constraints on which chemical reactions may take place in the aquifer (table 7). The thermodynamic state of various types of water in the study area (precipitation, BLR, and groundwater) was evaluated by calculating the mineral-water thermodynamic saturation index[8] (SI) (table 8) of individual water-quality samples with respect to albite and anorthite (plagioclase), forsterite (olivine), amorphous silica (representing volcanic glass with composition from McLing, 1994) (silicate minerals); gypsum, halite, fluorite, sylvite (evaporate minerals); ammonium nitrate; dolomite and calcite (carbonate minerals); and calcium montmorillonite and goethite (secondary minerals). Saturation indices were calculated using the computer code PHREEQC (Parkhurst and Appelo, 2013), the thermodynamic databases wateq4f.dat (for the mineral forsterite) and phreeqc.dat (for all other minerals in table 8) provided with PHREEQC, and the chemical composition of water-quality samples (tables 2, 3, and 4). Saturation indices (SIs) less than -0.1 were interpreted to indicate that the water is undersaturated with respect to the mineral (the mineral may dissolve into solution), SIs greater than 0.1 were interpreted to indicate that the water is supersaturated with respect to the mineral (the mineral may precipitate from solution), and SIs of -0.1–0.1 were interpreted to indicate that the water is in approximate equilibrium with the mineral (the mineral may dissolve or precipitate).

[8]The equation for calculating saturation indices is shown in Rattray (2019, appendix 1, eq. 1-2).

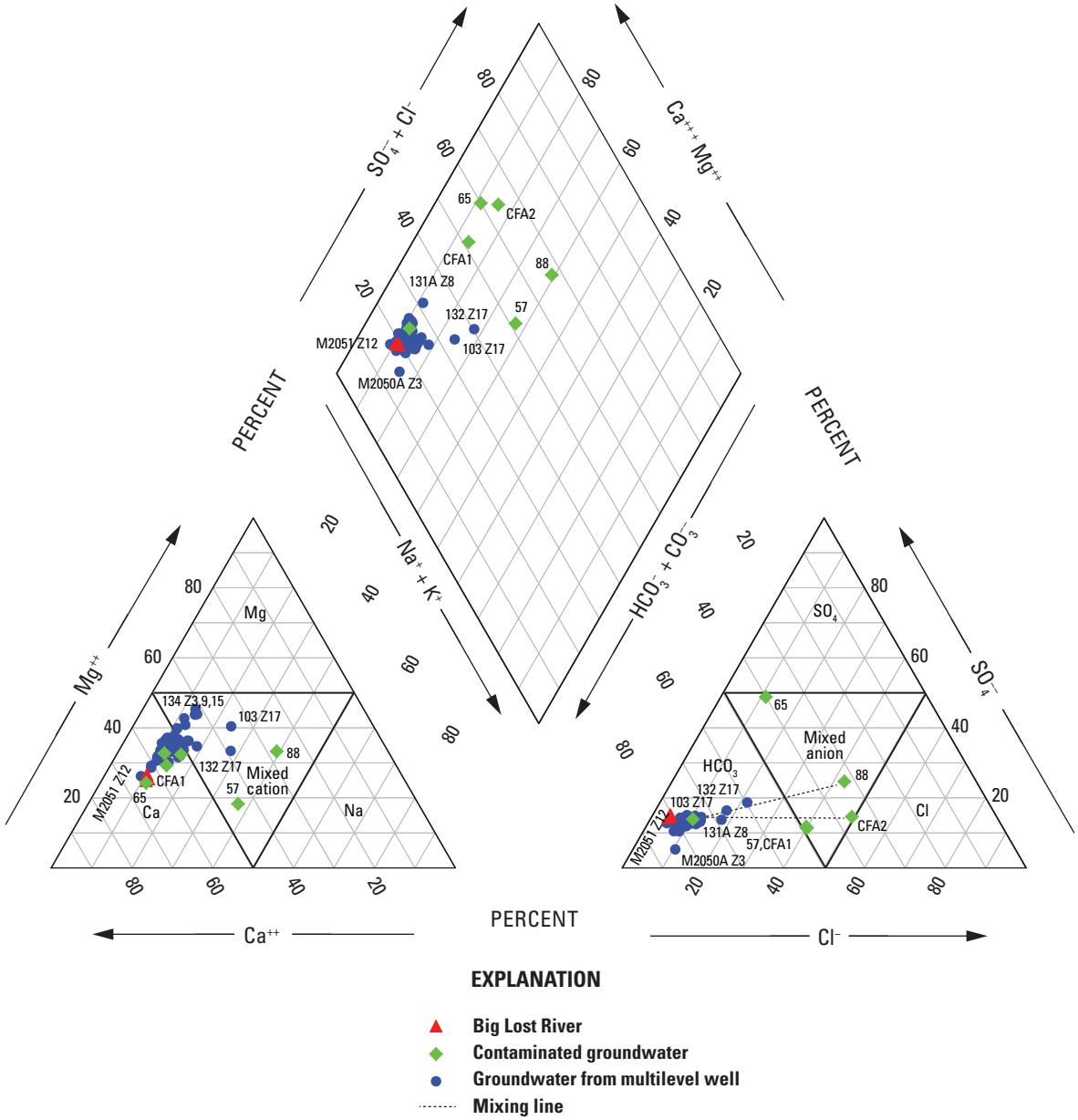

Figure 8. Water types (hydrochemical facies) of surface water and groundwater, Idaho National Laboratory, eastern Idaho. Abbreviations for site names are shown in table 1. More information is available from the National Water Information System (NWIS) at https://doi.org/10.5066/F7P55KJN (U.S. Geological Survey, 2021).

Table 7. Chemical reactions that may act as sources or sinks of gases and solutes to or from groundwater, Idaho National Laboratory, eastern Idaho.

[Adapted from Rattray (2019)]

Inputs	Chemical reactions
	Carbonate reactions
Calcite	$CaCO_3 + CO_2 + H_2O \leftrightarrow Ca^{2+} + 2HCO_3^-$
Dolomite	$CaMg(CO_3)_2 + 2CO_2 + 2H_2O \rightarrow Ca^{2+} + Mg^{2+} + 4HCO_3$
	Dissolution of evaporite minerals
Gypsum	$CaSO_4 \cdot H_2O \rightarrow Ca^{2+} + SO_4^{2-} + 2H_2O$
Halite	$NaCl \rightarrow Na^+ + Cl^-$
Fluorite	$CaF_2 \rightarrow Ca^{2+} + 2F^-$
Sylvite	$KCl \rightarrow K^+ + Cl^-$
	Dissolution of anthropogenic inputs
Inorganic fertilizer (ammonium nitrate)	$NH_4NO_3 + 2O_2 \rightarrow 2NO_3^- + 2H^+ + H_2O$
	Weathering of silicate minerals
Dissolution of Olivine (Forsterite, Fo_{85})	$Mg_{1.7}Fe_{0.3}SiO_4 + 4CO_2 + 4H_2O \rightarrow 1.7Mg^{2+} + 0.3Fe^{2+} + 4HCO_3^- + H_4SiO_4$
Plagioclase (An_{60}) to Ca-montmorillonite	$Ca_{0.6}Na_{0.4}Al_{1.6}Si_{2.4}O_8 + 0.13H_4SiO_4 + 1.36CO_2 + 1.12H_2O \rightarrow$ $0.69Ca_{0.17}Al_{2.33}Si_{3.67}O_{10}(OH)_2 + 0.48Ca^{2+} + 0.4Na^+ + 1.36HCO_3^-$
Volcanic glass (basalt) to Ca-montmorillonite	$SiAl_{0.08}Fe_{0.19}Mg_{0.1}Ca_{0.26}Na_{0.03}K_{0.01}O_{2.69} + 1.12CO_2 + 2.36H_2O \rightarrow$ $0.034Ca_{0.17}Al_{2.33}Si_{3.67}O_{10}(OH)_2 + 0.88H_4SiO_4 + 0.19Fe^{2+} + 0.1Mg^{2+} +$ $0.25Ca^{2+} + 0.03Na^+ + 0.01K^+ + 1.12HCO_3^-$
Precipitation of Ferric Oxyhydroxide	$Fe_3^+ + 2H_2O \rightarrow FeOOH + 3H^+$

Table 8. Mineral/water thermodynamic saturation indices for selected minerals with respect to chemical compositions for precipitation, surface water, and groundwater, Idaho National Laboratory, eastern Idaho.

[Snow core sample location was a snow grab-sample collected at USGS 83 (Rightmire and Lewis, 1987). **Site name:** Alternate names used in other reports shown in table 6. Saturation indexes are log (IAP/K) (ion activity product/equilibrium constant); negative values not in colored cells indicate undersaturation, positive values indicate saturation (light gray colored cells), and zero plus or minus 0.10 indicates equilibrium (dark gray colored cells). **Symbol:** –, missing chemistry data for calculation of saturation index]

Site name (fig. 1)	Albite	Anorthite	Forsterite	Amorphous silica	Gypsum	Halite	Fluorite	Sylvite	Dolomite	Calcite	Calcium montmorillonite	Goethite
SNOW CORE												
USGS 83	–	–	–26.39	–1.67	–5.53	–11.27	–5.25	–8.91	–16.89	–8.55	–	–
SURFACE WATER												
Big Lost River below INL Diversion (BLRINL)	–2.59	–3.53	–6.88	–0.91	–2.50	–9.32	–2.50	–8.58	0.52	0.48	0.51	7.03
Big Lost River below lower Lincoln Blvd Bridge (BLRLB)	–1.53	–1.45	–10.09	–0.93	–2.54	–9.35	–2.45	–8.48	–1.10	–0.32	4.62	7.86
DEEP GROUNDWATER												
EBR1	–1.32	–2.93	–6.19	–0.49	–2.76	–8.79	–2.75	–7.87	0.50	0.20	1.96	7.43
CONTAMINATED GROUNDWATER												
USGS 65	–1.69	–3.33	–7.78	–0.65	–1.37	–8.09	–3.43	–7.43	0.38	0.42	1.70	8.32
CFA 1	–1.65	–3.56	–8.32	–0.64	–2.17	–7.51	–2.09	–6.85	0.11	0.23	1.93	7.83
CFA 2	–1.31	–3.41	–8.03	–0.59	–1.93	–7.16	–1.67	–6.54	0.21	0.24	2.15	8.20
USGS 104	–1.83	–3.87	–7.66	–0.57	–2.49	–8.55	–2.48	–7.73	0.19	0.22	1.48	7.85
USGS 57	–0.83	–2.73	–8.45	–0.62	–2.06	–6.90	–1.95	–6.63	–0.07	0.15	2.86	6.52
RWMC M3S	–1.59	–3.14	–7.44	–0.60	–2.33	–8.49	–2.07	–7.67	0.47	0.37	2.05	7.73
USGS 88	–0.70	–3.39	–6.59	–0.50	–2.07	–6.96	–2.24	–6.46	0.30	0.13	1.81	6.87
NATURAL GROUNDWATER												
Fire Station 2	–1.48	–3.01	–8.04	–0.60	–2.26	–8.38	–2.35	–7.59	0.43	0.38	2.58	7.80
Site 4	–1.50	–3.08	–7.83	–0.60	–2.40	–8.63	–2.37	–7.95	0.42	0.39	2.36	7.56
Site 19	–2.14	–3.69	–7.62	–0.71	–2.42	–8.57	–2.51	–7.87	0.50	0.33	1.32	7.71
USGS 8	–1.85	–3.36	–8.24	–0.68	–2.36	–8.77	–2.36	–8.03	0.30	0.32	2.11	7.70
USGS 83	–1.42	–3.47	–7.51	–0.55	–2.55	–8.50	–2.40	–7.77	–0.03	0.11	1.91	7.50
USGS 86	–1.64	–4.10	–7.40	–0.54	–2.39	–8.19	–2.61	–7.45	0.23	0.33	1.08	7.70
USGS 107	–1.34	–3.53	–7.11	–0.51	–2.38	–8.02	–2.05	–7.34	0.50	0.32	1.65	7.53
USGS 119	–1.34	–3.38	–6.69	–0.50	–2.29	–8.41	–1.78	–7.71	0.26	0.26	1.52	6.77

Table 8. Mineral/water thermodynamic saturation indices for selected minerals with respect to chemical compositions for precipitation, surface water, and groundwater, Idaho National Laboratory, eastern Idaho.—Continued

[Snow core sample location was a snow grab-sample collected at USGS 83 (Rightmire and Lewis, 1987). **Site name:** Alternate names used in other reports shown in table 6. Saturation indexes are log (IAP/K) (ion activity product/equilibrium constant); negative values indicate undersaturation, positive values not in colored cells indicate saturation (light gray colored cells), and zero plus or minus 0.10 indicates equilibrium (dark gray colored cells). **Symbol:** –, missing chemistry data for calculation of saturation index]

Site name (fig. 1)	Albite	Anorthite	Forsterite	Amorphous silica	Gypsum	Halite	Fluorite	Sylvite	Dolomite	Calcite	Calcium montmorillonite	Goethite
GROUNDWATER FROM MULTILEVEL WELLS												
MIDDLE 2050A												
Zone 15	–1.76	–3.57	–9.26	–0.62	–2.23	–8.37	–2.32	–7.64	–0.22	0.07	2.45	6.43
Zone 12	–2.07	–3.76	–9.26	–0.67	–2.38	–8.63	–2.41	–7.80	–0.38	–0.04	2.12	6.45
Zone 9	–1.96	–3.72	–9.07	–0.66	–2.36	–8.56	–2.40	–7.90	–0.17	0.04	2.14	6.44
Zone 6	–2.27	–4.09	–9.43	–0.69	–2.40	–8.63	–2.45	–7.97	–0.42	–0.10	1.81	6.33
Zone 3	–2.32	–4.49	–8.86	–0.71	–2.77	–8.28	–2.12	–7.65	–0.11	0.02	1.04	7.07
MIDDLE 2051												
Zone 12	–2.10	–4.11	–10.35	–0.57	–2.32	–9.02	–2.35	–8.07	–0.91	–0.22	2.36	6.10
Zone 9	–1.79	–3.48	–9.43	–0.62	–2.29	–8.59	–2.42	–7.82	–0.48	–0.11	2.63	6.33
Zone 6	–1.94	–3.71	–9.05	–0.64	–2.28	–8.57	–2.43	–7.82	–0.26	0.00	2.13	6.45
Zone 3	–1.83	–3.53	–9.11	–0.60	–2.42	–8.58	–2.53	–7.75	–0.50	–0.19	2.51	6.35
Zone 1	–1.56	–3.08	–9.08	–0.59	–2.41	–8.56	–2.51	–7.73	–0.48	–0.19	3.05	6.59
USGS 103												
Zone 17	–3.47	–5.57	–7.18	–1.14	–2.61	–8.09	–2.10	–7.45	0.27	0.13	–1.61	7.21
Zone 15	–1.31	–3.52	–8.88	–0.49	–2.45	–8.27	–2.18	–7.59	–0.57	–0.20	2.63	6.46
Zone 12	–1.35	–3.35	–9.04	–0.50	–2.53	–8.55	–2.54	–7.75	–0.65	–0.24	2.92	6.46
Zone 9	–1.58	–3.56	–8.99	–0.53	–2.45	–8.49	–2.49	–7.69	–0.45	–0.13	2.57	6.45
Zone 6	–1.59	–3.42	–9.07	–0.57	–2.41	–8.45	–2.47	–7.65	–0.45	–0.12	2.69	6.45
Zone 3	–1.59	–3.55	–9.06	–0.54	–2.40	–8.43	–2.45	–7.64	–0.44	–0.11	2.58	6.45
Zone 1	–1.13	–2.60	–9.03	–0.54	–2.40	–8.43	–2.46	–7.66	–0.45	–0.12	3.67	6.63
USGS 105												
Zone 13	–1.51	–3.43	–8.38	–0.59	–2.37	–8.38	–2.45	–7.67	–0.08	0.09	2.27	6.84
Zone 11	–1.39	–3.25	–8.38	–0.58	–2.37	–8.38	–2.45	–7.69	–0.04	0.11	2.49	6.47
Zone 8	–1.38	–3.22	–7.87	–0.56	–2.37	–8.37	–2.45	–7.65	0.19	0.22	2.31	6.50
Zone 5	–1.36	–3.20	–8.31	–0.56	–2.38	–8.38	–2.45	–7.64	–0.04	0.11	2.55	6.83
Zone 2	–1.33	–3.11	–8.40	–0.58	–2.36	–8.41	–2.08	–7.72	–0.03	0.13	2.65	6.60

Table 8. Mineral/water thermodynamic saturation indices for selected minerals with respect to chemical compositions for precipitation, surface water, and groundwater, Idaho National Laboratory, eastern Idaho.—Continued

[Snow core sample location was a snow grab-sample collected at USGS 83 (Rightmire and Lewis, 1987). **Site name:** Alternate names used in other reports shown in table 6. Saturation indexes are log (IAP/K) (ion activity product/equilibrium constant); negative values indicate undersaturation, positive values not in colored cells indicate saturation (light gray colored cells), and zero plus or minus 0.10 indicates equilibrium (dark gray colored cells). **Symbol:** –, missing chemistry data for calculation of saturation index]

Site name (fig. 1)	Albite	Anorthite	Forsterite	Amorphous silica	Gypsum	Halite	Fluorite	Sylvite	Dolomite	Calcite	Calcium montmorillonite	Goethite
GROUNDWATER FROM MULTILEVEL WELLS—Continued												
USGS 108												
Zone 11	–1.48	–3.76	–8.27	–0.51	–2.41	–8.26	–2.13	–7.56	–0.08	0.05	2.07	7.82
Zone 9	–1.43	–3.29	–8.17	–0.52	–2.36	–8.37	–2.44	–7.61	0.05	0.12	2.53	6.30
Zone 7	–1.60	–3.50	–8.57	–0.54	–2.34	–8.39	–2.42	–7.63	–0.06	0.07	2.42	6.23
Zone 4	–1.51	–3.27	–8.53	–0.54	–2.30	–8.37	–2.39	–7.62	–0.02	0.10	2.66	6.23
Zone 1	–2.01	–4.15	–9.71	–0.57	–2.30	–8.37	–2.40	–7.59	–0.58	–0.19	2.17	5.84
USGS 131A												
Zone 12	–1.78	–3.78	–8.10	–0.57	–2.35	–8.42	–2.40	–7.62	0.13	0.21	1.79	6.35
Zone 8	–1.56	–3.44	–8.29	–0.55	–2.22	–8.14	–2.34	–7.37	0.12	0.22	2.23	6.95
Zone 5	–1.52	–3.06	–7.70	–0.59	–2.32	–8.50	–2.39	–7.76	0.46	0.35	2.35	6.86
Zone 3	–1.64	–3.13	–7.73	–0.62	–2.33	–8.51	–2.39	–7.79	0.50	0.37	2.22	6.31
USGS 132												
Zone 17	–1.04	–3.43	–8.31	–0.56	–2.20	–7.57	–2.15	–7.09	–0.08	0.03	2.46	6.60
Zone 14	–1.47	–3.39	–8.23	–0.56	–2.34	–8.45	–2.12	–7.71	0.01	0.11	2.31	6.59
Zone 11	–1.42	–3.19	–8.75	–0.55	–2.34	–8.57	–2.44	–7.78	–0.26	0.00	2.79	6.54
Zone 8	–1.48	–3.35	–9.19	–0.55	–2.35	–8.57	–2.44	–7.78	–0.51	–0.12	2.86	6.45
Zone 5	–1.49	–3.35	–8.34	–0.55	–2.34	–8.55	–2.44	–7.78	–0.07	0.10	2.41	6.60
Zone 1	–1.44	–3.55	–8.53	–0.56	–2.34	–8.43	–2.43	–7.73	–0.09	0.09	2.33	6.61
USGS 133												
Zone 10	–2.68	–4.77	–10.02	–0.79	–2.38	–8.50	–2.38	–7.63	–0.78	–0.21	1.15	6.17
Zone 7	–2.26	–4.75	–9.74	–0.56	–2.40	–8.54	–2.42	–7.67	–0.76	–0.22	1.45	6.30
Zone 4	–1.88	–3.84	–9.74	–0.58	–2.41	–8.58	–2.42	–7.79	–0.70	–0.19	2.47	6.54
Zone 1	–2.20	–4.29	–9.69	–0.67	–2.32	–8.44	–2.94	–7.82	–0.33	–0.01	1.81	6.87
USGS 134												
Zone 15	–1.78	–3.95	–8.19	–0.54	–2.60	–8.69	–2.63	–7.88	–0.25	–0.12	1.89	6.59
Zone 12	–1.83	–4.13	–9.17	–0.52	–2.49	–8.58	–3.10	–7.83	–0.40	–0.16	2.13	6.32
Zone 9	–1.73	–3.92	–7.69	–0.52	–2.63	–8.76	–2.63	–7.97	–0.01	0.01	1.66	6.61
Zone 6	–2.06	–4.29	–8.38	–0.57	–2.51	–8.63	–2.56	–7.84	–0.22	–0.07	1.38	6.52
Zone 3	–1.86	–4.67	–10.64	–0.39	–2.62	–8.76	–3.24	–7.91	–1.67	–0.83	2.49	5.93

Table 8. Mineral/water thermodynamic saturation indices for selected minerals with respect to chemical compositions for precipitation, surface water, and groundwater, Idaho National Laboratory, eastern Idaho.—Continued

[Snow core sample location was a snow grab-sample collected at USGS 83 (Rightmire and Lewis, 1987). **Site name:** Alternate names used in other reports shown in table 6. Saturation indexes are log (IAP/K) (ion activity product/equilibrium constant); negative values indicate undersaturation, positive values not in colored cells indicate saturation (light gray colored cells), and zero plus or minus 0.10 indicates equilibrium (dark gray colored cells). **Symbol:** –, missing chemistry data for calculation of saturation index]

Site name (fig. 1)	Albite	Anorthite	Forsterite	Amorphous silica	Gypsum	Halite	Fluorite	Sylvite	Dolomite	Calcite	Calcium montmorillonite	Goethite
GROUNDWATER FROM MULTILEVEL WELLS—Continued												
USGS 135												
Zone 10	–1.72	–3.13	–8.79	–0.67	–2.39	–8.80	–2.38	–8.10	–0.18	0.11	2.59	6.79
Zone 7	–1.78	–3.48	–9.54	–0.61	–2.45	–8.87	–2.44	–8.07	–0.79	–0.22	2.72	6.45
Zone 4	–1.83	–3.36	–9.16	–0.66	–2.39	–8.81	–2.38	–8.07	–0.35	0.03	2.53	6.54
Zone 1	–1.92	–3.45	–9.50	–0.69	–2.43	–8.84	–2.42	–8.06	–0.58	–0.12	2.60	6.32
USGS 137A												
Zone 5	–1.21	–3.14	–7.43	–0.53	–2.32	–8.29	–2.44	–7.60	0.42	0.32	2.26	6.35
Zone 4	–1.26	–3.07	–7.49	–0.55	–2.35	–8.41	–2.46	–7.68	0.37	0.30	2.35	6.35
Zone 3	–1.27	–3.05	–7.50	–0.55	–2.34	–8.45	–2.44	–7.75	0.41	0.33	2.35	6.83
Zone 1	–1.19	–2.94	–7.48	–0.55	–2.35	–8.43	–2.45	–7.74	0.40	0.32	2.47	6.89

Carbonate Reactions

Dissolution of carbonate minerals occurs in the aquifer, or in the unsaturated zone, because calcite and dolomite are present in surficial and interbed sediments and these minerals rapidly dissolve in solution. Calcite also may precipitate from solutions that are supersaturated with respect to calcite (fig. 9), but precipitation of dolomite is kinetically unlikely in the ESRP aquifer (Rattray and Ginsbach, 2014). Dissolution of calcite or dolomite will consume CO_2 while releasing Ca, Mg (from dolomite), and HCO_3 to solution (table 7). Precipitation of calcite is the reverse reaction.[9]

Dissolution of Evaporite Minerals

Gypsum present in sediment at the INL may be associated with eolian sediment or "ancient evaporative playas or evaporative marginal lacustrine environments" (Geslin and others, 2002, p. 23). Evaporative environments occurred in the Big Lost Trough and the Mud Lake subbasin (fig. 2), which were periodically filled with water as Pleistocene Lake Terreton advanced and receded in response to glacial and interglacial periods (Gianniny and others, 2002; Mark and Thackray, 2002). Gypsum is the only evaporate mineral that has been identified in surficial or interbed sediment at the INL, but other evaporate minerals such as halite, fluorite, and sylvite also may have been deposited. These evaporate minerals are undersaturated in all surface water and groundwater at the INL, rapidly dissolve in solution, and may release Ca^{2+}, SO_4^{2-}, Na^+, Cl^-, F^-, and K^+ to solution (table 7). Evaporite minerals may be most common inside the area encompassed by the Big Lost Trough (fig. 2).

Weathering of Silicate Minerals

The silicate minerals that compose the aquifer within the study area (plagioclase, olivine, volcanic glass; represented with albite, anorthite, forsterite, and amorphous silica in table 8) were always undersaturated in groundwater at the INL in our data and may chemically weather (dissolve) through hydrolysis reactions (table 7). However, most silicate minerals dissolve slowly in groundwater due to kinetic and (or) diffusive limitations on the rate of dissolution (Gronow, 1987; Lasaga and others, 1994). Dissolution rates for these minerals, from calculations of the mean lifetime of 1-millimeter (mm) crystals in a dilute solution at 25 °C and pH of 5 (pH dependence of dissolution rates is slight at near-neutral pH of 4–8), were on the order of 10^2 years for anorthite, 10^3 years for forsterite, and 10^4 years for pyroxene (Lasaga and others, 1994). Volcanic glass should dissolve rapidly because it is metastable due to its lack of crystallinity and large surface area (Deutsch and others, 1982).

Given the slow rates of dissolution for silicate minerals, except for volcanic glass, the amount of dissolution of silicate minerals as groundwater flows through the INL should be small. This interpretation is supported by the fresh, unaltered appearance of most basalt mineral grains in the shallow ESRP aquifer (Nace and others, 1956), although alteration of basalt minerals is evident in deeper parts of the aquifer (Doherty and others, 1979; Mazurek, 2004). The silicate minerals most likely to undergo some dissolution in the shallow aquifer were those minerals having the most rapid dissolution rates, such as volcanic glass, plagioclase, and olivine. Alteration of volcanic glass was described as conversion to a mass of opaque minerals and pyroxene, and the rims of olivine crystals were observed to alter to opaque minerals or iddingsite (Nace and others, 1956; Lanphere and others, 1993). Rightmire and Lewis (1987) suggested that ferric oxyhydroxide in sediment may be related to weathering of olivine and pyroxene.

Plagioclase and volcanic glass are aluminosilicate minerals that should dissolve incongruently to produce ions in solution and a secondary aluminosilicate mineral (Knobel and others, 1997). Knobel and others (1997) suggested that the secondary aluminosilicate mineral formed by incongruent dissolution of plagioclase was smectite because authigenic smectite was observed in basalt (Wood and Low, 1988) and conditions favorable for smectite formation are present in the ESRP aquifer (Rightmire and Lewis, 1987). The specific smectite mineral forming as an alteration product has not been well defined, but calcic plagioclase in basalt (An_{50-70}) and calcium-rich basalt volcanic glass should weather to calcium smectite (such as calcium montmorillonite) (Knobel and others, 1997, figs. 15–20).

Stability diagrams were prepared to identify which clay minerals (kaolinite and smectites) are thermodynamically stable relative to the composition of surface-water and groundwater samples. On a stability diagram representing stable fields for kaolinite and calcium montmorillonite (fig. 10*A*) all groundwater samples, except for USGS 103, Zone 17, plot in the calcium montmorillonite field,[10] and on a stability diagram prepared for calcium and sodium beidellite, all water samples plot in the calcium beidellite field (fig. 10*B*). Consequently, calcium smectite is the secondary aluminosilicate mineral that should form in the aquifer from incongruent dissolution of plagioclase (and volcanic glass).

Precipitation of Ferric Oxyhydroxide

Ferrous iron released to groundwater from weathering of olivine, pyroxene, and basalt volcanic glass becomes oxidized to ferric iron and forms opaque minerals (Nace and others, 1956; Lanphere and others, 1993) such as ferric oxyhydroxide (Rightmire and Lewis, 1987). Precipitation of ferric oxyhydroxide makes solutions more acidic (table 7).

[9]Molar ratios of Mg^{2+}:Ca^{2+} of less than 1 in water at the INL indicate that $CaCO_3$, and not Ca_xMg_1-xCO_3, is the carbonate mineral that should precipitate (Knobel and others, 1997). Most Mg^{2+}:Ca^{2+} molar ratios in water from the study area are less than 1.

[10]Stability diagrams were prepared using The Geochemist's Workbench computer code and the thermos.tdat database provided with the code (Bethke and Yeakel, 2017).

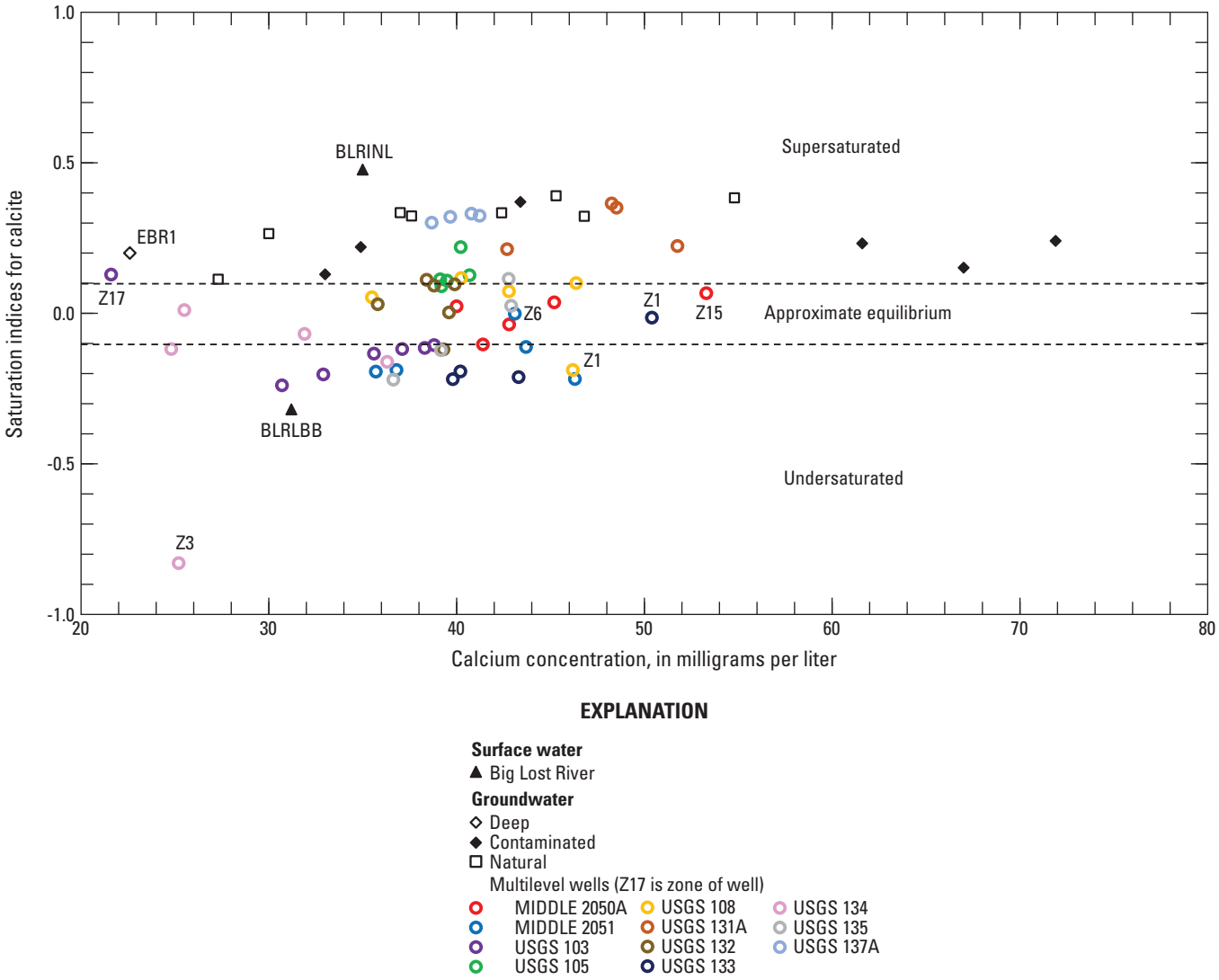

Figure 9. Calcium concentrations versus saturation indices for calcite for surface water and groundwater, Idaho National Laboratory, eastern Idaho. Location of sites shown in figure 1.

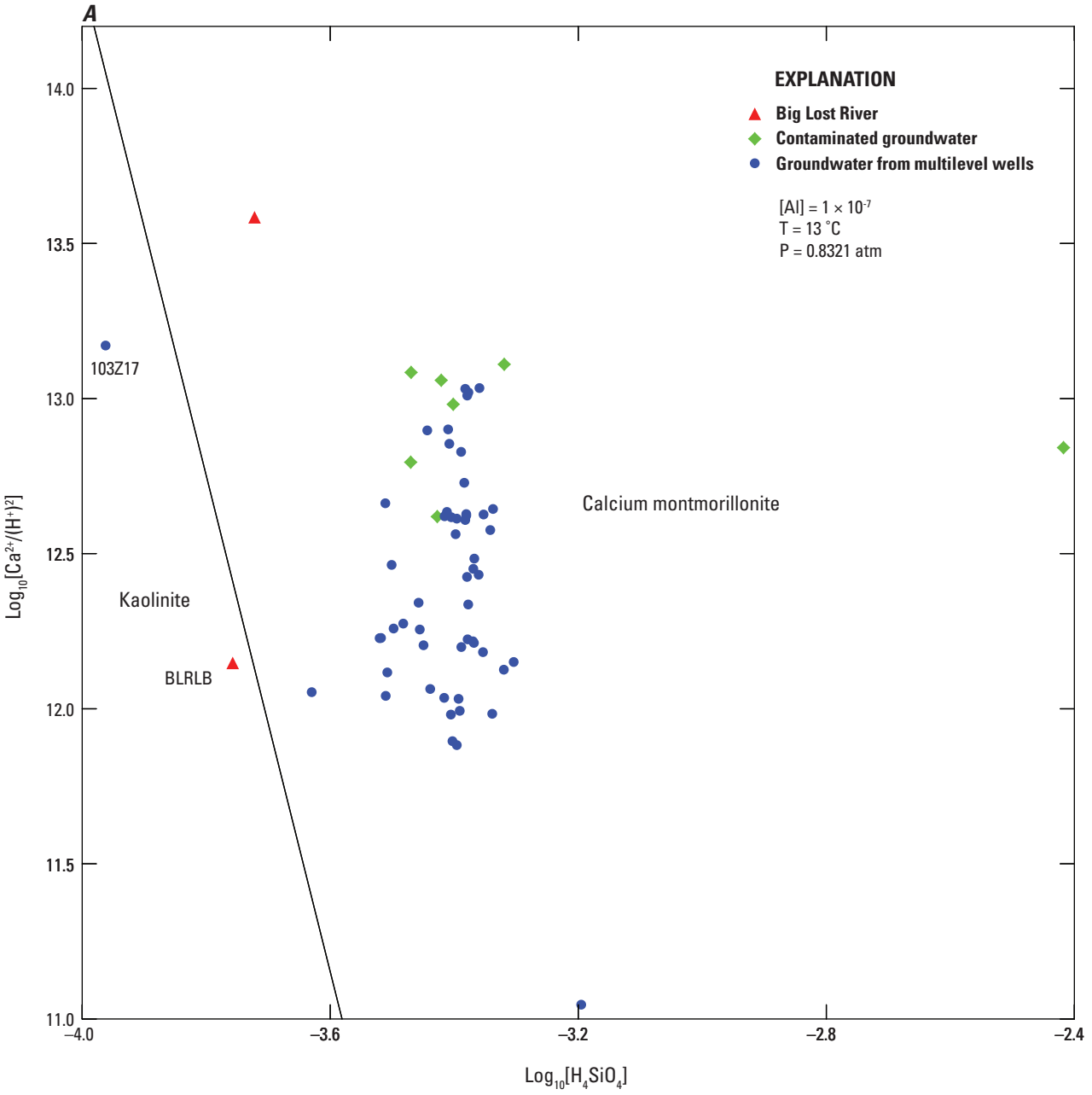

Figure 10. Selected clay minerals with superposed compositions of water samples, Idaho National Laboratory, eastern Idaho. *A.* Stability relations between kaolinite and calcium montmorillonite. *B.* Stability relations between calcium beidellite and sodium beidellite. Brackets indicate thermodynamic activity of indicated species. Abbreviated names are shown in table 1. atm, atmosphere (a measure of pressure); °C, degrees Celsius.

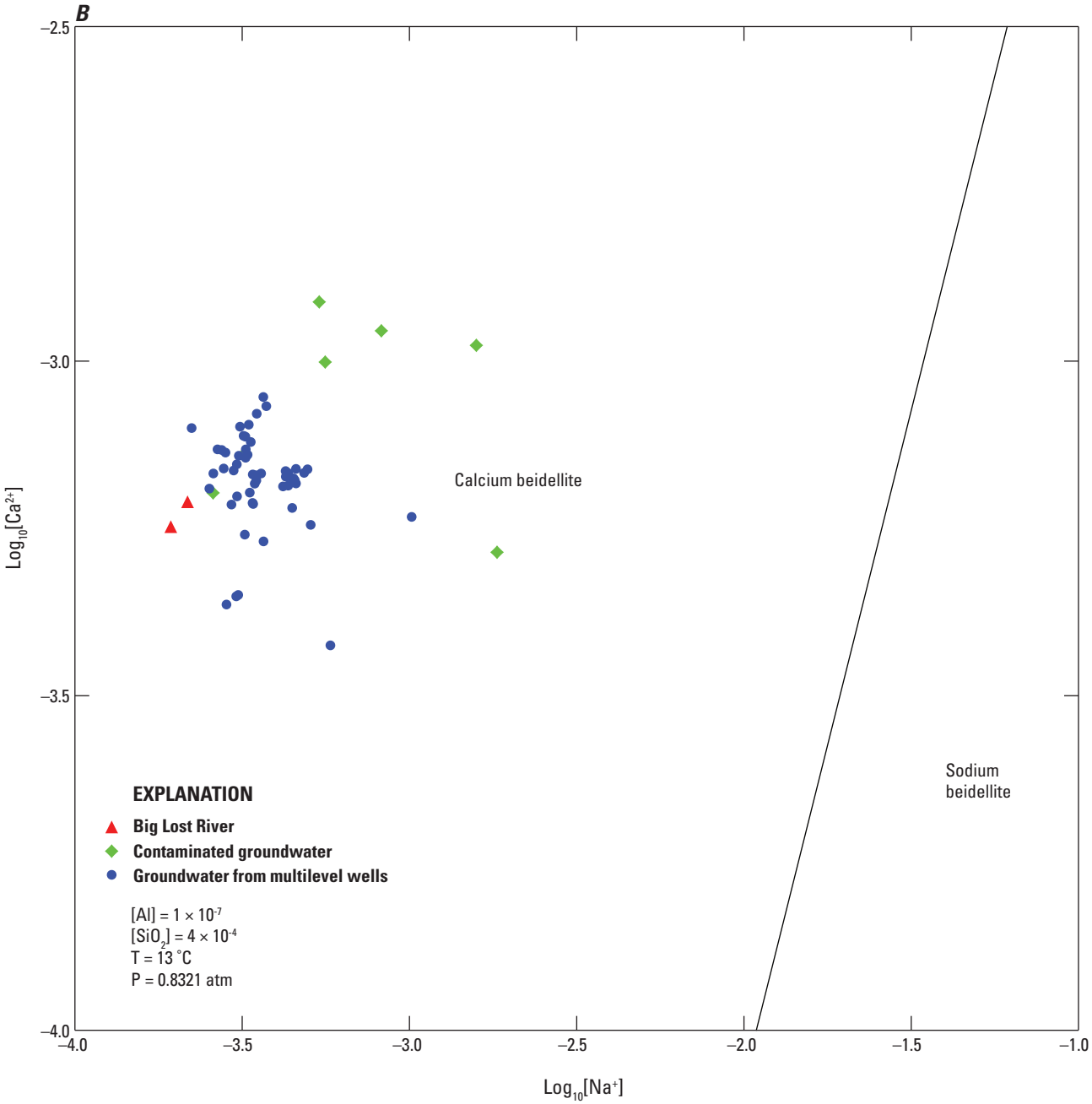

Figure 10.—Continued

Identifying Sources of Water from Water Chemistry

Differences in groundwater chemistry in the aquifer are due to the multiple sources of water to the aquifer, each with a unique water chemistry, and water-rock interaction as groundwater travels through the aquifer. Examination of the groundwater chemistry at MLW can provide information on these processes, and this information may then be used to construct hydrologically and geochemically plausible geochemical models.

Groundwater flows through the study area in approximately a north-northeast to south-southwest direction (figs. 5 and 6). Groundwater north of the study area is a mixture of surface water and groundwater from the Little Lost River (LLR) valley, groundwater from the Lost River Range, and water from the Big Lost River (BLR) (Rattray, 2018, 2019). The chemistry of this groundwater is modified by local sources of recharge that either have a recognizable influence on groundwater chemistry or an identifiable chemical signature. These local sources of recharge include (1) infiltration recharge from the BLR channel and Idaho National Laboratory (INL) spreading areas and (or) (2) injection and (or) infiltration of wastewater from the Advanced Test Reactor Complex (ATRC), Idaho Nuclear Technology and Engineering Center (INTEC), and Radioactive Waste Management Complex (RWMC) (fig. 1). Recharge from the BLR should dilute groundwater, whereas recharge from wastewater should cause groundwater concentrations of sodium, chloride, sulfate, and tritium to increase (Bartholomay, Maimer, and others, 2017).

Field Parameters and Major Ions

Concentrations of field parameters and major ions at depth-discrete sampling zones of the MLW are shown in figure 11. Some wells, such as USGS 105, USGS 108, USGS 135, and USGS 137A, have nearly uniform major ion concentrations throughout their sampling zones (fig. 11*D,* 11*E*, 11*H,* 11*I*). These MLW are in the Arco-Big Southern Butte rift zone, and the nearly uniform major ion concentrations probably result from a downward flow of water that results in a mixture of surface water and groundwater to depths at least equivalent to the bottom of these MLW. Other MLW have one or more zones with field parameters and (or) major ion concentrations that deviate from the chemistry of the other zones at that MLW (Bartholomay and Twining, 2010; Bartholomay and others, 2015). For example, at MIDDLE 2050A, the calcium concentration highest in zone 15, and sulfate and dissolved oxygen concentrations were lower for zone 3 (fig. 11*A*) than for the other zones at this MLW. This well is located within the Big Lost Trough (BLT) (fig. 2) and zone 3 is located about 701 to 748 feet below water table (ft bwt) (table 1). At the INL, higher sodium, chloride, and sulfate concentrations are often associated with groundwater containing wastewater (Rattray, 2018, p. 58), and wastewater from the ATRC and (or) INTEC are probable sources of water to zone 15. However, due to the depth of zone 3, and the abundance of sediment layers in the BLT, the source of the larger amounts of sodium and chloride to this zone may be dissolution of evaporite minerals.

Water temperature and concentrations of dissolved oxygen, specific conductance, magnesium, sodium, chloride, and sulfate were lower, and concentrations of calcium and silica were higher in zone 12 (the shallowest zone at MIDDLE 2051) than in other zones at this MLW (fig. 11*B*). Shallow groundwater at the INL that is more dilute than underlying groundwater indicates recharge from the BLR and (or) precipitation.

Dissolved oxygen, specific conductance, bicarbonate, calcium, and silica were lower, and sodium and chloride concentrations were higher in zone 17 (the shallowest zone at USGS 103) than in other zones at this MLW (fig. 11*C*). The dilute water, relative to water from underlying zones, indicates recharge from the BLR and (or) precipitation. The higher concentrations of sodium and chloride are typical of recharge of wastewater from the INTEC, although they also may reflect dissolution of halite.

Specific conductance, calcium, chloride, and sulfate concentrations were higher in zone 8 at USGS 131A than in other zones at this MLW (fig. 11*F*). High chloride and sulfate concentrations typically indicate the presence of wastewater. USGS 131A is downgradient from the INTEC and ATRC (figs. 1 and 5), so both facilities are possible sources of wastewater.

Specific conductance, sodium, chloride, and sulfate concentrations were higher in zone 17 at USGS 132 than in other zones at this MLW (fig. 11*G*). USGS 132 is near and downgradient of the RWMC (figs. 1 and 5), and high concentrations of these constituents may be due to application of a Mg-Cl brine to roads at the RWMC.

Trilinear Diagrams

Trilinear diagrams can be used to indicate broad differences in the major ion chemistry of water-quality samples and can be used to identify specific sources of recharge at MLW sampling zones that have uncharacteristic major ion concentrations. Water from the BLR, MLW, and wastewater-influenced (contaminated) groundwater from the ATRC, INTEC, and RWMC are plotted on the trilinear diagram shown in figure 8. Groundwater from the MLW is either a Ca- or mixed cation-HCO_3-type water and cluster in a small area on the cation and anion parts of the diagram.

Some groundwater from MLW, however, plot outside of these clusters. For example, the trilinear diagram shows that water from zone 3 at MIDDLE 2050A has a smaller percentage of sulfate than water from other zones at this MLW. The small percentage of sulfur in this groundwater sample is unique among water-quality samples in this study and, along with other geochemical evidence such as low concentrations of dissolved oxygen, nitrate, and a slightly elevated concentration of iron (tables 2, 3, and 4), indicates that redox reactions are taking place in zone 3.

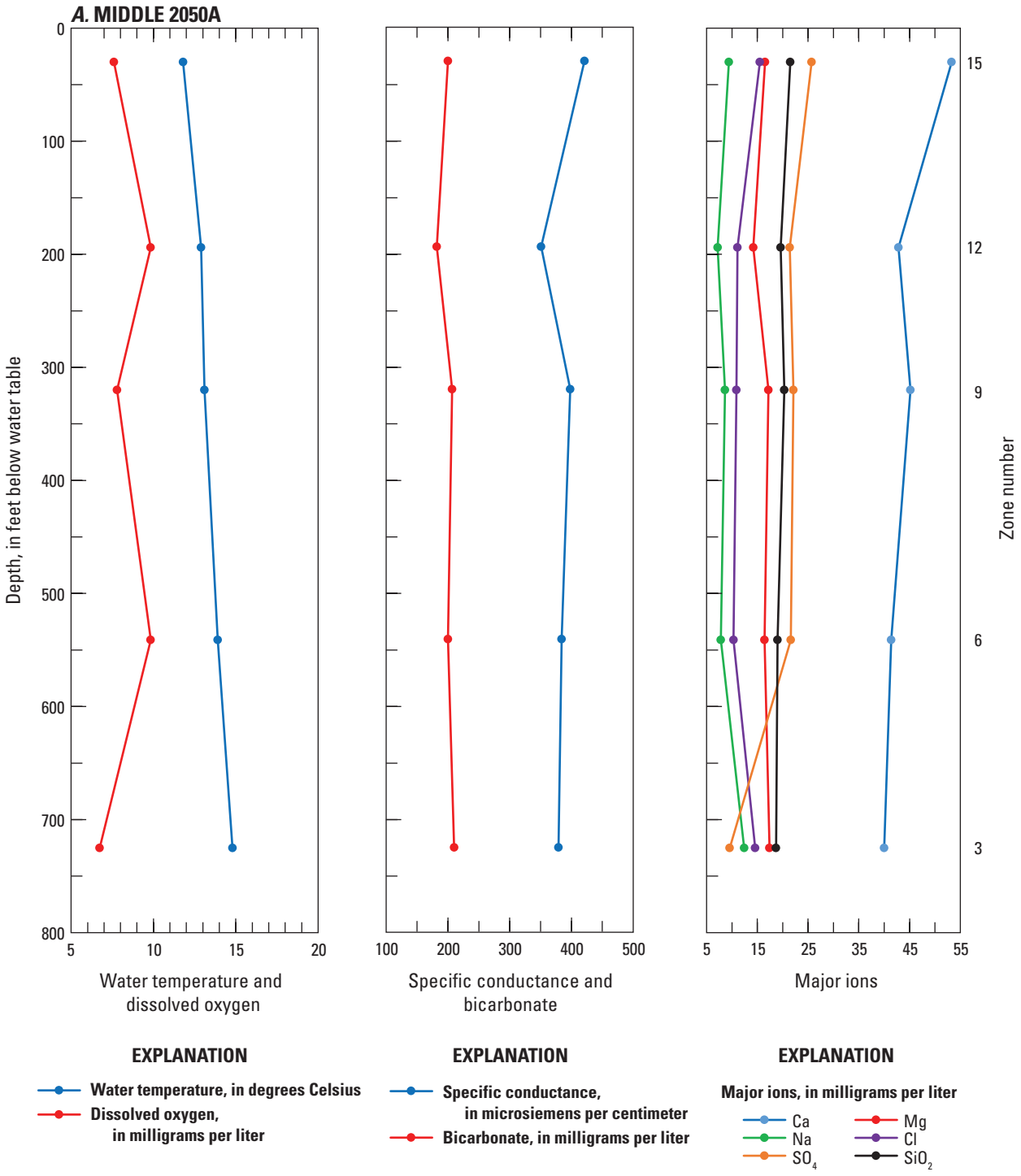

Figure 11. Selected field parameter values and major ion concentrations, Idaho National Laboratory, eastern Idaho. *A.* MIDDLE 2050A. *B.* MIDDLE 2051. *C.* USGS 103. *D.* USGS 105. *E.* USGS 108. *F.* USGS 131A. *G.* USGS 132. *H.* USGS 135. *I.* USGS 137A. Ca, calcium; Na, sodium, SO_4, sulfate; Mg, magnesium; Cl, chloride, SIO_2, silica. Location of sites is shown in figure 1. More information is available from the National Water Information System (NWIS) at https://doi.org/10.5066/F7P55KJN (U.S. Geological Survey, 2021).

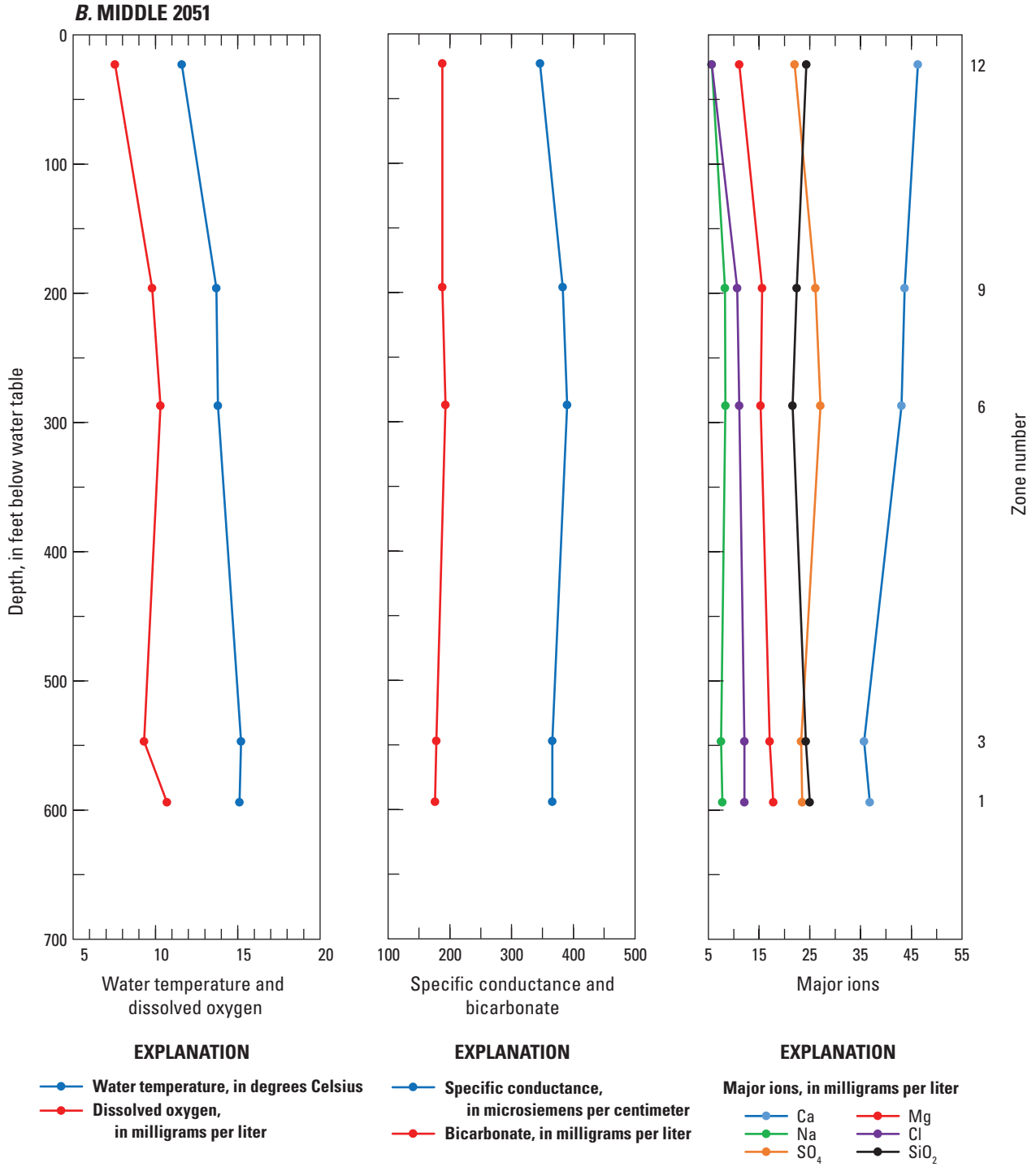

Figure 11.—Continued

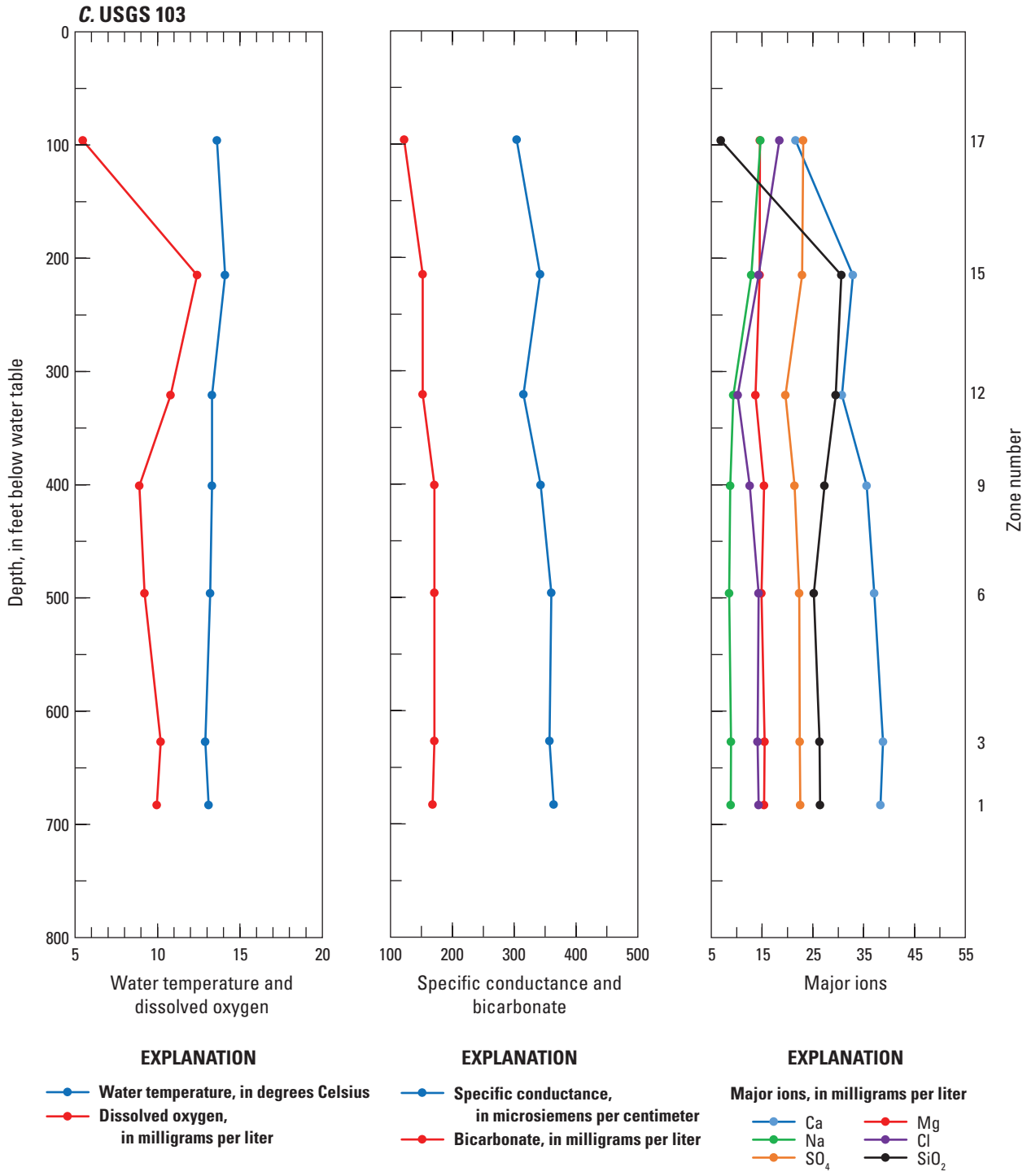

Figure 11.—Continued

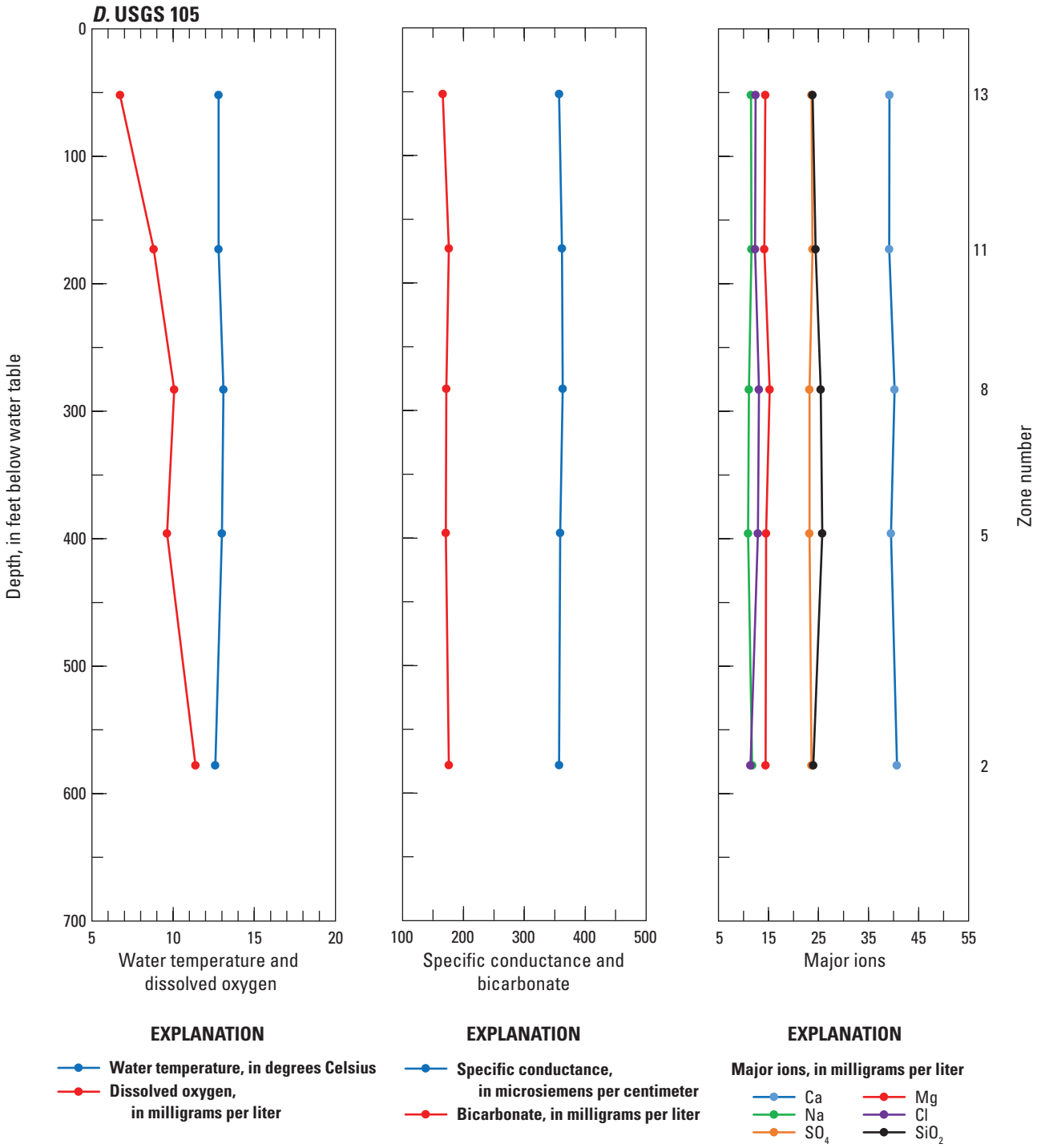

Figure 11.—Continued

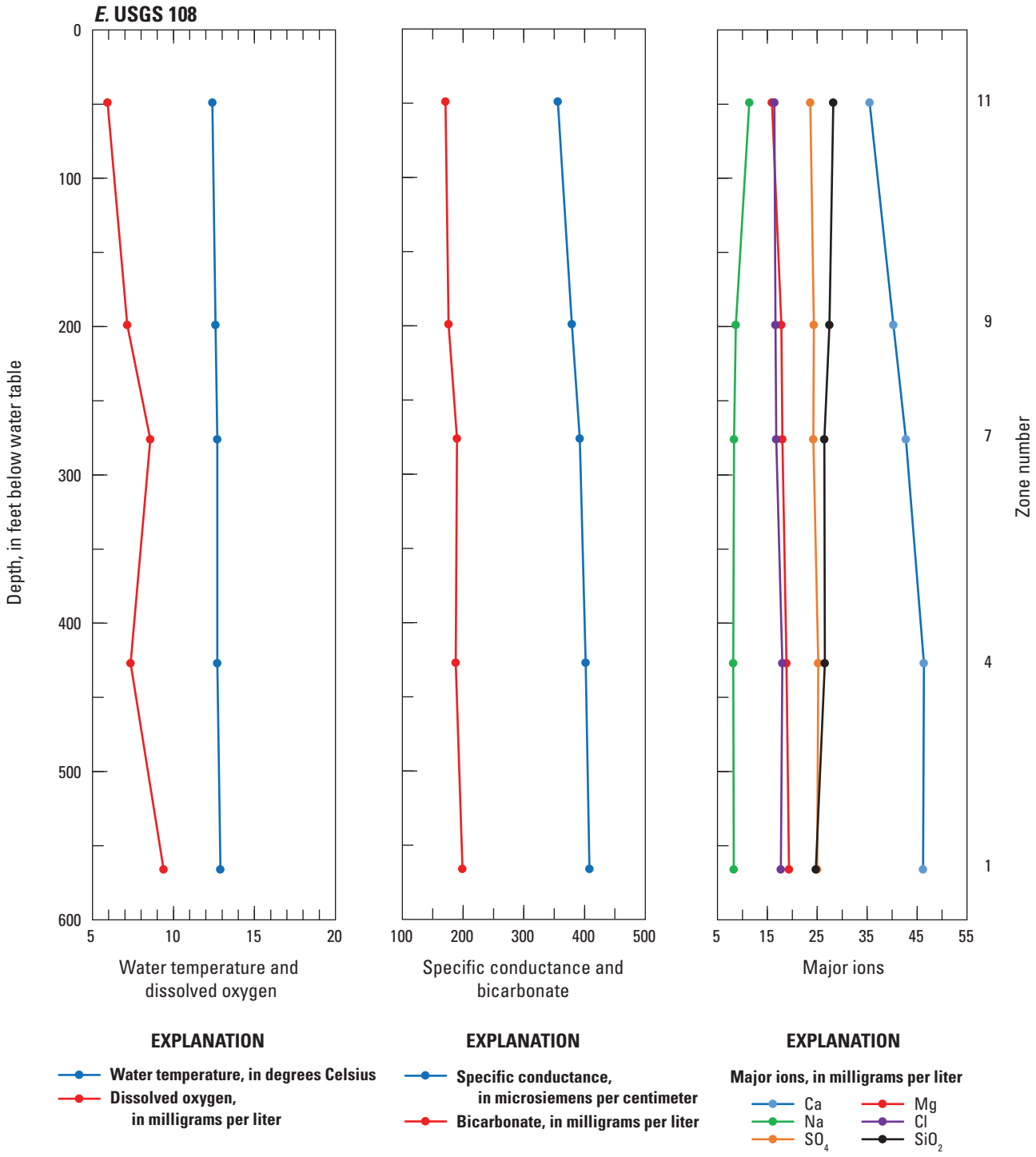

Figure 11.—Continued

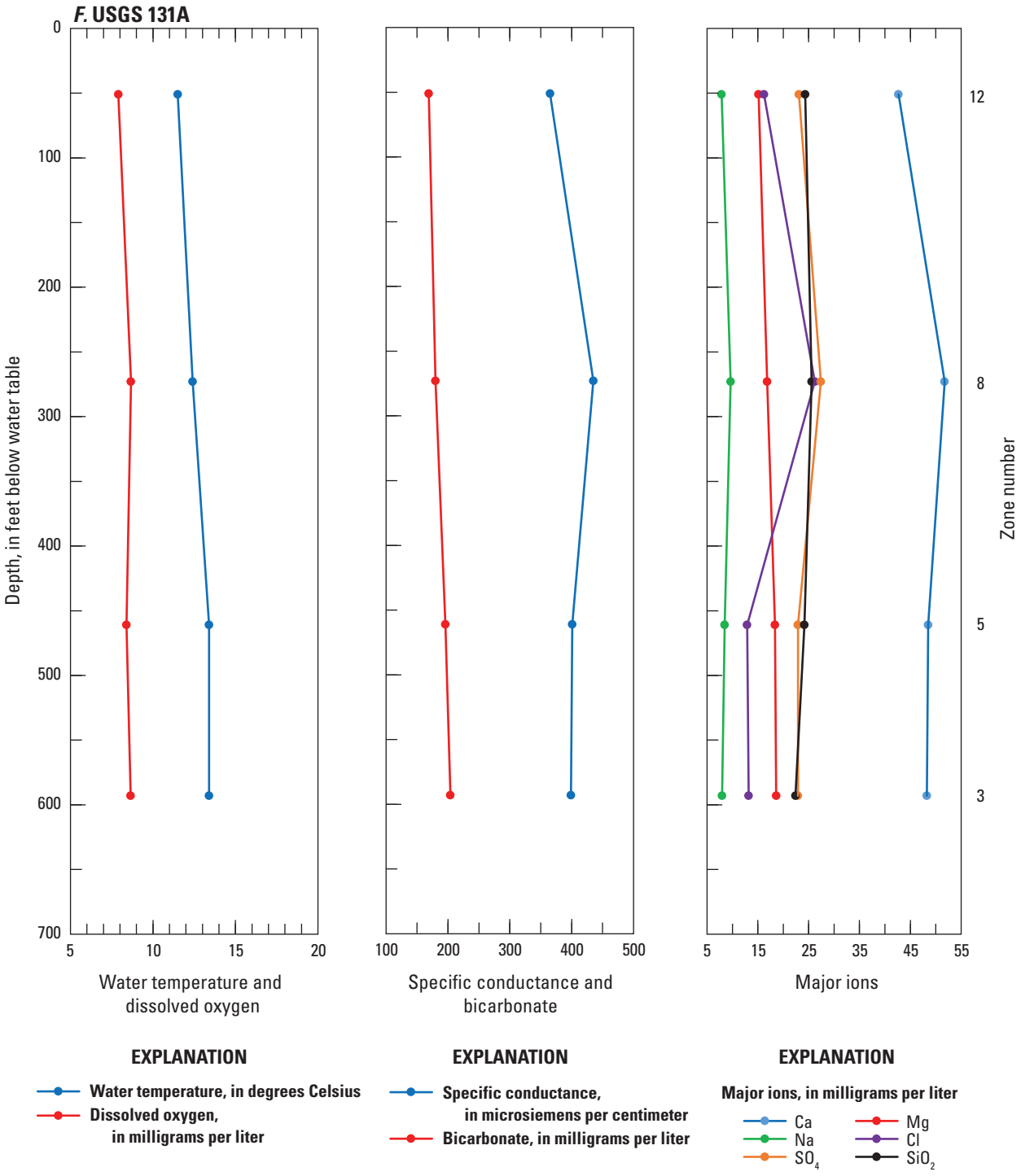

Figure 11.—Continued

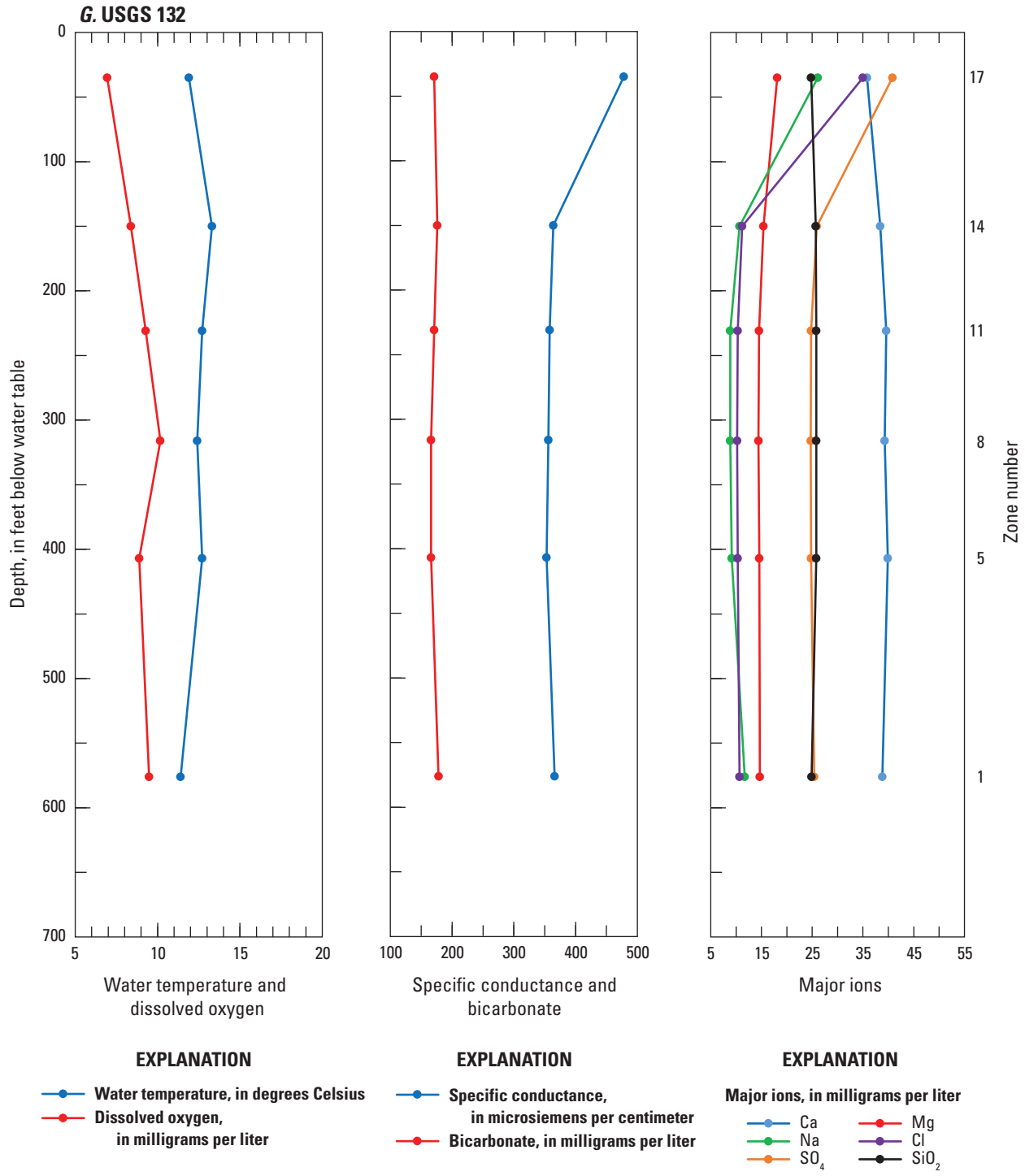

Figure 11.—Continued

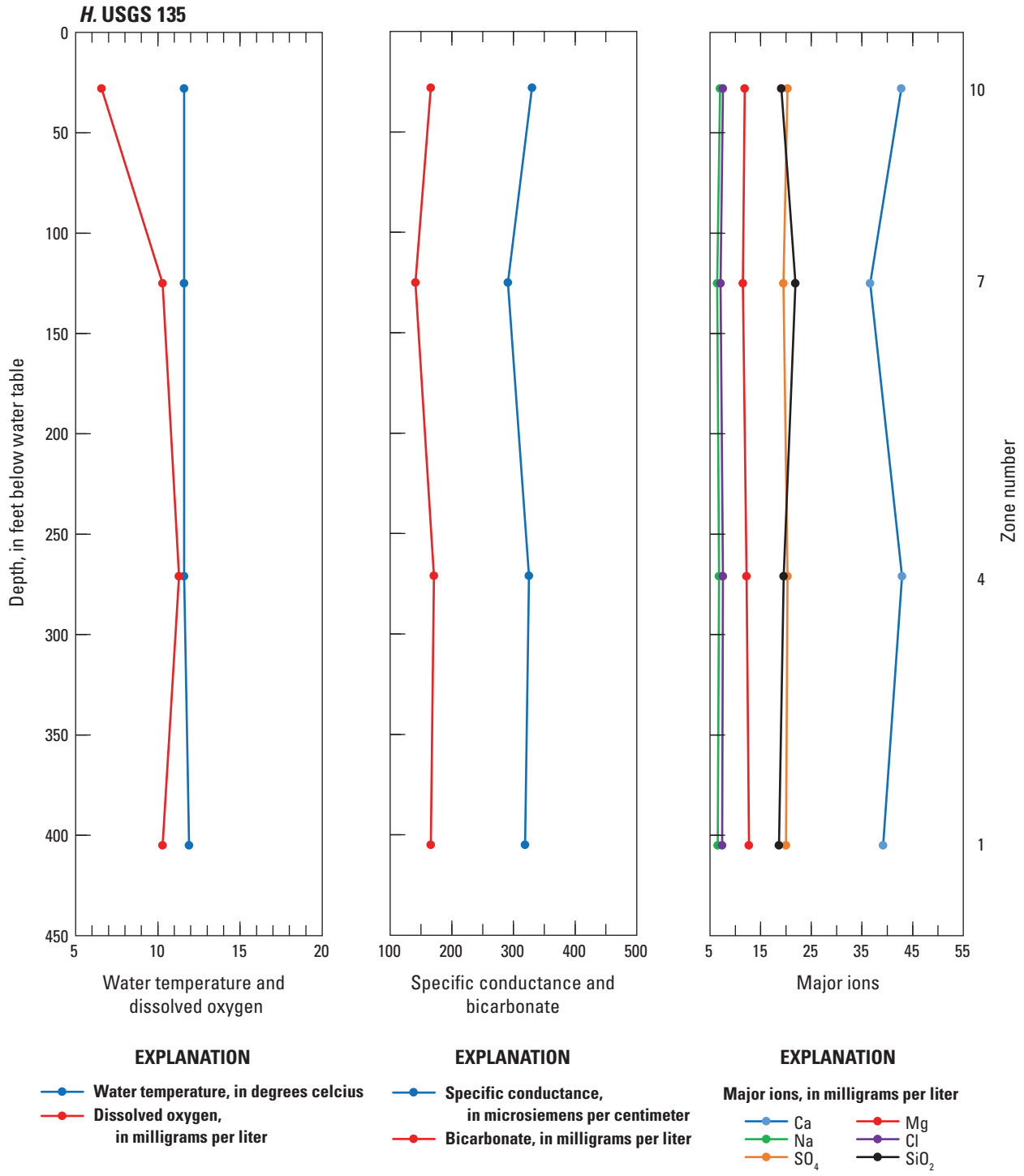

Figure 11.—Continued

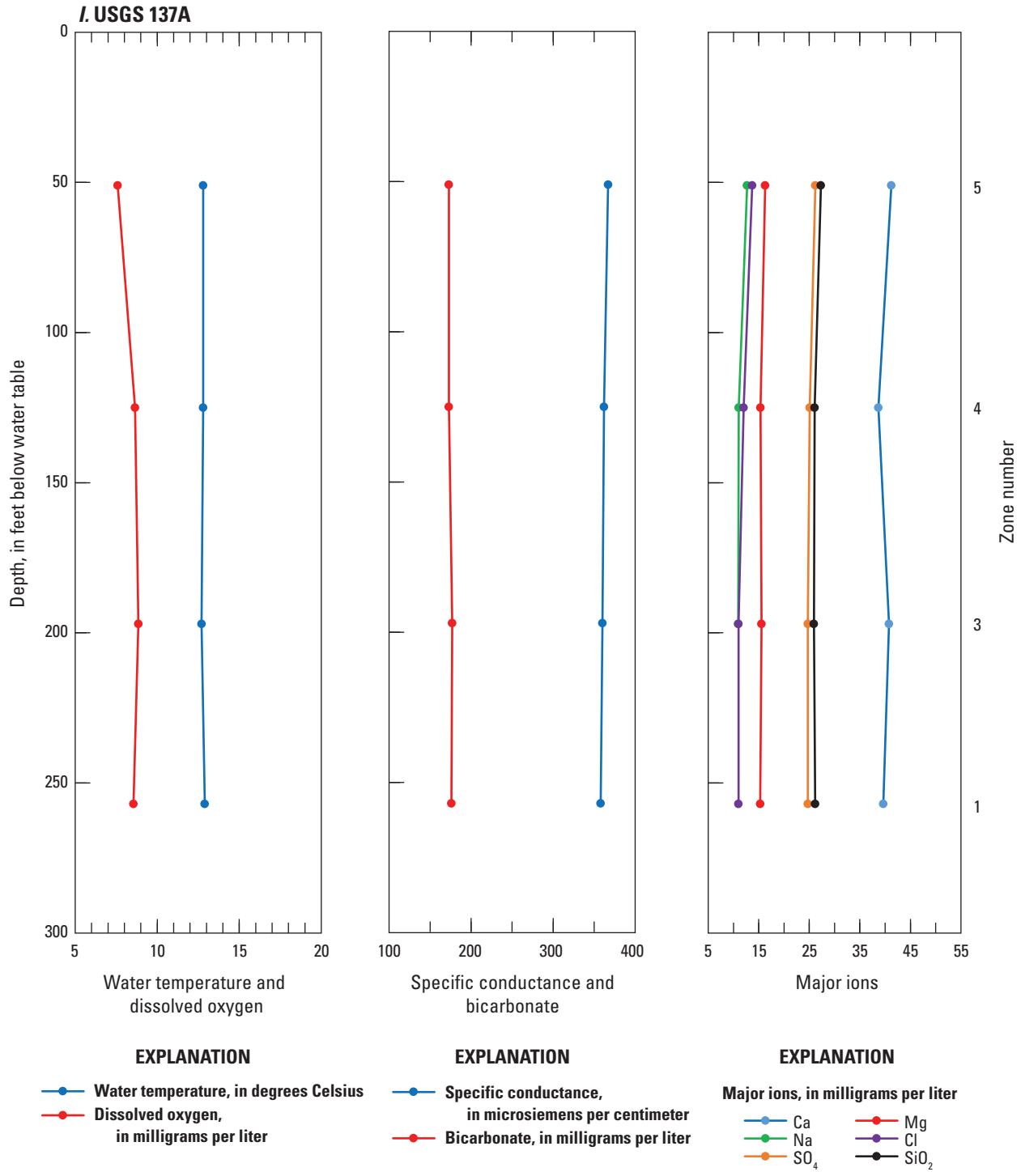

Figure 11.—Continued

The trilinear diagram shows that water from zone 12 from MIDDLE 2051 contains a smaller percentage of magnesium and chloride, as a percentage of total cations and anions, compared to water from other MLW. Water from this zone plots adjacent to water from the BLR, which indicates that the BLR may be a source of water to this zone. This interpretation is consistent with (1) zone 12 being the shallowest water sampling zone at MIDDLE 2051 (table 1) and (2) the proximity of MIDDLE 2051 to the BLR (fig. 1) (Bartholomay and Twining, 2010, p. 17).

In the trilinear diagram, percentages of some or all of sodium, chloride, and (or) sulfate in water from zone 8 from USGS 131A and zones 17 from USGS 103 and USGS 132 were larger relative to total cations and anions than other MLW. These high percentages are typically representative of wastewater in groundwater at the INL. However, determining which INL facility is the source of contamination by examining the cation part of the trilinear diagram is unreliable because cation concentrations near site facilities are affected by cation exchange (Rattray, 2019). In contrast, in the dilute, oxidizing environment of the ESRP aquifer, chloride and sulfate behave as conservative solutes and are good tracers of wastewater discharge at site facilities.

Wastewater discharged from the ATRC and INTEC is represented by USGS 65 and CFA 1/CFA 2/USGS 57, respectively, and groundwater contamination from a Mg-Cl brine applied to roads at the RWMC (U.S. Department of Energy, 2011) is represented by USGS 88. Concentrations of sulfate and chloride were high in wastewater from the ATRC and INTEC (table 4), respectively, so USGS 65 plots well above, and CFA 1/CFA 2/USGS 57 plots well to the right, of the cluster of MLW on the anion part of the trilinear diagram (fig. 8). Concentrations of chloride and sulfate were high in contaminated groundwater at USGS 88, so USGS 88 plots to the right of the cluster of MLW but above CFA 1/CFA 2/USGS 57. Water from USGS 131A, zone 8 plots on a mixing line between the cluster of MLW and CFA 2, which indicates that the source of wastewater at this zone is the INTEC. Water from USGS 132, zone 17 plots on mixing lines (anion and cation parts of the trilinear diagram) between the cluster of MLW and USGS 88, which indicates that the source of contaminants in groundwater at this zone is the Mg-Cl brine. USGS 103, zone 17 plots on the mixing line between the cluster of MLW and USGS 88, but also plots near the mixing line between the cluster of MLW and CFA 2. Because USGS 103 is downgradient of the INTEC (Rattray, 2019), but not downgradient of the RWMC, the INTEC is the most likely source of wastewater at zone 17.

Stable Isotopes

The stable isotope ratios δ^2H, $\delta^{18}O$, and $\delta^{13}C$ provide information about sources of recharge and the gas-water-rock interaction of carbonate species in the study area. Values for δ^2H and $\delta^{18}O$ are influenced by altitude, precipitation, and evaporation (Hem, 1992). The effects of altitude and precipitation produce lower δ^2H and $\delta^{18}O$ values in water from the LLR valley than the BLR valley, and evaporation of the BLR and wastewater in infiltration ponds cause the δ^2H and $\delta^{18}O$ values in this water to move towards higher values along evaporation lines (fig. 12).

The various sources of carbon in the study area influence the $\delta^{13}C$ values in groundwater at the INL. For example, $\delta^{13}C$ values were high in groundwater in the carbonate terranes north and northwest of the INL (Rattray, 2018, 2019). Consequently, recharge of groundwater from the Lost River Range[11] and the LLR valley produces relatively high $\delta^{13}C$ values in groundwater in the western part of the INL. Similarly, dissolution of carbonate rocks in sediment at the INL, with $\delta^{13}C$ values near zero, will cause $\delta^{13}C$ values in groundwater at the INL to increase. In contrast, infiltration recharge through the soil zone dissolves gaseous CO_2 with low $\delta^{13}C$ values. Transport of soil zone water to the aquifer will cause $\delta^{13}C$ values in groundwater at the INL to decrease.

δ^2H and $\delta^{18}O$ Stable Isotope Ratios

The δ^2H and $\delta^{18}O$ values for the BLR; deep, contaminated, and natural groundwater; groundwater from MLW; and a local meteoric water line for winter precipitation (Benjamin and others, 2004) are shown in figure 12. The δ^2H and $\delta^{18}O$ values for natural groundwater from USGS 8 and Site 19 are representative of the values for recharge from the BLR and LLR valleys (Rattray, 2019), respectively, and show that δ^2H and $\delta^{18}O$ values were higher in recharge from the BLR valley than in recharge from the LLR valley. High δ^2H and $\delta^{18}O$ values for the BLR,[12] USGS 65, USGS 113, USGS 120, and CFA 2 reflect the influence of evaporation from the BLR, INL spreading areas, and infiltration ponds at the ATRC and INTEC (Rattray, 2018).

Most δ^2H and $\delta^{18}O$ values for groundwater from the MLW are similar, and 87 percent of these values plot in a cluster (circle in fig. 12) near, and to the right of, the local meteoric water line for winter precipitation (fig. 12). However, δ^2H and $\delta^{18}O$ values in seven MLW sampling zones (MIDDLE 2050A, zones 3 and 15; MIDDLE 2051, zone 12; USGS 103, zones 3 and 17; and USGS 132, zones 14 and 17;) plot outside of the cluster of δ^2H and $\delta^{18}O$ values from MLW. The bulk of MLW wells with δ^2H and $\delta^{18}O$ values clustered to the right of the meteoric water line suggests most of the MLW, and corresponding zones, contain mixtures of evaporated water as recharge sources.

[11]Groundwater from USGS 23 (table 1) is representative of groundwater from the Lost River Range northwest of the INL (Busenberg and others, 2001; Rattray, 2018, 2019).

[12]The high δ^2H and $\delta^{18}O$ values for the Big Lost River (BLR) below INL Diversion (BLRINL in fig. 12) reflect significant evaporation. However, δ^2H and $\delta^{18}O$ values for the BLR near Arco (Rattray, 2019, fig. 7) are low (Rattray, 2018, table 15), which indicates that the δ^2H and $\delta^{18}O$ values in recharge from the BLR in the study area may not have undergone as much evaporation as the values for the BLR below INL Diversion would suggest.

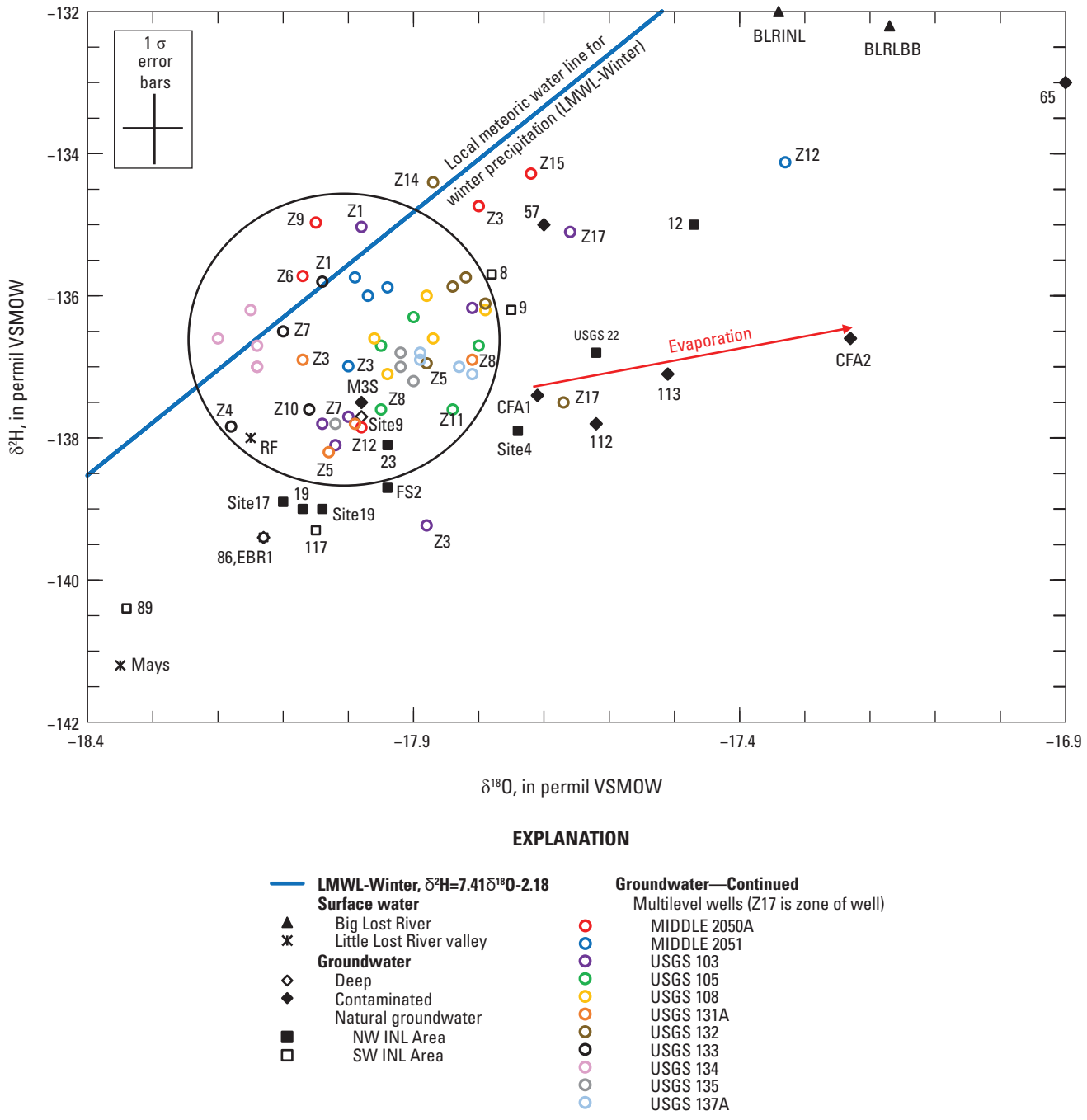

Figure 12. Local meteoric water line (LMWL) for winter and stable isotope ratios of hydrogen and oxygen (δ^2H and $\delta^{18}O$, respectively) for surface-water and groundwater samples, Idaho National Laboratory, eastern Idaho. Arrow shows evaporation trend line and ellipse encircles δ^2H and $\delta^{18}O$ (Vienna Standard Mean Ocean Water [VSMOW]) values representative of most groundwater from multilevel wells in the study area (table 6). Location of sites shown in figure 1 or in Rattray (2019, fig. 7, sites Ruby Farms, Site 17, USGS 12, USGS 22, and USGS 23). Abbreviated names are shown in table 1.

Four of these zones (MIDDLE 2050A, zones 3 and 15; MIDDLE 2051, zone 12; and USGS 103, zone 17) plot between the cluster of δ^2H and $\delta^{18}O$ values for groundwater from MLW and the high δ^2H and $\delta^{18}O$ values for the BLR (fig. 12). The BLR probably is a source of recharge at MIDDLE 2050A, zone 15; MIDDLE 2051, zone 12; and USGS 103, zone 17—an interpretation that is consistent with the shallow depth of these zones (table 1), the proximity of MIDDLE 2050A and MIDDLE 2051 to the BLR (fig. 1), and a previous study indicating that the BLR is a source of recharge to USGS 103 (Rattray, 2019). MIDDLE 2050A, zone 3 is located more than 700 ft bwt (table 1) and situated below three zones (zones 6, 9, and 12) that, based on δ^2H and $\delta^{18}O$ values, do not appear to have the BLR as a source of water. Consequently, if the BLR is a source of recharge to MIDDLE 2050A, zone 3, then the recharge from BLR must move downward and bypass zones 6, 9, and 12 via fracture/preferential flow (fig. 3).

The δ^2H and $\delta^{18}O$ values for groundwater from USGS 132, zones 14 and 17 plot above and to the right of the cluster of δ^2H and $\delta^{18}O$ values for groundwater from MLW, respectively. USGS 132 is near the INL spreading areas and south of the RWMC (fig. 1), and zones 14 and 17 are the two shallowest sampling zones at this MLW (fig. 3*C*). Consequently, both the BLR and Mg-Cl brine applied to roads at the RWMC are potential sources of surface-water recharge to zones 14 and 17. Because the δ^2H and $\delta^{18}O$ values for groundwater from zone 14 plot above the cluster of δ^2H and $\delta^{18}O$ values for groundwater from MLW, the BLR is the likely source of recharge to this zone. The δ^2H and $\delta^{18}O$ values for groundwater from zone 17 plot near the δ^2H and $\delta^{18}O$ values for groundwater from USGS 120 (fig. 12), which is located near USGS 132 (fig. 1). A previous study (Rattray, 2019) indicated that sources of water at USGS 120 included the BLR and wastewater (Mg-Cl brine) from the RWMC, so both are possible sources of water to zone 17.

The δ^2H and $\delta^{18}O$ values for groundwater from zone 3 at USGS 103 plot below the cluster of δ^2H and $\delta^{18}O$ values for groundwater from MLW and near the δ^2H and $\delta^{18}O$ values for groundwater from Fire Station 2 (FS2; figs. 1 and 12). Well Fire Station 2 is about an even mixture of water from the BLR and groundwater originating from the LLR valley (Rattray, 2019), so water from either or both sources may be sources of water to zone 3 at USGS 103.

$\delta^{13}C$ and $\delta^{18}O$ Stable Isotope Ratios

The $\delta^{18}O$ and $\delta^{13}C$ values for the BLR; deep, contaminated, and natural groundwater; and groundwater from MLW are plotted in figure 13. High $\delta^{18}O$ values indicate an increasing amount of recharge from a source of water that has undergone evaporation, such as the BLR or wastewater, whereas low $\delta^{18}O$ values indicate an increasing amount of recharge from the LLR valley or the Lost River Range. High $\delta^{13}C$ values indicate dissolution of carbonates and low $\delta^{13}C$ values indicate infiltration recharge from the BLR or wastewater.

Eighty-seven percent of groundwater samples from MLW plot in a cluster (within the ellipse) in figure 13 that indicates the groundwater contains dissolved carbonates and primarily originates from the LLR valley or the Lost River Range. Groundwater from six zones from MLW (MIDDLE 2050A, zones 3, 12, and 15; MIDDLE 2051, zone 12; and USGS 103 and 132, zones 17) however, plot in areas in figure 13 that indicate the water contains recharge from the BLR, wastewater, or precipitation.

Low $\delta^{13}C$ values in groundwater from MIDDLE 2050A, zones 3, 12, and 15 indicate that this water contains infiltration recharge of surface water. Due to the proximity of MIDDLE 2050A to the BLR (fig. 1), this stream is the most likely source of water to the two shallow zones (zones 12 and 15). The higher $\delta^{18}O$ value from the shallowest (zone 15) sampling zone, compared to the $\delta^{18}O$ value from zone 12, indicates that water from zone 15 contains infiltration recharge that underwent greater amounts of evaporation than the infiltration recharge at zone 12. The $\delta^{18}O$ and $\delta^{13}C$ values for zone 3 are unusual compared to $\delta^{18}O$ and $\delta^{13}C$ values from other MLW. These zone 3 values plot near the values for USGS 22[13] (fig. 13), which has precipitation as a source of water (Rattray, 2019), so the source of water to zone 3 could be precipitation that underwent less evaporation than water at USGS 22.

High $\delta^{18}O$ and low $\delta^{13}C$ values in groundwater from MIDDLE 2051, zone 12 indicate that infiltration recharge was a significant source of water to this zone. The proximity of the BLR to this MLW indicates that the BLR was the most likely source of infiltration recharge.

The $\delta^{18}O$ and $\delta^{13}C$ values are intermediate in groundwater from USGS 103, zone 17. The $\delta^{18}O$ value indicates that water from this zone contains infiltration recharge, either from the BLR, precipitation, and (or) wastewater. Significant infiltration recharge should produce low $\delta^{13}C$ values in groundwater. However, dissolution of carbonates as this water traveled about 8 miles (mi) through the ESRP aquifer, from recharge areas at the BLR or INTEC to USGS 103, may have produced the intermediate $\delta^{13}C$ value.

USGS 132 is near the INL spreading areas, the RWMC, and USGS 120 (fig. 1). The $\delta^{18}O$ and $\delta^{13}C$ values in groundwater from zone 17 at USGS 132 plots near groundwater from USGS 120, slightly to the right of the data within the ellipse (fig. 13). Sources of water at USGS 120 include the BLR and wastewater from the RWMC (Rattray, 2019, table 11). Consequently, both the BLR and wastewater from the RWMC are possible sources of surface-water recharge to zone 17.

[13]Isotopic data for USGS 22 are presented in Rattray (2019, table 8).

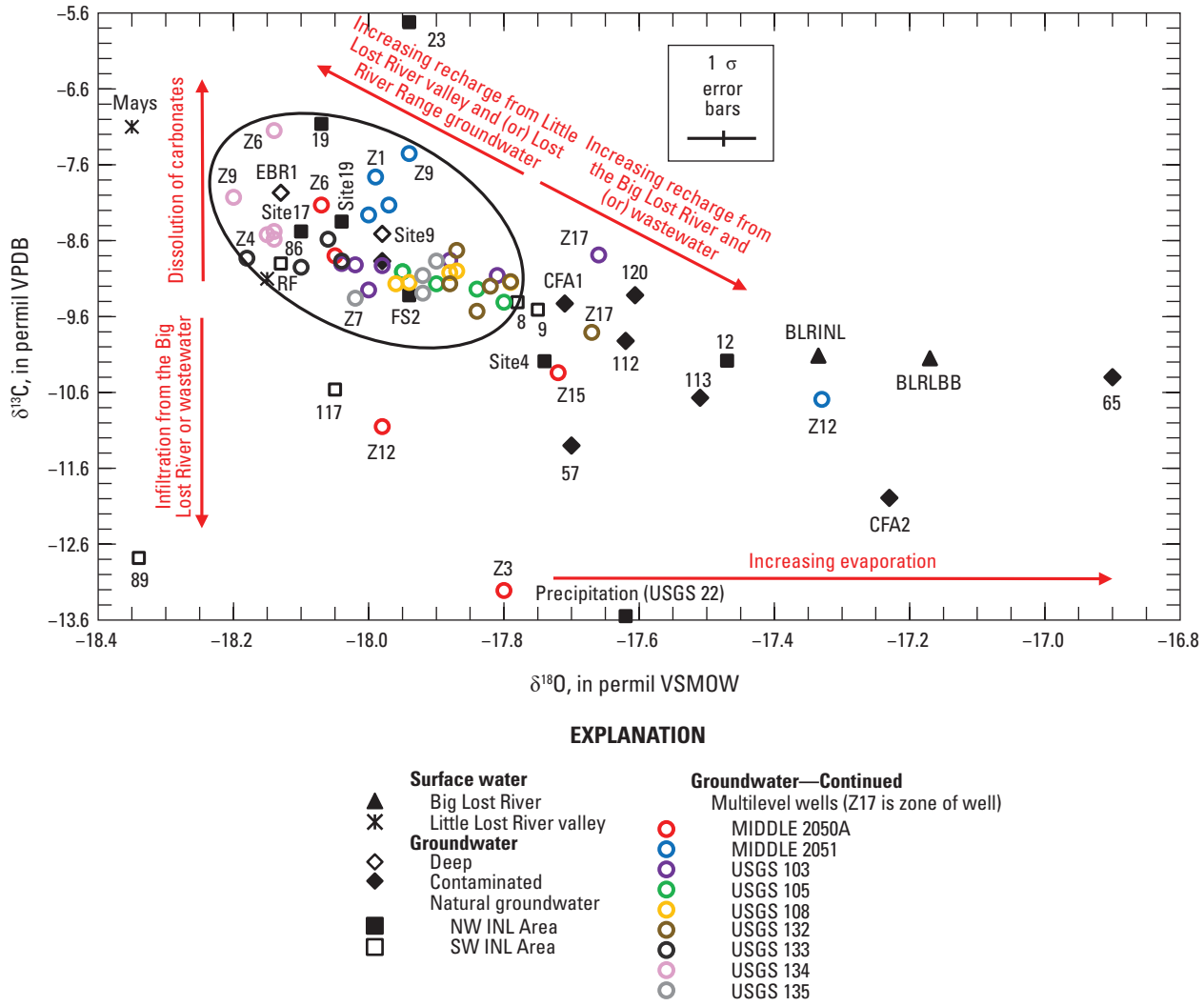

Figure 13. Stable isotope ratios of oxygen and carbon ($\delta^{18}O$ and $\delta^{13}C$, respectively) for surface- water and groundwater samples; arrows showing influence of physical, chemical, and hydrologic processes on $\delta^{18}O$ and $\delta^{13}C$ (Vienna Standard Mean Ocean Water [VSMOW]; Vienna Pee Dee Belemnite [VPDB]) values; and ellipse encircling $\delta^{18}O$ and $\delta^{13}C$ values representative of most natural groundwater in the study area, Idaho National Laboratory, eastern Idaho. Actual values are shown in table 6; abbreviated names are shown in table 1. Location of sites shown in figure 1 or in Rattray (2019, fig. 7, sites Ruby Farms, Site 17, USGS 12, USGS 22, and USGS 23).

Tritium

Tritium activities in groundwater in the study area are influenced by tritium in (1) wastewater discharged at the ATRC and the INTEC and (2) atmospheric deposition transported from land surface to the aquifer in infiltration recharge of the BLR and (or) precipitation. Disposal of tritium in wastewater began in 1952 and 1953 at the ATRC and INTEC (fig. 14), respectively. Much greater activities of tritium were disposed at the INTEC than the ATRC, with maximum estimated yearly disposal activities of about 3,500 Curies (Ci) at the INTEC in 1958 and 800 Ci at the ATRC in 1969. Tritium activities in wastewater discharge steadily decreased from their peaks to activities of zero Ci at the INTEC in 1989 and about 100 to 200 Ci at the ATRC in 1983. The activity of tritium in groundwater from CFA 2, about 3 mi downgradient of the INTEC, reached a peak activity in 1974 of more than 50,000 picocuries per liter (pCi/L), decreased to an activity of about 15,000 pCi/L in 1993, and decreased to an activity of about 4,000 to 5,000 pCi/L during 2011–12 (figs. 14 and 15; Bartholomay, 2022).

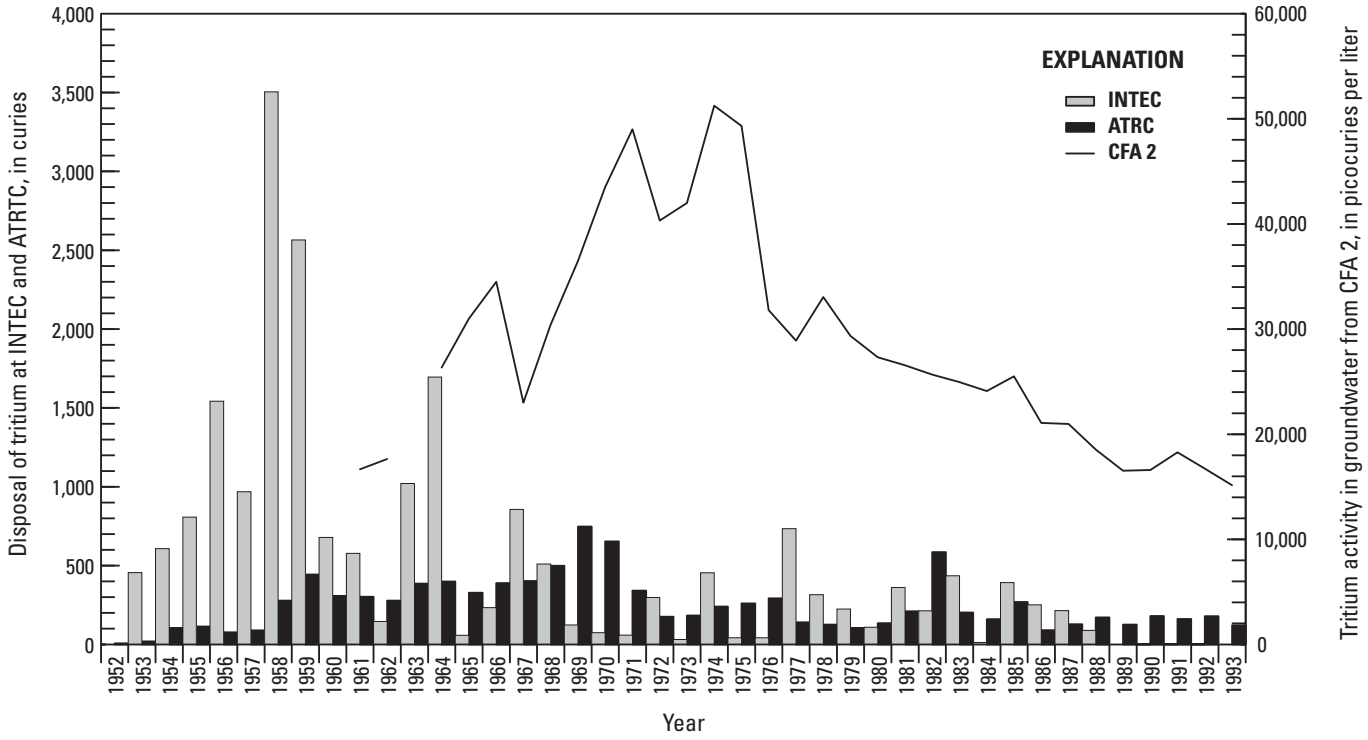

Figure 14. Disposal amounts of tritium at the Idaho Nuclear Technology and Engineering Center (INTEC) and Advanced Test Reactor Complex (ATRC) and the tritium activities in groundwater from Central Facilities Area 2 (CFA 2), Idaho National Laboratory, eastern Idaho, 1952–93.

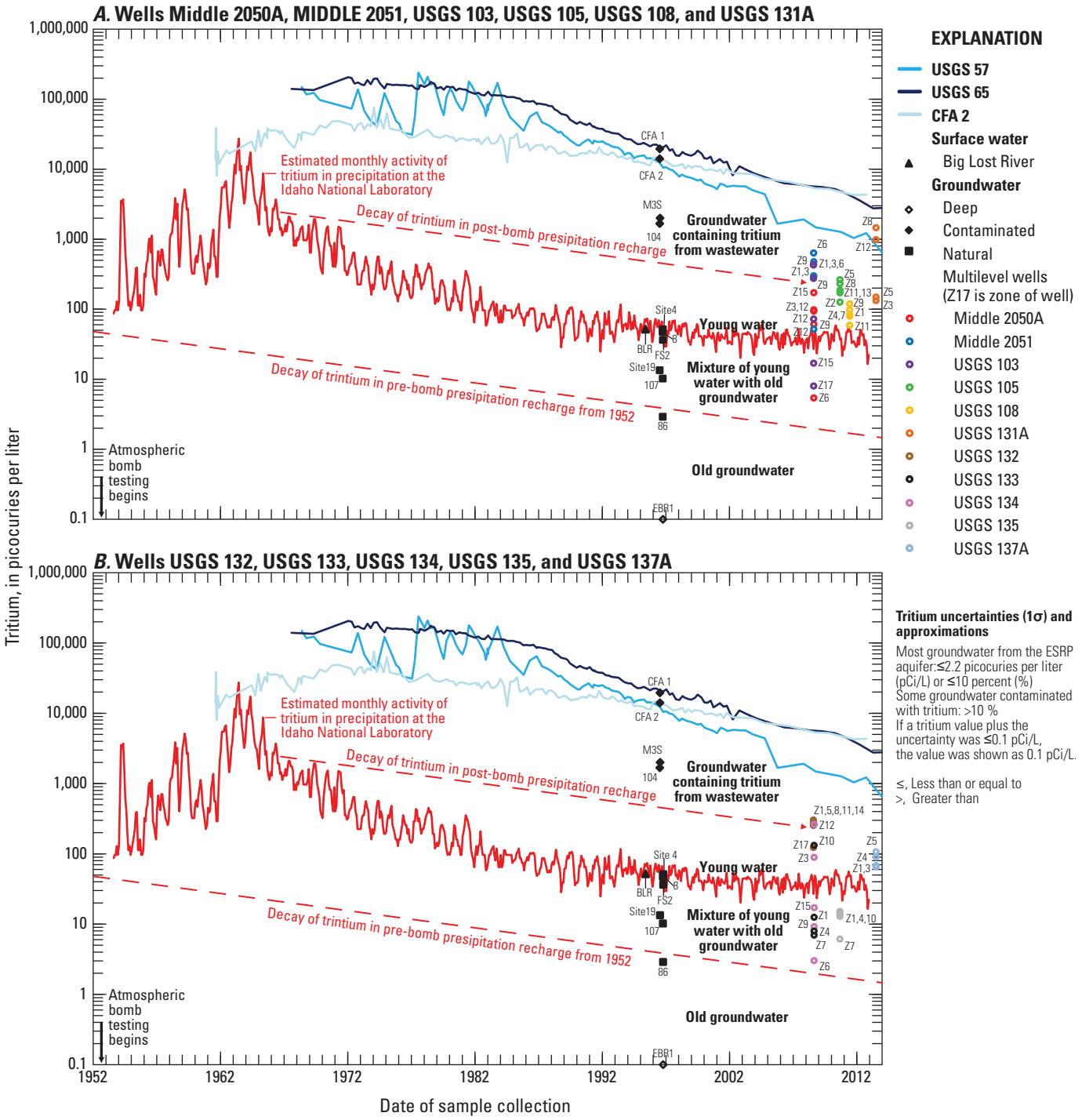

Figure 15. Activity of tritium in surface water and groundwater; estimated activity of tritium in precipitation; decay curves representing the possible evolution of tritium activities in pre-bomb and post-bomb recharge from precipitation; and areas on the graphs representing old groundwater, young water, mixtures of young and (or) contaminated water with old groundwater, and wastewater, Idaho National Laboratory, eastern Idaho. *A.* MIDDLE 2050A, MIDDLE 2051, USGS 103, USGS 105, USGS 108, and USGS 131A. *B.* USGS 132, USGS 133, USGS 134, USGS 135, and USGS 137A.

Tritium activities in atmospheric deposition (represented by the estimated monthly activity of tritium in precipitation[14] at the INL in fig. 15) increased substantially due to atmospheric bomb testing that began in 1952, with tritium activities peaking at about 27,000 pCi/L during June 1963. Tritium activities in atmospheric deposition decreased from 1963 to 2000 due to discontinuation of bomb testing and radioactive decay (half-life of tritium is 12.3 years) and ranged from about 20 to 60 pCi/L from 2000 to 2012.

The age of groundwater was qualitatively estimated by plotting the date of sample collection versus tritium activity of a water-quality sample on a graph with defined areas for **old groundwater**, **young groundwater**, a mixture of young and old groundwater, and groundwater containing tritium from wastewater (fig. 15). Old groundwater was defined as a tritium activity equal to or less than the line representing the radioactive decay (the equation for radioactive decay of tritium is shown in Rattray, 2018, app. 2, eq. 2–12) of tritium in precipitation recharge from 1952, using a pre-bomb 1952 tritium activity in precipitation of 48 pCi/L (Morris and others, 1963).

Young water (surface water and groundwater) was defined as a tritium activity within the area containing the line representing the activity of tritium in precipitation at the INL from the late 1980s through 2012 (lower bound). Groundwater plotting between the squiggly line and the line representing the decay of tritium in precipitation recharge from 1952 is likely a mixture of young and old groundwater, although this groundwater also could be precipitation recharge from the mid-1950s. Groundwater plotting above the line representing the activity of tritium in precipitation at the INL probably contains some tritium from wastewater, and any groundwater plotting above the line representing the decay of tritium in groundwater recharged from precipitation during the mid-1960s certainly contains tritium from discharge of wastewater. The other plausible scenario for elevated tritium values compared to precipitation input would be a dominant signature from recharge from the 1960s, which would show an elevated signature compared to background, or pre-bomb testing tritium values. This scenario is not considered likely given the rapid infiltration of natural recharge sources and mixing behavior of these recharge sources with wastewater inputs at the INL.

Tritium activities at MIDDLE 2050A suggest that water in zones 3, 12, and 15 may contain wastewater, as these zones have a higher tritium activity than observed in water from zone 9, which is mostly young water. Water from zone 6 is a mixture of young water and old water (fig. 15). Large tritium activities in water from MIDDLE 2051, USGS 105, USGS 108, USGS 131A, and USGS 132 indicate that water from most sampling zones at these MLW contains some wastewater, although MIDDLE 2051, zone 12 and USGS 108, zone 11 may be mostly young water. At USGS 103, water from the five deeper sampling zones contains wastewater, whereas the two shallower zones do not. Water from USGS 135 is primarily a mixture of young and old water, and water from USGS 137A, which is adjacent to the INL spreading areas and south of the RWMC (fig. 1), probably contains some wastewater.

Tritium activities in most groundwater from MLW ranged from 50 to 100 pCi/L indicating that the groundwater contained some wastewater (fig. 15). However, tritium activities exceeded 100 pCi/L in groundwater from at least one zone from all MLW except for USGS 135, indicating that some groundwater at each of these MLW undoubtably contained wastewater. At least one zone contained groundwater from MLW (MIDDLE 2050A, USGS 103, and USGS 135) that was a mixture of young and old groundwater, but none of the groundwater from MLW was entirely old groundwater.

Tritium and Chloride

Tritium activities are not unique among the various surface-water sources of recharge (precipitation, BLR, ATRC, INTEC, and RWMC). Tritium activity was low at the BLR, high in wastewater discharged at the ATRC (USGS 65) and INTEC (USGS 57, CFA 1, and CFA 2) (table 6), and uncertain in recharge water at the RWMC (represented with tritium at USGS 88, 90±160 pCi/L; table 6). However, tritium activities used in conjunction with other chemistry data may provide enough information to identify sources of recharge. For example, chloride concentrations in the BLR (3 and 3.1 mg/L, table 4) were low relative to most other chloride concentrations in the study area (chloride concentrations in study area ranged from 0.8 to 115 mg/L and 25th, 50th, and 75th ranked percentile concentrations were 10.34, 12.35, and 15.31 mg/L, respectively) and chloride concentrations in groundwater near wastewater discharge areas were 21, 110, and 82 mg/L at the ATRC, INTEC, and RWMC (table 4), respectively. In addition, chloride is a conservative element in the ESRP aquifer. Consequently, the combination of chloride concentrations and tritium activities may be used to identify sources of surface-water recharge at MLW.

[14]Estimated monthly activity of ^{3}H in precipitation at the INL was calculated for 1953 through 2012 with data and information from Jurgens (2018) and Michel and others (2018).

Chloride concentrations and tritium activities for the BLR; deep, contaminated, and natural groundwater; and groundwater from MLW are plotted in figure 16. Groundwater from 30 MLW zones forms a cluster (within the ellipse) in figure 16 where chloride concentrations and tritium activities range from 10.2 to 18.0 mg/L and 58.8±3 to 301±8.9 pCi/L, respectively. Groundwater from 24 MLW zones plot outside of the cluster, and their location on the diagram may be due to low or high chloride concentrations and tritium activities in particular sources of water. For example, data points for the BLR and groundwater representing recharge water from the RWMC (USGS 88), ATRC (USGS 65), and INTEC (USGS 57, CFA 1, and CFA 2) plot to the left, right, above, and above and right, respectively, of the cluster of data points from most MLW. High tritium activities in some groundwater within the cluster of MLW show that wastewater provided recharge to some of these MLW. However, none of the data points within the cluster of MLW clearly indicate a specific source of the wastewater. However, MLW sampling zones that plot outside of the cluster of MLW data points may fall along a mixing line between the cluster of data points and tritium activities and chloride concentrations from sources of surface water, thus providing an indication of sources of surface water to these sampling zones.

Groundwater from MIDDLE 2051, zones 6, 9, and 12 plot above (zones 6 and 9) and to the left (zone 12) of the cluster of MLW (fig. 16), towards USGS 65 and the BLR, respectively, indicating that wastewater from the ATRC was a source of recharge to zones 6 and 9 and that the BLR was source of recharge to zone 12. Groundwater from USGS 103 zones 1, 3, 6, and 9 and USGS 131A, zones 8 and 12 also plot above the cluster of MLW, in a direction towards either USGS 65 or USGS 57, CFA 1, and CFA 2, indicating that wastewater from either the ATRC or the INTEC was a source of water to these zones. However, because of their location downgradient from the INTEC, wastewater from the INTEC probably was the source of wastewater at these MLW.

Groundwater from USGS 132, zone 17 plots to the right of the cluster of MLW (fig. 16), which shows that chloride concentrations are elevated in this groundwater. The source of the extra chloride in groundwater from this zone probably was a Mg-Cl brine (Roddy, 2007; U.S. Department of Energy, 2011). Groundwater from one or more zones from MIDDLE 2050A (zone 6), USGS 103 (zones 15 and 17), USGS 134 (zones 6, 9, and 15), and USGS 135 (zones 1, 4, 7, and 10) plot below the cluster of MLW. This groundwater probably contains mostly old groundwater.

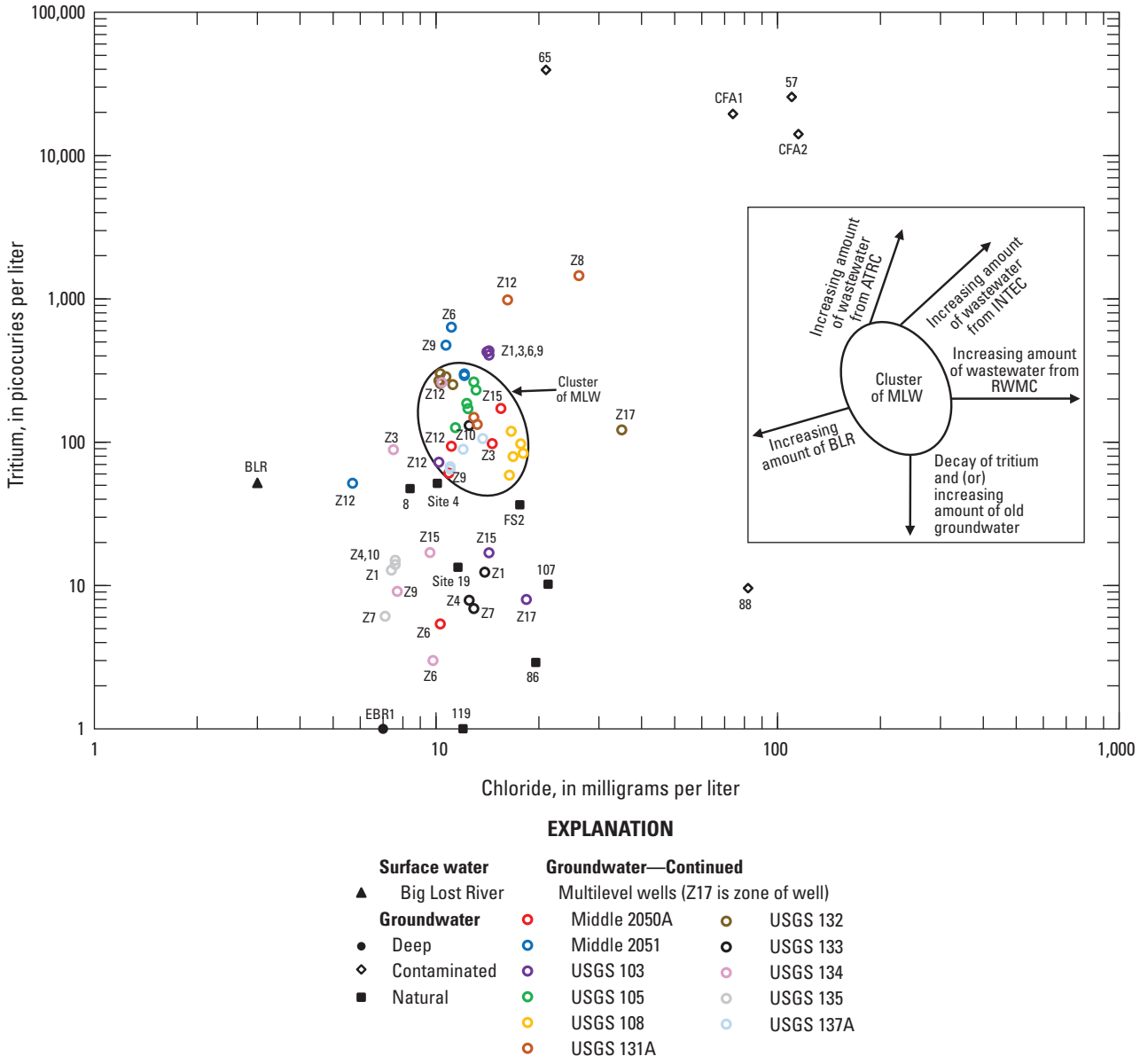

Figure 16. Chloride concentrations versus tritium activities, arrows showing how concentrations and activities trend when influenced by physical and hydrologic processes, and ellipse encircling chloride concentrations and tritium activities representative of most natural groundwater in the study area, Idaho National Laboratory, eastern Idaho. ATRC, Advanced Test Reactor Complex; BLR, Big Lost River; MLW, multilevel wells; RWMC, Radioactive Waste Management Complex.

Geochemical Modeling

Geochemical modeling was done with the inverse, mass-balance modeling capability of PHREEQC (Parkhurst and Appelo, 2013). Inverse modeling attempts to identify the net chemical reactions that account for observed changes in chemistry between initial (one or more) and final (one) water compositions along a single flowline or joined flowlines (Parkhurst and Appelo, 2013, p. 7). Changes in water chemistry taking place in the aquifer were accounted for through (1) addition of gases because surface water recharge to the aquifer in the southwestern part of the INL causes this part of the aquifer to behave as an open system, (2) removal or addition of solutes to the aquifer through water-rock interaction, and (3) mixing of two or more initial solutions. The nonunique model results were the sets of gas and solid phase mass transfers into or out of solution and the percentage contributions of initial solutions that accounted for the change in chemistry between the initial and final solutions.

Model Inputs and Constraints

Model inputs consist of the chemical and isotopic compositions of aqueous solutions (tables 2–5), the gas and solid (mineral) phases that represent plausible chemical reactions in the aquifer (table 7), and the set of chemical elements (hydrogen, oxygen, carbon, calcium, magnesium, sodium, potassium, chloride, sulfur, fluoride, nitrogen, silica, aluminum, and iron) that describe the solutions and phases. Model constraints include chemical constraints, which are the chemical and isotopic constituents used in models (tables 2–5), and the uncertainties assigned to the aqueous solutions, individual chemical constituents, and stable isotope ratios. These uncertainties include the uncertainties in collecting water samples, chemical analysis of the water samples, and from the spatial and temporal variability of the water chemistry (Parkhurst, 1997).

Aqueous Solutions

Aqueous solutions used in the models were the chemical and isotopic compositions of precipitation, the BLR, and groundwater (–). The global uncertainty for solutions with a charge balance[15] (CB) of 5 percent or less was set to 5 percent in PHREEQC. If a solution had a CB greater than 5 percent (table 3) the global uncertainty was set to the smallest value within CB + 1 percent that would produce an electrically balanced solution in PHREEQC. The redox state of the solutions, specified with pe, was set to 4. This pe value was appropriate for the oxic water conditions in the study area.

Inorganic constituents with (1) censored concentrations (<, less than) were assigned model concentrations of one-half the censored concentration with an uncertainty of ±100 percent and (2) estimated concentrations (E, estimated) were assigned model concentrations of the estimated concentration with an uncertainty of ±10 percent. These uncertainties were assigned using the "balances"[16] identifier in PHREEQC. A few water samples did not have a measured concentration (ND, not determined; tables 2 and 3) for nitrate (1 water sample), aluminum (14 water samples) and iron (4 water samples) and were assigned approximate concentrations, based on concentrations in nearby wells, with an uncertainty of ±10 percent. Uncertainty in stable isotope ratios results from variability in the origin of the water, seasonal weather and short-term climate variability, and variability caused by transport of surface water through the unsaturated zone to the aquifer (Rattray, 2018). Uncertainties assigned to stable isotope ratios were ±1 permil for δ^2H and ±0.1 permil for $\delta^{18}O$ and $\delta^{13}C$ (table 5). Estimated stable isotope ratios for the snow core sample from USGS 83 (table 5) were assigned the same uncertainties and carbon stable isotope ratios for solid and gas phases were assigned values of 0±1 permil for calcite and dolomite and -18±4 permil for carbon dioxide (Rattray, 2018).

Larger uncertainties for some stable isotope ratios, fluoride, nitrate, and (or) potassium were required in some model simulations to produce plausible model results. The uncertainty limits were increased for fluoride, nitrate, and potassium concentrations using the "balances" identifier in PHREEQC, and the larger isotope, fluoride, nitrate, and (or) potassium uncertainties were noted in the "comments" column in the table of model results (table 9). The accuracy of the geochemical models in this report is largely dependent on major ion concentrations, with minor elements and stable isotope ratios used to further constrain model results. Thus, models produced with larger uncertainties for stable isotope ratios (or no isotope ratios), fluoride, nitrate, and (or) potassium are less constrained, but probably have a similar accuracy, as models produced with smaller uncertainties for those chemical constituents.

Gas and Solid Phases

The ESRP aquifer generally behaves as a closed aquifer system with respect to atmospheric gases (Schramke and others, 1996; Busenberg and others, 2001). However, in the study area the aquifer behaves as an open system due to infiltration recharge of precipitation, the BLR, and wastewater discharge. Recharge of this surface water transports atmospheric O_2 and soil zone CO_2 through the unsaturated zone to the aquifer. Consequently, these two gas phases were included in geochemical models that had surface water as an initial solution.

Solid phases in the aquifer system are the minerals and other solid phases described in the sections, "Anthropogenic Inputs" and "Water-Rock Interaction." Anthropogenic inputs represented in geochemical modeling included nitrate and potassium (represented with ammonium nitrate and sylvite in table 7) in fertilizer applied to irrigated land and sodium, chloride, and nitrate (represented with halite and ammonium nitrate) discharged in wastewater. Potassium may also be present in detritus from silicic rocks such as sandstone in the southern extent of the Lost River Range (fig. 2).

Water-rock interaction was restricted to geologically, thermodynamically, and kinetically plausible chemical reactions between the gaseous, aqueous, and solid phases in the aquifer system. Solid phases included in all geochemical models were calcite, gypsum, halite, fluorite, olivine (Fo_{85}), plagioclase (An_{60}), basalt volcanic glass, calcium montmorillonite, and goethite. Pyroxene (as augite to ferroaugite) was a ubiquitous mineral in the aquifer system. However, pyroxene was not included in model simulations because only one of either olivine or pyroxene was required to obtain plausible model results.

For a mineral to be allowed to dissolve or precipitate in a model simulation that mineral had to be undersaturated or supersaturated, respectively, or be near equilibrium with

[15]The equation for calculating charge balance is shown in equation 1-3 in appendix 1 from Rattray (2019).

[16]"Balances" is a uniquely specified uncertainty for a specific chemical constituent for a specific model simulation (Parkhurst and Appelo, 2013).

at least one of the initial or final solutions in the model. The snow core from USGS 83 was undersaturated with respect to every mineral included in geochemical modeling[17] (table 8); consequently, every mineral could dissolve in models where the snow core was an initial solution. The BLR was undersaturated with respect to plagioclase, forsterite (representing olivine), amorphous silica (representing basalt volcanic glass), and evaporate minerals; supersaturated with respect to calcium montmorillonite and goethite; and either undersaturated (BLR LB) or supersaturated (BLR DIV) with respect to dolomite and calcite. Groundwater was undersaturated with respect to plagioclase, forsterite, amorphous silica, and evaporate minerals; supersaturated with respect to calcium montmorillonite, goethite, and quartz; and undersaturated, supersaturated, or in equilibrium with respect to dolomite and calcite.

Dissolution of olivine and basalt volcanic glass releases silica to solution, whereas the incongruent dissolution of plagioclase does not (table 7). Consequently, the model decision of which silicate phase(s) will dissolve in geochemical models depended on the need to balance the concentrations of silica in the initial and final solutions. If the concentration of silica resulting from the initial solutions was equivalent (within uncertainties) to the concentration of silica in the final solution, then plagioclase would be the preferred silicate mineral that dissolves. However, if the concentration of silica resulting from the initial solutions was less (including uncertainties) than the concentration of silica in the final solution, then either olivine and (or) basalt volcanic glass would be the preferred silicate mineral that dissolves. Dissolution of specific silicate minerals also is influenced by the need to balance concentrations of calcium, sodium, and bicarbonate between the initial and final solutions.

Model Results for Groundwater in Multilevel Wells

Geochemical models were run for groundwater from nine MLW with a combined 45 sampling zones in the southwestern part of the INL (table 9). Geochemical models were run in minimal mode, which means that the models were reduced to the minimum number of phases required to satisfy the model constraints and solution composition uncertainties (Parkhurst and Appelo, 2013, p. 89). Use of the minimal mode means that the model results do not include every possible combination of phases that could result in a successful model. However, the models produced in the minimal mode were suitable for determining the (1) physical and chemical processes influencing the geochemistry of groundwater and (2) sources of water to individual MLW zones.

Valid geochemical models should have initial and final solutions that generally align with groundwater-flow directions. Consequently, inferred information from water-table contours (fig. 5), hydraulic head contours at three discrete aquifer depths (fig. 6), and estimated groundwater-flow directions (Rattray, 2019) were used to guide selection of initial solutions that were hydrologically upgradient of, and reasonably close to, final solutions (figs. 1 and 5). In addition, hydraulic head and water temperature data (fig. 7) in the unconfined, fractured basalt ESRP aquifer indicated there is a downward vertical flow component for groundwater in the Arco-Big Southern Butte rift zone. Therefore, preference in model simulations for groundwater located in the rift zone was given to initial solutions that were shallower, instead of about equivalent depth (relative to the water table), than the depth of the MLW sampling zone of the final solution (fig. 3). Based on this inferred information, initial model simulations typically included about four to six initial solutions chosen from the closest sites hydrologically upgradient of the site of the final solution.

If no successful models were found, then additional model simulations were run using different combinations of initial solutions and (or) adjusting the uncertainties of some model constraints (isotopes, nitrate, fluoride, and potassium) until successful models were produced.

Successful models were then evaluated to identify plausible models. Plausible models are those model simulations that met thermodynamic, kinetic, and phase transfer constraints such as:

- dissolution or precipitation of each reacting phase was consistent with the thermodynamic state of at least one of the initial or final solutions (table 8);
- reacting phases should include dissolution of basalt minerals because the ESRP aquifer is a basalt aquifer;
- individual phase mass transfers were on the order of micromoles per kilogram of water (µmol/kg water) (Rattray, 2019), consistent with the dilute nature of natural groundwater at MLW (specific conductance of 291–478 microsiemens per centimeter (µS/cm); table 3) and the small dissolution rate of silicate minerals (Lasaga and others, 1994); and
- mass transfer amounts associated with incongruent dissolution of aluminosilicate phases and the concurrent precipitation of calcium montmorillonite were consistent with their reaction ratios (table 7).

[17]There were no data for aluminum and iron for the snow core, so saturation indexes were not calculated for feldspars, clays, and goethite.

Table 9. Geochemical mass-balance modeling results, Idaho National Laboratory, eastern Idaho.

[Positive numbers indicate dissolution, negative numbers indicate precipitation, and shaded rows indicate preferred model solution. **Solution names:** 83, snow core collected at site USGS 83; 57, USGS 57; 65, USGS 65, etc.; see table 6 for other site names and figure 1 for site locations. **Percentage (+, –):** Plus or minus range of percentages when more than one model solution for the set of initial solutions. **Phase mole transfer:** For solutions or mixtures of solutions that were evaporated (that is, sum of initial solutions exceeds 100), kilograms of water = sum of percent of initial solution(s)/100 = evaporation factor. –, the phase was not identified in the calculated unique model solution. **Solid and gas phases:** Cal, calcite; Dol, dolomite; Gyp, gypsum; Hal, halite; Flu, fluorite; Syl, sylvite; Amm nit, ammonium nitrate; Oliv Fo85, olivine with composition Fo85; Plag An60, plagioclase with composition An60; B-glass, basaltic volcanic glass; Ca mnt, calcium montmorillonite; CO_2, carbon dioxide; O_2, dissolved oxygen; Goe, goethite. **Comments:** %, percent; ‰, permil; unc, uncertainty; tr, trace]

Solution			Number of plausible (P) and unique (U) models (P/U)	Phase mole transfer (micromoles per kilogram of water)														Comments
Initial	Percentage (+, –)	Final		Cal	Dol	Gyp	Hal	Flu	Syl	Amm nit	Oliv Fo85	Plag An60	B-glass	Ca mnt	CO_2	O_2	Goe	
DEEP GROUNDWATER																		
M2051Z12, BLRINL, 83	55(+5), 26(+6), 19(+1)	EBR1	3/2	–698	292	–	61	–	22	6	–	185	350	–139	–	–	–66	No isotopes
M2051Z12, 83	75, 25			–766	277	–	55	1	16	3	–	237	321	–174	–	–	–60	
GROUNDWATER FROM MULTILEVEL WELLS																		
MIDDLE 2050A																		
FS2, BLRLBB, 57, 65	53(+8), 40(–9), 4(–1), 3(+2)	Zone 15	2/1	–	–	–	–	0.1	–	–	71	188	18	–130	366	–	–26	
Site 4, BLRINL, 83, 57	38, 34, 24, 5	Zone 12	4/4	–	103	58	–	0.5	12	–	92	53	–	–37	760	–	–28	No $\delta^{13}C$
83, BLRLBB, 57	52, 40, 8			420	–	103	–	1	–	–	236	198	–	–137	1,514	41	–71	
83, BLRINL, Site 19, 57	43, 33, 16, 8			–	314	82	–	1	–	–	–	–	221	–8	923	–	–42	
Site 4, BLRINL, 83	63, 21, 16			–	–	69	70	–	17	–	75	19	–	–13	552	–	–23	
Site 19	100	Zone 9	1/1	–84	–	–	–	–	–	–	–	85	12	–59	–	–	–3	δ^2H unc 2‰
Site 19, 134Z3	81, 19	Zone 6	1/1	–	–	–	–	1	–	–	–	102	–	–70	–	–	–1	Gbl unc, 7%; K unc, 9%; δ^2H unc 2‰
–	–	Zone 3	–	–	–	–	–	–	–	–	–	–	–	–	–	–	–	No successful models
MIDDLE 2051																		
BLRINL, Site19, 65	85, 12, 3	Zone 12	4/4	–	87	–	–	–	21	9	–	–	214	–7	681	35	–41	
BLRINL, Site19	73, 27			–	47	48	–	–	20	5	–	–	200	–7	597	–	–38	
BLRINL, 65	96, 4			–	124	–	17	–	27	12	–	–	228	–8	754	46	–44	
BLRINL, 134Z15	93, 7			–	119	44	25	–	27	13	–	–	216	–8	745	43	–41	
134Z15, BLRINL, Site19, 65	87, 6, 5, 3	Zone 9	2/2	299	–	35	–	0.1	–	7	–	81	–	–56	–	17	–	134Z15 unc 6%

Table 9. Geochemical mass-balance modeling results, Idaho National Laboratory, eastern Idaho.—Continued

[Positive numbers indicate dissolution, negative numbers indicate precipitation, and shaded rows indicate preferred model solution. **Solution names:** 83, snow core collected at site USGS 83; 57, USGS 57; 65, USGS 65, etc.; see table 6 for other site names and figure 1 for site locations. **Percentage (+, –):** Plus or minus range of percentages when more than one model solution for the set of initial solutions. **Phase mole transfer:** For solutions or mixtures of solutions that were evaporated (that is, sum of initial solutions exceeds 100), kilograms of water = sum of percent of initial solution(s)/100 = evaporation factor. –, the phase was not identified in the calculated unique model solution. **Solid and gas phases:** Cal, calcite; Dol, dolomite; Gyp, gypsum; Hal, halite; Flu, fluorite; Syl, sylvite; Amm nit, ammonium nitrate; Oliv Fo85, olivine with composition Fo85; Plag An60, plagioclase with composition An60; B-glass, basaltic volcanic glass; Ca mnt, calcium montmorillonite; CO_2, carbon dioxide; O_2, dissolved oxygen; Goe, goethite. **Comments:** %, percent; ‰, permil; unc, uncertainty; tr, trace]

Solution			Number of plausible (P) and unique (U) models (P/U)	Phase mole transfer (micromoles per kilogram of water)														Comments
Initial	Percentage (+, –)	Final		Cal	Dol	Gyp	Hal	Flu	Syl	Amm nit	Oliv Fo85	Plag An60	B-glass	Ca mnt	CO_2	O_2	Goe	
GROUNDWATER FROM MULTILEVEL WELLS—Continued																		
134Z15, BLRINL, 57, 134Z12	72, 25, 3, tr			275	–	59	–	–	7	10	–	179	–	–123	–	–	–	
134Z15, BLRINL, 65	82, 11, 8	Zone 6	1/1	285	–	–	–	–	6	11	–	112	–	–77	139	43	–0.3	134Z15 unc 6%
Site19, 65	99, 1	Zone 3	3/2	–125	–	–	–	–	12	–	–	–	78	–3	–	41	–16	$\delta^{13}C$ unc 0.2‰
Site19	100(0)			–239	42	47	–	–	12	–	–	–	62	–2	–	40	–13	
Site19, BLRINL, 65	76, 23, 1	Zone 1	3/3	–336	159	–	32	–	17	4	–	–	107	–4	–	101	–21	$\delta^{13}C$ unc 0.4‰
Site19, BLRINL	76, 24			–344	163	34	38	–	17	4	–	–	112	–4	–	102	–22	
Site19, BLRINL, 134Z3, 65	73, 16, 7, 4			–261	122	–	–	–	17	–	–	–	106	–4	–	85	–21	
USGS 103																		
BLRINL, 83, 107	56(–1), 39(0), 5(0)	Zone 17	6/2	–614	378	111	400	6	32	–	0.4	256	–	–176	527	–	–	No $\delta^{13}C$
BLRINL/ BLRLBB, 83	53(+2), 47(–3)			–487	367	129	433	6	30	–	41	232	–	–160	652	–	–13	
83, 107, BLRINL	47(–4), 42 (+5), 11(–1)	Zone 15	6/5	–	–	–	–	–	2	–	40	32	–	–22	104	157	–12	No $\delta^{13}C$
83, BLRINL	84, 16			–	121	31	132	2	14	4	–	–	121	–4	–	205	–23	
104, 83, BLRINL	43, 43, 15			–	–	36	129	2	15	4	56	75	88	–54	–	169	–34	
104, BLRINL	84, 16			–233	–	40	112	3	15	4	–	251	187	–179	–	133	–36	
107, BLRINL, 104	59, 21, 20			–118	–	–	–	–	–	–	–	–	108	–4	–	122	–21	
83, 104, BLRINL	53(0), 26(–7), 21(+8)	Zone 12	4/3	–	–	–	–	–	14	–	79	26	–	–18	323	122	–24	No $\delta^{13}C$
104, BLRINL	71, 29			–270	–	–	–	–	16	–	–	239	193	–171	345	82	–38	
104, BLRINL, 107, 83	48, 29, 12, 11			–124	–	–	9	–	8	–	–	–	156	–5	224	90	–30	

Table 9. Geochemical mass-balance modeling results, Idaho National Laboratory, eastern Idaho.—Continued

[Positive numbers indicate dissolution, negative numbers indicate precipitation, and shaded rows indicate preferred model solution. **Solution names:** 83, snow core collected at site USGS 83; 57, USGS 57; 65, USGS 65, etc.; see table 6 for other site names and figure 1 for site locations. **Percentage (+, –):** Plus or minus range of percentages when more than one model solution for the set of initial solutions. **Phase mole transfer:** For solutions or mixtures of solutions that were evaporated (that is, sum of initial solutions exceeds 100), kilograms of water = sum of percent of initial solution(s)/100 = evaporation factor. –, the phase was not identified in the calculated unique model solution. **Solid and gas phases:** Cal, calcite; Dol, dolomite; Gyp, gypsum; Hal, halite; Flu, fluorite; Syl, sylvite; Amm nit, ammonium nitrate; Oliv Fo85, olivine with composition Fo85; Plag An60, plagioclase with composition An60; B-glass, basaltic volcanic glass; Ca mnt, calcium montmorillonite; CO_2, carbon dioxide; O_2, dissolved oxygen; Goe, goethite. **Comments:** %, percent; ‰, permil; unc, uncertainty; tr, trace]

Solution			Number of plausible (P) and unique (U) models (P/U)	Phase mole transfer (micromoles per kilogram of water)														Comments
Initial	Percentage (+, –)	Final		Cal	Dol	Gyp	Hal	Flu	Syl	Amm nit	Oliv Fo85	Plag An60	B-glass	Ca mnt	CO_2	O_2	Goe	
GROUNDWATER FROM MULTILEVEL WELLS—Continued																		
104, 83	92,8 (–1,+1)	Zone 9	9/2	–87	74	–	–	–	–	–	–	97	62	–69	–	–	–13	No $\delta^{13}C$
104	100(0)			–	–	22	–	–	5	tr	41	70	–	–48	–	–	–13	
104	100	Zone 6	1/1	–	–	31	33	–	3	4	–	15	–	–10	246	13	–1	No $\delta^{13}C$
104	100	Zone 3	1/1	–	57	32	–	–	5	4	–	52	–	–35	–	45	–1	
104	100	Zone 1	1/1	–	–	33	10	–	–	4	–	149	101	–106	–	43	–20	δ^2H unc 2.1‰; $\delta^{13}C$ unc 0.2‰
USGS 105																		
131AZ12, EBR1	69, 31	Zone 13	1/1	–169	–	29	–	–	–	1	–	386	32	–266	–	–	–6	No $\delta^{13}C$
131AZ12, EBR1	64, 36	Zone 11	1/1	–	–	34	–	–	–	–	–	292	–	–201	–	42	–0.2	No $\delta^{13}C$
131AZ12, EBR1	72, 29	Zone 8	1/1	–	–	–	–	–	–	–	–	242	–	–166	–	79	–0.1	No $\delta^{13}C$
131AZ12, EBR1, 131AZ8	53, 35, 12	Zone 5	5/3	–	–	–	–	–	–	–	–	270	–	–185	–	63	–0.1	No $\delta^{13}C$
131AZ12, EBR1	78(–13), 22(+13)			–	–	–	–	–	2	–	–	222	–	–152	–	61	–	
EBR1, 131AZ8	62, 38			–	–	32	–	–	–	–	–	287	–	–197	–	67	–0.3	
M2051Z12, M2051Z9, EBR1	49, 36, 15	Zone 2	3/3	–	–	–	121	3	–	–	–	147	–	–101	–	98	–0.1	
M2051Z9, M2051Z12	56, 44			–197	–	–	76	3	9	–	–	223	–	–153	–	80	–	
M2051Z12, EBR1	54, 46			–	–	47	136	3	–	7	–	282	–	–194	–	146	–0.2	
USGS 108																		
83, 131AZ12, BLRINL	63, 23, 14	Zone 11	2/2	–	126	22	140	2	9	–	–	–	92	–3	354	–	–17	No $\delta^{13}C$
83, BLRINL	82, 18			–	177	32	148	2	12	4	–	–	97	–3	425	–	–18	
104, BLRINL, CFA2	73, 21, 6	Zone 9	3/2	–	116	31	–	–	–	7	–	–	106	–4	–	–	–21	
104, BLRINL	91(0), 9(0)			–	122	53	90	–	8	12	–	–	60	–2	129	–	–12	

Table 9. Geochemical mass-balance modeling results, Idaho National Laboratory, eastern Idaho.—Continued

[Positive numbers indicate dissolution, negative numbers indicate precipitation, and shaded rows indicate preferred model solution. **Solution names:** 83, snow core collected at site USGS 83; 57, USGS 57; 65, USGS 65, etc.; see table 6 for other site names and figure 1 for site locations. **Percentage (+, –):** Plus or minus range of percentages when more than one model solution for the set of initial solutions. **Phase mole transfer:** For solutions or mixtures of solutions that were evaporated (that is, sum of initial solutions exceeds 100), kilograms of water = sum of percent of initial solution(s)/100 = evaporation factor. –, the phase was not identified in the calculated unique model solution. **Solid and gas phases:** Cal, calcite; Dol, dolomite; Gyp, gypsum; Hal, halite; Flu, fluorite; Syl, sylvite; Amm nit, ammonium nitrate; Oliv Fo85, olivine with composition Fo85; Plag An60, plagioclase with composition An60; B-glass, basaltic volcanic glass; Ca mnt, calcium montmorillonite; CO_2, carbon dioxide; O_2, dissolved oxygen; Goe, goethite. **Comments:** %, percent; ‰, permil; unc, uncertainty; tr, trace]

Solution			Number of plausible (P) and unique (U) models (P/U)	Phase mole transfer (micromoles per kilogram of water)														Comments
Initial	Percentage (+, –)	Final		Cal	Dol	Gyp	Hal	Flu	Syl	Amm nit	Oliv Fo85	Plag An60	B-glass	Ca mnt	CO_2	O_2	Goe	
GROUNDWATER FROM MULTILEVEL WELLS—Continued																		
104, 131AZ8, BLRINL	48, 42, 11	Zone 7	3/3	–	94	17	–	–	–	–	–	–	52	–2	–	–	–10	No $\delta^{13}C$
131AZ8, BLRINL, 83	65, 29, 6			–162	178	–	–	–	–	–	–	–	91	–3	–	–	–17	
131AZ12, BLRINL	100, tr			–	–	–	–	–	–	–	52	44	–	–30	344	–	–16	
131AZ8, 104, BLRINL	50(+10), 34(–17), 16(+7)	Zone 4	15/7	–	124	–	–	–	–	4	–	–	65	–2	–	–	–13	No $\delta^{13}C$
131AZ5, 131AZ8, 83	61(–9), 28(+8), 11(+1)			–	–	14	–	–	–	–	–	–	34	–1	–	–	–7	
131AZ8, 131AZ5, BLRINL	54(–23), 24(+37), 21(–13)			–144	136	–	–	–	–	–	–	–	79	–3	–	–	–15	
131AZ5, 131AZ8, 104, BLRINL	37, 31, 25, 6			–	–	18	2	–	–	5	–	–	47	–2	187	–	–9	
131AZ5, 104, 131AZ8	57(–33), 22(+34), 20(+7,–2)			–41	–	–	22	–	–	4	–	–	7	–0.2	111	–	–20	
131AZ8, BLRINL, 104, 83	60, 22, 14, 5			–	116	–	–	–	–	–	–	–	73	–3	–	–	–14	
131AZ8, 83, BLRINL	55, 26, 19			–	150	–	–	–	–	4	–	–	66	–2	–	–	–13	
M2051Z3, 131AZ5, 131AZ8	54, 30, 16	Zone 1	1/1	–	–	30	42	–	–	–	–	–	36	–1	–	–	–7	No $\delta^{13}C$
USGS 131A																		
M2051Z12, EBR1, BLRINL, CFA2	36, 36, 19, 9	Zone 12	1/1	–	–	21	–	–	–	10	29	56	–	–38	–	41	–9	No $\delta^{13}C$; $\delta^{18}O$ unc 0.2‰
M2051Z12, EBR1, CFA1	41, 30, 29	Zone 8	3/3	–	92	58	–	–	–	–	–	71	–	–49	–	25	–0.4	No $\delta^{13}C$
M2051Z9, CFA1	77, 23			–	–	–	–	–	–	–	–	–	72	–2	–	–	–14	

Table 9. Geochemical mass-balance modeling results, Idaho National Laboratory, eastern Idaho.—Continued

[Positive numbers indicate dissolution, negative numbers indicate precipitation, and shaded rows indicate preferred model solution. **Solution names:** 83, snow core collected at site USGS 83; 57, USGS 57; 65, USGS 65, etc.; see table 6 for other site names and figure 1 for site locations. **Percentage (+, –):** Plus or minus range of percentages when more than one model solution for the set of initial solutions. **Phase mole transfer:** For solutions or mixtures of solutions that were evaporated (that is, sum of initial solutions exceeds 100), kilograms of water = sum of percent of initial solution(s)/100 = evaporation factor. –, the phase was not identified in the calculated unique model solution. **Solid and gas phases:** Cal, calcite; Dol, dolomite; Gyp, gypsum; Hal, halite; Flu, fluorite; Syl, sylvite; Amm nit, ammonium nitrate; Oliv Fo85, olivine with composition Fo85; Plag An60, plagioclase with composition An60; B-glass, basaltic volcanic glass; Ca mnt, calcium montmorillonite; CO_2, carbon dioxide; O_2, dissolved oxygen; Goe, goethite. **Comments:** %, percent; ‰, permil; unc, uncertainty; tr, trace]

Solution			Number of plausible (P) and unique (U) models (P/U)	Phase mole transfer (micromoles per kilogram of water)													Comments
Initial	Percentage (+, –)	Final		Cal	Dol	Gyp	Hal	Flu	Syl	Amm nit	Oliv Fo85	Plag An60	B-glass	Ca mnt	CO_2	O_2	Goe	
GROUNDWATER FROM MULTILEVEL WELLS—Continued																		
EBR1, CFA1, BLRINL	45, 30, 25			–	160	79	–	–	–	2	–	36	–	–25	–	37	–1	
M2051Z6, EBR1, CFA1	80, 17, 2	Zone 5	1/1	–	124	–	–	–	–	6	–	5	–	–3	–	–	–	'No $\delta^{13}C$
M2051Z3, M2051Z6	84, 16	Zone 3	4/3	–	146	–	–	–	–	7	–	68	–	–47	–	–	–	No $\delta^{13}C$; K unc, 2%
M2051Z6, M2051Z1	50(0), 50(0)			–	101	–	18	–	–	12	–	23	30	–17	–	–	–6	
M2051Z3	100			–	135	7	–	–	–	7	–	139	–	–95	–	–	–	
USGS 132																		
88, M3S, BLRINL	39(–14), 32(+15), 29(+10)	Zone 17	18/8	–	–	–	–	–	–	13	50	130	–	–90	560	–	–15	No isotopes
M3S, 88	68(–2), 32(+2)			–171	75	–	86	–	–	9	–	168	7	–116	–	–	–2	
BLRINL, 88, 119	42, 39, 19			–	–	–	–	–	–	13	92	278	–	–191	852	–	–28	
M3S	100(0)			–537	155	172	647	–	31	21	–	168	–	–115	–	–	–1	
BLRINL, 88	56(+1), 44(–1)			–	92	–	–	1	–	18	43	–	43	–2	648	–	–21	
M3S, BLRINL	53, 47			–538	287	202	762	1	44	33	–	–	126	–4	–	59	–25	
BLRINL	100			–343	–	238	842	3	61	46	245	258	–	–178	1,081	102	–73	
BLRINL, 119	74(–18), 26(+18)			–342	–	195	734	–	53	34	207	400	–	–275	1,123	65	–62	
M3S, 119, BLRINL	53(–22), 26(+7), 22(+13)	Zone 14	3/2	–	–	–	–	–	12	–	66	170	–	–117	429	–	–20	No isotopes
BLRINL, 119	65, 35			–	–	–	103	–	25	9	158	142	–	–97	878	53	–47	
M2051Z9, BLRINL, M3S	65(+13), 19(+2,–15), 16(+5,–14)	Zone 11	5/2	–	–	–	–	–	10	–	–	31	102	–25	225	–	–20	
M2051Z9, BLRINL	76(+10), 24(–8)			–	–	–	28	–	12	3	–	–	112	–4	244	–	–21	
M2051Z6, BLRINL	78(+10,–8), 22(+8,–9)	Zone 8	12/6	–199	–	–	–	–	13	–	–	117	137	–85	–	–	–26	

Table 9. Geochemical mass-balance modeling results, Idaho National Laboratory, eastern Idaho.—Continued

[Positive numbers indicate dissolution, negative numbers indicate precipitation, and shaded rows indicate preferred model solution. **Solution names:** 83, snow core collected at site USGS 83; 57, USGS 57; 65, USGS 65, etc.; see table 6 for other site names and figure 1 for site locations. **Percentage (+, –):** Plus or minus range of percentages when more than one model solution for the set of initial solutions. **Phase mole transfer:** For solutions or mixtures of solutions that were evaporated (that is, sum of initial solutions exceeds 100), kilograms of water = sum of percent of initial solution(s)/100 = evaporation factor. –, the phase was not identified in the calculated unique model solution. **Solid and gas phases:** Cal, calcite; Dol, dolomite; Gyp, gypsum; Hal, halite; Flu, fluorite; Syl, sylvite; Amm nit, ammonium nitrate; Oliv Fo85, olivine with composition Fo85; Plag An60, plagioclase with composition An60; B-glass, basaltic volcanic glass; Ca mnt, calcium montmorillonite; CO_2, carbon dioxide; O_2, dissolved oxygen; Goe, goethite. **Comments:** %, percent; ‰, permil; unc, uncertainty; tr, trace]

Solution			Number of plausible (P) and unique (U) models (P/U)	Phase mole transfer (micromoles per kilogram of water)														Comments
Initial	Percentage (+, –)	Final		Cal	Dol	Gyp	Hal	Flu	Syl	Amm nit	Oliv Fo85	Plag An60	B-glass	Ca mnt	CO_2	O_2	Goe	
GROUNDWATER FROM MULTILEVEL WELLS—Continued																		
M2051Z9, M3S, BLRINL, M2051Z6	43, 21, 20, 16			–	–	–	–	–	11	–	–	35	63	–26	152	45	–12	
M2051Z9, M3S, BLRINL	78, 19, 3			–170	–	–	–	–	–	–	–	–	67	–2	167	–	–13	
M2051Z6, M2051Z9, BLRINL	64, 25, 11			–214	–	–	27	–	4	–	–	–	141	–5	–	–	–27	
M2051Z6, BLRINL, M3S	85, 14, 1			–189	–	–	–	–	12	–	–	–	105	–4	16	–	–20	
M2051Z9, BLRINL	88(–4), 13(+3)			–205	–	–	–	–	10	–	–	97	103	–70	140	–	–20	
M2051Z6, BLRINL	78(–20), 22(+20)	Zone 5	4/1	–199	–	–	–	–	13	–	–	149	141	–107	–	–	–26	
M2051Z6, BLRINL	78(+3), 22(–3)	Zone 1	3/2	–283	–	–	20	–	18	–	–	369	153	–258	–	–	–29	
M2051Z3, BLRINL	78, 22			–211	–	34	–	–	15	–	–	483	131	–336	138	–	–25	
USGS 135																		
BLRINL, 86	72, 28	Zone 10	2/2	–	164	–	–	–	–	15	–	–	64	–2	134	–	–12	$\delta^{18}O$ unc 0.2‰
BLRINL, 86, 8	62, 21, 17			–	123	–	–	–	–	12	–	–	58	–2	–	–	–11	
BLRINL, 8, 86	44, 39, 16	Zone 7	1/1	–150	26	–	–	–	–	–	–	–	70	–2	–	69	–14	$\delta^{2}H$, $\delta^{18}O$, $\delta^{13}C$ unc; 2, 0.2, 0.4‰
BLRINL, 86	73, 27	Zone 4	10/2	–	141	–	–	0.3	–	15	–	–	72	–2	429	125	–14	$\delta^{18}O$ unc 0.2‰
8, BLRINL	76(+1), 24(–1)			–66	–	0.1	12	–	2	4	–	–	43	–1	–	119	–9	
BLRINL, 86	73, 27	Zone 1	1/1	–	137	–	–	–	–	11	–	–	55	–2	355	86	–11	$\delta^{18}O$ unc 0.2‰

Table 9. Geochemical mass-balance modeling results, Idaho National Laboratory, eastern Idaho.—Continued

[Positive numbers indicate dissolution, negative numbers indicate precipitation, and shaded rows indicate preferred model solution. **Solution names:** 83, snow core collected at site USGS 83; 57, USGS 57; 65, USGS 65, etc.; see table 6 for other site names and figure 1 for site locations. **Percentage (+, –):** Plus or minus range of percentages when more than one model solution for the set of initial solutions. **Phase mole transfer:** For solutions or mixtures of solutions that were evaporated (that is, sum of initial solutions exceeds 100), kilograms of water = sum of percent of initial solution(s)/100 = evaporation factor. –, the phase was not identified in the calculated unique model solution. **Solid and gas phases:** Cal, calcite; Dol, dolomite; Gyp, gypsum; Hal, halite; Flu, fluorite; Syl, sylvite; Amm nit, ammonium nitrate; Oliv Fo85, olivine with composition Fo85; Plag An60, plagioclase with composition An60; B-glass, basaltic volcanic glass; Ca mnt, calcium montmorillonite; CO_2, carbon dioxide; O_2, dissolved oxygen; Goe, goethite. **Comments:** %, percent; ‰, permil; unc, uncertainty; tr, trace]

Solution			Number of plausible (P) and unique (U) models (P/U)	Phase mole transfer (micromoles per kilogram of water)														Comments
Initial	Percentage (+, –)	Final		Cal	Dol	Gyp	Hal	Flu	Syl	Amm nit	Oliv Fo85	Plag An60	B-glass	Ca mnt	CO_2	O_2	Goe	
GROUNDWATER FROM MULTILEVEL WELLS—Continued																		
USGS 137A																		
131AZ12, EBR1, 132Z17, BLRINL	34(+17,–5), 29(+2,–18), 20(+1,–5), 17(+8)	Zone 5	27/6	–	–	–	–	–	–	–	48	191	–	–131	298	–	–15	No $\delta^{13}C$
EBR1, 131AZ12, 132Z17	48, 41, 10			–	–	50	–	–	–	–	–	313	–	–215	–	–	–0.3	
131AZ12, EBR1, BLRINL	50(+3,–13), 47(+10,–3), 4(+2,–1)			–	–	70	64	–	–	–	–	313	63	–217	283	–	–12	
BLRINL, 131AZ12, 132Z17	41(–11), 38(+19), 21(–9)			–	66	–	–	–	11	3	–	77	162	–59	–	–	–31	
EBR1, 132Z17, BLRINL	66(–20), 21(0), 13(+20)			–	78	75	–	–	–	7	–	–	–	–170	–	39	–0.4	
BLRINL, EBR	55(+4,–22), 45(+22,–4)			–	–	110	211	–	21	19	122	243	–	–167	639	66	–37	
131AZ12, BLRINL, EBR1, 132Z17	29(–2), 29(–1), 26(+2), 17(0)	Zone 4	5/3	–	–	–	–	–	–	4	59	113	–	–77	368	56	–18	No δ13C
131AZ12, EBR1, BLRINL	56, 39, 5			–	–	53	–	–	–	–	–	256	–	–176	–	37	–0.2	
BLRINL, 131AZ12, 132Z17	48(0), 36(+1), 16(–2)			–	66	–	–	–	9	6	–	39	116	–31	–	55	–22	
BLRINL, 131AZ12, EBR1, 132Z17	39(+1), 24(+5,–14), 21(+9,–4), 16(+4,–2)	Zone 3	14/7	–	32	–	–	–	–	3	50	119	–	–81	423	63	–15	

Table 9. Geochemical mass-balance modeling results, Idaho National Laboratory, eastern Idaho.—Continued

[Positive numbers indicate dissolution, negative numbers indicate precipitation, and shaded rows indicate preferred model solution. **Solution names:** 83, snow core collected at site USGS 83; 57, USGS 57; 65, USGS 65, etc.; see table 6 for other site names and figure 1 for site locations. **Percentage (+, –):** Plus or minus range of percentages when more than one model solution for the set of initial solutions. **Phase mole transfer:** For solutions or mixtures of solutions that were evaporated (that is, sum of initial solutions exceeds 100), kilograms of water = sum of percent of initial solution(s)/100 = evaporation factor. –, the phase was not identified in the calculated unique model solution. **Solid and gas phases:** Cal, calcite; Dol, dolomite; Gyp, gypsum; Hal, halite; Flu, fluorite; Syl, sylvite; Amm nit, ammonium nitrate; Oliv Fo85, olivine with composition Fo85; Plag An60, plagioclase with composition An60; B-glass, basaltic volcanic glass; Ca mnt, calcium montmorillonite; CO_2, carbon dioxide; O_2, dissolved oxygen; Goe, goethite. **Comments:** %, percent; ‰, permil; unc, uncertainty; tr, trace]

Solution			Number of plausible (P) and unique (U) models (P/U)	Phase mole transfer (micromoles per kilogram of water)														Comments
Initial	Percentage (+, –)	Final		Cal	Dol	Gyp	Hal	Flu	Syl	Amm nit	Oliv Fo85	Plag An60	B-glass	Ca mnt	CO_2	O_2	Goe	
GROUNDWATER FROM MULTILEVEL WELLS—Continued																		
BLRINL, 132Z14, EBR1, 131AZ12	44, 21, 19, 16			–	–	66	111	–	8	8	87	–	35	–1	493	69	–33	
131AZ12, 132Z14, BLRINL, EBR1	55, 21, 20, 4			–	–	–	–	–	1	–	–	229	95	–160	–	39	–18	
EBR1, 131AZ12, 132Z14	41, 38, 21			–	–	42	–	–	–	–	–	258	–	–177	–	43	–0.2	
131AZ12, BLRINL, 132Z14	55, 24, 21			–	–	–	–	–	5	–	61	225	–	–155	–	38	–18	
131AZ12, BLRINL,132Z14, EBR1, 132Z17	52(–28), 20(+19), 20(–14), 6(+19), 1(+14)			–	–	–	–	–	–	–	–	218	90	–153	–	40	–17	
EBR1, 131AZ12	57(0), 43(0)			–	–	60	–	–	–	–	–	320	–	–220	363	52	–0.3	
BLRINL, EBR1, 131AZ12, 132Z17	38(–12), 26(+8,–8), 19(+15,–12), 17(+4,–8)	Zone 1	21/9	–	–	–	–	–	–	7	70	165	–	–113	482	65	–21	No $\delta^{13}C$
131AZ12, 132Z14, EBR1, BLRINL	50(–40), 21(0), 19(+5), 9(+36)			–	–	30	–	–	–	0.8	–	235	–	–161	–	29	–	
131AZ12, EBR1, 132Z14	43, 35, 21			–	–	38	–	–	–	–	–	246	–	–169	–	32	–0.1	
131AZ12, BLRINL, 132Z14, EBR1, 132Z17	50(–16), 22(+4), 19(–7), 6(+12), 2(+7)			–	–	–	–	–	3	–	54	243	–	–167	–	31	–16	
131AZ12, BLRINL, 132Z14, 132Z17	41, 38, 15, 6			–	–	–	–	–	13	5	58	210	84	–147	366	49	–43	
EBR1, BLRINL, 132Z17	44(+14), 39(–15), 17(+2,–2)			–	–	44	–	–	–	11	63	265	–	–182	566	79	–19	

Table 9. Geochemical mass-balance modeling results, Idaho National Laboratory, eastern Idaho.—Continued

[Positive numbers indicate dissolution, negative numbers indicate precipitation, and shaded rows indicate preferred model solution. **Solution names:** 83, snow core collected at site USGS 83; 57, USGS 57; 65, USGS 65, etc.; see table 6 for other site names and figure 1 for site locations. **Percentage (+, –):** Plus or minus range of percentages when more than one model solution for the set of initial solutions. **Phase mole transfer:** For solutions or mixtures of solutions that were evaporated (that is, sum of initial solutions exceeds 100), kilograms of water = sum of percent of initial solution(s)/100 = evaporation factor. –, the phase was not identified in the calculated unique model solution. **Solid and gas phases:** Cal, calcite; Dol, dolomite; Gyp, gypsum; Hal, halite; Flu, fluorite; Syl, sylvite; Amm nit, ammonium nitrate; Oliv Fo85, olivine with composition Fo85; Plag An60, plagioclase with composition An60; B-glass, basaltic volcanic glass; Ca mnt, calcium montmorillonite; CO_2, carbon dioxide; O_2, dissolved oxygen; Goe, goethite. **Comments:** %, percent; ‰, permil; unc, uncertainty; tr, trace]

Solution			Number of plausible (P) and unique (U) models (P/U)	Phase mole transfer (micromoles per kilogram of water)														Comments
Initial	Percentage (+, –)	Final		Cal	Dol	Gyp	Hal	Flu	Syl	Amm nit	Oliv Fo85	Plag An60	B-glass	Ca mnt	CO_2	O_2	Goe	
GROUNDWATER FROM MULTILEVEL WELLS—Continued																		
EBR1, 132Z14, BLRINL	60, 21, 19			–	–	83	85	–	–	11	–	256	–	–176	471	68	–0.3	
131AZ12, EBR1	52(+4), 48(–4)			–	–	54	–	–	–	–	–	376	–	–258	314	40	–0.2	
EBR1, BLRINL	80(–32), 20(+32)			237	–	89	135	–	–	14	–	88	–	–60	346	83	0.5	

From 1 to 27 plausible models were produced for groundwater from 44 zones from MLW (no successful models were produced at MIDDLE 2050A, zone 3). Consequently, many of the model results included plausible models that have a range of solution percentages and (or) different combinations of initial solutions. Each different combination of initial solutions, for a particular final solution, was considered a unique model, and these unique models were further evaluated for hydrologic and (or) chemical constraints, such as minimizing precipitation as an initial solution and evaluating the consistency of tritium activities between initial and final solutions, to select the best model or models. Table 9 presents a summary of the model results (sets of initial solutions, solution percentages and range of solution percentages, number of plausible and unique models, and mass transfer of phases) for each final solution. The first result in the list of models for each final solution represents the "best" unique model that was used in calculations and interpretations described in section, "Hydrologic Processes."

The dominant chemical reactions simulated in the geochemical models were dissolution of plagioclase (An_{60}) and basalt volcanic glass (table 9). Other minerals simulated as dissolving into solution were dolomite, olivine (Fo_{85}), evaporite minerals (gypsum, halite, fluorite, and sylvite), and ammonium nitrate. Calcite was simulated as dissolving or precipitating into solution. Recharge of surface water was a common occurrence in the southwestern part of the Idaho National Laboratory (INL), making this part of the eastern Snake River Plain (ESRP) aquifer an open system. Therefore, model simulations included carbon dioxide and dissolved oxygen as reacting phases.

Two solid phases, calcium montmorillonite and goethite, were simulated as precipitating and were reaction products (tables 7 and 9). For example, precipitation of calcium montmorillonite occurred in all geochemical models and was a result of incongruent dissolution of plagioclase and (or) volcanic glass. Precipitation of goethite (>1 µmol/kg water) was represented in geochemical models if the iron-bearing solid phases, basalt volcanic glass and olivine, were represented as dissolving into solution. Dissolution of these minerals releases ferrous iron into solution (table 7), and ferrous iron subsequently becomes oxidized to ferric iron in the well-oxygenated ESRP aquifer. A ferric iron oxide/hydroxide, represented with goethite in geochemical models, precipitates from solution because ferric iron is nearly insoluble in the oxygenated slightly alkaline conditions (Manahan, 1991, fig. 4-4) present in the aquifer.

Recharge from the Big Lost River (BLR) is episodic and ephemeral, which creates a dynamic aquifer system in the southwestern part of the INL. The multilevel well (MLW) groundwater samples were collected during 2007–13, a period when the BLR was providing minimal or no recharge to the ESRP aquifer at the INL (fig. 4). Thus, geochemical modeling results could vary depending on the amount of recharge from the BLR compared to the timing of sample collection at the MLW. Results from Busenberg and others (2001) show that tritium-helium-3 age-dating of groundwater from wells dominated by BLR recharge have an approximate age of 10-15 years. These age-dating results support the timing of recharge between 1995 and 2000 for groundwater from the MLW sampled between 2007 and 2013.

MIDDLE 2050A

MIDDLE 2050A is located adjacent to the BLR and close to the Advanced Test Reactor Complex (ATRC) and Idaho Nuclear Technology and Engineering Center (INTEC) (fig. 1). MIDDLE 2050A consists of five zones (from shallowest to deepest: zones 15, 12, 9, 6, and 3) that extend from the water table to about 748 ft bwt (table 1). Plausible geochemical models were produced for all zones except zone 3[18]. There was one unique model for zones 15, 9, and 6 and four unique models for zone 12 (table 9).

Modeling indicates that water at zones 15 and 12 is primarily from the BLR, precipitation, and groundwater from Fire Station 2 and Site 4 (table 9). Modeling also indicates that wastewater at zone 15 is from the INTEC (USGS 57) and ATRC (USGS 65) and that wastewater at zone 12 is from the INTEC. Water at zones 9 and 6 is primarily groundwater from Site 19, although the deeper zone, zone 6, also contains groundwater from the deepest zone (zone 3) at USGS 134.

The sources of water identified from model results are consistent with the sources of water interpreted from chemistry data. For example, chemistry data indicate that young water and wastewater from the ATRC and (or) INTEC are sources of water to zones 15 and 12 (table 10). Consequently, the "best" models for zones 15 and 12 contain an initial solution that includes wastewater and, because precipitation should be a small source of recharge, the "best" model for zone 12 contains the smallest amount of precipitation as an initial solution. At zone 9, the model indicates that water from Site 19 is the source of water and tritium activities indicate that wastewater and (or) young water is a source of water. Tritium activities were lower in water at Site 19 (13.4±1.0 pCi/L) than at zone 9 (60.9±2.9 pCi/L) (table 6), which indicates that some wastewater should contribute water at zone 9. Tritium activities also indicated that water at zone 6 was a mixture of young and old water (fig. 15*A*). This is consistent with model results indicating that water at this zone is from Site 19 and zone 3 from USGS 134. Hydraulic head and water temperature profiles indicated that horizontal flow was the predominant flow type at MIDDLE 2050A (fig. 7). However, because most of the water at zone 12 is from surface-water recharge (table 9), there must be some vertical flow in the shallow part of the aquifer near MIDDLE 2050A.

[18]The chemistry of groundwater at zone 3 (low concentrations of dissolved oxygen, sulfate, nitrate, uranium, and high concentrations of iron; tables 2–4) indicates that redox reactions are taking place in this groundwater, perhaps due to upwelling of anoxic geothermal water similar in chemical composition to INEL-1 (Rattray, 2019). However, no successful models were produced for groundwater from zone 3 even when using water from INEL-1 as an initial solution.

Table 10. Summary of geologic province, dominant type of water flow, and source or age of water based on hydraulic, physical, and chemistry data, Idaho National Laboratory, eastern Idaho.

[Location of sites shown in figure 1. **Geologic province**: ABSB, Arco-Big Southern Butte rift zone; BLT, Big Lost Trough. **Dominant type of water flow:** Horizontal, horizontal groundwater flow; Vertical, vertical groundwater flow. **Source or age or water:** ATRC, Advanced Test Reactor Complex; BLR, Big Lost River; INTEC, Idaho Nuclear Technology and Engineering Center; RWMC, Radioactive Waste Management Complex. **Major ion concentrations:** precip, precipitation. **Tritium activity and chloride concentration:** Young, primarily young water; Mixture, mixture of young and (or) wastewater with old water; Wastewater, contains wastewater; /, and/or. **Symbol:** –, no source identified]

Zone	Geologic province	Dominant type of water flow based on hydraulic head and water temperature profiles	Source or age of water (based on)				
			Major ion concentrations	Trilinear diagram	$\delta^{18}O$–$\delta^{2}H$	$\delta^{18}O$–$\delta^{13}C$	Tritium activity and chloride concentration
GROUNDWATER FROM MULTILEVEL WELLS							
MIDDLE 2050A							
Zone 15	BLT	Horizontal	ATRC/INTEC	–	BLR	BLR	Young/wastewater
Zone 12	BLT		–	–	–	BLR	Young/wastewater
Zone 9	BLT		–	–	–	–	Young/wastewater
Zone 6	BLT		–	–	–	–	Mixture
Zone 3	BLT		–	–	BLR	Precipitation	Young/wastewater
MIDDLE 2051							
Zone 12	BLT	Horizontal	BLR/precipitation	BLR	BLR	BLR	BLR
Zone 9	BLT		–	–	–	–	ATRC
Zone 6	BLT		–	–	–	–	ATRC
Zone 3	BLT		–	–	–	–	Wastewater
Zone 1	BLT		–	–	–	–	Wastewater
USGS 103							
Zone 17	ABSB	Vertical	BLR/precip/INTEC	INTEC	BLR	BLR/INTEC	Mixture
Zone 15	ABSB		–	–	–	–	Mixture
Zone 12	ABSB		–	–	–	–	Young/wastewater
Zone 9	ABSB		–	–	–	–	INTEC
Zone 6	ABSB		–	–	–	–	INTEC
Zone 3	ABSB		–	–	–	–	INTEC
Zone 1	ABSB		–	–	–	–	INTEC
USGS 105							
Zone 13	ABSB	Vertical	–	–	–	–	Young/wastewater
Zone 11	ABSB		–	–	–	–	Young/wastewater
Zone 8	ABSB		–	–	–	–	Wastewater
Zone 5	ABSB		–	–	–	–	Wastewater
Zone 2	ABSB		–	–	–	–	Young/wastewater

Table 10. Summary of geologic province, dominant type of water flow, and source or age of water based on hydraulic, physical, and chemistry data, Idaho National Laboratory, eastern Idaho.—Continued

[Location of sites shown in figure 1. **Geologic province**: ABSB, Arco-Big Southern Butte rift zone; BLT, Big Lost Trough. **Dominant type of water flow:** Horizontal, horizontal groundwater flow; Vertical, vertical groundwater flow. **Source or age or water:** ATRC, Advanced Test Reactor Complex; BLR, Big Lost River; INTEC, Idaho Nuclear Technology and Engineering Center; RWMC, Radioactive Waste Management Complex. **Major ion concentrations:** precip, precipitation. **Tritium activity and chloride concentration:** Young, primarily young water; Mixture, mixture of young and (or) wastewater with old water; Wastewater, contains wastewater; /, and/or. **Symbol:** –, no source identified]

Zone	Geologic province	Dominant type of water flow based on hydraulic head and water temperature profiles	Source or age of water (based on)				
			Major ion concentrations	Trilinear diagram	$\delta^{18}O$–$\delta^{2}H$	$\delta^{18}O$–$\delta^{13}C$	Tritium activity and chloride concentration
GROUNDWATER FROM MULTILEVEL WELLS—Continued							
USGS 108							
Zone 11	ABSB	Vertical	–	–	–	–	Young
Zone 9	ABSB		–	–	–	–	Young/wastewater
Zone 7	ABSB		–	–	–	–	Young/wastewater
Zone 4	ABSB		–	–	–	–	Young/wastewater
Zone 1	ABSB		–	–	–	–	Young/wastewater
USGS 131A							
Zone 12	BLT	Horizontal	–	–	–	–	INTEC
Zone 8	BLT		INTEC/ATRC	INTEC	–	–	INTEC
Zone 5	BLT		–	–	–	–	Young/wastewater
Zone 3	BLT		–	–	–	–	Young/wastewater
USGS 132							
Zone 17	ABSB	Vertical	–	RWMC	Wastewater	RWMC/BLR	RWMC
Zone 14	ABSB		–	–	BLR	–	Wastewater
Zone 11	ABSB		–	–	–	–	Wastewater
Zone 8	ABSB		–	–	–	–	Wastewater
Zone 5	ABSB		–	–	–	–	Wastewater
Zone 1	ABSB		–	–	–	–	Wastewater
USGS 135							
Zone 10	ABSB	Vertical	–	–	–	–	Mixture
Zone 7	ABSB		–	–	–	–	Mixture
Zone 4	ABSB		–	–	–	–	Mixture
Zone 1	ABSB		–	–	–	–	Mixture
USGS 137A							
Zone 5	ABSB	Vertical	–	–	–	–	Young/wastewater
Zone 4	ABSB		–	–	–	–	Young/wastewater
Zone 3	ABSB		–	–	–	–	Young/wastewater
Zone 1	ABSB		–	–	–	–	Young/wastewater

The primary chemical reactions were dissolution of silicate minerals, with plagioclase dissolving in models for all four zones, basalt volcanic glass dissolving in models for the upper three zones, and olivine dissolving in models for the upper two zones (table 9). Carbonate reactions, represented with dissolution of calcite, dolomite, and (or) carbon dioxide, were important reactions in the upper two zones.

MIDDLE 2051

MIDDLE 2051 is located adjacent to the BLR and about 4.5 mi southwest of the ATRC and INTEC (fig. 1). MIDDLE 2051 consists of five zones (from shallowest to deepest: zones 12, 9, 6, 3, and 1) that extend from the water table to about 612 ft bwt (table 1).

Modeling indicates that the BLR and Site 19 contribute water to most zones at MIDDLE 2051 and that small amounts of wastewater from the ATRC (USGS 65) is present in some models in all zones (table 9). The primary source of water to zone 12 is the BLR, consistent with the interpretation from chemistry data (table 10). The primary source of water to zones 9 and 6 is zone 15 (shallowest zone) from USGS 134, and the primary source of water to zones 3 and 1 is water from Site 19.

Tritium activities indicate that the four deeper zones at MIDDLE 2051 contain wastewater, with the chloride-tritium graph indicating that wastewater from zones 9 and 6 are from the ATRC (fig. 16). The highest tritium activity, and therefore the largest amount of wastewater, was measured in water from zone 6 (table 6). This is consistent with model results that show wastewater from the ATRC (USGS 65) as a source of water to all sampling zones at MIDDLE 2051, with the highest percentage of wastewater (8 percent) from the ATRC in water from zone 6 (table 9). Horizontal flow was interpreted to be the dominant type of flow at MIDDLE 2051 based on interpretation from hydraulic head and water temperature profiles. Nevertheless, the presence of wastewater at all zones does support some downward movement of groundwater flowing to MIDDLE 2051.

There were four unique models for zone 12, three for zone 1, two for zones 9 and 3, and one for zone 6 (table 9). Wastewater from the ATRC (USGS 65) is an initial solution in one unique model for each of zones 9, 6, and 3, so each of these models are the “best” models for their respective zone. Wastewater from the ATRC is an initial solution in two unique models for zone 1. Because both models have similar initial solutions and solution percentages, each of them is an acceptable “best” model. The four unique models for zone 12 are similar in that they all indicate that 73 percent or more of the water at this zone is from the BLR. Consequently, each of these four models are an acceptable “best” model.

Silicate and carbonate reactions were the primary chemical reactions for all zones at MIDDLE 2051, and a large amount of carbon dioxide was modeled as dissolving into solution at zone 12, the shallowest zone, due to the large amount of infiltration recharge from the BLR to this zone (table 9). Silicate reactions consisted of either plagioclase or basalt volcanic glass dissolving into solution, and carbonate reactions consisted of either calcite or dolomite dissolving into solution in the shallowest three zones and calcite and dolomite precipitating and dissolving, respectively, in the deeper two zones. The dissolution of calcite in models for zones 9 and 6 were among the few zones at MLW where modeling indicated required dissolution of calcite. Calcite was modeled as dissolving at these two zones because water from zone 15 at USGS 134, the primary modeled source of water to these two zones, is undersaturated with respect to calcite.

USGS 103

USGS 103 is located about 8.1 mi south of the BLR and the INTEC (fig. 1). USGS 103 consists of seven zones (from shallowest to deepest: zones 17, 15, 12, 9, 6, 3, and 1) that extend from about 85 to 694 ft bwt (table 1).

Modeling indicates that the primary sources of water at USGS 103 are the BLR and precipitation at zone 17; USGS 83, USGS 104, or USGS 107, and the BLR at zones 15 and 12; and USGS 104 at zones 9, 6, 3, and 1 (table 9). Chemistry data support model results that show the BLR and precipitation are sources of water to zone 17 at USGS 103 (table 10), although the low tritium activity (8±1.9 pCi/L; table 6) in water from zone 17 indicates that this water also must contain some old groundwater (fig. 15*A*). The high sodium and chloride concentrations in groundwater from zone 17, relative to total cations or anions (fig. 8), may be due to dissolution of halite (table 9) as surface water infiltrates through the unsaturated zone and aquifer to zone 17.

Tritium activities in water from the four deepest zones at USGS 103 are high (fig. 3*B*; table 6), indicating that wastewater from the INTEC is a source of water to these zones (fig. 16; table 10). Vertical profiles showing a relatively constant hydraulic head and decreasing water temperature with depth suggest that vertical flow is the dominant flow type at USGS 103 (fig. 7), and the presence of wastewater in the four deep zones at USGS 103 supports the interpretation that groundwater moves downward to these zones.

There was one unique model for each of zones 6, 3, and 1, two for zones 17 and 9, and three and five for zones 12 and 15, respectively (table 9). The initial solutions and solution percentages for the two unique models for zone 17 are similar. However, because tritium activities indicate that zone 17 contains some old groundwater, the model that includes groundwater from USGS 107, which has a low tritium activity (10.2±1.0 pCi/L, table 6), as an initial solution is the “best” model. The initial solutions and solution percentages for the two unique models for zone 9 also are similar. However, matching of tritium activities (table 6) between initial and final solutions (and considering decay of tritium and groundwater travel time) suggests that the “best” model for zone 9 is the model that includes old groundwater (USGS 83, tritium activity of -190±70 pCi/L; table 6) as an initial solution. Because the tritium activity in groundwater from zone 12

(72.4±2.9 pCi/L; table 6) indicates the presence of only a small amount of wastewater, the unique model for zone 12 that minimized the percentage of USGS 104, which has a high tritium activity (1,670±240 pCi/L; table 6), as an initial solution was considered the "best" model. The low tritium activity of 16.9±1.9 pCi/L (table 6) in groundwater from zone 15 shows that this groundwater does not contain wastewater. Three of the five unique models for zone 15 include USGS 104 as an initial solution, so these three unique models were eliminated as "best" models. The other two unique models consist of a large percentage of groundwater and a small percentage of the BLR as initial solutions, and either of these two models are an acceptable "best" model.

Silicate reactions were important chemical reactions for all zones at USGS 103 (table 9), with plagioclase dissolving into solution in models for all zones and either olivine or basalt volcanic glass dissolving into solution in models for most zones. Carbonate reactions and dissolution of evaporite minerals were important reactions for the shallowest zone, probably because infiltration recharge of dilute surface water from the BLR and precipitation were large sources of water to this zone. Dissolution of carbon dioxide and dissolved oxygen was represented at many of the zones and reflects infiltration of surface water.

USGS 105

USGS 105 is located about 9.1 mi south-southwest of the INTEC (fig. 1). USGS 105 consists of five zones (from shallowest to deepest: zones 13, 11, 8, 5, and 2) that extend from about 34 to 603 ft bwt (table 1).

Modeling indicates that the primary sources of water at USGS 105 are (1) EBR1 at all zones, (2) zone 12 from USGS 131A at the upper four zones, (3) zone 8 from USGS 131A at zone 5, and (4) zones 9 and 12 from MIDDLE 2051 at zone 2 (table 9). Tritium activities in water from USGS 105 indicate that wastewater was a source of recharge (fig. 15*A*). Tritium activities increase with depth for the shallowest four zones, ranging from 171.3±5.4 to 262.9±7.7 pCi/L, while the deepest zone had a slightly smaller tritium activity of 126.3±4.1 pCi/L (fig. 13; table 6). The high tritium activities at the deepest zones indicate that significant downward movement of surface water has occurred, an interpretation that is consistent with hydraulic head and water temperature profiles that suggest vertical movement of water is the dominant type of flow at USGS 105 (fig. 7). However, the low tritium activity at the deepest zone indicates that less wastewater reaches this zone, which suggests that there may be less downward movement of groundwater to this zone than for the shallow zones.

Zones 13, 11, and 8 each have one unique model and zones 5 and 2 each have three unique models (table 9). Initial solutions for the three unique models for zone 5 are groundwater from EBR1 and USGS 131A. None of these models is clearly better than the other models, so each of these models is an acceptable "best" model. In the three unique models for zone 2, only zone 9 from MIDDLE 2051 is an initial solution that has a high tritium activity (table 6). Consequently, either of the two models that include zone 9 from MIDDLE 2051 as an initial solution are acceptable "best" models.

Dissolution of plagioclase was the dominant chemical reaction at USGS 105 (table 9). Calcite was modeled as precipitating out of solution for the shallowest zone, and dissolution of gypsum and halite were modeled for the two shallowest zones and the deepest zone, respectively.

USGS 108

USGS 108 is located about 8.6 mi south-southwest of the INTEC (fig. 1). USGS 108 consists of five zones (from shallowest to deepest: zones 11, 9, 7, 4, and 1) that extend from about 30 to 582 ft bwt (table 2).

Modeling indicates that the sources of water at USGS 108 are (1) USGS 83, zone 12 from USGS 131A, and the BLR at zone 11; (2) USGS 104, the BLR, and CFA2 at zone 9; (3) USGS 83, USGS 104, zones 12, 8, and 5 from USGS 131A, and the BLR at zones 7 and 4; and (4) zone 3 from MIDDLE 2051 and zones 8 and 5 from USGS 131A at zone 12 (table 9). Tritium activities indicate that sources of water at USGS 108 include a small amount of wastewater. For example, the lowest (58.8±3 pCi/L, table 6) and highest (119±3 pCi/L, table 6) tritium activities, in water from the two shallowest zones at this MLW, zones 11 and 9 (fig. 3*D*), respectively, exceed the estimated tritium activity of current or recent (since 1998) recharge of young water (fig. 15*A*). However, some large sources of water to USGS 108, such as zones 12 and 8 from USGS 131A, CFA2, and USGS 104, have much higher tritium activities (ranging from 983±26.3 to 1,670±240 pCi/L, table 6) than the tritium activities at USGS 108 (table 6). Although some dilution of tritium occurs through mixing with water with low tritium activities, such as USGS 83 and the BLR, the small solution percentages of these sources of water (table 9) does not provide enough dilution to account for the large difference in tritium activities between the initial solutions and USGS 108. Consequently, flow rates between the source waters and USGS 108 may be slow to allow enough time for decay of tritium to reduce tritium activities to those measured in water from USGS 108. Tritium has a half-life of 12.3 years, and a time lapse of about two to three half-lives (24.6–36.9 years) probably is required to sufficiently reduce (through dilution plus decay of tritium) tritium activities in initial solutions to the tritium activities measured in water from USGS 108. With distances between the initial solutions and USGS 108 of about 3 to 5.7 mi, average linear groundwater-flow rates between the source waters and USGS 108 must range from about 1.2 to 3.3 ft/d. These flow rates are lower than the 4 to 20 ft/d flow rates estimated for the southwestern part of the INL (Ackerman and others, 2006). Low hydraulic conductivities in the aquifer north of USGS 108 (Rattray, 2018, fig. 7) may be a cause of these apparent slow flow rates.

There was one unique model result for zone 1, two for zones 11 and 9, three for zone 7, and 7 for zone 4 (table 9). Only one unique model for zone 11 includes an initial solution, zone 12 from USGS 131A (tritium activity of 983±26.3 pCi/L, table 6), that contains wastewater, so this is the "best" model for zone 11. Both unique models for zone 9 have initial solutions that contain wastewater, and matching tritium activities between initial and final solutions indicates that either model could be the "best" model. The unique models for zones 7 and 4 all include groundwater, and most also include the BLR, as an initial solution. Any of these unique models are acceptable "best" models, although because the solution percentage of the BLR in these models ranges from 0 to 29 percent there is some uncertainty about the precise relative amounts of surface-water and groundwater sources of recharge to these zones.

The primary silicate and carbonate reactions were dissolution of basalt volcanic glass and dolomite. Dissolution of gypsum, halite, and carbon dioxide were important chemical reactions for zones 11, 9, and 1 (table 9).

USGS 131A

USGS 131A is located about 4.5 mi south-southwest of the INTEC (fig. 1). USGS 131A consists of four zones (from shallowest to deepest: zones 12, 8, 5, and 3) that extend from about 16 to 611 ft bwt (table 1).

Modeling indicates that water at (1) zones 12 and 8 consist of water from zones 12 and 9 at MIDDLE 2051A, EBR1, CFA1 or CFA2, and the BLR; (2) zone 5 consists of water from EBR 1, zone 6 at MIDDLE 2051, and CFA1; and (3) zone 3 consists of water from zones 6, 3, and 1 at MIDDLE 2051 (table 9). Chemistry data, including high tritium activities, indicate that a significant amount of wastewater from the INTEC is a source of water to zones 12 and 8, the upper two zones, at USGS 131A (table 10; fig. 15*A*). Low tritium activities in zones 3 and 5, the bottom two zones at USGS 131A, indicate that a small amount of wastewater provides water to these zones (fig. 15*A*). This interpretation is consistent with groundwater from CFA1 or CFA2, with very high tritium activities (18,800±1,600 and 14,100±1,400 pCi/L, respectively; table 6), modeled as providing higher percentages of water to the upper two zones than the lower two zones (table 9).

Groundwater from MIDDLE 2051 is modeled as a source of water to zones 5 and 3 at USGS 131A (table 9). However, this would require groundwater to flow southeast from MIDDLE 2051 to USGS 131A, in contrast to the south to southwest direction of groundwater flow in the southwestern part of the INL (Rattray, 2019, fig. 19). Consequently, MIDDLE 2051 may be representative of groundwater north of USGS 131A.

There was one unique model for zones 12 and 5 and three for zones 8 and 3 (table 9). All three models for zone 8 include 23 to 30 percent water from CFA1 as an initial solution, so any of these three models are possible "best" models. However, because EBR1 is an initial solution for the zones directly above and below zone 8 (table 9), either of the two models for zone 8 that include EBR1 as an initial solution are acceptable "best" models. The initial solutions for one of the unique models for zone 3 include zones 6 and 1, but not zone 3, from MIDDLE 2051. This vertical inconsistency in sources of water to zone 3 at USGS 131A is unlikely. Consequently, either of the other two models are acceptable "best" models.

The primary silicate reaction was dissolution of plagioclase (table 9). Carbonate reactions consisted of dissolution of dolomite for the three deepest zones, and gypsum and dissolved oxygen were modeled as dissolving into solution for the shallowest two zones.

USGS 132

USGS 132 is located about 1.0 mi south-southwest of the RWMC and 0.5 mi east-southeast of INL spreading area B (fig. 1). USGS 132 consists of six zones (from shallowest to deepest: zones 17, 14, 11, 8, 5, and 1) that extend from about 17 to 607 ft bwt (table 1).

Modeling indicates that sources of water at USGS 132 are the BLR at all six zones, USGS 88 and (or) USGS 119 at the two shallowest zones, RWMC M3S at the shallowest four zones, and zones 6 or 9 from MIDDLE 2051 at the four deepest zones (table 9). The trilinear diagram (fig. 8) and a graph of chloride concentrations (fig. 16) show that zone 17 has a high chloride concentration. This high concentration probably originates from application of a Mg-Cl brine at the RWMC (Roddy, 2007; U.S. Department of Energy, 2011), and mixing lines on the trilinear diagram (fig. 9) indicate that groundwater from USGS 88 may be a good representation of the chemistry of brine-influenced groundwater. Hydrogen and oxygen stable isotope values in water from zone 14 are slightly higher than most values at MLW, indicating that recharge of water from the BLR that has undergone evaporation (fig. 12) may be a source of water to this zone.

Tritium activities are lowest, 122±4.1 pCi/L, in water from the shallowest zone (zone 17), and tritium activities in water from deeper zones (zones 1 to 14;) range from 252±7.7 to 301±8.9 pCi/L. These high tritium activities indicate the presence of wastewater in groundwater at these zones (fig. 15*B*), and wastewater in the models is present as initial solutions from zones 6 and 9 at MIDDLE 2051 and RWMC M3S (table 9). The high tritium activities and low chloride concentrations at the five deeper zones indicate that wastewater at these zones probably is from the ATRC (fig. 16).[19]

There was one unique model for zone 5, two for zones 14, 11, and 1, six for zone 8, and eight for zone 17 (table 9). Only one model for zone 14 includes an initial solution

[19]The presence of carbon tetrachloride (tetrachloromethane) at all six zones at USGS 132 (Bartholomay, Maimer, and others, 2017) indicates that some constituents in waste disposed at RWMC also are present in groundwater throughout this MLW.

(RWMC M3S) that has high tritium activities, so this model is the "best" model for zone 14. Zones 11 and 1 each have two models, and the models for each zone have similar initial solutions, solution percentages, and an initial solution that is a large source of tritium. Consequently, either model in these two zones is an acceptable "best" model. The six models for zone 8 consist largely of groundwater from zones 9 and (or) 6 from MIDDLE 2051 with lesser amounts of water from the BLR. The similar initial solutions and solution percentages of these models makes any of them an acceptable "best" model. Tritium activities in groundwater from zone 17 indicate the presence of a small amount of wastewater (fig. 15*B*). Chloride concentrations and tritium activities are high in water from zone 17 (table 6), so the "best" model for zone 17 is the model that includes USGS 88 and the smallest solution percentage of water from RWMC M3S, which contains wastewater, as initial solutions.

Silicate weathering consisted of dissolution of plagioclase and (or) basalt volcanic glass at all zones and of forsterite in the shallowest two zones (table 9). Carbon dioxide and sylvite were simulated as dissolving, and calcite was simulated as precipitating, in most models.

USGS 135

USGS 135 is located about 4.9 mi south of the BLR (fig. 1). USGS 135 consists of four zones (from shallowest to deepest: zones 10, 7, 4, and 1) that extend from about 10 to 420 ft bwt (table 1).

Modeling indicates that sources of water at USGS 135 are the BLR and USGS 86 at all four zones and USGS 8 at the shallowest three zones (table 9). Tritium activities in water from sampling zones at USGS 135 range from 6.1±1.9 to 15±2.2 pCi/L (table 6) and indicate that groundwater at this MLW may be a mixture of old groundwater and young water (table 10). Low tritium activities and chloride concentrations indicate that wastewater is not present in water at this MLW (fig. 16; Bartholomay, Maimer, and others, 2017). The BLR is a significant source of water to all sampling zones (table 9), which indicates that groundwater moving to this MLW has a vertical component. This interpretation is consistent with the narrow range of hydraulic head and water temperature observed in vertical profiles of these parameters for USGS 135 (fig. 7).

There was one unique model for zones 7 and 1 and two for zones 10 and 4 (table 9). The two models for zone 10 have similar initial solutions and solution percentages, so either model is an acceptable "best" model. USGS 86 is an initial solution in all models for all four zones at USGS 135 except for one model for zone 4. Because USGS 86 is an initial solution for zones above and below zone 4, it is likely that USGS 86 also provides water to zone 4. Therefore, the "best" model for zone 4 is the model that includes USGS 86 as an initial solution.

Carbonate and silicate reactions were simulated in models for all zones at USGS 135 (table 9). Dolomite was simulated as dissolving for all zones, and calcite was simulated as precipitating for zone 7. Dissolution of basalt volcanic glass was the only silicate reaction and was simulated for all zones. Dissolution of carbon dioxide and (or) dissolved oxygen was simulated for all zones, reflecting the significant amount of surface-water recharge reaching USGS 135.

USGS 137A

USGS 137A is located about 3.4 mi south of the RWMC and adjacent to INL spreading area D (fig. 1). USGS 137A consists of four zones (from shallowest to deepest: zones 5, 4, 3, and 1) that extend from about 12 to 267 ft bwt (table 1).

Modeling indicates that sources of water at all four zones at USGS 137A are zone 12 from USGS 131A, the BLR, EBR 1, and zone 17 from USGS 132 (table 9). In addition, some models in the deeper two zones include zone 14 from USGS 132 as a source of water.

Tritium activities decreased with depth at USGS 137A and ranged from 106±3.83 pCi/L in water from zone 5 to 64.8±2.97 pCi/L in water from zone 1 (table 6). These activities are slightly higher than activities that would be measured in recharge of young water and indicate that a small amount of wastewater is present throughout the vertical extent of this MLW (fig. 15*B*). Tritium activity is high in water from zone 12 at USGS 131A (table 6), so water from this zone should only contribute a small amount of water to USGS 137A. The BLR should be a frequent source of water to USGS 137A because USGS 137A is located adjacent to the INL spreading areas (fig. 1), and the presence of surface water at all depths at USGS 137A (table 9) indicates that groundwater flowing to this MLW includes a vertical component of flow. This interpretation is supported by the nearly uniform hydraulic head and water temperature shown in vertical profiles (fig. 7).

There were three unique models for zone 4, six for zone 5, seven for zone 3, and nine for zone 1 (table 9). The "best" models for each zone at USGS 137A include the BLR and the smallest possible solution percentage of water from zone 12 from USGS 131A as initial solutions.

The model with the estimated lowest tritium activity for zone 3 at USGS 137A, based on solution percentages and tritium activities of initial solutions, includes zone 14 from USGS 132 as an initial solution. However, the "best" model for zone 1 at USGS 137A, which is deeper than zone 3, includes zone 17 from USGS 132, a zone that is shallower than zone 14, as an initial solution. Other models for zone 1 at USGS 137A are unsatisfactory alternatives as "best" models for zone 1 because they have much higher percentages of zone 12 from USGS 131A (table 9). Because it is improbable that zone 3 at USGS 137A would have a deeper source of groundwater than the stratigraphically deeper zone 1, the "best" model for zone 3 at USGS 137A is the model with the lowest percentage of zone 12 from USGS 131A as an initial solution where zone 17, and not zone 14, from USGS 132 is an initial solution.

Dissolution of plagioclase and carbon dioxide were the primary silicate carbonate reactions, respectively, for all zones at USGS 137A. Reactions of smaller magnitude and prominence included dissolution of olivine, volcanic glass, and gypsum (table 3).

Hydrologic Processes

Results from geochemical modeling, consisting of the first model result listed for each final solution ("best" model) in table 9, were used to make interpretations about sources of recharge, mixing of water, and groundwater-flow directions. The sources of recharge and mixing of water were extrapolated from the initial solutions, and groundwater-flow directions were identified from the three-dimensional spatial coordinates between initial and final solutions.

Sources of Recharge

Sources and amounts of recharge to EBR1 and sampling zones at multilevel wells (MLW) (table 11) were determined by extrapolating backward through initial solutions in geochemical models as described by Rattray (2019, p. 35) and table 11. Figure 17 shows the calculated sources of recharge to sampling zones at MLW, with sources of recharge to each sampling zone equal to 100 percent and the total recharge from a specific source of recharge to each MLW shown as cumulative percent.[20] The approximate percentage each source of recharge supplies to the total recharge to the upper 600–700 feet (ft) of the aquifer in the southwestern part of the INL was estimated by summing the percentages for each source of recharge for all sampling zones at MLW and dividing these percentages by the total number of sampling zones (table 12 and fig. 18).[21]

Big Lost River

The Big Lost River (BLR) is a major source of recharge to all nine MLW (fig. 17) and contributes about 60 percent of the total recharge (table 12; fig. 18) to the southwestern part of the Idaho National Laboratory (INL). These results are consistent with Rattray (2019) in that the BLR is a significant source of recharge throughout the southwestern part of the INL.

The amount of recharge from the BLR to MLW, relative to total recharge from all sources, increases in a direction south of the BLR channel. This is evident by comparing the two primary sources of recharge to MLW, the BLR and groundwater from the Little Lost River (LLR) valley (fig. 17). At MIDDLE 2050A, MIDDLE 2051, USGS 131A, and USGS 132, all located within about 3 mi of the BLR (fig. 1), groundwater from the LLR valley is a larger source of recharge than the BLR. This relationship is reversed at USGS 103, USGS 105, USGS 108, USGS 135, and USGS 137A, all located about 5 or more miles south of the BLR, where the BLR is a much larger source of recharge than groundwater from the LLR valley.

There is a distinct vertical distribution to recharge from the BLR. For example, at MIDDLE 2050A, MIDDLE 2051, and USGS 131A only the upper one or two sampling zones have the BLR as the primary source of recharge; recharge from the BLR in the deeper zones at these MLW generally is much smaller and ranges from 7 to 31 percent (table 11). Recharge from the BLR was significant at all zones at USGS 132 and USGS 135, with percentages of recharge from the BLR ranging from 29 to 73 percent. At MLW farther south, along the southern boundary of the INL, USGS 103, USGS 105, USGS 108, and USGS 137A, the BLR is primary source of recharge at all sampling zones (except for the deepest zone at USGS 108) and the percentage of recharge ranges from 56 to 95 percent. These results show that recharge from the BLR affects the shallow aquifer near the BLR channel, but that groundwater containing recharge from the BLR moves to deeper parts of the aquifer as it travels south of the BLR.

Structural features of the aquifer may contribute to the downward movement of groundwater as groundwater flows south of the BLR channel. For example, the Big Lost Trough (BLT), located in the northern part of the study area (fig. 2), has extensive horizontal layers of sediment that impede the downward movement of groundwater. Consequently, horizontal flow predominates near the BLR. In contrast, the Arco-Big Southern Butte rift zone, located near the southern boundary of the INL (fig. 2), contains volcanic vents and fissures that facilitates the downward movement of groundwater. Consequently, vertical flow predominates in the southern part of the study area. These flow directions are consistent with interpretations of flow by Twining and Fisher (2015) based on vertical profiles of hydraulic head and temperature (fig. 11). The downward movement of groundwater also may be enhanced by the southerly dip of stratigraphic units south of the BLR (fig. 3). In addition, the increasing thickness of the aquifer south of the BLR may cause groundwater to flow downward (Ackerman and others, 2006, fig. 24).

[20]Sum of cumulative percent from all sources of recharge to a specific MLW is 100 percent times the number of sampling zones at that MLW (fig. 17).

[21]Including USGS 137A in these calculations adds a slight bias for the Big Lost River (BLR). This is because USGS 137A only extends about 267 feet below water table (ft bwt) (table 1), depths at which the BLR is still the primary source of recharge at MLW along the southern boundary of the INL. As depths increase, groundwater from the Little Lost River (LLR) valley becomes the primary source of recharge (fig. 17).

Table 11. Sources of recharge at EBR1 and multilevel wells, Idaho National Laboratory, eastern Idaho.

[**Initial**: See table 1 for site names and figure 1 for site locations. **Source of recharge:** BC, Birch Creek; BLR, Big Lost River; gw, groundwater; LLR, Little Lost River; LRR, Lost River Range; Reg, regional. **Symbol:** –, none]

Solution			Sources of recharge (percent)							
Initial	Percentage	Final	Wastewater	Precipitation	BLR	LLR valley gw	BLR valley gw	LRR gw	BC valley gw	Reg gw
DEEP GROUNDWATER										
M2051Z12, BLRINL, 83	55, 26, 19	EBR1	2	19	74	6	–	–	–	–
GROUNDWATER FROM MULTILEVEL WELLS										
MIDDLE 2050a										
FS2, BLRLBB, 57, 65	53, 40, 4, 3	Zone 15	5	–	67	27	–	–	–	–
Site 4, BLRINL, 83, 57	38, 34, 24, 5	Zone 12	2	24	59	15	–	–	–	–
Site19	100	Zone 9	–	–	11	90	–	–	–	–
Site19, 134Z3	81, 19	Zone 6	–	–	9	92	–	–	–	–
MIDDLE 2051										
BLRINL, Site19, 65	85, 12, 3	Zone 12	3	–	86	11	–	–	–	–
134Z15, BLRINL, Site19, 65	87, 6, 5, 3	Zone 9	3	10	7	82	–	–	–	–
134Z15, BLRINL, 65	82, 11, 8	Zone 6	8	10	11	72	–	–	–	–
Site19, 65	99, 1	Zone 3	1	–	11	89	–	–	–	–
Site19, BLRINL, 65	76, 23, 1	Zone 1	1	–	31	68	–	–	–	–
USGS 103										
BLRINL, 83, 107	56, 39, 5	Zone 17	–	39	59	–	–	–	1	1
83, 107, BLRINL	47, 42, 11	Zone 15	–	–	78	3	–	–	8	11
83, 104, BLRINL	53, 26, 21	Zone 12	1	–	94	3	–	–	2	–
104, 83	92, 8	Zone 9	2	–	93	2	–	–	1	–
104, BLRINL, 83	90, 7, 4	Zone 6	2	–	95	2	–	–	1	–
104	100	Zone 3	2	–	93	2	–	–	1	–
104	100	Zone 1	2	–	93	2	–	–	1	–
USGS 105										
131AZ12, EBR1	69, 31	Zone 13	6	11	78	7	–	–	–	–
131AZ12, EBR1	64, 36	Zone 11	5	11	77	6	–	–	–	–
131AZ12, EBR1	72, 29	Zone 8	6	11	79	7	–	–	–	–
131AZ12, EBR1, 131AZ8	53, 35, 12	Zone 5	6	12	77	7	–	–	–	–
M2051Z12, M2051Z9, EBR1	49, 36, 15	Zone 2	2	7	56	36	–	–	–	–

Table 11. Sources of recharge at EBR1 and multilevel wells, Idaho National Laboratory, eastern Idaho.—Continued

[**Initial**: See table 1 for site names and figure 1 for site locations. **Source of recharge:** BC, Birch Creek; BLR, Big Lost River; gw, groundwater; LLR, Little Lost River; LRR, Lost River Range; Reg, regional. **Symbol:** –, none]

Solution			Sources of recharge (percent)							
Initial	Percentage	Final	Wastewater	Precipitation	BLR	LLR valley gw	BLR valley gw	LRR gw	BC valley gw	Reg gw
GROUNDWATER FROM MULTILEVEL WELLS—Continued										
USGS 108										
83, 131AZ12, BLRINL	63, 23, 14	Zone 11	2	2	90	5	–	–	2	–
104, BLRINL, CFA2	73, 21, 6	Zone 9	4	–	91	1	–	–	1	–
104, 131AZ8, BLRINL	48, 42, 11	Zone 7	5	3	87	5	–	–	1	–
131AZ8, 104, BLRINL	50, 34, 16	Zone 4	7	3	85	6	–	–	–	–
M2051Z3, 131AZ5, 131AZ8	54, 30, 16	Zone 1	4	2	21	76	–	–	–	–
USGS 131A										
M2051Z12, EBR1, BLRINL, CFA2	36, 36, 19, 9	Zone 12	7	7	80	7	–	–	–	–
M2051Z12, EBR1, CFA1	41, 30, 29	Zone 8	11	6	74	10	–	–	–	–
M2051Z6, EBR1, CFA1	80, 17, 2	Zone 5	7	11	23	59	–	–	–	–
M2051Z3, M2051Z6	84, 16	Zone 3	2	2	11	87	–	–	–	–
USGS 132										
88, M3S, BLRINL	39, 32, 29	Zone 17	39	–	40	21	–	–	–	–
M3S, 119, BLRINL	53, 26, 22	Zone 14	3	–	63	35	–	–	–	–
M2051Z9, BLRINL, M3S	65, 19, 16	Zone 11	2	7	29	64	–	–	–	–
M2051Z6, BLRINL	78, 22	Zone 8	6	8	31	56	–	–	–	–
M2051Z6, BLRINL	78, 22	Zone 5	6	8	31	56	–	–	–	–
M2051Z6, BLRINL	78, 22	Zone 1	6	8	31	56	–	–	–	–
USGS 135										
BLRINL, 86	72, 28	Zone 10	–	13	72	–	9	6	–	–
BLRINL, 8, 86	44, 39, 16	Zone 7	–	8	44	–	29	18	–	–
BLRINL, 86	73, 27	Zone 4	–	13	73	–	9	5	–	–
BLRINL, 86	73, 27	Zone 1	–	13	73	–	9	5	–	–

Table 11. Sources of recharge at EBR1 and multilevel wells, Idaho National Laboratory, eastern Idaho.—Continued

[**Initial**: See table 1 for site names and figure 1 for site locations. **Source of recharge:** BC, Birch Creek; BLR, Big Lost River; gw, groundwater; LLR, Little Lost River; LRR, Lost River Range; Reg, regional. **Symbol:** –, none]

Solution			Sources of recharge (percent)							
Initial	Percentage	Final	Wastewater	Precipitation	BLR	LLR valley gw	BLR valley gw	LRR gw	BC valley gw	Reg gw
GROUNDWATER FROM MULTILEVEL WELLS—Continued										
USGS 137A										
131AZ12, EBR1, 132Z17, BLRINL	34, 29, 20, 17	Zone 5	11	8	73	8	–	–	–	–
131AZ12, BLRINL, EBR1, 132Z17	29, 29, 26, 17	Zone 4	10	7	78	8	–	–	–	–
BLRINL, 131AZ12, EBR1, 132Z17	39, 24, 21, 16	Zone 3	8	6	79	6	–	–	–	–
BLRINL, EBR1, 131AZ12, 132Z17	38, 26, 19, 17	Zone 1	9	6	79	7	–	–	–	–

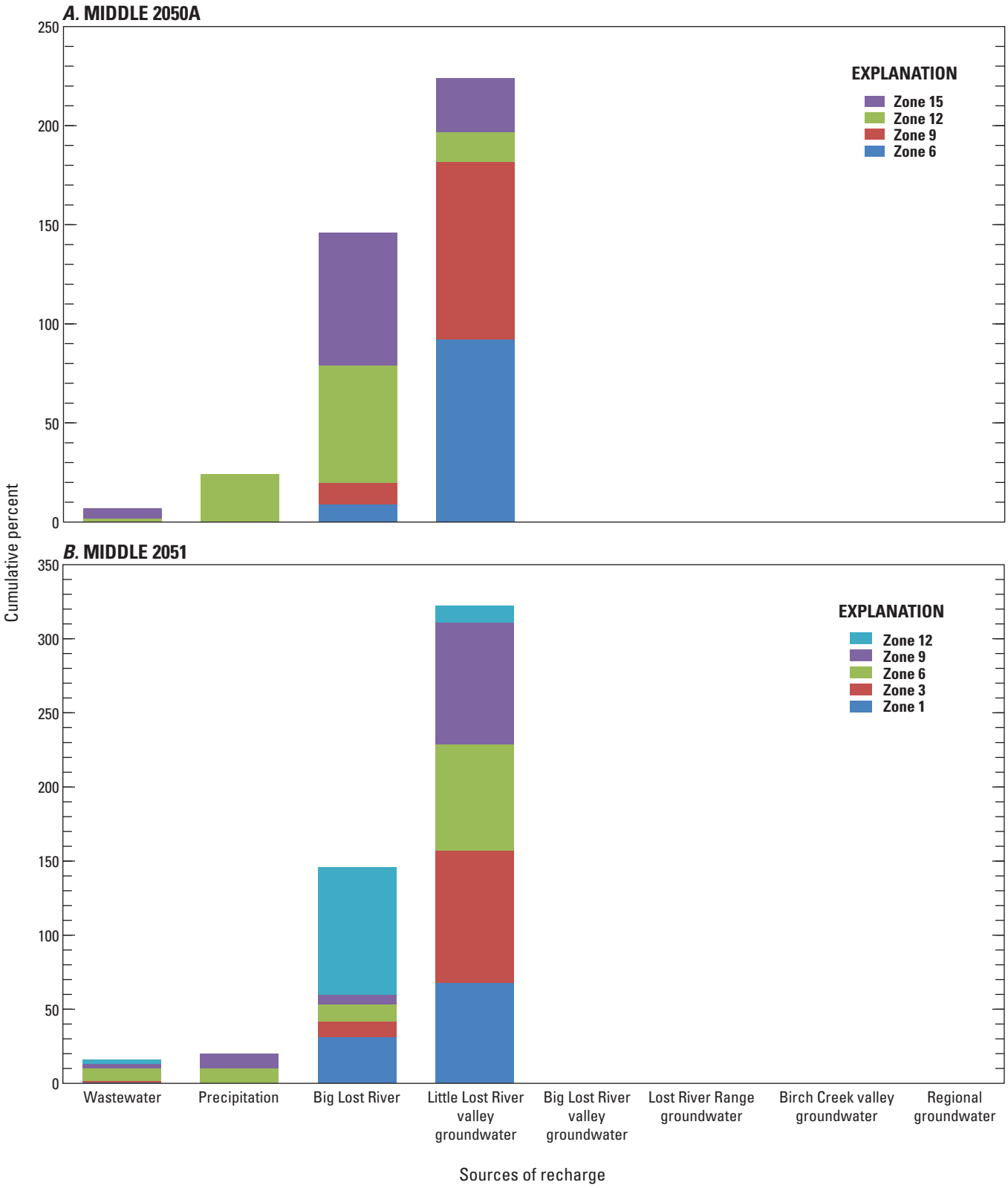

Figure 17. Percentage of various sources of recharge to sampling zones and the cumulative percentage of individual sources of recharge to multilevel wells, Idaho National Laboratory, eastern Idaho. *A*. MIDDLE 2050A. *B*. MIDDLE 2051. *C*. USGS 103. *D*. USGS 105. *E*. USGS 108. *F*. USGS 131A. *G*. USGS 132. *H*. USGS 135. *I*. USGS 137A.

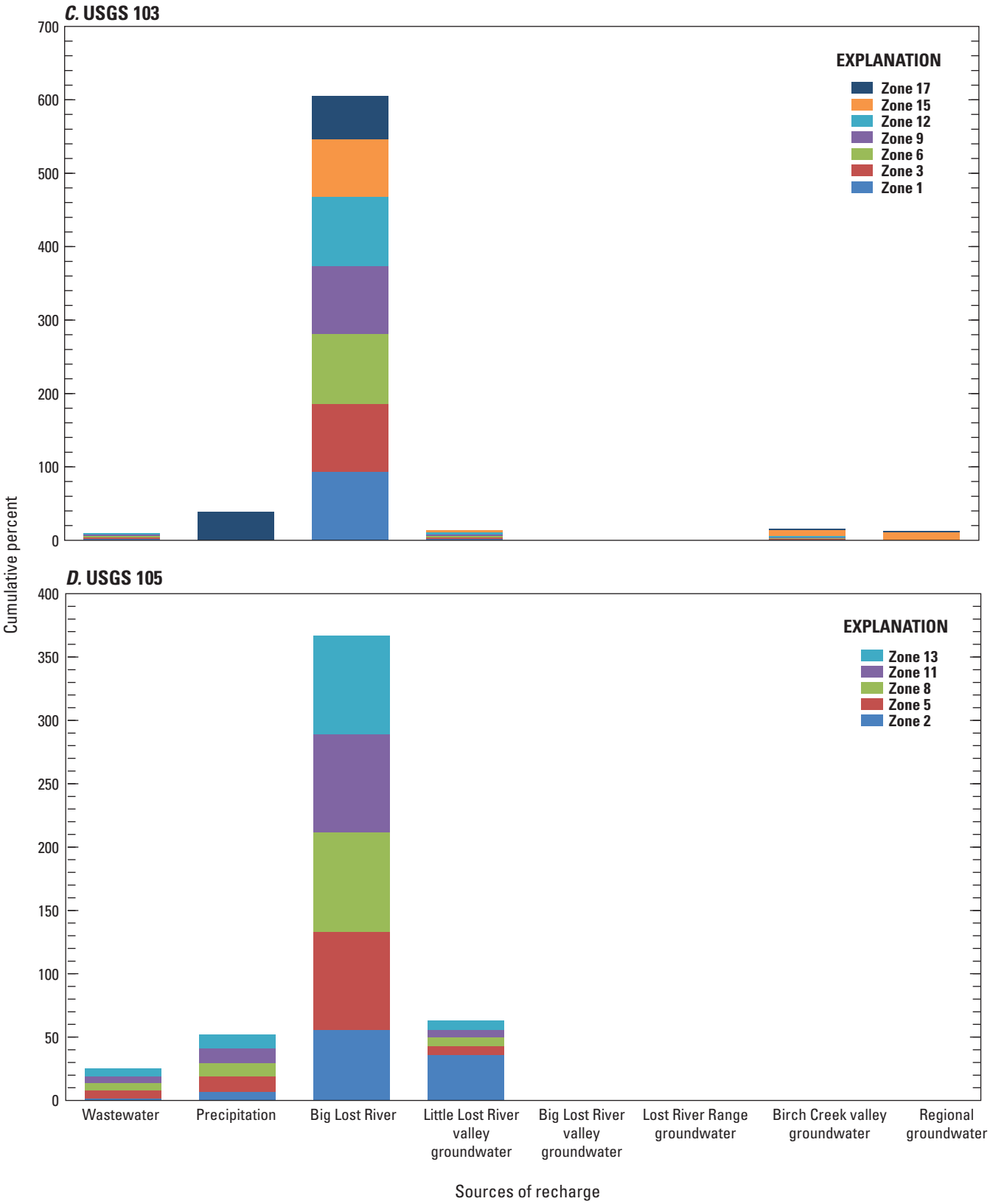

Figure 17.—Continued

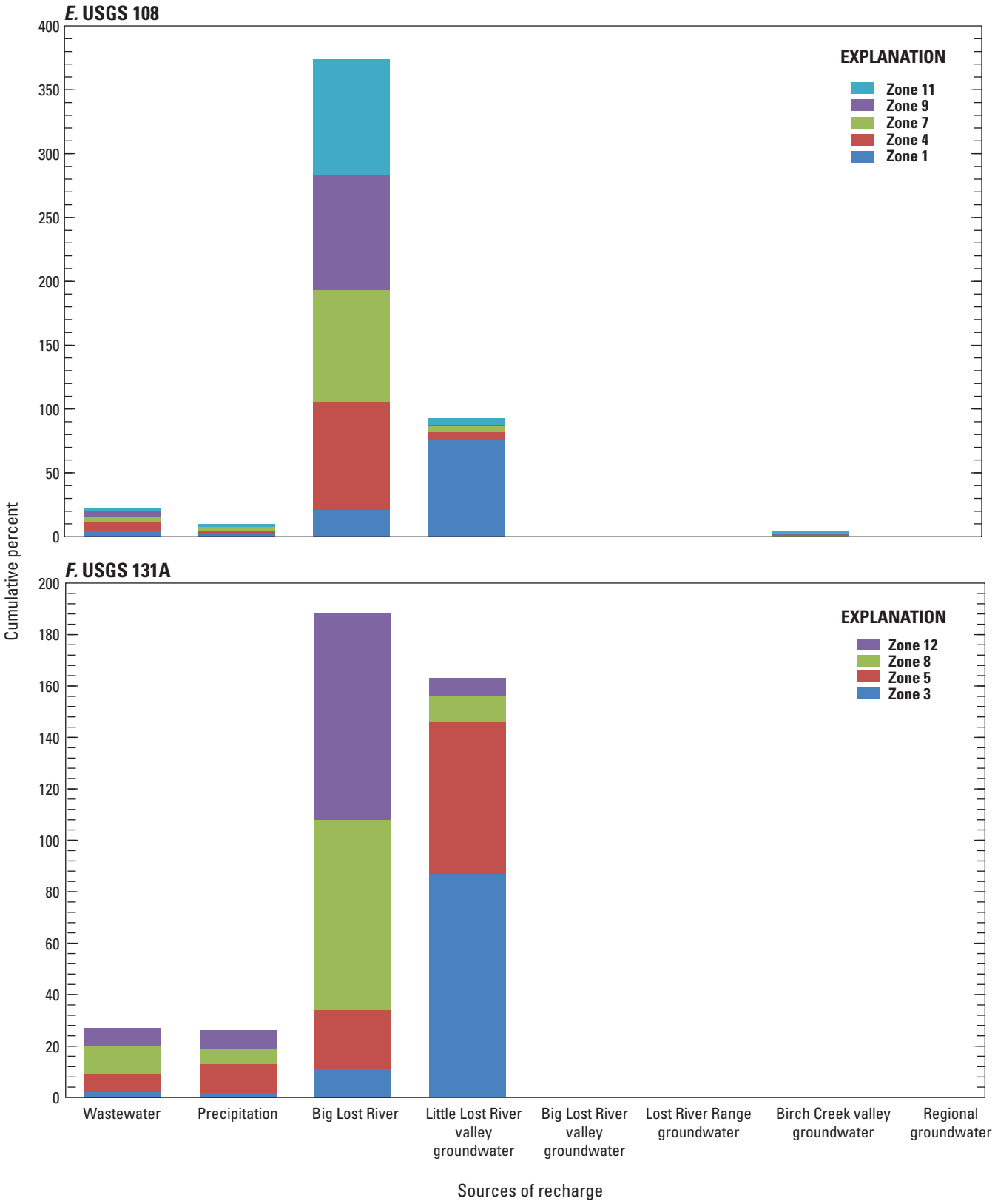

Figure 17.—Continued

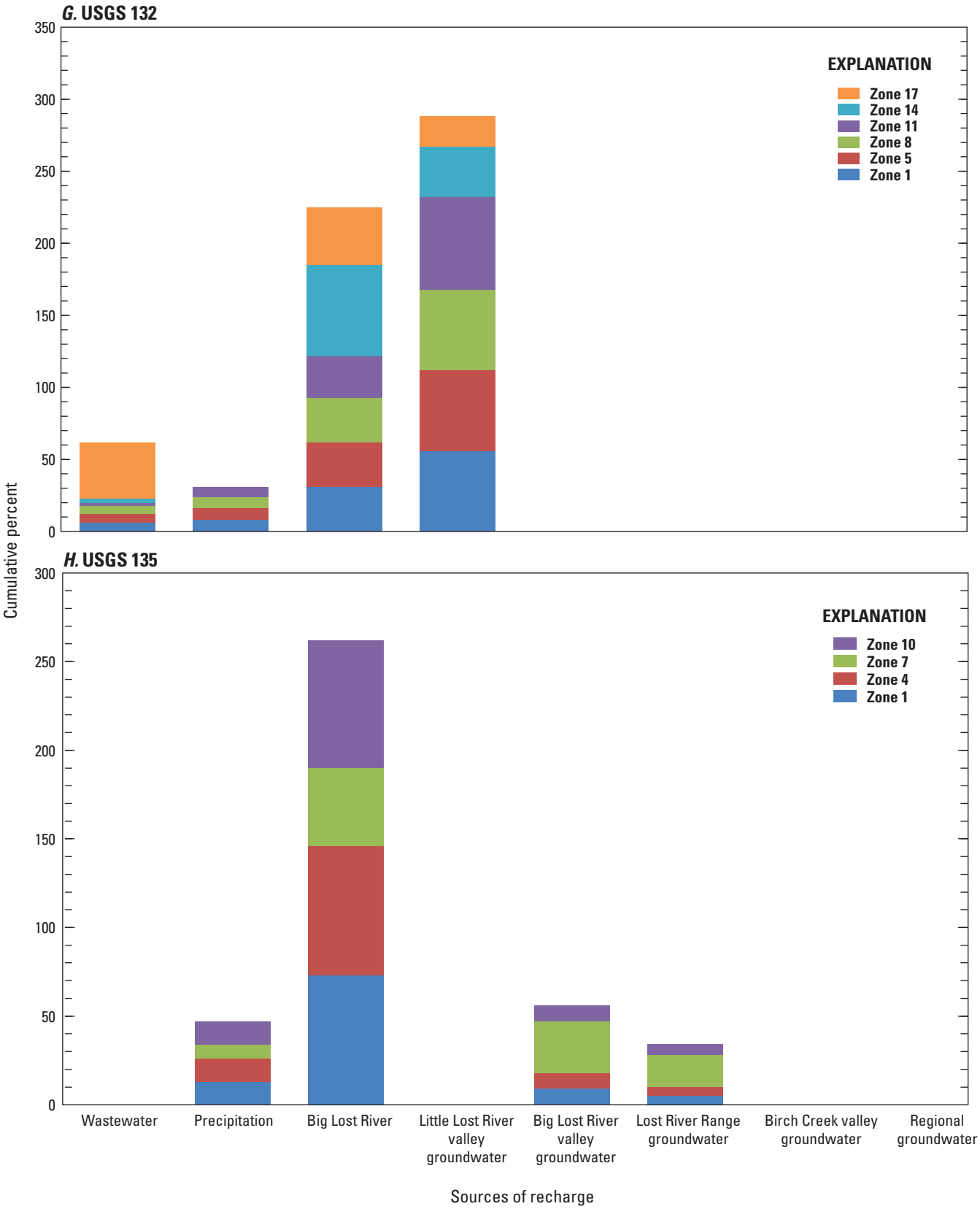

Figure 17.—Continued

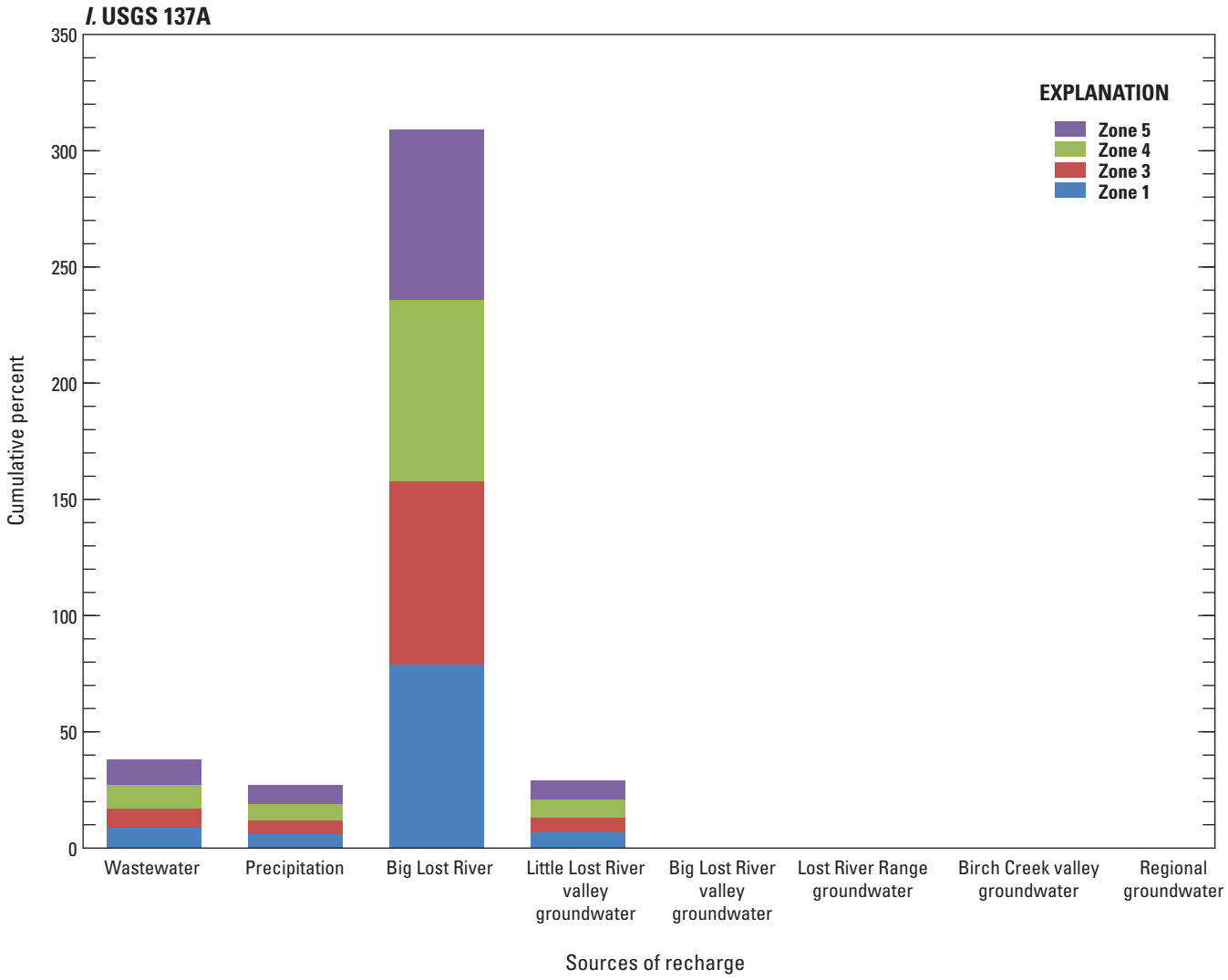

Figure 17.—Continued

Table 12. Sources of recharge and their percentage of total recharge to the southwestern part of the Idaho National Laboratory, eastern Idaho.

[<, less than]

Source of recharge	Percentage of total recharge
Big Lost River	60
Little Lost River valley groundwater	27
Precipitation	6
Wastewater	5
Big Lost River valley groundwater	1
Lost River Range groundwater	<1
Birch Creek valley groundwater	<1
Regional groundwater	<1

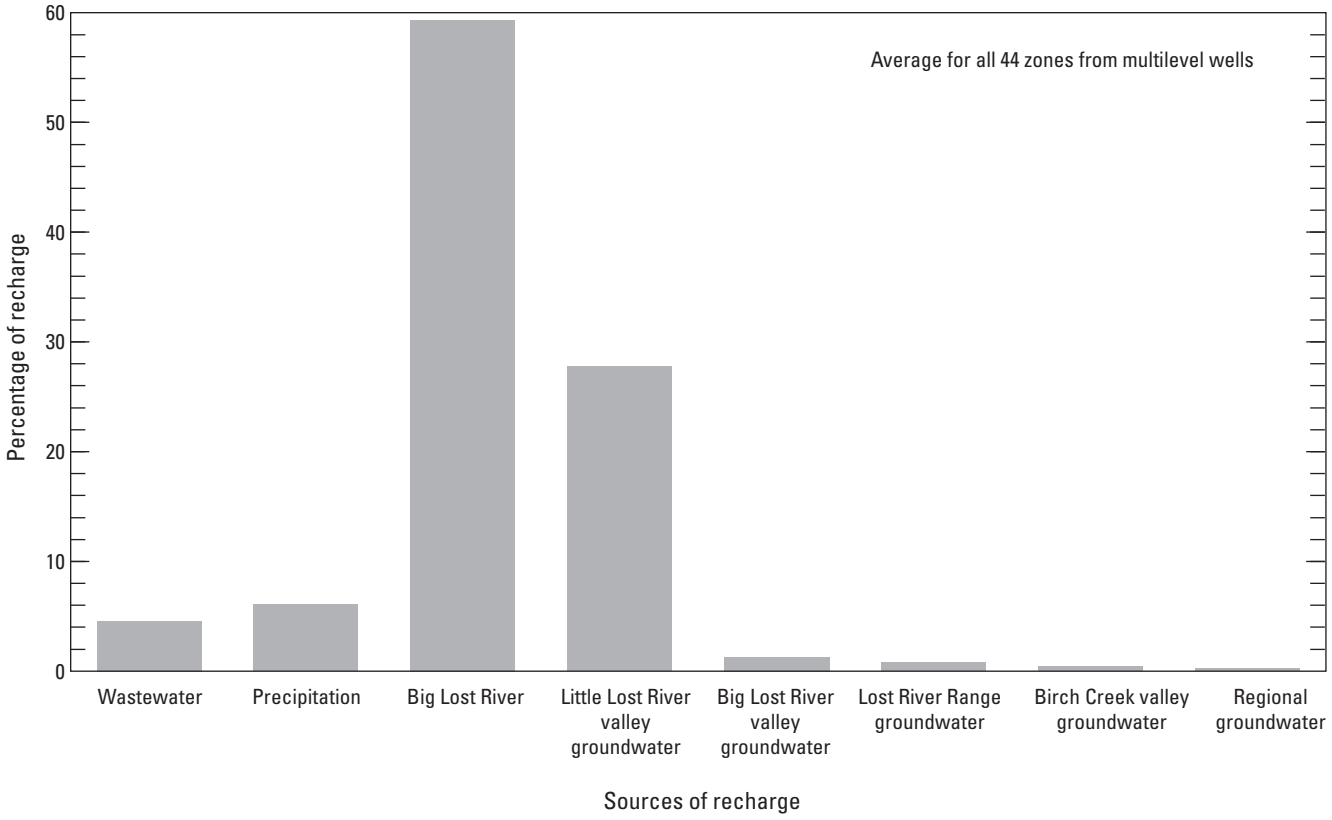

Figure 18. Percentage of recharge that each recharge source contributes to groundwater in the southwestern part of the Idaho National Laboratory, eastern Idaho.

Little Lost River Valley Groundwater

Groundwater from the LLR valley contributes about 27 percent of the total recharge to the southwestern part of the INL (table 12; fig. 18) and is the second most important source of recharge, after the BLR, to this area. Recharge of groundwater from the LLR valley, relative to total recharge from all sources, is largest at MLW near the BLR and generally decreases, in a southward direction, with distance from the BLR (fig. 17). Groundwater from the LLR valley, however, is not present at USGS 135 and provides negligible recharge to USGS 103, MLW that reside in the southwestern and southeastern parts of the study area, respectively (fig. 1). Consequently, these two MLW approximately represent the western and eastern boundaries of groundwater from the LLR valley in the upper 600 to 700 ft of the aquifer beneath the southern boundary of the INL.

The percentage of recharge from groundwater from the LLR valley generally increases with depth at individual MLW (table 11). For example, at MIDDLE 2050A, MIDDLE 2051, and USGS 131A, groundwater from the LLR valley contributes small percentages of recharge (7– 27 percent) to the upper one or two sampling zones (less than 300 ft bwt) and large percentages (59–92 percent) to deeper zones (greater than 180–400 ft bwt). Further south, at USGS 105 and USGS 108, groundwater from the LLR valley is a major source of recharge (36 and 76 percent, respectively) at about 550 to 600 ft bwt (the deepest sampling zone) but provides minimal recharge to shallower sampling zones. Thus, the percentage of recharge from groundwater from the LLR valley not only increases in magnitude with depth, but the depth at which the magnitude increases becomes deeper as groundwater flows south of the BLR.

Precipitation

Recharge from precipitation is ubiquitous in geochemical modeling of groundwater from the southwestern part of the INL (fig. 17; Rattray, 2019, table 11). Compared to the BLR and groundwater from the LLR valley, however, it is a minor source of recharge (fig. 18) that contributes about 6 percent of the total recharge to groundwater in the study area (table 12).

Recharge from precipitation at the INL has been indicated from other geochemistry studies, although this recharge has been very localized (Busenberg and others, 2001; Rattray, 2018, 2019). The results from these other studies suggest that the ubiquitous recharge simulated with geochemical modeling may be incorrect. This discrepancy is probably because recharge from precipitation in the geochemical models represents more dilute recharge from the BLR than was incorporated in model simulations. This is because two, nearly uniform, chemical compositions of the BLR from 1995 and 1997 (tables 2–5) were used in geochemical modeling, and the amount of discharge in the BLR during 1995–97 was modest compared to larger discharge amounts during the 1970s and 1980s (fig. 4). Both the discharge and chemistry of the BLR vary in response to winter snowfall amounts in the BLR drainage basin. Spring runoff in the BLR following winters with well above average snowfall amounts, compared to spring runoff following drier winters, will contain greater amounts of dilute snowmelt and less amounts of saline groundwater (Rattray, 2018). Consequently, recharge from precipitation in the geochemical models may represent the more dilute chemistry in recharge from the BLR following winters that accumulated greater amounts of snow in the BLR drainage basin than the winters of 1995–97.

Wastewater

Wastewater is present at all MLW except USGS 135 (fig. 17) and is a minor source of recharge (fig. 18) that contributes about 5 percent of the total recharge to groundwater in the study area (table 12). Initial solutions from geochemical modeling (table 11; Rattray, 2019, table 11) indicate that (1) wastewater from the INTEC travels south to USGS 131A, USGS 103, USGS 105, and USGS 108; (2) wastewater from the ATRC primarily travels south-southwest to MIDDLE 2051 and USGS 132; and (3) water interacting with buried waste at RWMC travels south and is present in the upper zone at USGS 132. Wastewater is present in groundwater at the upper two zones at MIDDLE 2050A and generally at all zones at other MLW except USGS 135. The presence of wastewater at deep sampling zones supports the hypothesis that groundwater moves downward in the southwestern part of the INL, although the downward movement of wastewater may partly be due to direct injection of wastewater into the aquifer through a 600-ft injection well at the INTEC (Bartholomay, Maimer, and others, 2017).

Other Sources of Recharge

Other sources of recharge to the southwestern part of the INL include regional groundwater, groundwater from the Lost River Range, and groundwater from the BLR and Birch Creek (BC) valleys (fig. 18). Each of these sources of recharge contributed 1 percent or less of the total recharge to the study area (table 12). Regional groundwater and groundwater from the BC valley originate northeast of the study area and are sources of water to USGS 103 and USGS 108 (table 11). Groundwater from the Lost River Range and the BLR valley originates northwest of the study area and are sources of water to USGS 135.

Mixing of Water

Mixing of water in the study area primarily occurs between surface water (BLR, precipitation, and wastewater) and groundwater (regional groundwater, groundwater from the Lost River Range, and groundwater from the LLR, BLR, and BC valleys). Mixing between different sources of groundwater is negligible because of the small amount of groundwater in the study area from sources other than the LLR valley. Mixing between surface water and groundwater was estimated, from the sources of recharge shown in table 11, by calculating the percentage of surface water, relative to surface water plus groundwater, for each MLW sampling zone.

Mixing at Different Aquifer Depths

Mixing between surface water and groundwater at different aquifer depths was evaluated by calculating the percentage of surface water at MLW at six discrete depth ranges. These depth ranges were determined by using the midpoint of each sampling zone open interval (in feet below water table [bwt], table 1) as a reference for depth and balancing possible depth ranges with the need to maximize the number of MLW represented in each depth range. The resulting range of sampling zone open intervals included in each of the six depth ranges are 0–90, 85–189, 159–257, 247–335, 362–564, and 545–655 ft bwt. These discrete depth ranges are nearly exclusive, but a slight overlap between some of the depth ranges does occur. The number of MLW in the depth ranges ranged from five to nine (table 13).

Contours of the percentage of surface water (fig. 19), for each discrete aquifer depth range, were interpolated from the data using the natural neighbor technique (Sibson, 1981). The limited number of data points means that the contours may be imprecise, but the contours are useful for broadly illustrating how the percentage of surface water across the study area changes with depth. Upward and downward pointing arrows adjacent to MLW sampling zones (fig. 19) indicate an increase or decrease in the percentage of surface water of at least 20 percent at the sampling zone relative to the sampling zone directly above.

The percentage of surface water in the shallowest depth range, 0–90 ft bwt, ranges from 72 to 95 percent (table 13). The smallest percentage of surface water occurs at MIDDLE 2050A, adjacent to the BLR, and percentages greater than 90 percent occur at MLW along the southern boundary of the INL (fig. 19*A*). In the next lower depth range, 85–189 ft bwt, the percentage of surface water ranges from 52 to 98 percent (table 13). The percentage of surface water along the southern boundary of the INL is still greater than 90 percent, but data are not available from MLW near the BLR (fig. 19*B*). One significant change from the shallowest depth range was that the percentage of surface water at USGS 135 decreased from 85 to 52 percent (table 13).

The percentage of surface water in the 159–257 ft bwt depth ranges from 20 to 95 percent (table 13). The percentage of surface water along the southern boundary of the INL is still generally greater than 90 percent, although the percentage of surface water at USGS 103 decreased to 78 percent. Other changes in the percentage of surface water were a slight increase at MIDDLE 2050A and large decreases at MIDDLE 2051 and USGS 132 (fig. 19*C*). The percentage of surface water in the 247–335 ft bwt depth ranges from 11 to 96 percent (table 13). The percentage of surface water decreases substantially at MIDDLE 2050A but remained greater than 90 percent at USGS 131A and along the southern boundary of the INL (fig. 19*D*).

The percentage of surface water ranges from 9 to 96 percent in the 362–445 ft bwt depth range (table 13). The distribution of the percentage of surface water in this depth range is like the overlying depth range except that the percentage of surface water decreases substantially at USGS 131A (fig. 19*E*). The percentage of surface water ranges from 15 to 95 percent in the 545–655 ft bwt depth range (table 13). The most substantial changes at this depth range were the large decreases in the percentage of surface water at USGS 105 and USGS 108 (fig. 19*F*).

Evaluation of the percentage of surface water in the six depth ranges indicates that the percentage of surface water in the aquifer increases south of the BLR and decreases with depth. At the deepest depth range, only at USGS 103 and USGS 105, along the southern boundary of the INL, does surface water remain the primary source of water. The consistently large percentage of surface water at MLW along the southern boundary of the INL in the upper five depth ranges indicates that groundwater is flowing downward as a uniform, well-mixed body of water. If continual mixing were occurring between surface water and groundwater, then the percentage of surface water should steadily decrease with increasing depth.

Increasing amounts of surface water with increasing distance from the BLR seems counterintuitive. However, this is because BLR is an ephemeral stream. The last period when substantial recharge from the BLR occurred was during 1995–2000 (fig. 4), about 10–15 years before sample collection at MLW (table 3). Thus, recharge from surface water during 1995–2000 has moved downgradient from the BLR during the intervening years before sample collection, with the largest amount of this recharge residing near the southern boundary of the INL. The average linear groundwater velocity between the BLR near the INTEC and USGS 103 (about 8.5 mi apart, fig. 1), assuming a 10- to 15-year travel time, is about 8–12 feet per day (ft/d). This is a rapid groundwater velocity, but this velocity falls within the estimated velocity range of 4–20 ft/d for groundwater south of the INTEC (Ackerman and others, 2006).

Table 13. Percentage of surface water at multilevel wells for discrete depth ranges, Idaho National Laboratory, eastern Idaho.

[All values in table are in percentage of surface water. –, no data]

Site name	Discrete depth ranges (feet below water table)					
	0–90	85–189	159–257	247–335	362–564	545–655
MIDDLE 2050A	72	–	85	11	9	–
MIDDLE 2051	89	–	20	29	12	32
USGS 103	–	98	78	95	96	95
USGS 105	95	93	–	96	95	65
USGS 108	94	–	95	95	95	27
USGS 131A	94	–	–	91	41	15
USGS 132	79	66	38	45	45	45
USGS 135	85	52	–	86	86	–
USGS 137A	92	95	93	94	–	–

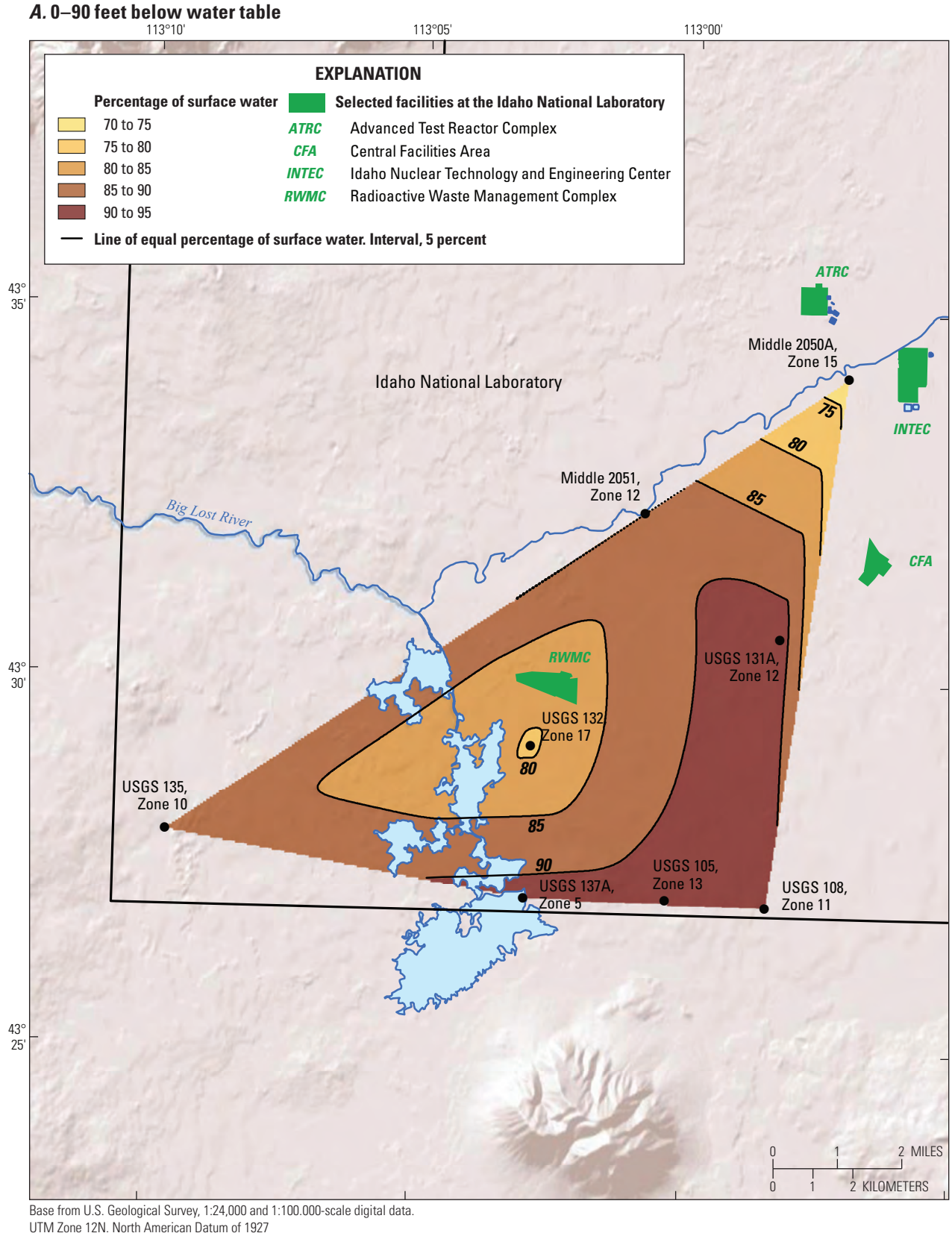

Figure 19. Percentage of surface water, relative to the total amount of surface water plus groundwater, at six discrete depth ranges in the eastern Snake River Plain aquifer, Idaho National Laboratory, eastern Idaho. *A.* 0–90 feet below the water table (ft bwt). *B.* 85–189 ft bwt. *C.* 159–257 ft bwt. *D.* 247–335 ft bwt. *E.* 362–564 ft bwt. *F.* 545–655 ft bwt.

***B.* 85–189 feet below water table**

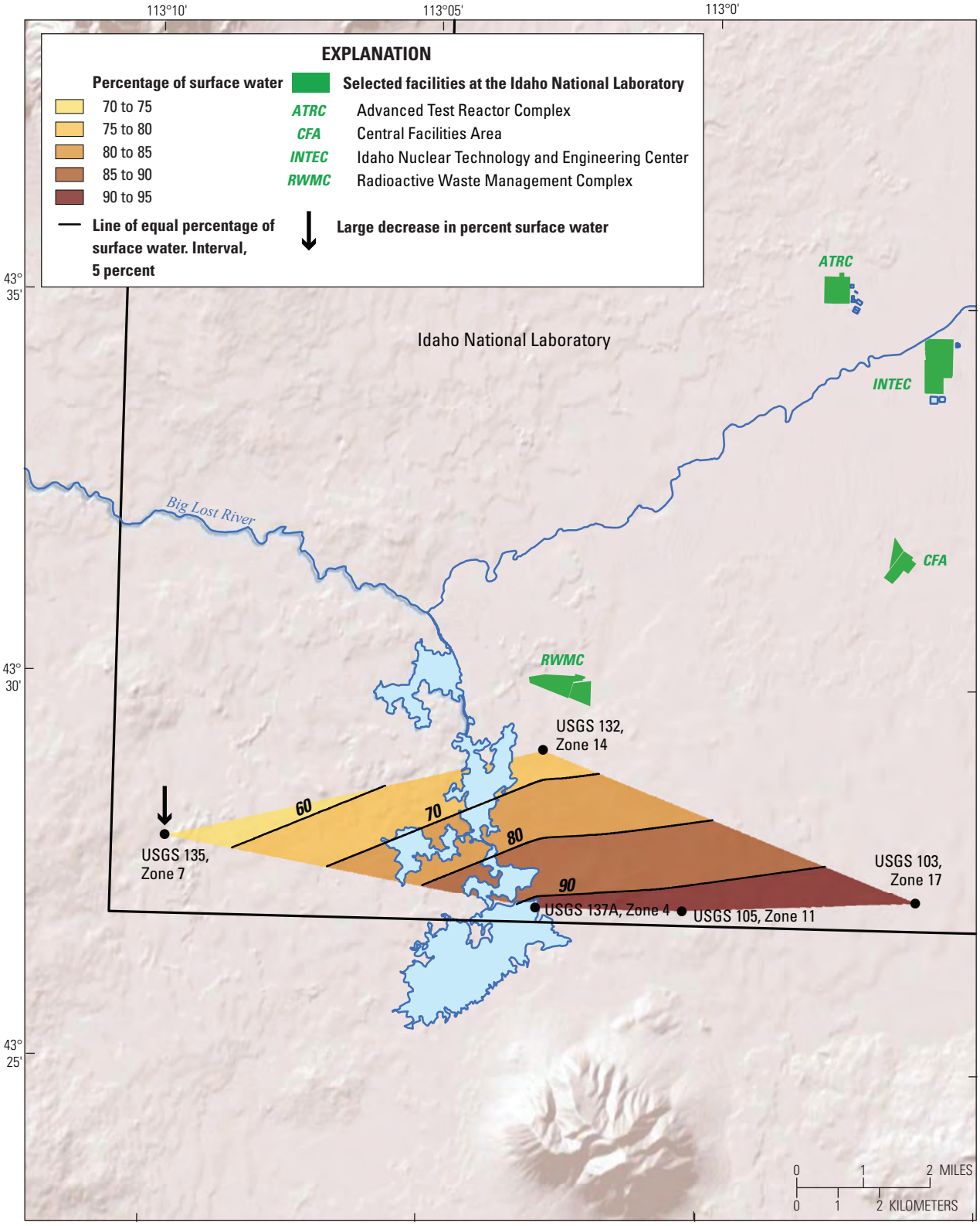

Base from U.S. Geological Survey, 1:24,000 and 1:100.000-scale digital data.
UTM Zone 12N. North American Datum of 1927

Figure 19.—Continued

***C.* 159–257 feet below water table**

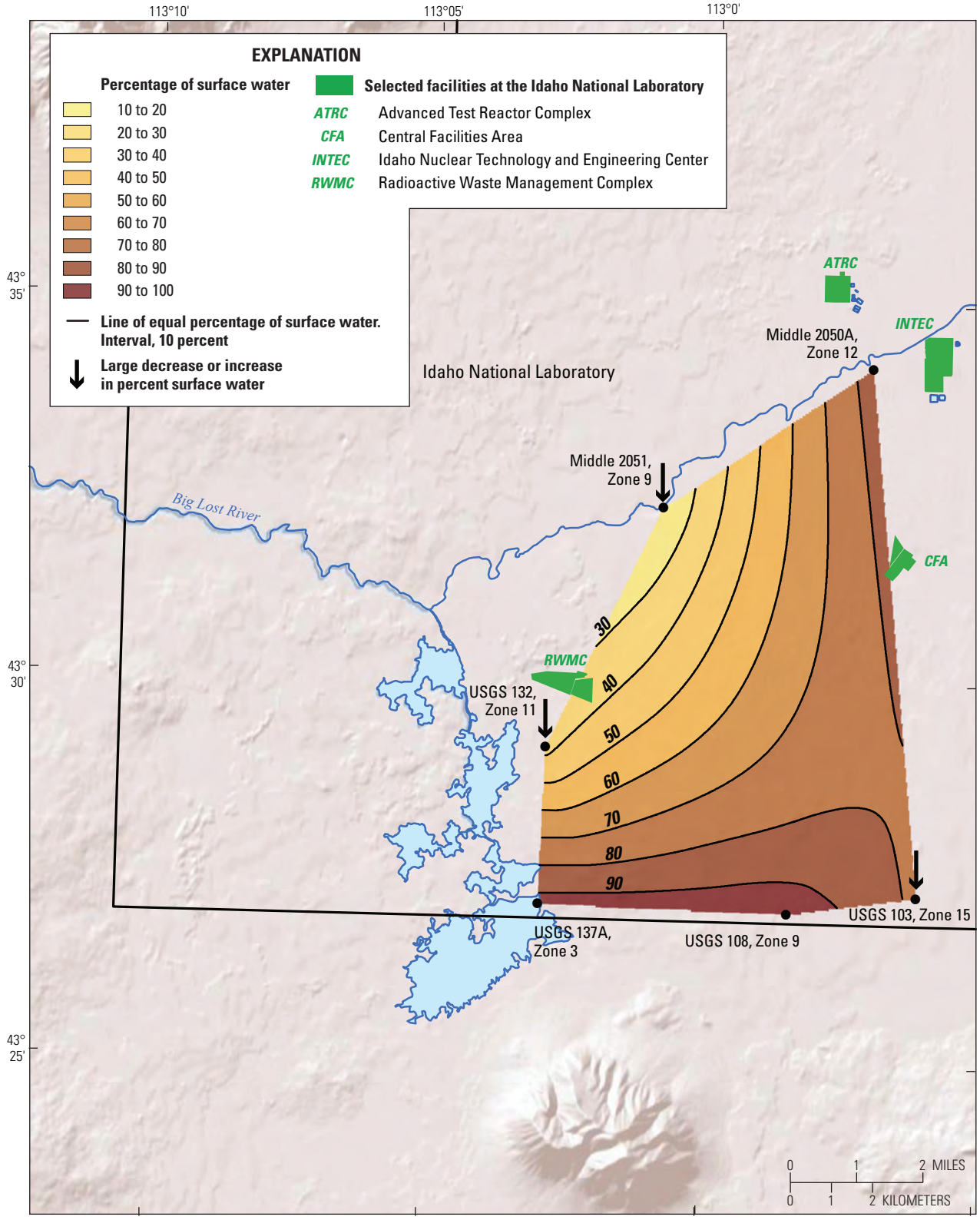

Base from U.S. Geological Survey, 1:24,000 and 1:100.000-scale digital data.
UTM Zone 12N. North American Datum of 1927

Figure 19.—Continued

***D.* 247–335 feet below water table**

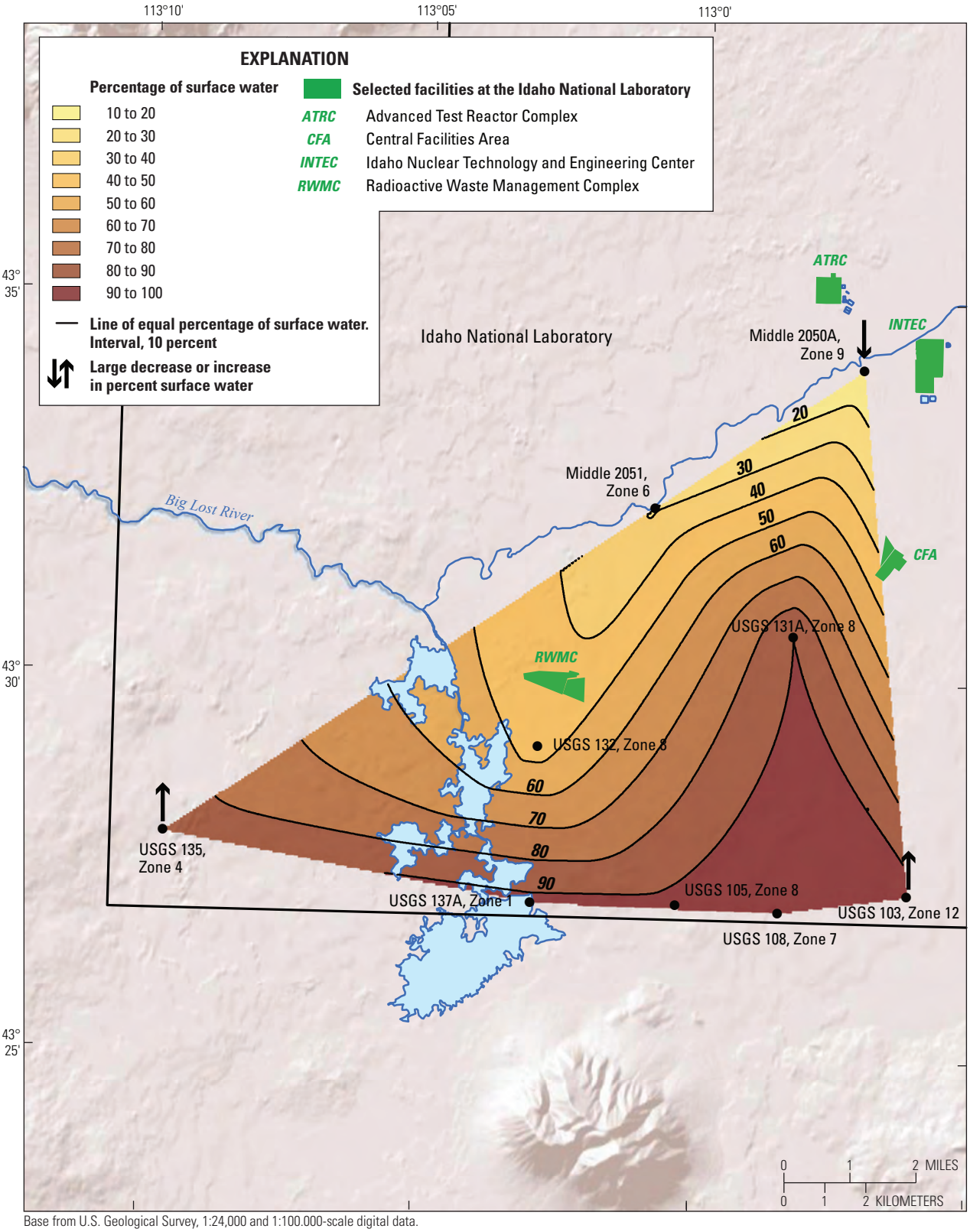

Base from U.S. Geological Survey, 1:24,000 and 1:100.000-scale digital data.
UTM Zone 12N. North American Datum of 1927

Figure 19.—Continued

***E.* 362–564 feet below water table**

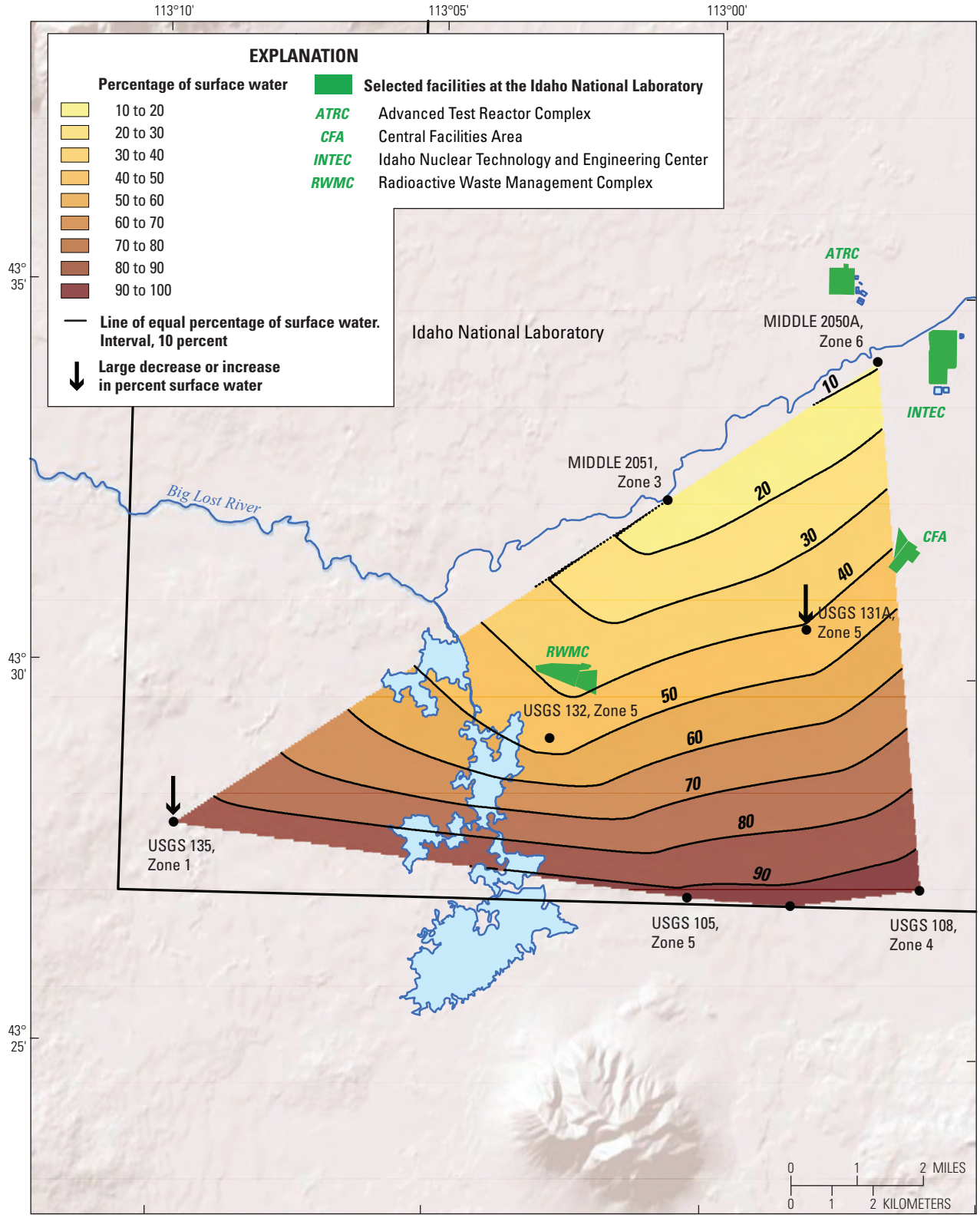

Base from U.S. Geological Survey, 1:24,000 and 1:100.000-scale digital data.
UTM Zone 12N. North American Datum of 1927

Figure 19.—Continued

F. 545–655 feet below water table

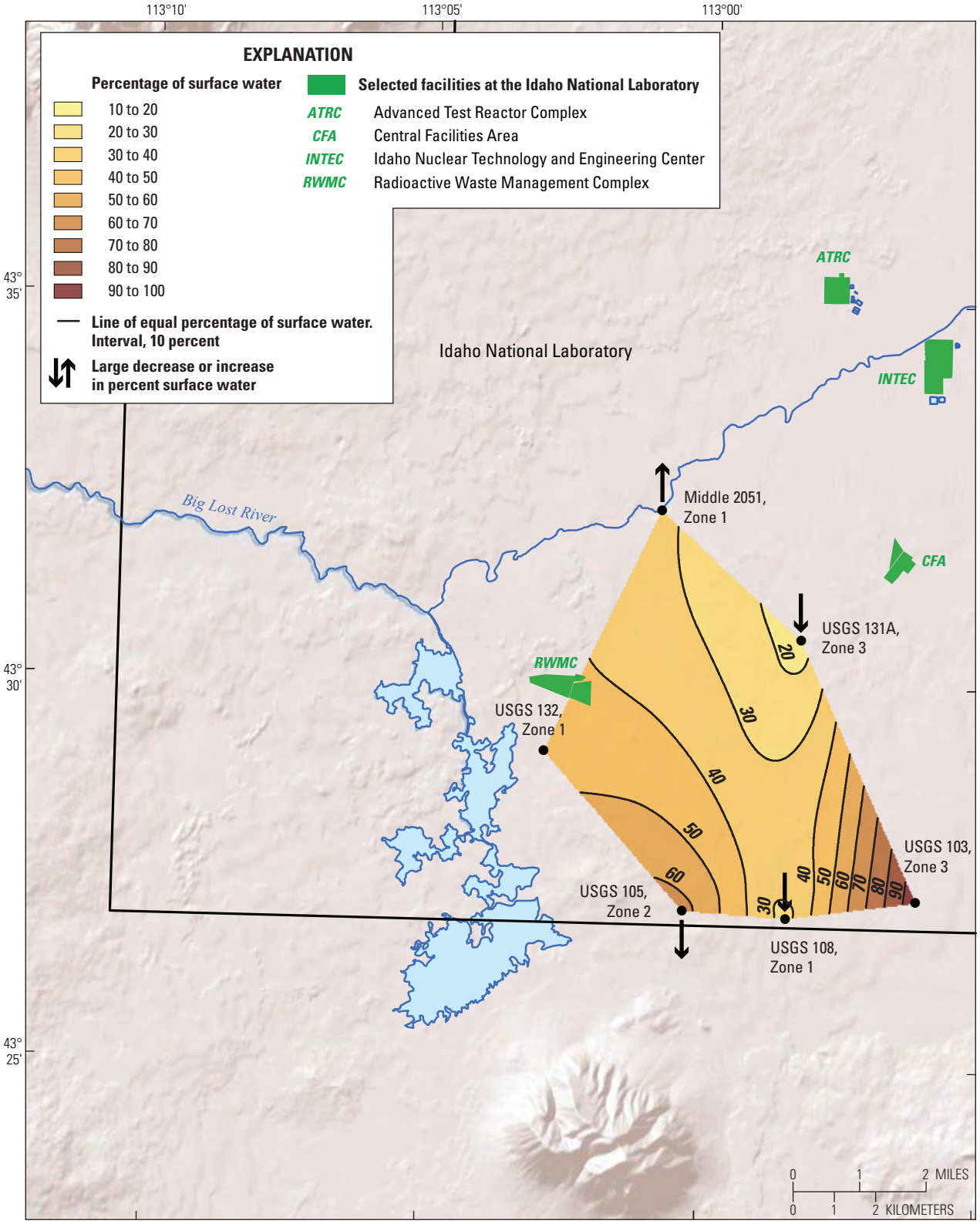

Base from U.S. Geological Survey, 1:24,000 and 1:100.000-scale digital data.
UTM Zone 12N. North American Datum of 1927

Figure 19.—Continued

Influence of Stratigraphic Units on Mixing of Water

The ESRP aquifer is an unconfined aquifer composed of subhorizontal stratigraphic layers of basalt and sediment. However, any impermeable or semi-impermeable layers of dense basalt or fine-grained sediment could create conditions that restrict the downward movement of surface water. Because the mixing investigated here identifies the presence of surface water at various depths in the aquifer, any restriction in the ability of water to move downward past a relatively impermeable layer should be revealed by a decrease in the percentage of surface water at or directly below that layer. Thus, significant decreases in the percentage of surface water at discrete depth ranges at MLW may provide evidence for relatively impermeable stratigraphic layers in the aquifer.

Table 14 shows the discrete depth range (feet below water table), sampling zone, and stratigraphic unit where a decrease in the percentage of downward flowing surface water exceeds 20 percent. A decrease exceeding 20 percent was chosen because this value was thought to be large enough to represent a significant change in the amount of surface water that is unlikely to be due to uncertainties associated with water-quality sampling and geochemical modeling. There are seven MLW, and eight sampling zones, where a decrease in the percentage of downward flowing surface water exceeds 20 percent.

A decreasing percentage of surface water at depth at MLW may be due either to variable amounts of surface-water recharge in response to short-term climate cycles (fig. 4) or downward flowing water reaching stratigraphic units with reduced permeability relative to overhead units. If short-term climate cycles were the cause of decreasing percentages of surface water with depth, the variable distances of MLW and depths of stratigraphic units from the source of surface-water recharge, the BLR, should cause the decreased percentages to occur at random, and different, stratigraphic units. However, if a relatively impermeable stratigraphic unit is the cause of the decreased percentages of surface water, then the decreased percentages should all occur at this specific stratigraphic unit. In table 14, the stratigraphic units with decreased percentages of surface water are all within, or directly above or below, the Matuyama flow. Thus, the Matuyama flow appears to be semi-impermeable to the downward flow of groundwater.

Neither USGS 103 nor USGS 137A showed a decrease in percentage of surface water of more than 20 percent. However, the depth of USGS 137A is shallow compared to other MLW and does not reach the depth of the Matuyama flow (fig. 3*B*). Zone 3 at USGS 103 (fig. 3*B*; discrete depth range 545–655 ft bwt, table 13) is partly located within the Matuyama flow, but there is no decrease in the percentage of surface water at this zone or the underlying zone. Possible reasons why the Matuyama flow does not restrict the downward flow of surface water at USGS 103 are (1) the Matuyama flow is too thin beneath USGS 103 to act as a relatively impermeable zone, (2) zone 3 extends into the Post Jaramillo flow (fig. 3*B*), and the Post Jaramillo flow of Hodges and Champion (2016) is connected to stratigraphic units above the Matuyama flow by fractures, tension cracks, or fissures that allow surface water to bypass the Matuyama flow, and (or) (3) the features that cause the Matuyama flow to act as a relatively impermeable unit are not present near USGS 103.

The percentage decrease in surface water ranges from 26 to 75 percent. However, there is a geographic distribution in the percentage decrease of surface water, with western (USGS 105, USGS 132, USGS 135) and eastern (MIDDLE 2050A, MIDDLE 2051, USGS 108, USGS 131A) groups of MLW that have a decrease ranging from 28 to 33 percent and 68 to 76 percent[22] (table 14), respectively. This disparity may indicate that the permeability of the Matuyama flow is larger near the western group of MLW and smaller in the vicinity of the eastern group of MLW (Hodges and Champion, 2016).

Groundwater Flow Directions

The horizontal and vertical groundwater flow direction(s) between initial and final solutions in the geochemical models give an indication of the direction that groundwater flows in the ESRP aquifer (fig. 20). Because inferred information about horizontal groundwater-flow directions were used to construct geochemical models, model results merely provide supporting evidence that the inferred information was accurate. In contrast, differences in elevation (fig. 20; elevation represented as depth below water table) between initial and final solutions provide an unbiased indication of the vertical or downward movement of groundwater. If an initial solution originates from an open borehole, however, any downward movement of groundwater between initial and final solutions is poorly constrained. However, if an initial solution originates from a sampling zone at MLW, then any downward movement of groundwater between the initial and final solutions is well constrained. Downward movement of water may be facilitated by fissures, fractures, and volcanic vents (Anderson and others, 1999); increasing aquifer depth in the downgradient direction (Ackerman and others, 2006); or increased head potential at the water table from recharge of surface water.

When surface water is an initial solution, recharge of the surface water is presumed to occur near the source of the surface water, such as the BLR channel, INL spreading areas, and (or) wastewater disposal sites. Thus, when final solutions in deeper parts of the aquifer include initial solutions that are surface water, the initial solutions are assumed to represent recharge at the source location of the surface water that subsequently traveled the necessary distance and depth to the final solution as groundwater.

[22]The 76-percent value is for the combined decrease in the percentage of surface water for zones 5 and 3 from USGS 131A (table 14).

Table 14. Stratigraphy at multilevel wells at discrete depth range where percentage of surface water decreases by more than 20 percent (for downward flowing water), Idaho National Laboratory, eastern Idaho.

[Discrete depth range and decrease in percentage of surface water from table 13, sampling zone from table 1, and stratigraphic unit from figure 3. Stratigraphic unit and flow names are modified from Hodges and Champion (2016)]

Multilevel well name	Discrete depth range (feet below water table)	Sampling zone	Decrease in percentage of surface water	Stratigraphic unit
USGS 132	159–257	11	28	South Late Matuyama, Matuyama flow
USGS 105	545–655	2	30	Matuyama flow
USGS 135	85–189	7	33	South Late Matuyama flow
USGS 108	545–655	1	68	Matuyama flow
MIDDLE 2051	159–257	9	69	Unknown (directly above Matuyama flow)
MIDDLE 2050A	247–335	9	74	Matuyama flow
USGS 131A	362–564	5	50	Jaramillo flow (directly below Matuyama flow)
USGS 131A	545–655	3	26	Jaramillo flow (directly below Matuyama flow)

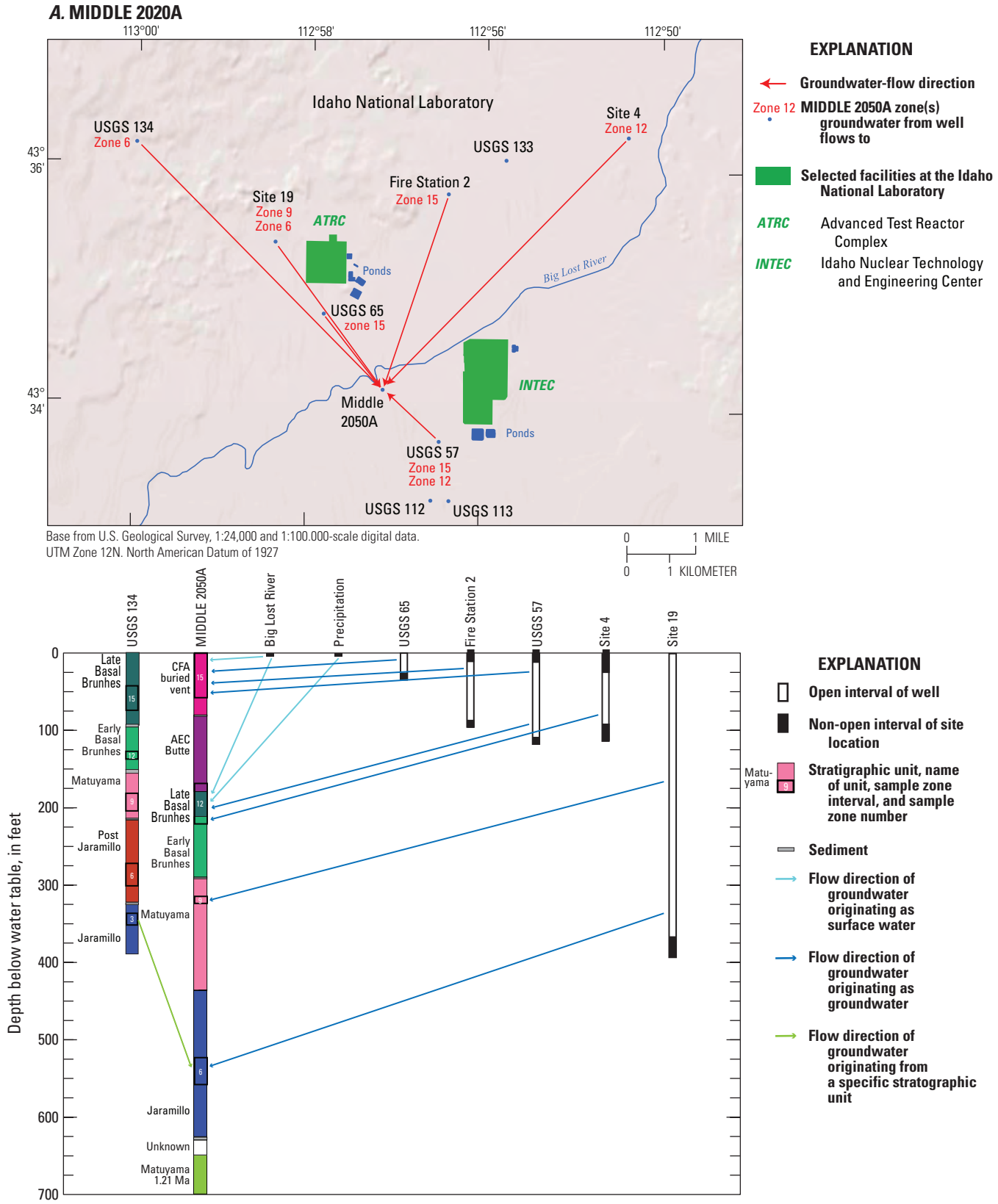

Figure 20. Horizontal (top images) and diagrams showing vertical (bottom images) groundwater-flow directions between initial and final solutions in geochemical models, Idaho National Laboratory, eastern Idaho. *A.* MIDDLE 2020A. *B.* MIDDLE 2051. *C.* USGS 103. *D.* USGS 105. *E.* USGS 108. *F.* USGS 131A. *G.* USGS 132. *H.* USGS 135. *I.* USGS 137A. Informal flow names from Hodges and Champion (2016) are abbreviated here owing to spacing issues.

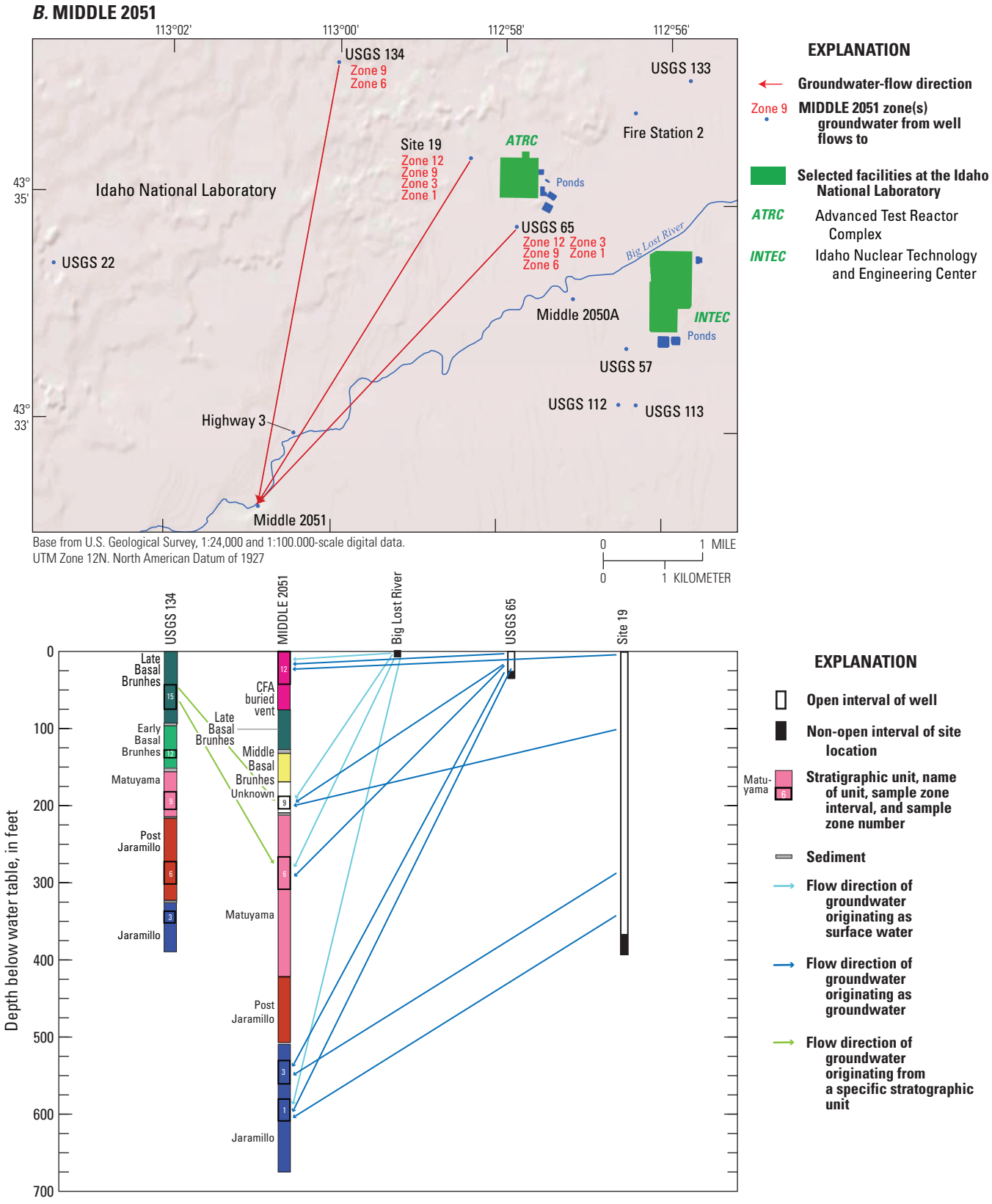

Figure 20.—Continued

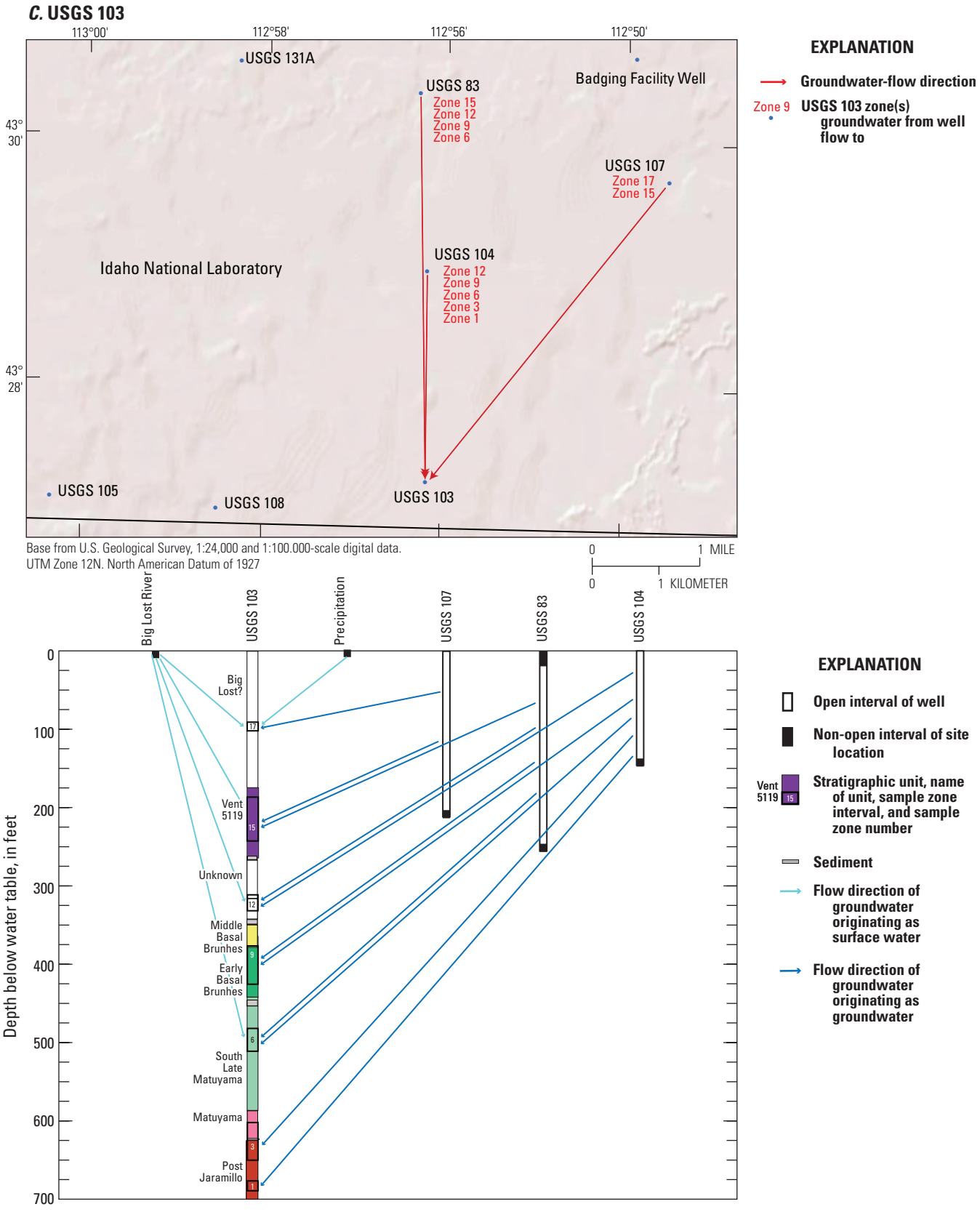

Figure 20.—Continued

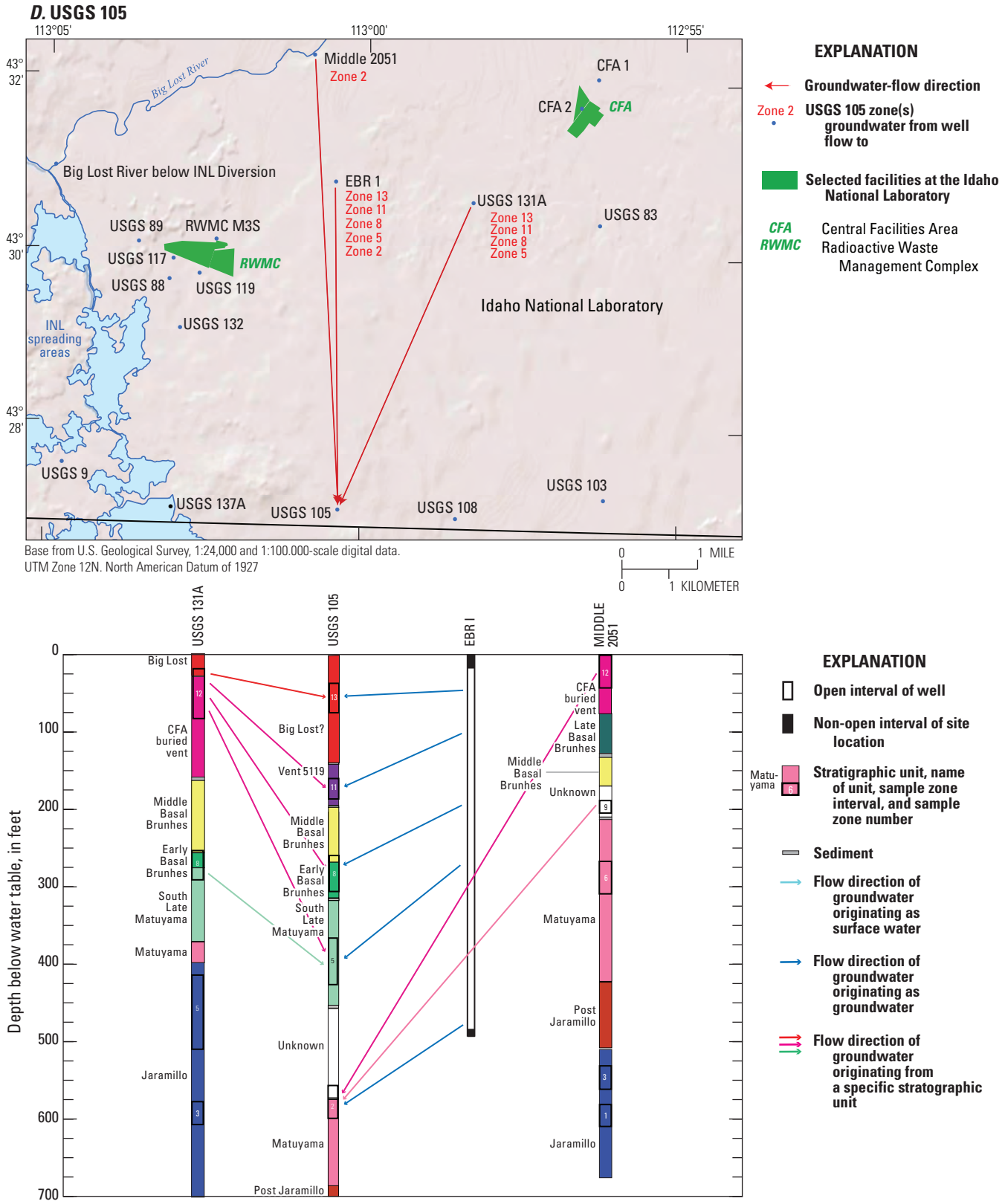

Figure 20.—Continued

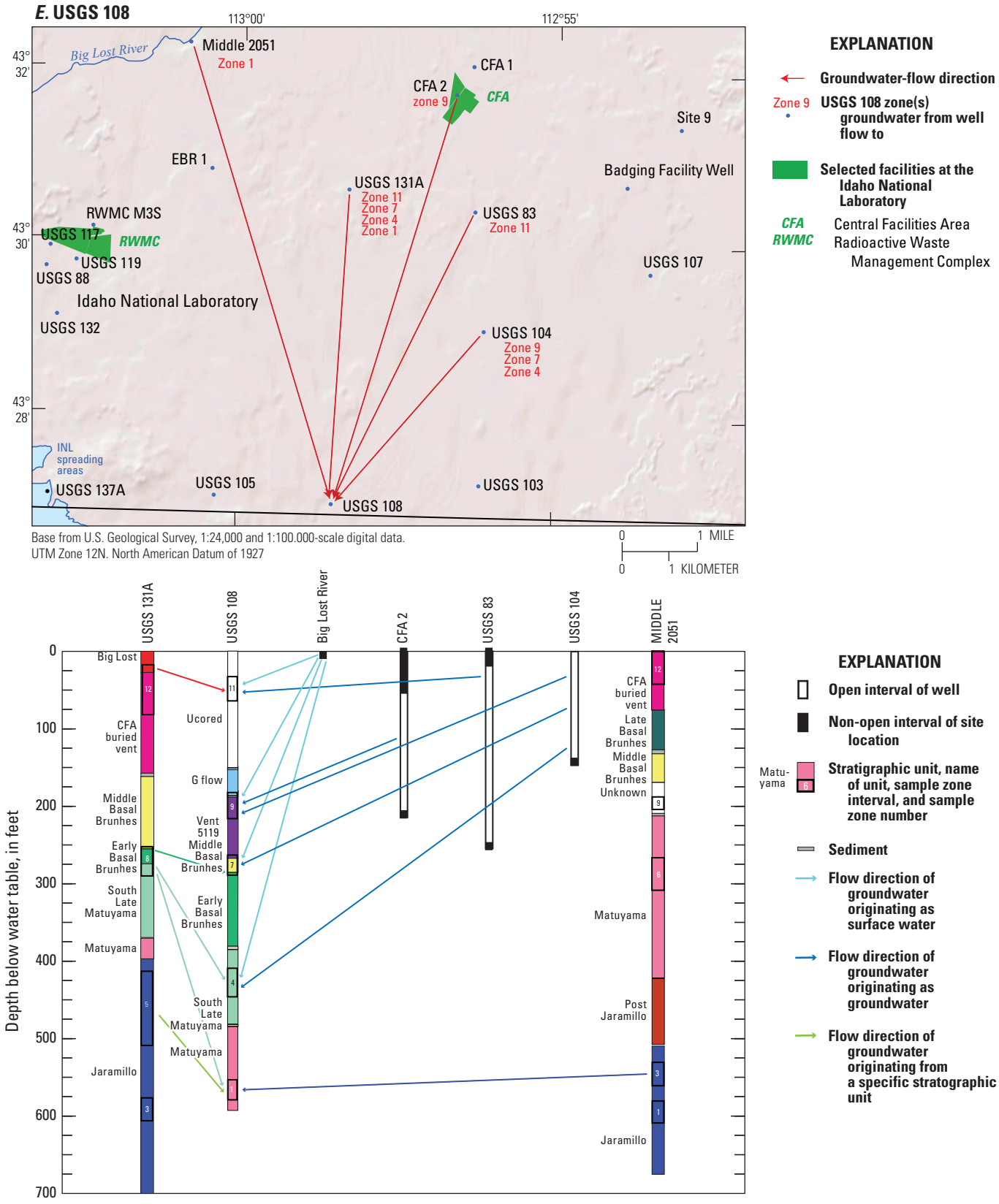

Figure 20.—Continued

F. USGS 131A

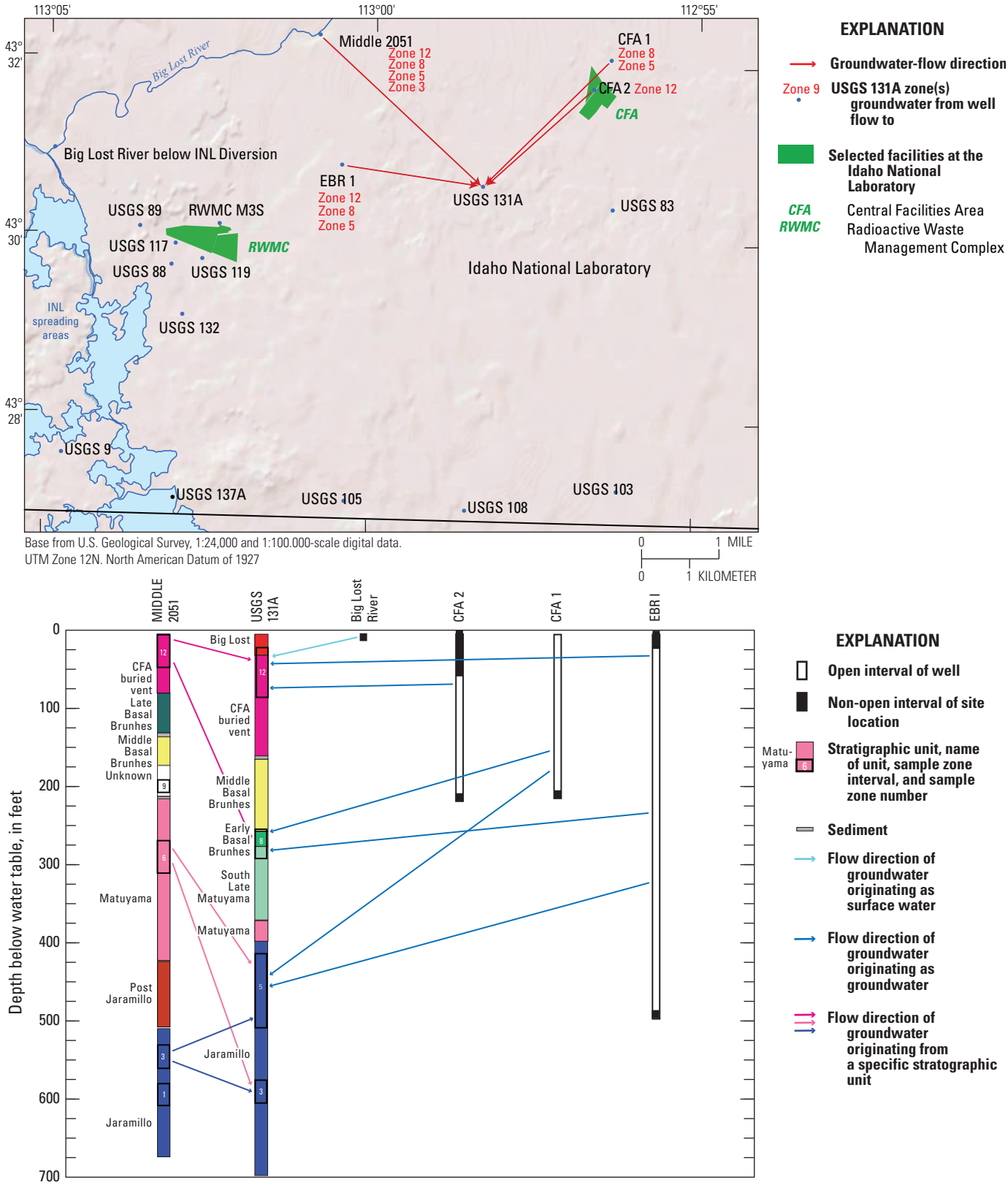

Figure 20.—Continued

G. USGS 132

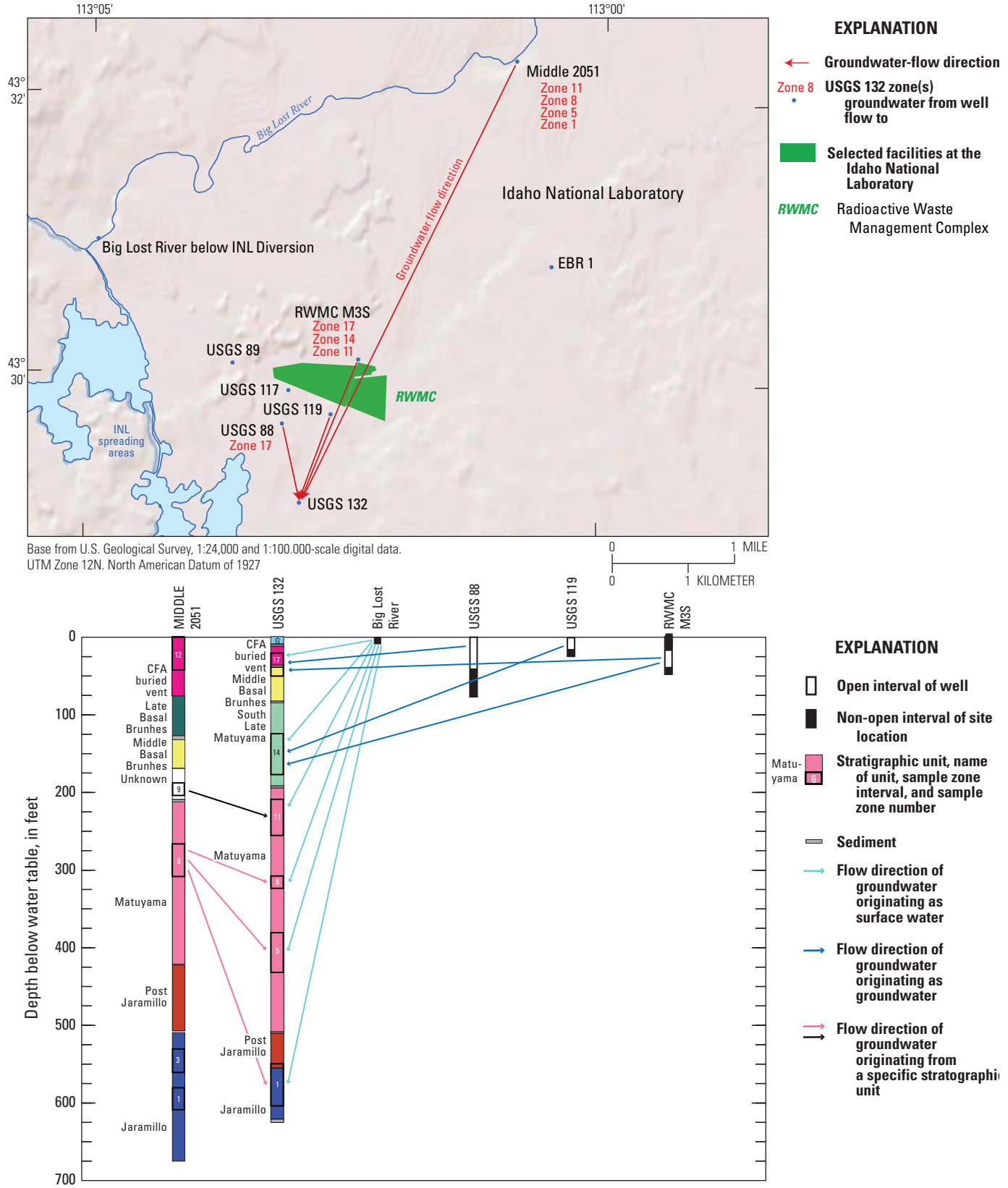

Figure 20.—Continued

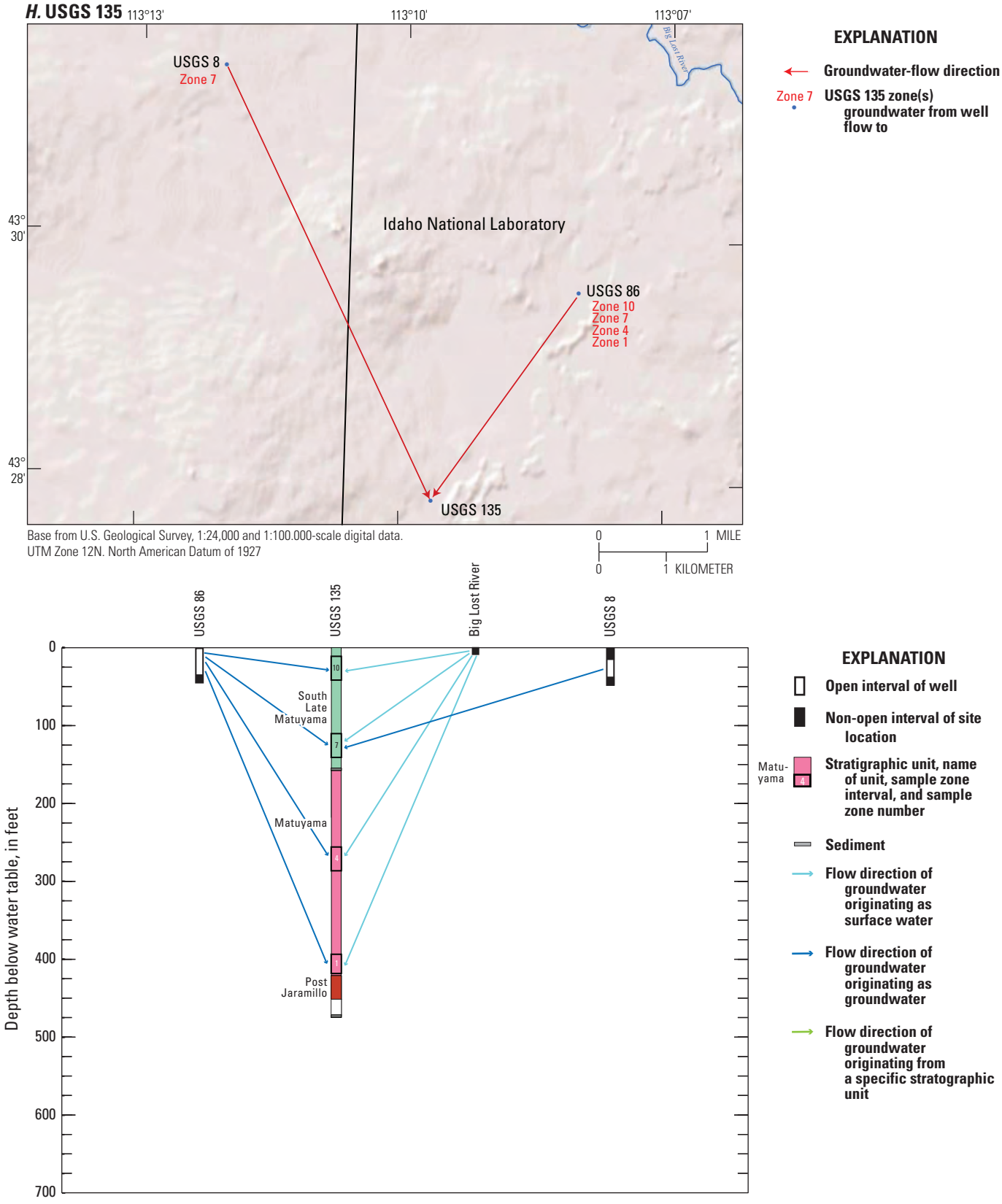

Figure 20.—Continued

I. USGS 137A

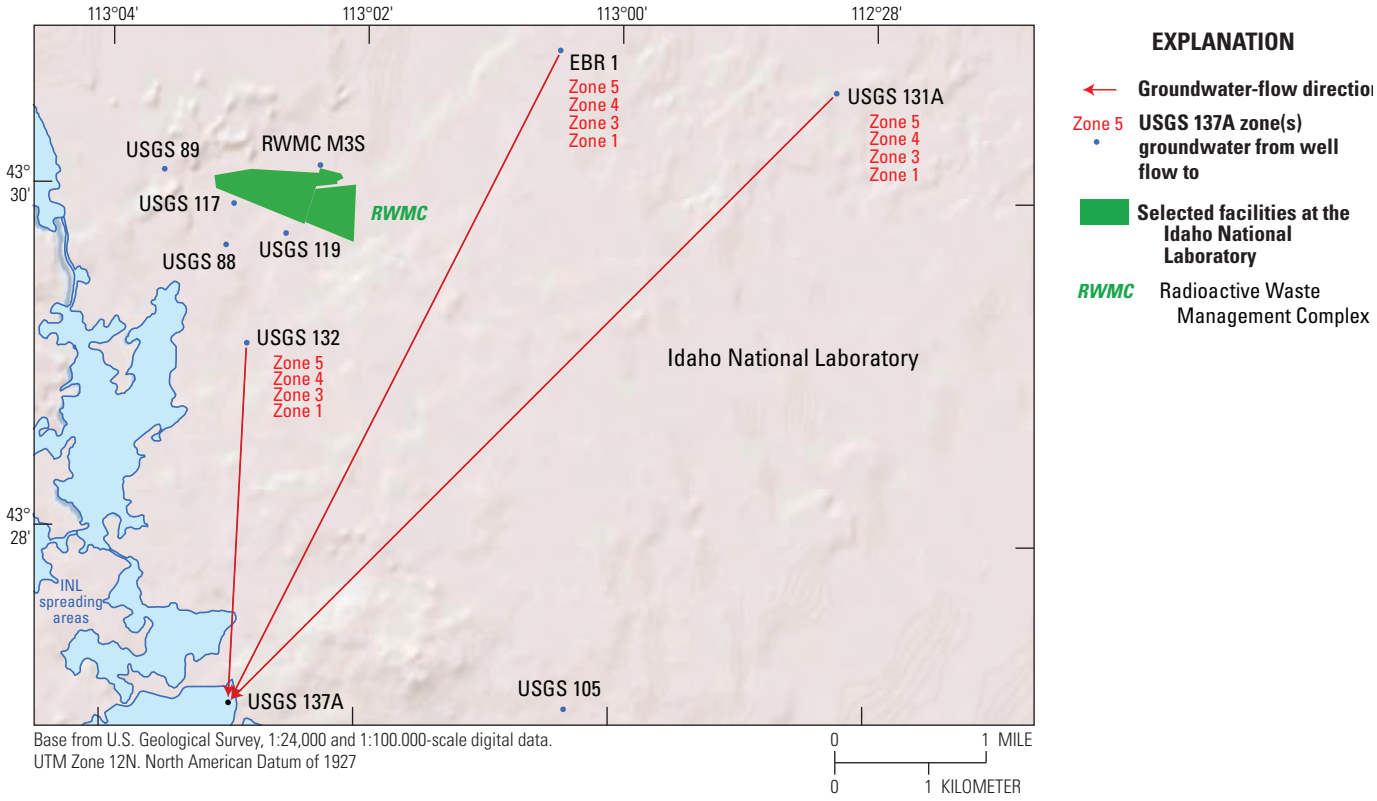

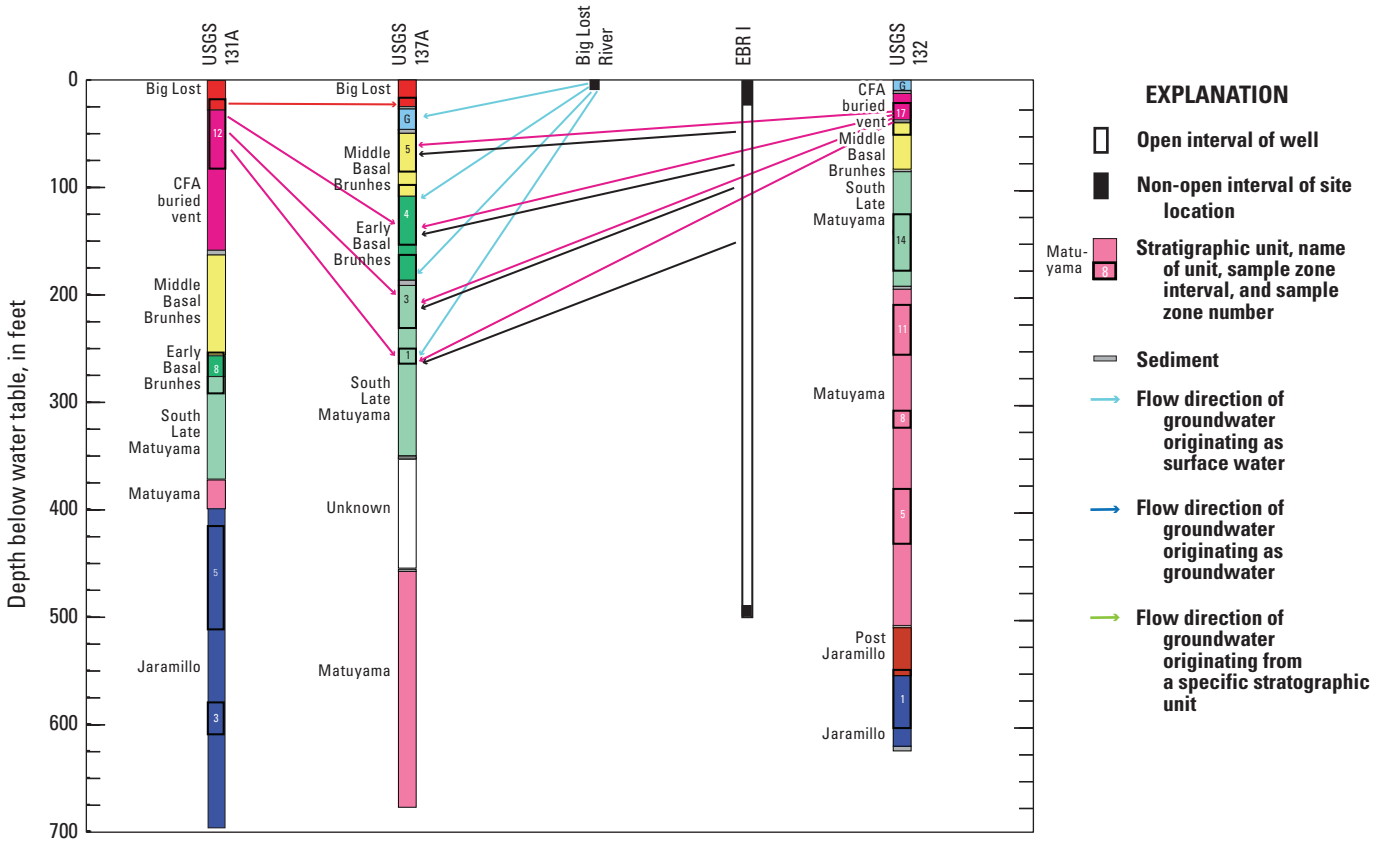

Figure 20.—Continued

MIDDLE 2050A

Water at the two shallowest sampling zones (zones 15 and 12) at MIDDLE 2050A is a mixture of water from the BLR, precipitation, wastewater from the ATRC and INTEC, and groundwater from Fire Station 2 and Site 4 (fig. 20*A*). Excluding wastewater sources of water, for which the direction of movement may be affected by flow through the unsaturated zone and local mounding of the aquifer from discharged wastewater, modeled groundwater-flow directions were southerly or southwesterly, which is consistent with the flow directions indicated from inferred information. Initial solutions included surface water in the upper two zones, indicating that some downward movement of groundwater occurs in the upper part of the aquifer near MIDDLE 2050A. Tritium activities of about 94–172 pCi/L (fig. 15*A*) also support the downward movement of wastewater to the upper two zones.

The next two deeper sampling zones, zones 9 and 6, include water from Site 19 (both zones) and zone 3 from USGS 134 (zone 6). Groundwater is represented as moving in a southeasterly direction to both zones (fig. 20*A*), although inferred information indicates that groundwater moving to these zones probably flows in a southerly or southwesterly direction (fig. 5). This unsupported model flow direction may be due to the limited availability of deep wells with water-quality data in the aquifer north or northeast of MIDDLE 2050A.

Groundwater moves downward from zone 3 at USGS 134 to zone 6 at MIDDLE 2050A (fig. 20*A*). Both these zones are located within the Jaramillo flow (of Hodges and Champion, 2016). Because the bottom of USGS 134 ends within the Jaramillo flow, the full depth of this unit at USGS 134 is unknown. Consequently, it is possible that the water chemistry at zone 3 from USGS 134 is representative of deeper groundwater within the Jaramillo flow. Thus, the vertical movement of groundwater between these two zones is uncertain.

MIDDLE 2051

Water at MIDDLE 2051 is a mixture of water from the BLR, wastewater from the ATRC (USGS 65), and groundwater from Site 19 and USGS 134 (fig. 20*B*). Modeled groundwater flow directions are south to southwest.

Surface water is an initial solution at all zones at MIDDLE 2051, which indicates that water has a downward component of flow in this part of the aquifer. Wastewater modeled at all five zones also supports the downward movement of surface water and groundwater to all zones. Tritium activities in the top zone are small (51.7±2.9 pCi/L, table 6), indicating that wastewater has a small presence at this zone, but larger activities (about 292–635 pCi/L, table 6) at the deeper four zones support a larger presence of wastewater at each of these zones. Downward flow also is indicated for the shallow aquifer from the downward direction of groundwater movement between zone 15 at USGS 134, located in the Late Basal Brunhes flow of Hodges and Champion (2016), and zones 9 and 6 at MIDDLE 2051, located just above and within the Matuyama flow, respectively (fig. 20*B*).

The downward movement of surface water and groundwater is consistent at all aquifer depths at MIDDLE 2051. However, the magnitude of the downward flow decreases significantly below zone 12. At zone 12, recharge from surface water comprises 86 percent of the water, whereas at the four zones below zone 12 recharge from surface water comprises just 12–32 percent of the water (table 11). The four deeper zones are located just above, within, or below the Matuyama flow (fig. 20*B*), so the decrease in surface water at these zones may be due to the impermeability of the Matuyama flow and the presence of several thick sedimentary beds.

USGS 103

Water at USGS 103 is a mixture of water from the BLR, precipitation, and groundwater from USGS 107, USGS 83, and USGS 104 (fig. 20*C*). Modeled groundwater-flow directions are southerly plus a southwesterly component of flow for groundwater traveling from USGS 107 to zones 17 and 15 at USGS 103. However, groundwater from USGS 107 comprises 42 percent of the total initial solutions to zone 15 but only 5 percent at zone 17. Thus, except for zone 15, groundwater primarily flows south to USGS 103.

Initial solutions at zones 17, 15, 12, and 6 include surface water from the BLR, which indicates that groundwater moving to these zones at USGS 103 has a downward component of flow. In addition, large tritium activities in groundwater from the lower five zones (ranging from 72.4 to 434 pCi/L, table 6) at USGS 103 are representative of wastewater discharged at the INTEC (fig. 15*A*) and indicate that wastewater has traveled to great depths at this well. These interpretations and data are consistent with the large amount of surface water, ranging from 78 to 98 percent, providing recharge at all aquifer depths at USGS 103 (table 11).

USGS 105

Water at USGS 105 is a mixture of groundwater from the EBR 1, USGS 131A, and MIDDLE 2051 (fig. 20*D*). Modeled groundwater-flow directions to USGS 105 are southerly and southwesterly.

Surface water was not modeled as an initial solution to USGS 105. However, surface water (from the BLR, precipitation, and wastewater) provides from 65 to 96 percent of water to sampling zones at USGS 105 (table 11). Groundwater from all sampling zones at USGS 105 have large tritium activities, ranging from 126.3 to 262.9 pCi/L (table 6), that indicate wastewater is present at all zones. These large tritium activities are evidence that surface water is an important source of water at all zones at USGS 105.

Initial solutions to sampling zones at USGS 105 include (1) water from EBR1, which is a 1,075-foot deep well (table 1), to all zones, (2) water from the upper zone (zone 12) at USGS 131A to the upper four zones (zones 13, 11, 8, and 5), (3) water from the zone 8 at USGS 131A to zone 5, and (4) water from the upper two zones at MIDDLE 2051 to the deepest zone (zone 2). These results may indicate that (1) the upper four zones at USGS 105 consist of a thick zone of relatively well-mixed groundwater, (2) groundwater represented by the upper two zones at MIDDLE 2051 moves downward and flows beneath groundwater represented by the upper four zones at USGS 105, and (3) the thick zone of relatively well-mixed groundwater and the deeper groundwater are horizontally stratified. Because zone 2 at USGS 105 is located within the Matuyama flow (fig. 20*D*), the horizontal stratification of shallow, well-mixed groundwater and deep groundwater flowing to USGS 105 may result from the Matuyama flow acting as a semi-impermeable unit. This interpretation is consistent with the large decrease in recharge from surface water to zone 2 compared to the shallower zones (table 14).

USGS 108

Water at USGS 108 is a mixture of water from the BLR, wastewater from the INTEC (CFA 2; Rattray, 2019, table 11), and groundwater from USGS 83, USGS 104, USGS 131A, and MIDDLE 2051 (fig. 20*C*). Modeled groundwater-flow directions to USGS 108 are south and southwest plus a possible southeasterly component of flow to the deepest zone (zone 1). The upper four zones include surface water as an initial solution (table 9), which indicates that groundwater flowing to these zones has a downward component of flow. This interpretation is consistent with the large percentage of surface water calculated to be sources of water to these four zones (table 11).

The presence of water from the BLR in the upper four zones indicates that groundwater flowing to these zones mixed with surface water from the BLR. However, groundwater flowing from USGS 131A to all five zones at USGS 108 appears to be horizontally stratified (fig. 20*E*). A possible explanation for this discrepancy is that much of the downward movement of surface water in the aquifer may have occurred beneath the BLR streambed in response to the large head potential generated from downward infiltrating surface water ponding above the water table.

Zone 1, the deepest zone at USGS 108, is located within the Matuyama flow (fig. 20*E*). Initial solutions for zone 1 include zones 8 and 5 from USGS 131A and zone 3 from MIDDLE 2051, and zones 8 and 5 from USGS 131A and zone 3 from MIDDLE 2051 all represent relatively deep parts of the aquifer (table 11). This is a substantial difference compared to the deep zone at USGS 105, also located within the Matuyama flow (fig. 20*D*), that has initial solutions of shallow groundwater. It is not clear why shallow and deep groundwater are initial solutions for deep zones at USGS 105 and USGS 108, respectively, when USGS 105 is only about 1.5 mi west of USGS 108 (fig. 1). However, hydraulic conductivities determined from well tests in the southwestern part of the INL show that hydraulic conductivities in the aquifer range from small to large and are irregularly distributed. Small hydraulic conductivities of -1.03 and 0.58 ft/d were measured at wells USGS 83 and USGS 104 located north-northeast, or upgradient, of USGS 108 (Rattray, 2018, fig. 7), and these small hydraulic conductivities may impede the flow of shallow groundwater to USGS 108.

Groundwater flowing to zone 1 at USGS 108 is almost entirely from the Jaramillo flow, which is stratigraphically below the Matuyama flow (fig. 20*E*). Consequently, although groundwater from the Jaramillo flow may not flow vertically upward to zone 1 it does move stratigraphically upward into the Matuyama flow.

USGS 131A

Water at USGS 131A is a mixture of water from the BLR, wastewater from the INTEC (CFA 1 and CFA 2; Rattray, 2019, table 11) and ATRC (zones 3 and 6 at MIDDLE 2051, table 9), and groundwater from EBR1 and the upper four zones at MIDDLE 2051 (fig. 20*F*). Modeled groundwater-flow directions to USGS 131A are east, southeast, and southwest. Initial solutions from EBR1 and MIDDLE 2051, which are located east and southeast of USGS 131A, are not along groundwater-flow directions indicated from inferred information. The initial solutions from these wells may be representative of groundwater north of USGS 131A.

The initial solutions to the upper two zones (zones 12 and 9) at USGS 131A include the BLR, wastewater, groundwater from EBR1, and groundwater from zone 12 at MIDDLE 2051 (table 11), all of which are or may be (EBR1) shallow sources of water (fig. 20*F*). The initial solutions to the lower two zones (zones 5 and 3) at USGS 131A are primarily groundwater from zones 6 and 3 from MIDDLE 2051 (plus a small amount of water from EBR1 and CFA1 at zone 5; table 11) that are much deeper sources of water than were sources to the upper two zones. The two upper and lower zones at USGS 131A are located above and below the Matuyama flow, respectively, and the difference in the sources of water between the upper and lower two zones may indicate that the Matuyama flow is a semi-impermeable unit that segregates groundwater above and below this unit. Thus, downward flow or mixing of groundwater may occur within the groundwater above or below the Matuyama flow, but probably does not occur, or occurs in small amounts, across the Matuyama flow.

The shallow and deep sources of water to the upper and lower two zones at USGS 131A, respectively, reflect sources of recharge that are primarily the BLR to the upper two zones and groundwater from the LLR valley to the lower two zones (table 11). Wastewater, represented with tritium activities, also indicates that the flow characteristics of the upper and lower two zones are different. For example, tritium activities are much larger in groundwater from the upper two zones

(983 and 1,454 pCi/L, table 6) than the lower two zones (149 and 133 pCi/L, table 6). This discrepancy in tritium activities reflects the preponderance of surface-water recharge, including a significant amount of wastewater, to the upper two zones and the much larger amount of groundwater recharge, with much less influence from infiltrating wastewater, to the lower two zones.

USGS 132

Water at USGS 132 is a mixture of water from the BLR, wastewater from USGS 88, RWMC M3S, and zones 9 and 6 at MIDDLE 2051, and groundwater from these wells, zones, and USGS 119 (fig. 20*G*). Modeled groundwater-flow directions to USGS 132 are largely south-southwest.

Water from the BLR is present at all zones at USGS 132, which indicates that surface water moves downward in this part of the aquifer. Wastewater was modeled as being present at all zones at USGS 132 (table 11), a result that is consistent with the large tritium activities at all zones (ranging from 122 to 301 pCi/L, table 6). However, initial solutions of groundwater flowing to USGS 132 appear to be horizontally stratified by the Matuyama flow (fig. 20*G*), which may impede the downward movement of groundwater. For example, groundwater from the shallow wells USGS 88, USGS 119, and RWMC M3S flows to the shallowest two zones at USGS 132. These two zones are located above the Matuyama flow. Deeper groundwater, from zones 9 and 6 at MIDDLE 2051, zones that are located directly above or within the Matuyama flow, flow to the four deeper zones at USGS 132. These four zones are all located within or below the Matuyama flow.

These results appear to create a discrepancy at USGS 132 between surface water from the BLR, which is not horizontally stratified and moves downward across the Matuyama flow, and groundwater that is horizontally stratified and is segregated by the Matuyama flow. However, while surface water is a large source of recharge to all zones at USGS 132 (table 11), the large decrease in the percentage of recharge from surface water for the lower four zones, compared to the upper two zones, indicates that the Matuyama flow does impede the downward flow of water at USGS 132.

USGS 135

Water at USGS 135 is a mixture of water from the BLR and groundwater from USGS 8 and USGS 86 (fig. 20*H*). Modeled groundwater-flow directions to USGS 135 are south-southwest to all four zones plus south-southeast to zone 7.

Surface water from the BLR is present in all zones at USGS 135, which indicates that downward movement of water occurs in this part of the aquifer. Groundwater from USGS 86 also flows to all four zones at USGS 135, corresponds to the downward movement of surface water from the BLR, and provides additional evidence that water flowing to USGS 135 has a downward component. The two deepest zones at USGS 135 are in the Matuyama flow, and surface water provides 86 percent of the water to these zones (table 11). Because surface water constitutes most of the water in the Matuyama flow at USGS 132, the Matuyama flow may not act as a semi-impermeable unit in this area of the aquifer.

USGS 137A

Water at USGS 137A is a mixture of surface water from the BLR and groundwater from EBR1, USGS 131A, and USGS 132 (fig. 20*I*). Modeled groundwater-flow directions to USGS 137A are south and southwest.

Surface water is a large source of water to all zones at USGS 137A (table 11), which indicates that downward movement of water occurs in this part of the aquifer. Tritium activities at USGS 137A range from about 64.8 to 106 pCi/L (table 6), slightly larger than the 30 to 60 pCi/L activity in recent precipitation (fig. 15), indicating that a small amount of wastewater is probably present in groundwater at USGS 137A. Groundwater flowing to all four zones at USGS 137A are from unknown depths at EBR1 and the shallowest zones from USGS 131A and USGS 132 (fig. 20*I*). These results indicate that groundwater is moving downward to all zones at USGS 137A, consistent with the downward movement of surface water to all zones. All four zones at USGS 137A are located above the Matuyama flow, so vertical flow directions at this well do not provide any information about the permeability of the Matuyama flow.

Southwestern Part of Idaho National Laboratory

Horizontal groundwater-flow directions in the southwestern part of the INL are largely south to southwest in both the shallow and deep parts of the aquifer. Surface water from the BLR is the primary source of recharge at the shallow zones at MIDDLE 2050A, MIDDLE 2051, USGS 131A, and USGS 132 and at all sampling zones at the other MLW, all of which are near the southern boundary of the INL (fig. 1; table 11). The presence of surface water at deep sampling zones indicates that downward movement of groundwater occurs in the southwestern part of the INL. Some horizontal stratification of groundwater in the southwestern part of the INL is apparent, however. This horizontal stratification appears to be primarily controlled by the Matuyama flow, which appears to act as a semi-impermeable flow that partially segregates water above and below this flow.

Summary and Conclusions

Geochemical modeling indicated that the primary chemical reactions in the aquifer were dissolution of plagioclase, basalt volcanic glass, dolomite, and carbon dioxide and precipitation of calcite. Minor chemical reactions included the dissolution of olivine and gypsum.

Results from geochemical modeling indicate that most of the recharge to the southwestern part of the Idaho National Laboratory (INL) is from the Big Lost River (BLR) and groundwater from the Little Lost River valley, which contribute about 60 and 27 percent of the total recharge, respectively. Precipitation and wastewater contribute about 6 and 5 percent of the total recharge, and regional groundwater and groundwater from the BLR and Birch Creek valleys and Lost River Range each contribute 1 percent or less of the total recharge.

Evaluation of mixing between surface water and groundwater indicates that the percentage of surface water in the aquifer increases south of the BLR and decreases with aquifer depth. In the deepest part of the aquifer (545–655 feet below water table), only multilevel wells (MLW) USGS 103 and USGS 105, along the southern boundary of the INL, have surface water as the primary source of water.

Large decreases in the percentage of surface water in the aquifer, in a downward direction (that is, between one aquifer depth range and the underlying depth range), ranged from 26 to 74 percent. These large decreases in the percentage of surface water in the aquifer may indicate the presence of a semi-impermeable stratigraphic unit. These large decreases all occurred within, or directly above or below, the Matuyama flow, and indicate that the Matuyama flow and (or) associated sedimentary layers are semi-impermeable to the downward flow of groundwater.

There is an identifiable spatial distribution in the percentage decrease of surface water, with western (USGS 105, USGS 132, USGS 135) and eastern (MIDDLE 2050A, MIDDLE 2051, USGS 108, USGS 131A) groups of MLW that have a decrease ranging from 28 to 33 percent and 68 to 76 percent, respectively. This disparity may indicate that the permeability of the Matuyama flow is larger near the western group of MLW and smaller near the eastern group of MLW.

Horizontal groundwater-flow directions are largely south to southwest in both the shallow and deep parts of the aquifer. Surface water from the BLR is the primary source of recharge at the shallow zones at MIDDLE 2050A, MIDDLE 2051, USGS 131A, and USGS 132 and at all sampling zones at the other MLW, all of which are near the southern boundary of the INL. The presence of surface water as a source of water to groundwater from deep sampling zones at MLW along the southern boundary of the INL indicates that downward movement of groundwater occurs in the southwestern part of the INL.

Geochemical modeling indicates that wastewater and (or) waste constituents from the (1) Idaho Nuclear Technology and Engineering Center (INTEC) were present at USGS 131A, USGS 103, USGS 105, and USGS 108, (2) Advanced Test Reactor Complex (ATRC) were present at MIDDLE 2051 and USGS 132, (3) INTEC and ATRC were present at MIDDLE 2050A, and (4) INTEC and Radioactive Waste Management Complex were present at USGS 132 and USGS 137A. These results indicate that wastewater is present throughout the southwestern part of the INL and that wastewater generally travels in southern and (or) south-southwestern directions. These MLW, except MIDDLE 2050A, contain wastewater at deep sampling zones. These results show that wastewater has moved downward and support the interpretation that groundwater in the southwestern part of the INL moves downward.

Acknowledgments

The Idaho National Laboratory Project Chief expresses his gratitude to Kerri C. Treinen (U.S. Geological Survey [USGS]) for stewarding this report to completion upon author Gordon W. Rattray's retirement, working closely with the Science Publishing Network managing editor and the Bureau Approving Official to resolve all outstanding concerns. The author also thanks the field team for completing field work needed for this study.

References Cited

Ackerman, D.J., Rattray, G.W., Rousseau, J.P., Davis, L.C., and Orr, B.R., 2006, A conceptual model of ground-water flow in the Eastern Snake River Plain aquifer at the Idaho National Laboratory and vicinity with implications for contaminant transport: U.S. Geological Survey Scientific Investigations Report 2006–5122 (DOE/ID-22198), 62 p.

Anderson, S.R., Kuntz, M.A., and Davis, L.C., 1999, Geologic controls of hydraulic conductivity in the Snake River Plain aquifer at and near the Idaho National Engineering and Environmental Laboratory, Idaho: U.S. Geological Survey Water-Resources Investigations Report 99–4033 (DOE/ID-22155) 38 p., accessed November 1, 2020, at https://pubs.er.usgs.gov/publication/wri994033.

Anderson, S.R., and Liszewski, M.J., 1997, Stratigraphy of the unsaturated zone and the Snake River Plain aquifer at and near the Idaho National Engineering Laboratory, Idaho: U.S. Geological Survey Water-Resources Investigations Report 97–4183 (DOE/ID-22142), 65 p.

Barraclough, J.T., Lewis, B.D., and Jensen, R.G., 1981, Hydrologic conditions at the Idaho National Engineering Laboratory, Idaho, emphasis—1974–1978: U.S. Geological Survey Open-File Report 81–256 (IDO-22060), 116 p.

Bartholomay, R.C., 1990, Mineralogical correlation of surficial sediment from area drainages with selected sedimentary interbeds at the Idaho National Engineering Laboratory, Idaho: U.S. Geological Survey Water-Resources Investigations Report 90–4177 (DOE/ID-22092), 18 p.

Bartholomay, R.C., 2022, Historical development of the U.S. Geological Survey hydrological monitoring and investigative programs at the Idaho National Laboratory, Idaho, 2002–2020: U.S. Geological Survey Open-File Report 2022–1027 (DOE/ID-22256), 54 p., accessed December 2022, at https://doi.org/10.3133/ofr20221027.

Bartholomay, R.C., Hodges, M.K.V., and Champion, D.E., 2017, Correlation between basalt flows and radiochemical and chemical constituents in selected wells in the southwestern part of the Idaho National Laboratory, Idaho: U.S. Geological Survey Scientific Investigations Report 2017–5148 (DOE/ID-22245), 39 p., accessed November 1, 2020, at https://pubs.er.usgs.gov/publication/sir20175148.

Bartholomay, R.C., Hopkins, C.B., and Maimer, N.V., 2015, Chemical constituents in groundwater from multiple zones in the Eastern Snake River Plain aquifer at the Idaho National Laboratory, Idaho, 2009–13: U.S. Geological Survey Scientific Investigations Report 2015–5002 (DOE/ID-22232), 109 p., accessed November 1, 2020, at https://pubs.er.usgs.gov/publication/sir20155002.

Bartholomay, R.C., Knobel, L.L., and Davis, L.C., 1989, Mineralogy and grain size of surficial sediment from the Big Lost River drainage and vicinity, with chemical and physical characteristics of geologic materials from selected sites at the Idaho National Engineering Laboratory, Idaho: U.S. Geological Survey Open-File Report 89–384 (DOE/ID-22081), 74 p. [Also available at https://doi.org/10.3133/ofr89384.]

Bartholomay, R.C., Maimer, N.V., Rattray, G.W., and Fisher, J.C., 2017, An update of hydrologic conditions and distribution of selected constituents in water, eastern Snake River Plain aquifer and perched groundwater zones, Idaho National Laboratory, Idaho, emphasis 2012–15: U.S. Geological Survey Scientific Investigations Report 2017–5021 (DOE/ID-22242), 87 p., accessed November 1, 2020, at https://pubs.er.usgs.gov/publication/sir20175021.

Bartholomay, R.C., Maimer, N.V., and Wehnke, A.J., 2014, Field methods and quality-assurance plan for water-quality activities and water-level measurements, U.S. Geological Survey, Idaho National Laboratory, Idaho: U.S. Geological Survey Open-File Report 2014–1146 (DOE/ID-22230), 66 p., accessed November 1, 2020, at https://pubs.er.usgs.gov/publication/ofr20141146.

Bartholomay, R.C., and Tucker, B.J., 2000, Distribution of selected radiochemical and chemical constituents in perched ground water, Idaho National Engineering and Environmental Laboratory, Idaho, 1996-98: U.S. Geological Survey Water-Resources Investigations Report 2000–4222 (DOE/ID-22168), 51 p., accessed November 1, 2020, at https://pubs.usgs.gov/wri/2000/4222/report.pdf.

Bartholomay, R.C., and Twining, B.V., 2010, Chemical constituents in groundwater from multiple zones in the Eastern Snake River Plain aquifer at the Idaho National Laboratory, Idaho, 2005–08: U.S. Geological Survey Scientific Investigations Report 2010–5116 (DOE/ID-22211), 81 p.

Benjamin, L., Knobel, L.L., Hall, L.F., Cecil, L.D., and Green, J.R., 2004, Development of a local meteoric water line for southeastern Idaho, western Wyoming, and south-central Montana: U.S. Geological Survey Scientific Investigations Report 2004–5126 (DOE/ID-22191), 17 p.

Bennett, C.M., 1990, Streamflow losses and ground-water level changes along the Big Lost River at the Idaho National Engineering Laboratory, Idaho: U.S. Geological Survey Water-Resources Investigations Report 90–4067 (DOE/ID-22091), 49 p.

Bethke, C.M., and Yeakel, S., 2017, The Geochemist's workbench, release 11—GWB essentials guide: Aqueous Solutions, LLC, Champaign, Illinois, 180 p.

Blair, J.J., 2002, Sedimentology and stratigraphy of sediments of the Big Lost Trough subsurface from selected boreholes at the Idaho National Engineering and Environmental Laboratory, Idaho: Pocatello, Idaho State University, M.S. thesis, 162 p., accessed November 1, 2020, at https://isu.app.box.com/v/Blair-2002.

Busenberg, E., Plummer, L.N., and Bartholomay, R.C., 2001, Estimated age and source of the young fraction of ground water at the Idaho National Engineering and Environmental Laboratory: U.S. Geological Survey Water-Resources Investigations Report 01–4265 (DOE/ID-22177), 144 p., accessed November 1, 2020, at https://pubs.er.usgs.gov/publication/wri014265.

Busenberg, E., Plummer, L.N., Bartholomay, R.C., and Wayland, J.E., 1998, Chlorofluorocarbons, sulfur hexafluoride, and dissolved permanent gases in ground water from selected sites at and near the Idaho National Engineering and Environmental Laboratory: U.S. Geological Survey Open-File Report 98–274 (DOE/ID-22151), 72 p., accessed November 1, 2020, at https://pubs.er.usgs.gov/publication/ofr98274.

Busenberg, E., Plummer, L.N., Doughten, M.W., Widman, P.K., and Bartholomay, R.C., 2000, Chemical and isotopic composition and gas concentrations of ground water and surface water from selected sites at and near the Idaho National Engineering and Environmental Laboratory: U.S. Geological Survey Open-File Report 00–81 (DOE/ID-22164), 51 p., accessed November 1, 2020, at https://pubs.er.usgs.gov/publication/ofr0081.

Busenberg, E., Weeks, E.P., Plummer, L.N., and Bartholomay, R.C., 1993, Age dating groundwater by use of chlorofluorocarbons (CCl_3F and CCl_2F_2), and distribution of chlorofluorocarbons in the unsaturated zone, Snake River Plain aquifer, Idaho National Engineering Laboratory, Idaho: U.S. Geological Survey Water-Resources Investigations Report 93–4054 (DOE/ID-22107), 47 p., accessed November 1, 2020, at https://doi.org/10.3133/wri934054.

Cecil, L.D., Orr, B.R., Norton, T., and Anderson, S.R., 1991, Formation of perched ground-water zones and concentrations of selected chemical constituents in water, Idaho National Engineering Laboratory, Idaho, 1986–88: U.S. Geological Survey Water-Resources Investigations Report 91–4166 (DOE/ID-22100), 53 p., accessed November 1, 2020, at https://doi.org/10.3133/wri914166.

Cecil, L.D., Welhan, J.A., Green, J.R., Grape, S.K., and Sudicky, E.R., 2000, Use of chlorine-36 to determine regional-scale aquifer dispersivity, eastern Snake River Plain aquifer, Idaho/USA: Nuclear Instruments & Methods in Physics Research. Section B, Beam Interactions with Materials and Atoms, v. 172, nos. 1–4, p. 679–687, accessed November 1, 2020, at https://doi.org/10.1016/S0168-583X(00)00216-0.

Davis, L.C., 2010, An update of hydrologic conditions and distribution of selected constituents in water, Snake River Plain aquifer and perched groundwater zones, Idaho National Laboratory, Idaho, emphasis 2006–08: U.S. Geological Survey Scientific Investigations Report 2010–5197 (DOE/ID-22212), 80 p., accessed November 1, 2020, at https://pubs.er.usgs.gov/publication/sir20105197.

Davis, L.C., Bartholomay, R.C., Fisher, J.C., and Maimer, N.V., 2015, Water-quality characteristics and trends for selected wells possibly influenced by wastewater disposal at the Idaho National Laboratory, Idaho, 1981–2012: U.S. Geological Survey Scientific Investigations Report 2015–5003 (DOE/ID-22233), 105 p., accessed November 1, 2020, at https://pubs.er.usgs.gov/publication/sir20155003.

Davis, L.C., Bartholomay, R.C., and Rattray, G.W., 2013, An update of hydrologic conditions and distribution of selected constituents in water, eastern Snake River Plain aquifer and perched groundwater zones, Idaho National Laboratory, Idaho, emphasis 2009–11: U.S. Geological Survey Scientific Investigations Report 2013–5214 (DOE/ID-22226), 89 p., accessed November 1, 2020, at https://pubs.er.usgs.gov/publication/sir20135214.

Deer, W.A., Howie, R.A., and Zussman, J., 1983, An introduction to the rock forming minerals: Longman House, Essex, England, 528 p.

Deutsch, W.J., Jenne, E.A., and Krupka, K.M., 1982, Solubility equilibria in basalt aquifers—The Columbia Plateau, eastern Washington, U.S.A: Chemical Geology, v. 36, nos. 1–2, p. 15–34, accessed November 1, 2020, at https://doi.org/10.1016/0009-2541(82)90037-7.

Doherty, D.J., McBroome, L.A., and Kuntz, M.A., 1979, Preliminary geological interpretation and lithologic log of the exploratory geothermal test well (INEL-1), Idaho National Engineering Laboratory, eastern Snake River Plain, Idaho: U.S. Geological Survey Open-File Report 79–1248, 9 p., accessed November 1, 2020, at https://doi.org/10.2172/6515315.

Fisher, J.C., Rousseau, J.P., Bartholomay, R.C., and Rattray, G.W., 2012, A comparison of U.S. Geological Survey three-dimensional model estimates of groundwater source areas and velocities to independently derived estimates, Idaho National Laboratory and vicinity, Idaho: U.S. Geological Survey Scientific Investigations Report 2012–5152 (DOE/ID-22218), 130 p.

Fisher, J.C., and Twining, B.V., 2011, Multilevel groundwater monitoring of hydraulic head and temperature in the eastern Snake River Plain aquifer, Idaho National Laboratory, Idaho, 2007–08: U.S. Geological Survey Scientific Investigations Report 2010–5253 (DOE/ID-22213), 62 p.

Freeze, R.A., and Cherry, J.A., 1979, Groundwater: Englewood Cliffs, New Jersey, Prentice Hall, 604 p.

Fromm, J.R., Welhan, J.A., McCurry, M., and Hackett, W.R., 1994, Idaho Chemical Processing Plant (ICCP) injection well—Operations history and hydrochemical inventory of the waste stream, *in* Link, P.K., ed., Hydrogeology, waste disposal, science and politics: Proceedings of the 30th symposium on Engineering Geology and Geotechnical Engineering, Pocatello, Idaho, College of Engineering, Idaho State University, p. 221–237.

Geslin, J.K., Link, P.K., Riesterer, J.W., Kuntz, M.A., and Fanning, C.M., 2002, Pliocene and Quaternary stratigraphic architecture and drainage systems of the Big Lost Trough, northeastern Snake River Plain, Idaho, *in* Link, P.K., and Mink, L.L., eds., Geology, hydrogeology, and environmental remediation—Idaho National Engineering and Environmental Laboratory, Eastern Snake River Plain, Idaho: Geological Society of America Special Paper 353, p. 11–26, accessed November 1, 2020, at https://doi.org/10.1130/0-8137-2353-1.11.

Gianniny, G.L., Thackray, G.D., Kauffman, D.S., Forman, S.L., Sherbondy, M.J., and Findeisen, D., 2002, Late Quaternary highlands in the Mud Lake and Big Lost Trough subbasins of Lake Terreton, Idaho, *in* Link, P.K., and Mink, L.L., eds., Geology, hydrogeology, and environmental remediation—Idaho National Engineering and Environmental Laboratory, Eastern Snake River Plain, Idaho: Geological Society of America Special Paper 353, p. 77–90, accessed November 1, 2020, at https://doi.org/10.1130/0-8137-2353-1.77.

Ginsbach, M.L., 2013, Geochemical evolution of groundwater in the Medicine Lodge Creek drainage basin, eastern Idaho: Pocatello, Idaho State University, M.S. thesis, 241 p., accessed November 1, 2020, at https://isu.app.box.com/v/Ginsbach-2013.

Gronow, J.R., 1987, The dissolution of asbestos fibres in water: Clay Minerals, v. 22, no. 1, p. 21–35, accessed November 1, 2020, at https://doi.org/10.1180/claymin.1987.022.1.03

Hem, J.D., 1992, Study and interpretation of the chemical characteristics of natural water: U.S. Geological Survey Water-Supply Paper 2254 (3d ed.), 263 p., accessed November 1, 2020, at https://pubs.er.usgs.gov/publication/wsp2254.

Hodges, M.K.V., and Champion, D.E., 2016, Paleomagnetic correlation of basalt flows in selected coreholes near the Advanced Test Reactor Complex, the Idaho Nuclear Technology and Engineering Center, and along the southern boundary, Idaho National Laboratory, Idaho: U.S. Geological Survey Scientific Investigations Report 2016–5131 (DOE/ID-22240), 65 p., 1 pl., accessed November 1, 2020, at https://doi.org/10.3133/sir20165131.

Hodges, M.K.V., Orr, S.M., Potter, K.E., and LeMaitre, T., 2012, Construction diagrams, geophysical logs, and lithologic descriptions for boreholes USGS 103, 105, 108, 131, 135, NRF-15, and NRF-16, Idaho National Laboratory, Idaho: U.S. Geological Survey Data Series 660 (DOE/ID-22217), 34 p., accessed November 1, 2020, at https://pubs.er.usgs.gov/publication/ds660.

Idaho Department of Environmental Quality, 2015, Sole source aquifers: Idaho Department of Environmental Quality web page, accessed September 1, 2021, at https://www.deq.idaho.gov/water-quality/ground-water/aquifers/.

Idaho Department of Water Resources, 2014, Well driller reports: Idaho Department of Water Resources, accessed December 12, 2014, at https://research.idwr.idaho.gov/apps/wellconstruction/wcinfosearchexternal/.

Jones, P.H., 1961, Hydrology of waste disposal, National Reactor Testing Station, Idaho, an interim report: U.S. Atomic Energy Commission, Idaho Operations Office Publication IDO-22042-USGS, 152 p.

Jurgens, B.C., 2018, Data for tritium deposition in precipitation in the United States, 1953–2012: U.S. Geological Survey data release, accessed November 1, 2020, at https://doi.org/10.5066/P92CEFXN.

Knobel, L.L., Bartholomay, R.C., Cecil, L.D., Tucker, B.J., and Wegner, S.J., 1992, Chemical constituents in the dissolved and suspended fractions of ground water from selected sites, Idaho National Engineering Laboratory and vicinity, Idaho, 1989: U.S. Geological Survey Open-File Report 92–51 (DOE/ID-22101), 56 p., accessed November 1, 2020, at https://pubs.er.usgs.gov/publication/ofr9251.

Knobel, L.L., Bartholomay, R.C., and Orr, B.R., 1997, Preliminary delineation of natural geochemical reactions, Snake River Plain aquifer system, Idaho National Engineering Laboratory and vicinity, Idaho: U.S. Geological Survey Water-Resources Investigations Report 97–4093 (DOE/ID-22139), 52 p., accessed November 1, 2020, at https://pubs.er.usgs.gov/publication/wri974093.

Knobel, L.L., Bartholomay, R.C., Tucker, B.J., Williams, L.M., and Cecil, L.D., 1999, Chemical constituents in ground water from 39 selected sites with an evaluation of associated quality assurance data, Idaho National Engineering and Environmental Laboratory and vicinity, Idaho: U.S. Geological Survey Open-File Report 99–246 (DOE/ID-22159), 58 p., accessed November 1, 2020, at https://pubs.er.usgs.gov/publication/ofr99246.

Knobel, L.L., Tucker, B.J., and Rousseau, J.P., 2008, Field methods and quality-assurance plan for quality-of-water activities, U.S. Geological Survey, Idaho National Laboratory, Idaho: U.S. Geological Survey Open-File Report 2008–1165 (DOE/ID-22206), 36 p., accessed November 1, 2020, at https://pubs.er.usgs.gov/publication/ofr20081165.

Kuntz, M.A., Covington, H.R., and Schorr, L.J., 1992, An overview of basaltic volcanism of the eastern Snake River Plain, Idaho, *in* Link, P.K., Kuntz, M.A., and Platt, L.B., eds., Regional geology of Eastern Idaho and western Wyoming: Geological Society of America Memoir 179, p. 227–257, accessed November 1, 2020, at https://doi.org/10.1130/MEM179-p227.

Lanphere, M.A., Champion, D.E., and Kuntz, M.A., 1993, Petrography, age, and paleomagnetism of basalt lava flows in coreholes Well 80, NRF 89-04, NRF 89-05, and ICPP 123, Idaho National Engineering Laboratory: U.S. Geological Survey Open-File Report 93–327, 40 p., accessed November 1, 2020, at https://doi.org/10.2172/10192018.

Lasaga, A.C., Soler, J.M., Ganor, J., Burch, T.E., and Nagy, K.L., 1994, Chemical weathering rate laws and global geochemical cycles: Geochimica et Cosmochimica Acta, v. 58, no. 10, p. 2361–2386, accessed November 1, 2020, at https://doi.org/10.1016/0016-7037(94)90016-7.

Lewis, R.S., Link, P.K., Stanford, L.R., and Long, S.P., 2012, Geologic map of Idaho: Idaho Geological Survey Map 9, scale 1:750,000, accessed September 14, 2015, at https://www.idahogeology.org/pub/Maps/Geologic_Map_of_Idaho_M-9_2012_200DPI.pdf.

Manahan, S.E., 1991, Environmental chemistry: Chelsea, Mich., Lewis publishers, 583 p.

Mann, L.J., 1986, Hydraulic properties of rock units and chemical quality of water for INEL-1—A 10,365-foot deep test hole drilled at the Idaho National Engineering Laboratory, Idaho: U.S. Geological Survey Water-Resources Investigations Report 86–4020 (DOE/ID-22070), 23 p., accessed September 2020, at https://pubs.er.usgs.gov/publication/wri864020.

Mann, L.J., 1996, Quality-assurance plan and field methods for quality-of-water activities, U.S. Geological Survey, Idaho National Engineering Laboratory, Idaho: U.S. Geological Survey Open-File Report 96–615 (DOE/ID-22132), 37 p., accessed November 1, 2020, at https://pubs.usgs.gov/of/1996/0615/.

Mann, L.J., and Beasley, T.M., 1994, Iodine-129 in the Snake River Plain aquifer at and near the Idaho National Engineering Laboratory, Idaho, 1990–91: U.S. Geological Survey Water-Resources Investigations Report 94–4053 (DOE/ID-22115), 27 p., accessed November 1, 2020, at https://pubs.er.usgs.gov/publication/wri944053.

Mann, L.J., and Cecil, L.D., 1990, Tritium in ground water at the Idaho National Engineering Laboratory, Idaho: U.S. Geological Survey Water-Resources Investigations Report 90–4090 (DOE/ID-22090), 35 p., accessed November 1, 2020, at https://pubs.er.usgs.gov/publication/wri904090.

Mark, L.E., and Thackray, G.D., 2002, Sedimentologic and hydrologic characterization of surficial sedimentary facies in the Big Lost Trough, Idaho National Engineering and Environmental Laboratory, eastern Idaho, *in* Link, P.K., and Mink, L.L., eds., Geology, Hydrogeology, and Environmental Remediation—Idaho National Engineering and Environmental Laboratory, Eastern Snake River Plain, Idaho: Geological Society of America Special Paper 353, p. 61–75, accessed November 1, 2020, at https://doi.org/10.1130/0-8137-2353-1.61.

Mazurek, J., 2004, Genetic controls on basalt alteration within the eastern Snake River Plain aquifer system, Idaho: Pocatello, Idaho State University, M.S. thesis, 215 p., accessed November 1, 2020, at https://isu.app.box.com/v/Mazurek-2004.

McLing, T.L., 1994, The pre-anthropogenic groundwater evolution at the Idaho National Engineering Laboratory, Idaho: Pocatello, Idaho State University, M.S. thesis, 62 p., accessed November 1, 2020, at https://isu.app.box.com/v/McLing-1994.

Michel, R.L., Jurgens, B.C., and Young, M.B., 2018, Tritium deposition in the United States, 1953−2012: U.S. Geological Survey Scientific Investigations Report 2018–5086, 11 p., accessed November 1, 2020, at https://doi.org/10.3133/sir20185086.

Morris, D.A., Hogenson, G.M., Teasdale, W.E., and Shuter, E., 1963, Hydrology of waste disposal, National Reactor Testing Station, Idaho—Annual progress report, 1962: U.S. Atomic Energy Commission, Idaho Operations Office Publication IDO-22044-USGS, 99 p.

Nace, R.L., Deutsch, M., and Voegli, P.T., 1956, Geography, geology, and water resources of the National Reactor Testing Station, Idaho—Part 2. Geography and geology: U.S. Geological Survey Open-File Report (IDO-22033), 225 p.

National Oceanic and Atmospheric Administration, 2015, NOAA INL Weather Center: U.S. Department of Commerce, accessed on September 10, 2015, at https://niwc.noaa.inl.gov/climate.htm#.

Nimmo, J.R., Perkins, K.S., Rose, P.E., Rousseau, J.P., Orr, B.R., Twining, B.V., and Anderson, S.R., 2002, Kilometer-scale rapid transport of naphthalene sulfonate tracer in the unsaturated zone at the Idaho National Engineering and Environmental Laboratory: Vadose Zone Journal, v. 1, no. 1, p. 89–101, accessed November 1, 2020, at https://doi.org/10.2136/vzj2002.8900.

North Wind, Inc., 2006, Drilling, coring, and installation of two deep monitoring wells (MIDDLE 2051 and MIDDLE 2050A) in fiscal year 2005: Prepared under subcontract No. 00026016 for the U.S. Department of Energy, Rpt-178, Revision 0, [variously paged].

Olmsted, F.H., 1962, Chemical and physical character of ground water in the National Reactor Testing Station, Idaho: U.S. Atomic Energy Commission, Idaho Operations Office Publication IDO-22043-USGS, [variously paged].

Orr, B.R., Cecil, L.D., and Knobel, L.L., 1991, Background concentrations of selected radionuclides, organic compounds, and chemical constituents in ground water in the vicinity of the Idaho National Engineering Laboratory: U.S. Geological Survey Water-Resources Investigations Report 91–4015, 52 p.

Parkhurst, D.L., 1997, Geochemical mole-balance modeling with uncertain data: Water Resources Research, v. 33, no. 8, p. 1957–1970, accessed September 2020, at https://doi.org/10.1029/97WR01125.

Parkhurst, D.L., and Appelo, C.A.J., 2013, Description of input and examples for PHREEQC Version 3—A computer program for speciation, batch-reaction, one-dimensional transport, and inverse geochemical calculations: U.S. Geological Survey Techniques and Methods, book 6, chap. A43, 497 p., accessed November 1, 2020, at https://pubs.usgs.gov/tm/06/a43/.

Peckham, A.E., 1959, Investigations of underground waste disposal, Chemical Processing Plant area, National Reactor Testing Station, Idaho: U.S. Atomic Energy Commission, Idaho Operations Office Publication IDO-22039-USGS, 35 p.

Pittman, J.R., Jensen, R.G., and Fischer, P.R., 1988, Hydrologic conditions at the Idaho National Engineering Laboratory, 1982 to 1985: U.S. Geological Survey Water-Resources Investigations Report 89–4008 (DOE/ID-22078), 73 p.

Rattray, G.W., 2012, Evaluation of quality-control data collected by the U.S. Geological Survey for routine water-quality activities at the Idaho National Laboratory, Idaho, 1996–2001: U.S. Geological Survey Scientific Investigations Report 2012–5270 (DOE/ID-22222), 74 p., accessed November 1, 2020, at https://pubs.usgs.gov/sir/2012/5270/.

Rattray, G.W., 2014, Evaluation of quality-control data collected by the U.S. Geological Survey for routine water-quality activities at the Idaho National Laboratory, southeastern Idaho, 2002–2008: U.S. Geological Survey Scientific Investigations Report 2014–5027 (DOE/ID-22228), 66 p., accessed November 1, 2020, at https://pubs.usgs.gov/sir/2014/5027/.

Rattray, G.W., 2015, Geochemical evolution of groundwater in the Mud Lake area, eastern Idaho, USA: Environmental Earth Sciences, v. 73, p. 8251–8269, accessed November 1, 2020, at https://doi.org/10.1007/s12665-014-3988-9.

Rattray, G.W., 2018, Geochemistry of groundwater in the eastern Snake River Plain aquifer, Idaho National Laboratory and vicinity, eastern Idaho: U.S. Geological Survey Professional Paper 1837–A (DOE/ID-22246), 198 p., accessed November 1, 2020, at https://doi.org/10.3133/pp1837A.

Rattray, G.W., 2019, Evaluation of chemical and hydrologic processes in the eastern Snake River Plain aquifer based on results from geochemical modeling, Idaho National Laboratory, eastern Idaho: U.S. Geological Survey Professional Paper 1837–B (DOE/ID-22248), 85 p., accessed November 1, 2020, at https://doi.org/10.3133/pp1837B.

Rattray, G.W., and Ginsbach, M.L., 2014, Geochemistry of groundwater in the Beaver and Camas Creek drainage basins, eastern Idaho: U.S. Geological Survey Scientific Investigations Report 2013–5226 (DOE/ID-22227), 70 p., accessed November 1, 2020, at https://pubs.usgs.gov/sir/2013/5226/.

Reed, M.F., and Bartholomay, R.C., 1994, Mineralogy of selected sedimentary interbeds at or near the Idaho National Engineering Laboratory, Idaho: U.S. Geological Survey Open-File Report 94–374 (DOE/ID-22116), 19 p.

Rightmire, C.T., 1984, Description and hydrogeologic implications of cored sedimentary material from the 1975 drilling program at the Radioactive Waste Management Complex, Idaho: U.S. Geological Survey Water-Resources Investigations Report 84–4071 (DOE/ID-22067), 33 p.

Rightmire, C.T., and Lewis, B.D., 1987, Hydrogeology and geochemistry of the unsaturated zone, Radioactive Waste Management Complex, Idaho National Engineering Laboratory, Idaho: U.S. Geological Survey Water-Resources Investigations Report 87–4198 (DOE/ID-22073), 89 p.

Robertson, J.B., Schoen, R., and Barraclough, J.T., 1974, The influence of liquid waste disposal on the geochemistry of water at the National Reactor Testing Station, Idaho—1952–1970: U.S. Geological Survey Open-File Report 73–238 (IDO-22053), 231 p., accessed November 1, 2020, at https://doi.org/10.3133/ofr73238.

Roddy, M., 2007, Anthropogenic contaminants as groundwater flow tracers—Idaho Museum of Natural History: Idaho Falls, Idaho, Falls Printing, p. 123–132.

Schramke, J.A., Murphy, E.M., and Wood, B.D., 1996, The use of geochemical mass-balance and mixing models to determine groundwater sources: Applied Geochemistry, v. 11, no. 4, p. 523–539, accessed November 1, 2020, at https://doi.org/10.1016/0883-2927(96)00007-8.

Sibson, R., 1981, A brief description of natural neighbor interpolation, *in* Barnett, V., ed., Interpreting Multivariate Data: New York, John Wiley and Sons, p. 21–36.

Twining, B.V., and Fisher, J.C., 2012, Multilevel groundwater monitoring of hydraulic head and temperature in the eastern Snake River Plain aquifer, Idaho National Laboratory, Idaho, 2009–10: U.S. Geological Survey Scientific Investigations Report 2012–5259, 44 p., accessed November 1, 2020, at https://doi.org/10.3133/sir20125259.

Twining, B.V., and Fisher, J.C., 2015, Multilevel groundwater monitoring of hydraulic head and temperature in the eastern Snake River Plain aquifer, Idaho National Laboratory, Idaho, 2011–13: U.S. Geological Survey Scientific Investigations Report 2015–5042, 49 p., accessed November 1, 2020, at https://doi.org/10.3133/sir20155042.

Twining, B.V., Hodges, M.K.V., and Orr, S.M., 2008, Construction diagrams, geophysical logs, and lithologic descriptions for boreholes USGS 126a, 126b, 127, 128, 129, 130, 131, 132, 133, and 134, Idaho National Laboratory, Idaho: U.S. Geological Survey Digital Series 350, 27 p., accessed November 1, 2020, at https://doi.org/10.3133/ds350.

U.S. Department of Energy, 2004, Monitoring report/decision summary for operable unit 313, group 5, Snake River Plain aquifer: U.S. Department of Energy, Idaho Operations Office Publication DOE/ID-11098, revision 1, [variously paged].

U.S. Department of Energy, 2007, Waste area group 10, operable unit 10-08, remedial investigation/feasibility study annual status report for fiscal year 2006: U.S. Department of Energy, Idaho Operations Office Publication DOE/ID-11297, revision 0, 245 p. [Also available at https://www.osti.gov/bridge/product.biblio.jsp?osti_id=910308.]

U.S. Department of Energy, 2008, Waste area group 10, operable unit 10-08, annual monitoring status report for fiscal year 2007: U.S. Department of Energy, Idaho Operations Office Publication DOE/ID-11355, revision 0, 123 p.

U.S. Department of Energy, 2011, Idaho National Laboratory groundwater monitoring and contingency plan update: U.S. Department of Energy, DOE/ID-11034, revision 2, [variously paged].

U.S. Geological Survey, 2021, USGS water data for the Nation: U.S. Geological Survey National Water Information System database, accessed January 2020, at https://doi.org/10.5066/F7P55KJN.

U.S. Geological Survey, [variously dated], National field manual for the collection of water-quality data: U.S. Geological Survey Techniques of Water-Resources Investigations, book 9, chaps. A1–A9, accessed September 1, 2015, at https://water.usgs.gov/owq/FieldManual/.

Welhan, J.A., Clemo, T.M., and Gégo, E.L., 2002, Stochastic simulation of aquifer heterogeneity in a layered basalt aquifer system, eastern Snake River Plain, Idaho, *in* Link, P.K., and Mink, L.L., eds., Geology, hydrogeology, and environmental remediation—Idaho National Engineering and Environmental Laboratory, Eastern Snake River Plain, Idaho: Geological Society of America Special Paper 353, p. 225–247, accessed November 1, 2020, at https://doi.org/10.1130/0-8137-2353-1.225.

Welhan, J.A., Johannesen, C.M., Reeves, K.S., Clemo, T.M., Glover, J.A., and Bosworth, K.W., 2002, Morphology of inflated pahoehoe lavas and spatial architecture of their porous and permeable zones, eastern Snake River Plain, Idaho, *in* Link, P.K., and Mink, L.L., eds., Geology, hydrogeology, and environmental remediation—Idaho National Engineering and Environmental Laboratory, Eastern Snake River Plain, Idaho: Geological Society of America Special Paper 353, p. 135–150, accessed November 1, 2020, at https://doi.org/10.1130/0-8137-2353-1.135.

Whitehead, R.L., 1992, Geohydrologic framework of the Snake River Plain regional aquifer system, Idaho and eastern Oregon: U.S. Geological Survey Professional Paper 1408–B, 32 p., 6 pls., accessed November 1, 2020, at https://pubs.er.usgs.gov/publication/pp1408B.

Wood, W.W., and Low, W.H., 1988, Solute geochemistry of the Snake River Plain regional aquifer system Idaho and eastern Oregon: U.S. Geological Survey Professional Paper 1408–D, 79 p., accessed November 1, 2020, at https://doi.org/10.3133/pp1408D.

Glossary

contaminated groundwater Groundwater influenced by discharge of wastewater and waste constituents. Contaminated groundwater was identified from various chemical signatures. These included groundwater samples with (1) large tritium activities (>75 pCi/L), (2) large sodium and sulfate concentrations (>25 and > 40 mg/L, respectively), (3) large specific conductance values (>600 µS/cm at 25 °C), and, (4) in the area near the Naval Reactors Facility, large chloride/nitrate ratios (>75).

deep groundwater Groundwater that is more than the 250 feet below the water table (does not include geothermal water).

groundwater from multilevel wells Groundwater from wells with multiple, discrete sampling zones of various depths below the land surface. Provides a vertical profile of groundwater chemistry in the ESRP aquifer. Groundwater from multilevel wells may be either contaminated or natural groundwater.

natural groundwater All groundwater that is not contaminated groundwater at and south of the Idaho National Laboratory.

old groundwater Groundwater that is older than the onset of atmospheric bomb testing (pre-1952). In this report, this qualitative age was assigned to groundwater with tritium activities less than 4 pCi/L.

regional groundwater Groundwater in the eastern Snake River Plain aquifer east of the Idaho National Laboratory (INL).

tributary valley groundwater Groundwater from the Big Lost River, Little Lost River, and (or) Birch Creek valleys.

young groundwater Groundwater that is younger than the onset of atmospheric bomb testing (post-1952). This qualitative groundwater age was determined from tritium activities.

For more information concerning the research in this report, contact the

Director, Idaho Water Science Center
U.S. Geological Survey
230 Collins Road
Boise, Idaho 83702-4520
https://www.usgs.gov/centers/idaho-water-science-center

Manuscript approved on December 14, 2022.

Publishing support provided by the U.S. Geological Survey
Science Publishing Network, Tacoma Publishing Service Center

ISSN 2330-7102 (online)
https://doi.org/10.3133/pp1837C